Special Report: Careers in Translational Research >> page 966

Science

17 August 2007 | S10

AAAS

PCR Arrays

Profile your pathway using qRT-PCR.

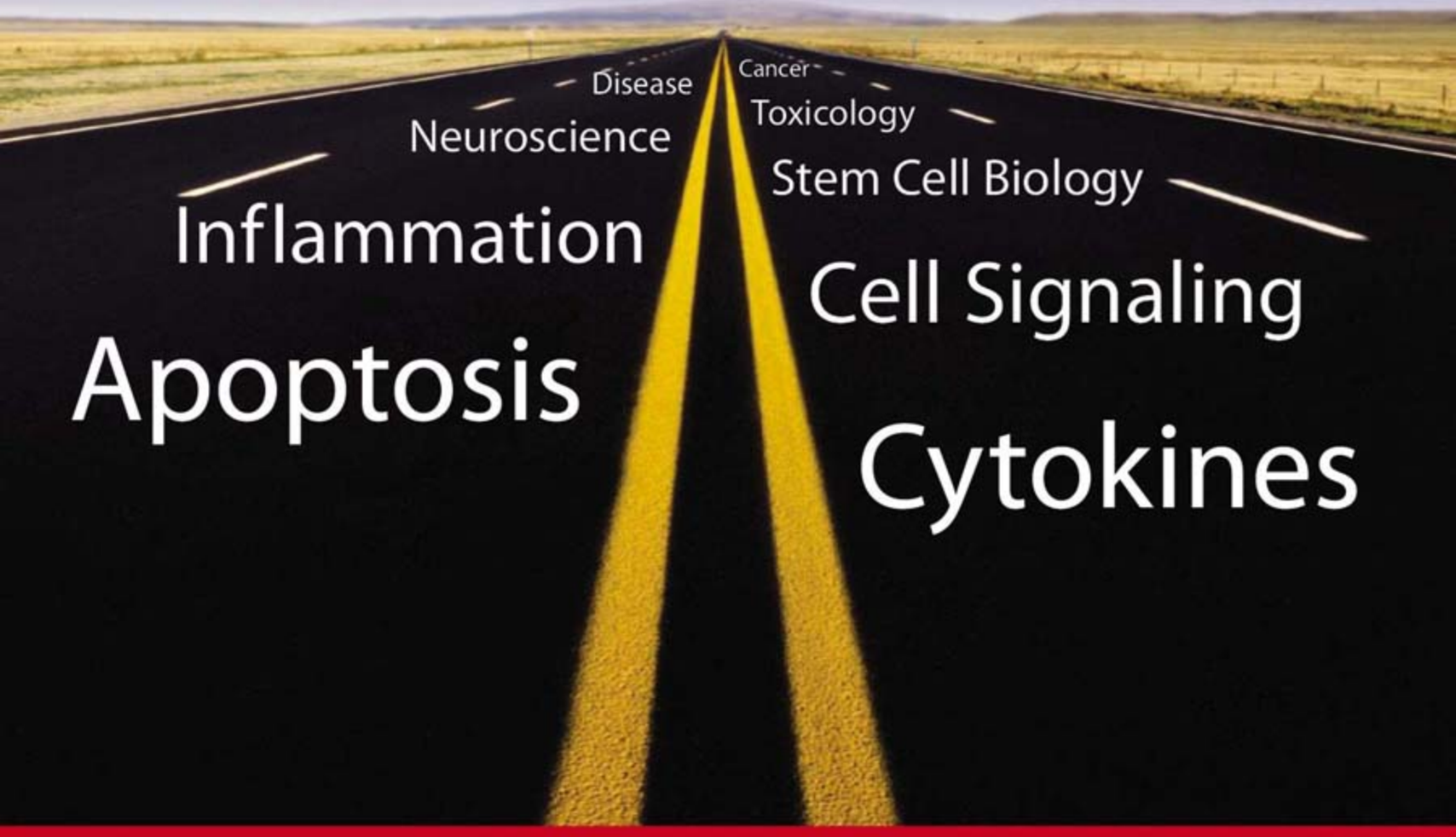

RT² *Profiler*™ PCR Arrays

RT² *Profiler*™ PCR Arrays are powerful new tools for monitoring the expression of focused gene panels. With PCR Arrays, you can accurately profile gene expression for a biological pathway or disease using the real-time quantitative PCR instrument in your lab.

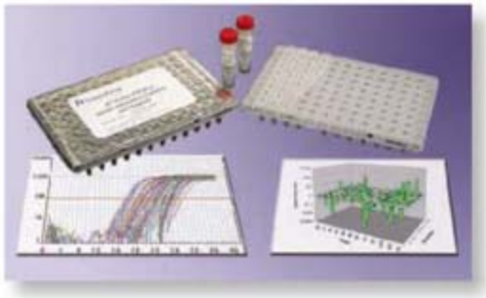

Focus on your Pathway

www.superarray.com

SuperArray
Bioscience Corporation

Q What can *Science* STKE give me?

A The definitive resource on cellular regulation

STKE – Signal Transduction Knowledge Environment offers:

- A weekly electronic journal
- Information management tools
- A lab manual to help you organize your research
- An interactive database of signaling pathways

STKE gives you essential tools to power your understanding of cell signaling. It is also a vibrant virtual community, where researchers from around the world come together to exchange information and ideas. For more information go to www.stke.org

To sign up today, visit promo.aaas.org/stkeas

Sitewide access is available for institutions.
To find out more e-mail stkelicense@aaas.org

Science stke AAAS

GE Healthcare

illustra™

Get attached to illustra for faster nucleic acid sample prep.

New illustra™ nucleic acid sample prep kits from GE Healthcare give you optimal yield and purity. What's more, they do this in as little as half the time it takes the best competing products. Whether you're purifying nucleic acids in plasmid, blood, tissue, cells or bacteria, you'll find that superior results and outstanding reproducibility come easily with illustra mini and midi kits.

With more than 20 years' experience in nucleic acid research, we're bringing science to life and helping transform healthcare. We call it Life Science Re-imagined.

www.gelifesciences.com/illustra

Speed is crucial to the sundew plant's success.
It reacts rapidly, bending its tentacles to bind its prey.
Some species can do this in just tenths of a second.

imagination at work

GE05-07. First printed 05/2007.

Volume 317, Issue 5840

COVER

In superb fairy-wrens (*Malurus cyaneus*), helper males can assist females by providing extra food to their chicks. When this is the case, females lay smaller eggs that give rise to lighter chicks. Females benefit from increased survival. See page 941.

Photo: BIOS Ruoso Cyril/Peter Arnold Inc.

DEPARTMENTS

EDITORIAL

NEWS OF THE WEEK

NEWS FOCUS

888

LETTERS

BOOKS *ET AL.*

900

POLICY FORUM

PERSPECTIVES

CONTENTS continued >>

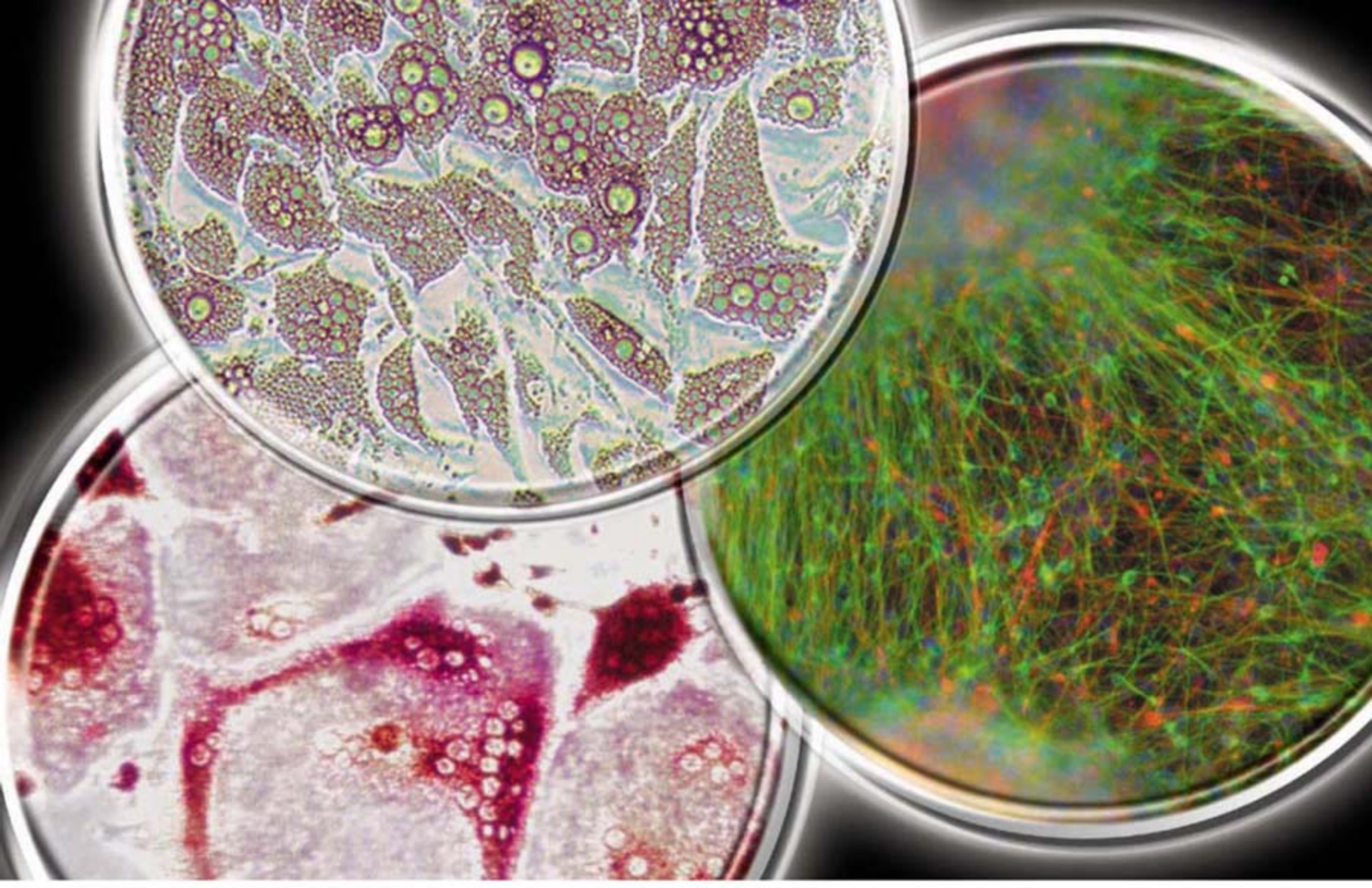

Poietics® Human Stem Cells & Media

In Vivo Relevance. *In Vitro* Results.

As the leader in primary cell culture, Lonza offers a variety of primary stem cells, including:

Human Stem Cells

- New! Poietics® Adipose-Derived Stem Cells purely characterized with relevant stromal and stem markers, and a media kit for growth and expansion
- Multipotent Mesenchymal Stem Cells isolated from bone marrow, and media kits for growth and differentiation of several lineages

Human Bone, Adipose, and Neural Progenitor Cells and Media Kits

- Cryopreserved osteoclast precursors, preadipocytes, and neural progenitors with media kits for growth and differentiation

Human Hematopoietic Progenitor Cells

- Variety of hematopoietic progenitors including CD34+, CD133+, and mononuclear cells isolated from peripheral blood, bone marrow, and umbilical cord blood

Visit our website at www.lonzabioscience.com/poietics to receive a FREE Lonza Cell Mug.

Lonza Walkersville, Inc., 8830 Biggs Ford Road, Walkersville, MD 21793

www.lonza.com

Lonza

Science

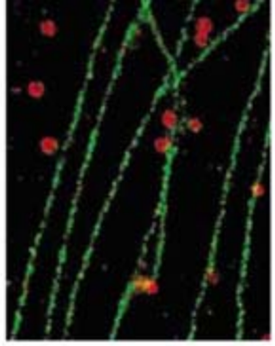

SCIENCE EXPRESS

www.sciencexpress.org

EVOLUTION

Crystal Structure of an Ancient Protein: Evolution by Conformational Epistasis

E. A. Ortlund, J. T. Bridgham, M. R. Redinbo, J. W. Thornton

The structure of a 450-million-year-old corticoid receptor, resurrected computationally and biochemically, suggests how modern hormone receptors evolved.

>> News story p. 884

10.1126/science.1142819

DEVELOPMENTAL BIOLOGY

Synchrony Dynamics During Initiation, Failure, and Rescue of the Segmentation Clock

I. H. Riedel-Kruse, C. Müller, A. C. Oates

A model of the segmentation clock, coupled genetic oscillators that sequentially generate the body segments of animals, successfully predicts the results of system perturbations.

10.1126/science.1142538

CELL BIOLOGY

Multicolor Super-Resolution Imaging with Photo-Switchable Fluorescent Probes

W. M. Bates, B. Huang, G. T. Dempsey, X. Zhuang

A super-resolution imaging method that uses a family of multicolor fluorescent probes yields images of fixed cells with a spatial resolution of 20 to 30 nanometers.

10.1126/science.1146598

PHYSICS

Signatures of Electron Fractionalization in Ultraquantum Bismuth

K. Behnia, L. Balicas, Y. Kopelevich

At very high magnetic fields, charge transport in bismuth crystals behaves like a quantum fluid, an effect previously seen only in two-dimensional materials.

10.1126/science.1146509

REVIEW

BREVIA

RESEARCH ARTICLE

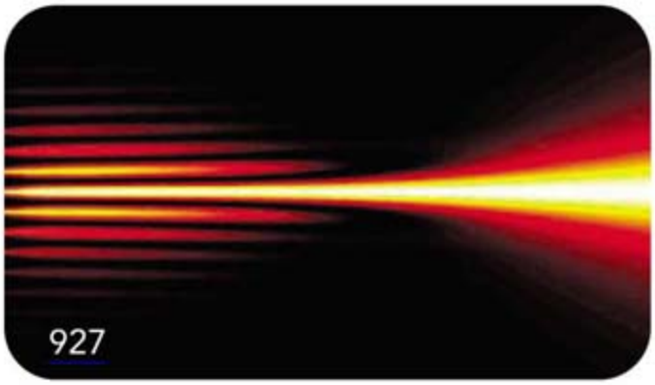

927

REPORTS

CONTENTS continued >>

Only Kentucky matches federal SBIR-STTR Phase 1 + Phase 2 awards

Kentucky will match both Phase 1 and Phase 2 federal SBIR and STTR awards to our high-tech small businesses – no other state has a program designed to do just that.

If you are looking for a place to locate or start a high-tech company, Kentucky's SBIR-STTR Matching Funds program is just one of many reasons to give our state a look.

We are now accepting applications from companies in Kentucky (or willing to relocate to Kentucky) for state funds to match federal Small Business Innovation Research (SBIR) and Small Business Technology Transfer Research (STTR) grants. Phase 1 awards are matched up to $100,000 and Phase 2 awards up to $500,000 per year for two years.

Kentucky offers a wide range of support for high-tech small businesses, including grants, tax incentives, and other forms of early-stage funding. Our statewide network of Innovation and Commercialization Centers can offer business management and entrepreneurial training, while helping find financing.

The Cabinet for Economic Development can make growing a business in Kentucky fast and easy. Our low cost of living, low-stress commutes, and high quality of life amid unrivaled natural beauty are why Kentucky communities are rated among the best places to start a business and raise a family.

For more information about our SBIR-STTR Matching Funds and other business support programs, visit www.ThinkKentucky.com/dci/sbir2.

Kentucky
UNBRIDLED SPIRIT

Cabinet for Economic Development

For more information about the SBIR-STTR program in Kentucky, call 1-800-626-2930 or visit www.ThinkKentucky.com/dci/sbir2.

REPORTS *CONTINUED...*

904 & 916

SPECIAL FEATURE

Careers in Translational Research

www.sciencecareers.org

AAAS

ADVANCING SCIENCE, SERVING SOCIETY

SCIENCE (ISSN 0036-8075) is published weekly on Friday, except the last week in December, by the American Association for the Advancement of Science, 1200 New York Avenue, NW, Washington, DC 20005. Periodicals Mail postage (publication No. 484460) paid at Washington, DC, and additional mailing offices. Domestic individual membership and subscription (51 issues): $142 ($74 allocated to subscription). Domestic institutional subscription (51 issues): $710; Foreign postage extra: Mexico, Caribbean (surface mail) $55; other countries (air assist delivery) $85. First class, airmail, student, and emeritus rates on request. Canadian rates with GST available upon request, GST #1254 88122. Publications Mail Agreement Number 1069624. **Printed in the U.S.A.**

Change of address: Allow 4 weeks, giving old and new addresses and 8-digit account number. **Postmaster:** Send change of address to AAAS, P.O. Box 96178, Washington, DC 20090–6178. **Single-copy sales:** $10.00 current issue, $15.00 back issue prepaid includes surface postage; bulk rates on request. *Science* is indexed in the *Reader's Guide to Periodical Literature* and in several specialized indexes.

CONTENTS continued >>

What makes a first-class news story?

Constance Holden
2004 National Mental Health Association: Media Award

Richard Kerr
2006 Geological Society of America: Public Service Award

Colin Norman
News Editor, *Science* magazine

Jennifer Couzin
Articles selected for inclusion in The Best American Science Writing 2007 and 2005

2003 Evert Clark/Seth Payne Award for Young Science Journalists

A first-class editorial team. Award-winning journalists write for *Science*—with 12 top awards in the last four years. That's why we have the most compelling stories, and the biggest readership of any general scientific publication. To see the complete list of awards go to:
sciencemag.org/newsawards

Science
AAAS

Paper power.

SCIENCENOW

www.sciencenow.org DAILY NEWS COVERAGE

New Battery Resembles Paper
Thin, flexible material could usher in new generation of power sources.

The Tail Is Mightier Than the Fang
Squirrels heat tail to scare off rattlesnakes.

The 1% Solution
Gene-regulating regions separate humans from chimps.

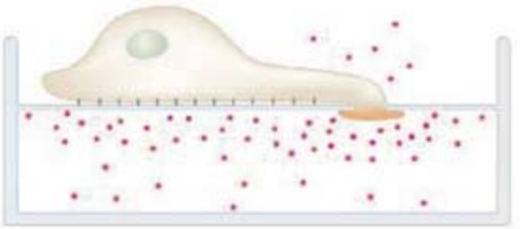

Extending a pseudopodium.

SCIENCE'S STKE

www.stke.org SIGNAL TRANSDUCTION KNOWLEDGE ENVIRONMENT

EDITORIAL GUIDE: Focus Issue—Cells on the Move
J. F. Foley and N. R. Gough
New research challenges some established models for multiple aspects of directed cell movement.

PERSPECTIVE: Signals on the Move—Chemokine Receptors and Organogenesis in Zebrafish
J. R. Perlin and W. S. Talbot
A single signal elicits distinct responses in different populations of cells in the zebrafish lateral line primordium.

REVIEW: Filopodia—The Fingers That Do the Walking
S. L. Gupton and F. B. Gertler
New and old players are involved in the formation of filopodia.

PROTOCOL: Methods for Pseudopodia Purification and Proteomic Analysis
Y. Wang et al.
Cells cultured on microporous filters allow the analysis of cellular extensions separately from the bulk of the cell body.

A new kind of researcher.

SCIENCECAREERS

www.sciencecareers.org CAREER RESOURCES FOR SCIENTISTS

>> Careers in Translational Research feature p. 966

GLOBAL: Special Feature—Translational Research Careers
K. Travis
Translational research is pushing a fundamental change in the way science operates, while giving rise to a new type of researcher: the translational scientist.

US: From the Archives—M.D.-Ph.D. Careers, Feature Index
J. Austin
M.D.-Ph.D. researchers are an important part of the translational-research workforce.

SCIENCEPODCAST

Listen to the 17 August *Science* Podcast to hear about ocean circulation changes in the North Atlantic, the latest on the ivory-billed woodpecker, helper effects in cooperatively breeding birds, and more.
www.sciencemag.org/about/podcast.dtl

CREDIT: (SCIENCE CAREERS) JOHANNA BLESS

Separate individual or institutional subscriptions to these products may be required for full-text access.

EDITED BY STELLA HURTLEY AND PHIL SZUROMI

Overturning Assumptions >>

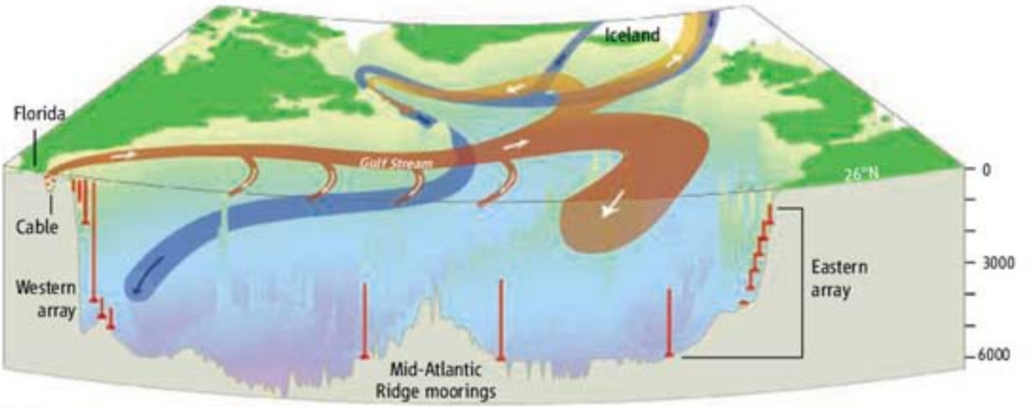

In the north Atlantic, warm surface waters flow northward and eastward from the Florida Strait, and the northward flows return as southward-flowing deep water. This meridional overturning circulation (MOC) transports huge quantities of heat from low to high northern latitudes. Global climate models have suggested that the flux of water transported might be decreased by global warming, which could have an important effect on climate, particularly that of Europe. However, there has not been a sufficiently long or detailed observational record to evaluate whether significant weakening has occurred (see the Perspective by **Church**). **Cunningham *et al.*** (p. 935) and **Kanzow *et al.*** (p. 938) now provide annual records of the strength of the MOC using an array of moored instruments deployed across the Atlantic basin at a latitude of 26.5°N. The strength of the MOC varied by more than a factor of 8 during a 1-year period from a low of 4.0 sverdrups (1 Sv equals 1 million cubic meters per second) to a high of 34.9 Sv, with an average flow of 18.7 ± 5.6 Sv. Fluctuations of the different transport components of the MOC largely compensate each other, which means that robust estimates of the flow can be made over intra-annual periods. Thus, an earlier claim that the MOC has decreased by 8 Sv during the past decade, made on the basis of only a few instantaneous measurements during that period, was premature and reflected short-term natural variability.

Giant Smoking Gun

Type 1a supernovae are valuable as cosmological distance probes because their intrinsic brightness can be inferred. However, we know little about how they occur or the nature of their progenitor star systems. It is widely thought that type 1a supernovae mark the catastrophic death of a white dwarf after it has cannibalized a companion star within a binary star system. By detecting a whiff of gas blown off during a type 1a supernova outburst, **Patat *et al.*** (p. 924, published online 12 July) determined the stellar type of its companion from its absorption line characteristics. The expansion velocities of the gas appear to favor a red-giant companion at the time of the explosion.

Bright Boron Nitride Crystals

The hexagonal form of boron nitride (hBN) resembles graphite in that it is used as a lubricant and has good thermal conductivity, but unlike graphite, it is an electrical insulator. The large direct band gap of hBN makes it a possible candidate for emission of deep ultraviolet light, which may be of use in the electronics industry or for medical treatments. **Kubota *et al.*** (p. 932) have developed a method to synthesize high-purity crystals at atmospheric pressure using nickel-molybdenum as a solvent. The crystals showed intense emission at a wavelength of 215 nanometers at room temperature.

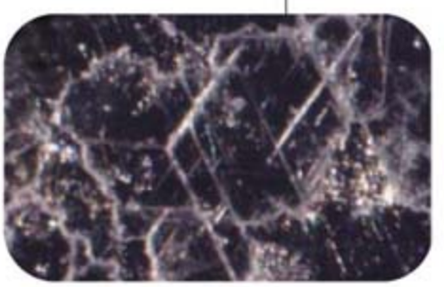

Into Sharper Focus

In high-end optical systems, zone plates cut off the out-of-phase components of light so that a sharp focus is achieved further down the optic axis. However, these patterned zone plates still create a focus that suffers from classical diffractive wavelength limitations. **Merlin** (p. 927, published online 12 July) presents theoretical work which shows that it should be possible to design planar structures that force convergence of the near-field component of the optical fields, which would provide a subwavelength focus at some point down the axis. This approach might lead to a general route for achieving subwavelength focusing and imaging that complements the negative refraction route to such superlensing effects.

Atom-Like Quantum Dots

Quantum dots are often referred to as artificial atoms because they exhibit discrete energy levels that arise through quantum-confinement effects. However, quantum dots are typically formed from hundreds if not thousands of individual atoms, so that many-body, or bulk-like, effects are also present under intense optical excitation. These effects have been used by **Xu *et al.*** (p. 929) to tune the absorption and gain of quantum dots driven by two different optical fields. They observed Autler-Townes splitting and the Mollow spectrum in the absorption spectrum of a single quantum dot, and they demonstrated gain without population inversion. These results should enable further well-controlled studies with quantum dots and open the way for applications such as quantum logic gates and optical switches.

One Too Many

Aneuploid cells, often observed in cancer, have at least one extra or missing chromosome, but little is known about the effects of aneuploidy on cell physiology. **Torres *et al.*** (p. 916; see the Perspective by **Jallepalli and Pellman**) systematically created strains of yeast that contained an extra copy of one or more yeast chromosomes and tested how this influenced cell function. Some effects, like a characteristic pattern of gene expression, seemed to result from the increase in DNA content itself, whereas others, like increased glucose uptake, depended on increased transcription or translation of the extra genes. Some properties were shared regardless

CREDITS (TOP TO BOTTOM): LOUISE BELL AND NEIL WHITE/CSIRO; KUBOTA *ET AL.*

of which chromosome was duplicated, including a surprising one—inhibition of cellular proliferation. This result calls into question whether aneuploidy might be a cause or an effect of cancer.

Plant Speciation

Much theory of speciation has focused on animal systems. Because plants are sessile organisms, they offer some advantages over animals in sampling, tracking, and measuring, as well as extended possibilities for manipulations in experimental gardens and growth chambers. **Rieseberg and Willis** (p. 910) review the mechanisms of reproductive isolation in plants and their underlying genetics, as well as focus on the role of polyploidy in speciation, which occurs much more in plants than in animals.

Mom's Anticipating Some Help

An almost universal observation in studies of cooperative vertebrates is that offspring receive more food in the presence of helpers than in their absence. Nevertheless, helper effects on offspring mass and survival have been surprisingly difficult to detect. **Russell *et al.*** (p. 941; cover) show that, in the presence of helpers, Australian female fairy-wrens lay smaller eggs, of lower nutritional content, that give rise to lighter chicks. Helper effects on chick provisioning rates are wholly obscured by this maternal reduction in egg investment, which in turn helps the mother survive into the next breeding season.

HIV-1 Goes Genome-Wide

Elucidating the genetic variability in the response of individuals to human immunodeficiency virus–1 (HIV-1) infection will play an increasing part in developing effective treatments. **Fellay *et al.*** (p. 944, published online 19 July) report a whole-genome association study of host response to HIV-1, focusing on viral load during the early stages of infection. Two immune-related polymorphisms were identified that together could account for 15% of the total variation seen in the viral load between patients.

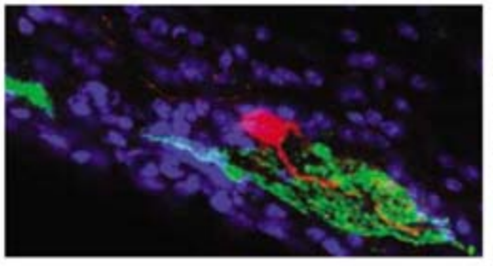

CREDIT: HU *ET AL.*

Smell the CO_2

Although invertebrates are known to sense and show behavioral responses to concentrations of CO_2 similar to those in the earth's atmosphere, it has been unclear whether the mammalian olfactory system also can sense such amounts of CO_2. **Hu *et al.*** (p. 953) describe a set of olfactory neurons that appear to allow detection of concentrations of CO_2 about 70% greater than those in air. The neurons express carbonic anhydrase II, which catabolizes CO_2, and appears to be required as part of the sensing mechanism.

Understanding Selective Synapse Elimination

Synapse elimination is a hallmark of neural circuit maturation during development. Many synapses are eliminated after an initial phase of synapse formation. However, little is known about the molecular machinery that executes synaptic elimination, nor why certain synapses are selectively eliminated while other synapses persist and grow. **Ding *et al.*** (p. 947; see the Perspective by **Miller**) examined synapse elimination in the nematode worm and found that a ubiquitin E3 ligase complex plays a key role. The activity of the ubiquitin-proteasome system was tightly regulated by a synaptic adhesion molecule, which protected certain synapses from selective elimination.

Fleeting Memories

How persistent is our memory, how is it maintained, and how can it be disrupted? It has recently been shown that PKMζ, a protein kinase C isoform, is critical for maintaining hippocampus-dependent spatial memory and long-term potentiation. Using a conditioning taste aversion paradigm, **Shema *et al.*** (p. 951; see the news story by **Miller**) found that long-term memory could be erased by infusion of a PKMζ inhibitor, ZIP, into the insular cortex. The activity of PKMζ was specifically involved in the storage of memories but not in their acquisition.

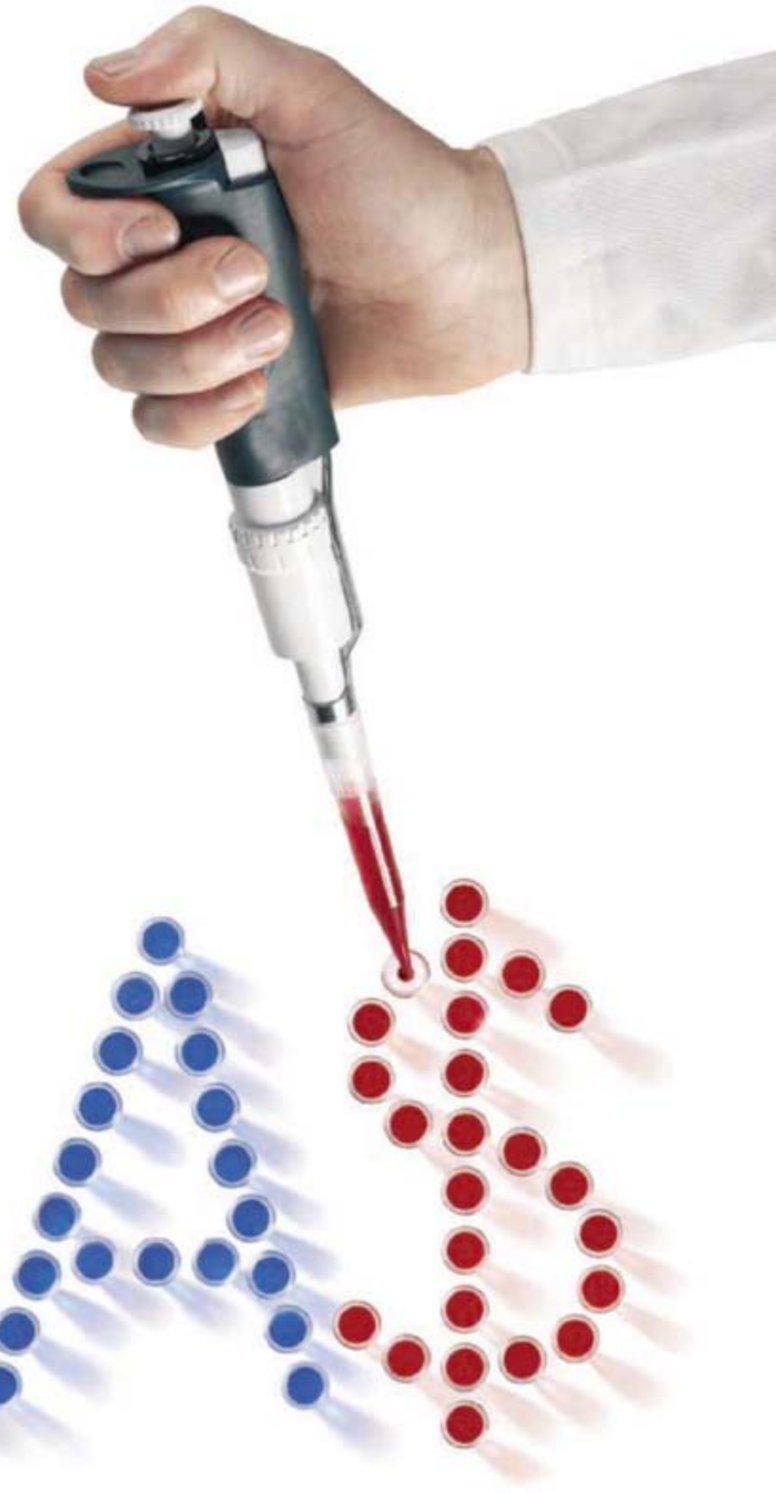

Q

Who's working to increase support for science?

Top quality research depends on comprehensive support. AAAS is present at every stage of the process – from advising on funding policy initiatives to tracking the US Federal R&D budgeting process. As the experts, we brief Congressional staffers and representatives from governments around the world. And only AAAS Funding Updates – sent out monthly – provide continual coverage of R&D appropriations. By actively working to increase support for research, AAAS advances science.

To see how, go to **www.aaas.org/support**

AAAS

ADVANCING SCIENCE, SERVING SOCIETY

Donald Kennedy is Editor-in-Chief of *Science*.

Pork and Punishment

THE CONGRESS OF THE UNITED STATES DOES SOME FUNNY THINGS WITH RESPECT TO some scientific projects. It either likes them enough to scoop them out of some priority line and give them special status, or it finds them, well, either dumb or disgusting and declines to give them money that their executive agency has asked for. In the first instance, it finds various ways of funneling federal support to them, often going outside various established procedures for competitive review. In the second case, it amends authorization or appropriation bills to require the removal of particular projects that members dislike for some reason or another.

We have long experience with both habits. The first has become so familiar that it has a pet name: pork, short for "pork-barrel funding," a term that first received public notice in the late 19th century, when individual members would compete for river and harbor projects. The process by which pork is actually distributed is "earmarking," after the practice of notching the ears of livestock to claim ownership. In the development of a research agency's budget, a member will specify a support line for a building, project, or research facility at an institution in the member's district; because the budget is limited, this means that funds will be diverted from projects that had been competitively approved.

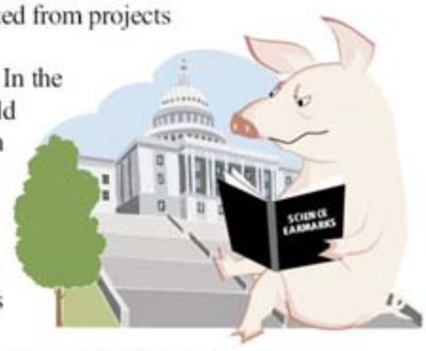

At one time this was just a cottage industry, perfected by a lone few. In the Northwest, for example, Senators Warren Magnuson and Mark Hatfield worked wonders for their medical schools. But the game changed when Gerald Cassidy and Kenneth Schlossberg put together a tiny organization that made pork-barrel strategizing a lobbyist's game. Their breakthrough was a special appropriation for Tufts University; once that happened, Columbia, Catholic University, and others found pork. The subsequent history of this malady was chronicled by Bob Kaiser in an excellent series in the *Washington Post* earlier this year.

While I was at the Association of American Universities, we made express objections to pork-barrel funding of academic science facilities and urged member presidents to resist temptation. Some did; Cornell was a heroic example. Others, alas, didn't, and the system continues to be broken. Indeed, despite recent efforts to control lobbying and other sins, set-asides are still in and growing, and bragged about by successful members.

Just as some members of Congress are working to support projects that probably wouldn't have survived the competition of peer review, their colleagues are busily trying to de-fund others that already have! This, too, is an ancient practice. One thing members don't like is studying sex; another is anything that sounds too "social-sciency." One year, a member objected strenuously to a National Science Foundation project with the word "ATM" in the title, wondering why we would spend tax money studying automated tellers; it turned out the grant was for asynchronous transfer modes used in communications technologies. Wisconsin Senator William Proxmire used to be fond of going after projects he thought silly and even created an award for proposals he found especially ridiculous called the Golden Fleece Award.

The most recent attempts attacked several projects that were identified as the National Science Foundation Authorization Act of 2007 was being considered. Representatives John Campbell (R-CA) and Scott Garrett (R-NJ) cited a total of nine grants between them for elimination, offering amendments that would have barred funding for them. What were the subjects that so troubled them? Well, one study was to analyze comparative features of menopause among six cross-cultural groups of women. A member defending the process asked Garrett how he would explain to the women in his constituency that he opposed studying menopause. His response is unrecorded, but both amendments failed and—at least for the moment—peer review and the competitive processes survived.

In both of these modes, Congress is acting to substitute its own judgments for priorities derived through competition in which expert judgments are taken into account. There is a case to be made for legislative authority to redress distributional or other issues in managing the federal science budget. But Congress should state clearly what it is doing and why, not take ad hoc bites out of a process that works fairly and well.

– Donald Kennedy

10.1126/science.1147818

EDITED BY GILBERT CHIN AND JAKE YESTON

APPLIED MATHEMATICS

Open and Shut

During photosynthesis, plants collect carbon dioxide through openings called stomata but also lose water vapor when these pores are open. Thus, the plant must continually optimize the aperture diameter, a process thought to be global (coordinated over large regions of the leaf surface). To better understand the optimization mechanism, researchers inject dye into a plant leaf and then use time-lapse videography to track fluorescence changes as the stomata open and close. However, processing the video sequence is mathematically tricky: Standard methods to identify the synchronized dynamics of fluorescing patches in two spatial dimensions and one time dimension can neglect important changes or overemphasize unimportant detail. Luttman and Bardsley have devised an algorithm based in variational calculus to extract the three-dimensional evolution of stomatal patch dynamics from experimental data. After preprocessing video of a fluorescing cocklebur leaf to remove noise and normalize changes in lighting, they identified the patches by looking for segmentations of the data that yielded the optimal division of light and dark regions. Processing of the spatial and temporal data as a whole proved essential; analyzing each frame independently resulted in meaningless segmentation. — DV

SIAM J. Sci. Comput. **29**, 1550 (2007).

Magnified stoma.

MOLECULAR BIOLOGY

Islands of Silence

In eukaryotes, DNA is packaged into chromatin, which serves as a platform for regulating access to the genome and modulating transcription, repair, and replication. Heterochromatin marks regions where, generally, genes are silenced; it is largely restricted to centromeres, the inactive X chromosome, and telomeres, and is thought to spread unless constrained by molecular barriers. Euchromatin, on the other hand, defines regions where genes are active. Yet silenced genes can be found among active genes. Do they exist as microdomains of heterochromatin, or are they some other form of repressive chromatin?

Regha *et al.* have examined the IgfR2 imprinted region on mouse chromosome 17. Here, the overlapping *Air* and *Igf2r* genes, with promoters a mere 28 kb apart, are reciprocally repressed on maternal and paternal chromosomes. Though silenced by different mechanisms—*Air* by DNA methylation and *Igf2r* via a noncoding RNA—the promoters of both genes bear highly localized marks on the histone components of their chromatin that match those found in classically defined regions of heterochromatin, specifically histone H4 trimethylated on lysine 20 (H4K20me3) and H3K9me3. Furthermore, these marks do not spread through the body of the gene. The results indicate that heterochromatin and euchromatin can be highly interspersed, even to the point where heterochromatin peaks can exist within the transcribed region of a neighboring active gene. In contrast, genes in regions that show tissue-specific repression are marked with broad swaths of H3K27me3, which delineates a second and perhaps long-term repressive chromatin state. — GR

Mol. Cell **27**, 353 (2007).

BIOMEDICINE

A Kick in the Kidneys

The unsurpassed filtration ability of the kidney is underpinned by the exquisite cellular architecture of the podocytes. These cells extend foot-like processes that abut the multilayered barrier of basement membrane and epithelial cells, on the other side of which lies the capillary lumen. The integrity of this barrier (which is permeable to water and small molecules), and in particular the mesh-like connections between the podocyte feet, are essential for preventing the escape of proteins into the urine (proteinuria). Sever *et al.* show that an intracellular GTPase, dynamin, is required for the maintenance of podocyte morphology. Dynamin contains a cleavage site for the intracellular protease cathepsin L, and in proteinuric kidney disease, cleavage leads to the rearrangement of the actin cytoskeleton in the podocytes and collapse of the feet. In a mouse model of proteinuria, introduction of a protease-resistant dynamin or a dynamin that assembled into protease-resistant higher-order structures restored podocyte function and resolved their symptoms. Dynamin has previously been implicated in endocytosis in neuronal and other cells, but a specific role in kidney anatomy was unanticipated. — SMH

J. Clin. Invest. **117**, 2095 (2007).

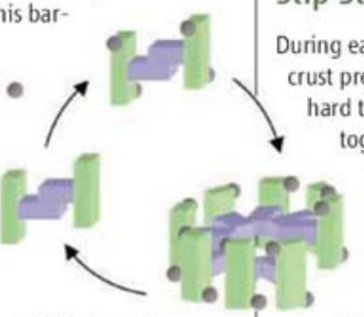

GTP (spheres) promotes higher-order assembly of dynamin (green/purple).

GEOPHYSICS

Slip Sliding Away

During earthquakes, very high stresses within the crust press the two sides of the fault together so hard that they should be effectively locked together by friction. In the laboratory, rocks are similarly difficult to rip apart. Yet in the landscape setting, faults rupture suddenly and easily. Various explanations for this conundrum have been put forward, including fault lubrication by fluids or weakening by seismic vibrations. Recent experiments suggested that the rocks themselves may become slippery during rupture if they are heated or interact with

CREDITS (TOP TO BOTTOM): BRIAN SULLIVAN/GETTY IMAGES; SEVER *ET AL.*, *J. CLIN. INVEST.* **117**, 2095 (2007)

fluids; silica gel may lubricate quartz rocks and fine powder may ease sliding in carbonate rocks. Hirose and Bystricky have found support for another hypothesis: fault weakening through dehydration of embedded phyllosilicate clays. They carried out high-velocity friction experiments on natural serpentinite (a phyllosilicate) under conditions mimicking an earthquake and measured the heat generated by friction and the resulting rock strength. An observed increase in humidity implied that water was lost from the serpentinite during sliding. Dehydration requires temperatures of about 500°C, which the authors argue might be attained where bumpy asperities rub together. — JB

Geophys. Res. Lett. **34**, L14311 (2007).

CLIMATE SCIENCE

Trop Chaud?

The summer of 2003 was the hottest on record in Europe over the past 500 years; the summer of 2006 was almost as hot, and the heat was even more widespread. Were these extremes part of a trend that can be expected to continue? Della-Marta *et al.* compiled 54 temperature records from western Europe (6 based in Scandanavia, 12 in the Iberian Peninsula, and 36 in the central region) to determine how the daily summer maximum temperatures there have changed since 1880. They found that the length of summer heat waves has doubled and that the frequency of hot days has nearly tripled over that interval. These changes are the result of a combination of a long-term trend toward higher temperatures and a significant increase in the intrinsic variability of western European daily summer maximum temperatures, particularly in the central region. — HJS

J. Geophys. Res. **112**, D15103 (2007).

IMMUNOLOGY

A Regulatory Trio

Immune responses rely on many regulatory strands that may act independently or cooperatively. Madhav *et al.* provide evidence for the intersection of three prominent regulatory mechanisms in mice that develop in response to tumors. Their study builds on the previous identification of an immune-suppressive dendritic cell (DC) subset present in lymph nodes that drain from tumors. Although the potent tryptophan-degrading enzyme indoleamine 2,3-dioxygenase (IDO) produced by these cells already has its own direct immune-suppressive credentials, it emerged that this source of IDO could rouse local regulatory T cells. These cells also possess their own direct suppressive activity, but in this case provided additional feedback on IDO-expressing DCs to induce the expression of the cell-surface protein PD-L1, which curbed the proliferation of T cells in culture. Blocking PD-L1 with antibodies or growing tumors in IDO-deficient mice interfered with the inhibitory activity exerted by regulatory T cells. This study raises the question of whether equivalent suppressive pathways induced by IDO-producing DCs and linked through the activity of regulatory T cells might also develop in response to tumors in humans. — SJS

J. Clin. Invest. **117**, 10.1172/JCI31911 (2007).

BIOCHEMISTRY

Studying Ions in Depth

Detailed understanding of how particular proteins function in human cells can provide the foundation for pathophysiology-based therapies, but it rarely is feasible to study these proteins directly. Instead, bacterial substitutes are usually more tractable, and the application of homology modeling and site-specific mutagenesis of mammalian proteins can yield useful insights. Forrest *et al.* offer a rigorous example of this approach, starting with a previously published structure of a bacterial amino acid transporter, LeuT, which is representative of transporters that couple the movement of small molecules, such as leucine and serotonin, to the transmembrane Na^+ gradient. From an analysis of a structure-based sequence alignment of LeuT with the serotonin transporter (SERT), they find that the carboxylate of a buried glutamate in LeuT, in which leucine transport is Cl-independent, occupies the same location as a chloride ion (coordinated by a serine) in SERT, which exhibits Cl-stimulated serotonin transport. Changing the serine to a glutamate or aspartate had no effect on the basal transport activity of SERT but fully abrogated the stimulation by Cl^-, and further mutagenesis of other Cl-coordinating residues in other amino acid transporters confirmed the predicted effects on activity. Other modulators of leucine transport by LeuT include the tricyclic antidepressants, as shown by Singh *et al.* (see also Zhou *et al.*, *Science* Express, 9 August 2007) — GJC

Proc. Natl. Acad. Sci. U.S.A. **104**, 12761 (2007); *Nature* **448**, 10.1038/nature06038 (2007).

CREDIT: PHILIPPE WOJAZER/REUTERS

www.sciencemag.org

Science

1200 New York Avenue, NW
Washington, DC 20005
Editorial: 202-326-6550, FAX 202-289-7562
News: 202-326-6581, FAX 202-371-9227

Bateman House, 82-88 Hills Road
Cambridge, UK CB2 1LQ
+44 (0) 1223 326500, FAX +44 (0) 1223 326501

SUBSCRIPTION SERVICES For change of address, missing issues, new orders and renewals, and payment questions: 866-434-AAAS (2227) or 202-326-6417, FAX 202-842-1065. Mailing addresses: AAAS, P.O. Box 96178, Washington, DC 20090-6178 or AAAS Member Services, 1200 New York Avenue, NW, Washington, DC 20005

INSTITUTIONAL SITE LICENSES please call 202-326-6755 for any questions or information

REPRINTS: Author Inquiries 800-635-7181
Commercial Inquiries 803-359-4578

PERMISSIONS 202-326-7074, FAX 202-682-0816

MEMBER BENEFITS Bookstore: AAAS/BarnesandNoble.com bookstore www.aaas.org/bn; Car purchase discount: Subaru VIP Program 202-326-6417; Credit Card: MBNA 800-847-7378; Car Rentals: Hertz 800-654-2200 CDP#343457, Dollar 800-800-4000 #AA1115; AAAS Travels: Betchart Expeditions 800-252-4910; Life Insurance: Seabury & Smith 800-424-9883; Other Benefits: AAAS Member Services 202-326-6417 or www.aaasmember.org.

science_editors@aaas.org	(for general editorial queries)
science_letters@aaas.org	(for queries about letters)
science_reviews@aaas.org	(for returning manuscript reviews)
science_bookrevs@aaas.org	(for book review queries)

Published by the American Association for the Advancement of Science (AAAS), *Science* serves its readers as a forum for the presentation and discussion of important issues related to the advancement of science, including the presentation of minority or conflicting points of view, rather than by publishing only material on which a consensus has been reached. Accordingly, all articles published in *Science*—including editorials, news and comment, and book reviews—are signed and reflect the individual views of the authors and not official points of view adopted by the AAAS or the institutions with which the authors are affiliated.

AAAS was founded in 1848 and incorporated in 1874. Its mission is to advance science and innovation throughout the world for the benefit of all people. The goals of the association are to: foster communication among scientists, engineers and the public; enhance international cooperation in science and its applications; promote the responsible conduct and use of science and technology; foster education in science and technology for everyone; enhance the science and technology workforce and infrastructure; increase public understanding and appreciation of science and technology; and strengthen support for the science and technology enterprise.

INFORMATION FOR AUTHORS

See pages 120 and 121 of the 5 January 2007 issue or access www.sciencemag.org/feature/contribinfo/home.shtml

EDITOR-IN-CHIEF **Donald Kennedy**
EXECUTIVE EDITOR **Monica M. Bradford**
DEPUTY EDITORS **R. Brooks Hanson, Barbara R. Jasny, Katrina L. Kelner**
NEWS EDITOR **Colin Norman**

EDITORIAL SUPERVISORY SENIOR EDITOR Phillip D. Szuromi; **SENIOR EDITOR/PERSPECTIVES** Lisa D. Chong; **SENIOR EDITORS** Gilbert J. Chin, Pamela J. Hines, Paula A. Kiberstis (Boston), Marc S. Lavine (Toronto), Beverly A. Purnell, L. Bryan Ray, Guy Riddihough, H. Jesse Smith, Valda Vinson, David Voss; **ASSOCIATE EDITORS** Jake S. Yeston, Laura M. Zahn; **ONLINE EDITOR** Stewart Wills; **ASSOCIATE ONLINE EDITOR** Tara S. Marathe; **BOOK REVIEW EDITOR** Sherman J. Suter; **ASSOCIATE LETTERS EDITOR** Etta Kavanagh; **EDITORIAL MANAGER** Cara Tate; **SENIOR COPY EDITORS** Jeffrey E. Cook, Cynthia Howe, Harry Jach, Barbara P. Ordway, Jennifer Sills, Trista Wagoner; **COPY EDITORS** Lauren Kmec, Peter Mooreside; **EDITORIAL COORDINATORS** Carolyn Kyle, Beverly Shields; **PUBLICATIONS ASSISTANTS** Ramatoulaye Diop, Chris Filiatreau, Joi S. Granger, Jeffrey Hearn, Lisa Johnson, Scott Miller, Jerry Richardson, Brian White, Anita Wynn; **EDITORIAL ASSISTANTS** Maris M. Bish, Emily Guise, Patricia M. Moore, Jennifer A. Seibert; **EXECUTIVE ASSISTANT** Sylvia S. Kihara; **ADMINISTRATIVE SUPPORT** Maryrose Madrid

NEWS SENIOR CORRESPONDENT Jean Marx; **DEPUTY NEWS EDITORS** Robert Coontz, Eliot Marshall, Jeffrey Mervis, Leslie Roberts; **CONTRIBUTING EDITORS** Elizabeth Culotta, Polly Shulman; **NEWS WRITERS** Yudhijit Bhattacharjee, Adrian Cho, Jennifer Couzin, David Grimm, Constance Holden, Jocelyn Kaiser, Richard A. Kerr, Eli Kintisch, Andrew Lawler (New England), Greg Miller, Elizabeth Pennisi, Robert F. Service (Pacific NW), Erik Stokstad; **INTERNS** Benjamin Lester, Marissa Cevallos, Veronica Raymond; **CONTRIBUTING CORRESPONDENTS** Barry A. Cipra, Jon Cohen (San Diego, CA), Daniel Ferber, Ann Gibbons, Robert Irion, Mitch Leslie, Charles C. Mann, Evelyn Strauss, Gary Taubes; **COPY EDITORS** Rachel Curran, Linda B. Felaco, Melvin Gatling; **ADMINISTRATIVE SUPPORT** Scherraine Mack, Fannie Groom; **BUREAUS** New England: 207-549-7755, San Diego, CA: 760-942-3252, FAX 760-942-4979, Pacific Northwest: 503-963-1940

PRODUCTION DIRECTOR James Landry; **SENIOR MANAGER** Wendy K. Shank; **ASSISTANT MANAGER** Rebecca Doshi; **SENIOR SPECIALISTS** Jay Covert, Chris Redwood; **SPECIALIST** Steve Forrester; **PREFLIGHT DIRECTOR** David M. Tompkins; **MANAGER** Marcus Spiegler; **SPECIALIST** Jessie Mudjitaba

ART DIRECTOR Kelly Buckheit Krause; **ASSOCIATE ART DIRECTOR** Aaron Morales; **ILLUSTRATORS** Chris Bickel, Katharine Sutliff; **SENIOR ART ASSOCIATES** Holly Bishop, Laura Creveling, Preston Huey, Nayomi Kevitiyagala; **ASSOCIATE** Jessica Newfield; **PHOTO EDITOR** Leslie Blizard

***SCIENCE* INTERNATIONAL**

EUROPE (science@science-int.co.uk) **EDITORIAL: INTERNATIONAL MANAGING EDITOR** Andrew M. Sugden; **SENIOR EDITOR/PERSPECTIVES** Julia Fahrenkamp-Uppenbrink; **SENIOR EDITORS** Caroline Ash (Geneva: +41 (0) 222 346 3106), Stella M. Hurtley, Ian S. Osborne, Stephen J. Simpson, Peter Stern; **ASSOCIATE EDITOR** Joanne Baker; **EDITORIAL SUPPORT** Deborah Dennison, Rachel Roberts, Alice Whaley; **ADMINISTRATIVE SUPPORT** Janet Clements, Jill White; **NEWS: EUROPE NEWS EDITOR** John Travis; **DEPUTY NEWS EDITOR** Daniel Clery; **CONTRIBUTING CORRESPONDENTS** Michael Balter (Paris), John Bohannon (Vienna), Martin Enserink (Amsterdam and Paris), Gretchen Vogel (Berlin); **INTERN** Krista Zala

ASIA Japan Office: Asca Corporation, Eiko Ishioka, Fusako Tamura, 1-8-13, Hirano-cho, Chuo-ku, Osaka-shi, Osaka, 541-0046 Japan; +81 (0) 6 6202 6272, FAX +81 (0) 6 6202 6271; asca@os.gulf.or.jp; **ASIA NEWS EDITOR** Richard Stone +66 2 662 5818 (rstone@aaas.org); **CONTRIBUTING CORRESPONDENTS** Dennis Normile (Japan: +81 (0) 3 3391 0630, FAX 81 (0) 3 5936 3531; dnormile@gol.com); Hao Xin (China: + 86 (0) 10 6307 4439 or 6307 3676, FAX +86 (0) 10 6307 4358; cindyhao@gmail.com); Pallava Bagla (South Asia: +91 (0) 11 2271 2896; pbagla@vsnl.com)

AFRICA Robert Koenig (contributing correspondent, rob.koenig@gmail.com)

EXECUTIVE PUBLISHER **Alan I. Leshner**
PUBLISHER **Beth Rosner**

FULFILLMENT & MEMBERSHIP SERVICES (membership@aaas.org) **MANAGER** Waylon Butler; **CUSTOMER SERVICE SUPERVISOR** Pat Butler; **SPECIALISTS** Tamara Alfson, Laurie Baker, Latoya Casteel, Lavanda Crawford, Vicki Linton; **DATA ENTRY SUPERVISOR** Cynthia Johnson; **SPECIALISTS** Tomeka Diggs, Tarrika Hill, Erin Layne, Sheila Thomas

BUSINESS OPERATIONS AND ADMINISTRATION DIRECTOR Deborah Rivera-Wienhold; **BUSINESS MANAGER** Randy Yi; **SENIOR FINANCIAL ANALYSTS** Michael LoBue, Jessica Tierney; **FINANCIAL ANALYSTS** Nicole Nicholson, Farida Yeasmin; **RIGHTS AND PERMISSIONS: ADMINISTRATOR** Emilie David; **ASSOCIATE** Elizabeth Sandler; **MARKETING DIRECTOR** John Meyers; **MARKETING MANAGERS** Darryl Walter, Allison Pritchard; **MARKETING ASSOCIATES** Julianne Wielga, Mary Ellen Crowley, Alison Chandler, Marcia Leach, Wendy Wise; **INTERNATIONAL MARKETING MANAGER** Wendy Sturley; **MARKETING EXECUTIVE** Jennifer Reeves; **MARKETING/MEMBER SERVICES EXECUTIVE** Linda Rusk; **JAPAN SALES** Jason Hannaford; **SITE LICENSE SALES DIRECTOR** Tom Ryan; **SALES MANAGER** Russ Edra; **SALES AND CUSTOMER SERVICE** Mehan Dossani, Iquo Edim, Kiki Forsythe, Catherine Holland; **ELECTRONIC MEDIA: MANAGER** Lizabeth Harman; **PROJECT MANAGER** Trista Snyder; **ASSISTANT MANAGER** Lisa Stanford; **SENIOR PRODUCTION SPECIALIST** Walter Jones; **PRODUCTION SPECIALISTS** Nichele Johnston, Kimberly Oster

ADVERTISING DIRECTOR WORLDWIDE AD SALES Bill Moran

PRODUCT (science_advertising@aaas.org); **CONSUMER & SPONSORSHIP SALES MANAGER** Tina Morra: 202-326-6542 **MIDWEST** Rick Bongiovanni: 330-405-7080, FAX 330-405-7081 • **WEST COAST/W. CANADA** Teola Young: 650-964-2266 **EAST COAST/E. CANADA** Christopher Breslin: 443-512-0330, FAX 443-512-0331 • **UK/EUROPE/ASIA** Michelle Field: +44 (0) 1223-326-524, FAX +44 (0) 1223-325-532 **JAPAN** Mashy Yoshikawa: +81 (0) 33235 5961, FAX +81 (0) 33235 5852; **SENIOR TRAFFIC ASSOCIATE** Deiandra Simms

COMMERCIAL EDITOR Sean Sanders: 202-326-6430

CLASSIFIED (advertise@sciencecareers.org); **U.S.: RECRUITMENT SALES MANAGER** Ian King: 202-326-6528, FAX 202-289-6742; **INSIDE SALES MANAGER: MIDWEST/CANADA** Daryl Anderson: 202-326-6543; **NORTHEAST:** Allison Millar: 202-326-6572; **SOUTHEAST:** Tina Burks: 202-326-6577; **WEST:** Nicholas Hintibidze: 202-326-6533; **SALES COORDINATORS** Erika Foard, Rohan Edmonson, Leonard Marshall, Shirley Young; **INTERNATIONAL: SALES MANAGER** Tracy Holmes: +44 (0) 1223 326525, FAX +44 (0) 1223 326532; **SALES** Marium Hudda, Alex Palmer; **SALES ASSISTANT** Louise Moore; **JAPAN:** Jason Hannaford: +81 (0) 52 757 5360, FAX +81 (0) 52 757 5361; **ADVERTISING PRODUCTION OPERATIONS MANAGER** Deborah Tompkins; **SENIOR PRODUCTION SPECIALISTS** Robert Buck, Amy Hardcastle; **SENIOR TRAFFIC ASSOCIATE** Christine Hall; **PUBLICATIONS ASSISTANT** Mary Lagnaoui

AAAS BOARD OF DIRECTORS RETIRING PRESIDENT, CHAIR John P. Holdren; **PRESIDENT** David Baltimore; **PRESIDENT-ELECT** James J. McCarthy; **TREASURER** David E. Shaw; **CHIEF EXECUTIVE OFFICER** Alan I. Leshner; **BOARD** John E. Dowling, Lynn W. Enquist, Susan M. Fitzpatrick, Alice Gast, Linda P. B. Katehi, Cherry A. Murray, Thomas D. Pollard, Kathryn D. Sullivan

AAAS
ADVANCING SCIENCE, SERVING SOCIETY

If you're looking for gene expression assays...we've got you covered.

The Most Comprehensive Gene Expression Assay Selection in the Industry.

Incredible selection and extraordinary quality. That's the definition of our TaqMan® Gene Expression Assays family of products. With over 700,000 pre-designed real-time PCR assays for 8 species and a variety of custom options, Applied Biosystems produces a TaqMan® Assay to enable virtually any experiment. A range of pre-designed assays for individual genes or multiplexed TaqMan® Array Gene Signature Panels simplify experimental design. Our TaqMan Assay family delivers the quality and breadth you've come to expect from Applied Biosystems. Get it all, get it right, and get it now with TaqMan Gene Expression Assays.

Get a free t-shirt! Visit www.allgenes.com, register for a free t-shirt*, and find a TaqMan Gene Expression Assay for any application, including:

- Microarray validation
- Biomarker discovery
- MicroRNA quantitation
- RNAi validation
- Custom assays for other applications

Applied Biosystems

*Limited to one (1) t-shirt per individual. Void where prohibited. Offer limited to persons directly involved in Life Sciences research, as determined at the sole discretion of Applied Biosystems.

From physics to nutrition

For careers in science, turn to *Science*

If you want your career to bear fruit, don't leave it to chance. At *Science* Careers we know science. We are committed to helping you find the right job, and to delivering the useful advice you need. Our knowledge is firmly founded on the expertise of *Science*, the premier scientific journal, and the long experience of AAAS in advancing science around the world. *Science* Careers is the natural selection.

www.ScienceCareers.org

Features include:

- Thousands of job postings
- Career advice
- Grant information
- Resume/CV Database
- Career Forum

Science Careers

From the journal *Science* AAAS

Opening NASA's Vault

The moon shots that researchers and the public have gazed at over the years are mainly copies—or copies of copies—that don't match the originals in clarity, color, or contrast.

But at last, we all will get to see the originals. Arizona State University (ASU) in Tempe, the Lunar and Planetary Institute, and NASA are posting high-resolution scans of the 35,000 photos from the Apollo missions—from film that has been chilling out in a freezer in Houston, Texas, for more than 30 years.

NET WATCH

The digitized images will enable researchers to draft more precise topographic maps of the lunar surface, for example, and to evaluate possible landing sites for future moon missions, says geologist Mark Robinson of ASU. The archive is just gearing up but will have several hundred images by next month. >> apollo.sese.asu.edu

What's My Bite

Using finite-element analysis, a computer-simulation technique employed in engineering, Australian scientists have put together a super-refined virtual skull that reflects the properties of different types of bone in measuring stresses. Paleontologist Stephen Wroe of the University of New South Wales in Sydney says models such as this chimp skull, based on hundreds of computed tomography scans, can be used for testing applications such as surgical procedures, crash helmets, and dental prosthetics.

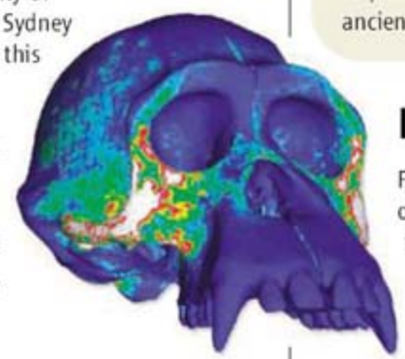

Chimp skull showing the distribution of stress during a bite at the second molar.

His team also hopes to model skulls of ancient human ancestors to see how their biomechanical features differed and illuminate their dietary leanings and limitations. It's a "novel and useful approach," says paleoanthropologist Dean Falk of Florida State University in Tallahassee. "I'd love to see what they come up with for *Paranthropus*"—a heavyset australopithecine believed to have favored plants and grubs.

FOREST PRIMEVAL

Archaeologists in Hungary announced this month that they have unearthed a 7-million-year-old forest that has resisted fossilization, the largest of its kind in the world.

Strip miners stumbled across stumps while digging for coal. Scientists from Eötvös University in Budapest have identified the remains of 16 *Taxodium* trees, similar to Florida cypress, standing as much as 6 meters tall and 3.5 meters in diameter. They were preserved in a Miocene swamp after sand engulfed them, shielding them from wind, rain, and degrading fungi, says paleontologist Miklós Kázmér.

The cellulose that makes up the cell walls of the tree has long since broken down, but the remaining lignin has kept the trees standing although very crumbly. Researchers are wrapping the stumps in plastic and submerging them in water to preserve them while they raise money for a costly several-year polymer bath.

The forest offers a rare "high-resolution photograph from the past," says Kázmér, who notes that almost all ancient nonfossilized wood so far found has been driftwood. Paleoecologist Christopher Williams of Franklin and Marshall College in Lancaster, Pennsylvania, says scientists can learn a lot from these trees, including the thickness of the canopy and how much carbon they sequestered. Kázmér adds that biologists are eager to collect DNA samples in hopes of finding ancient organisms.

Instant Milk

For visual-effects creators, rendering objects like the mist-emitting Pensieve in *Harry Potter* is no mean feat. Even creating a realistic glass of milk can take computer artists hours of tedious work. But a new image-generating technique may accurately replicate many substances given only the type and amount of their ingredients.

"If we know what it's made of, we can say what it looks like," says computer scientist Henrik Jensen of the University of California, San Diego, who outlined the technique last week at a computer-graphics conference in San Diego.

Jensen, who won a 2004 Academy Award for a novel method of rendering skin that was used to create *The Lord of the Rings*' Gollum, worked with colleagues from the Technical University of Denmark in Lyngby to broaden a 100-year-old model of optical scattering called Lorenz-Mie theory. The team extended it to include irregularly shaped particles like the constituents of milk, seawater, and other light-absorbing substances.

Glass of skim milk generated from its optical properties.

The technique can also be run in reverse to derive a substance's composition from digital photographs. Commercially, this could make it possible to spot spoiled or contaminated food. A Danish company, Danisco, is interested in using it to check the freshness of milk and ice cream.

CREDITS (TOP TO BOTTOM): REUTERS/OTTO HERMAN MUSEUM/LANDOV; COMPUTATIONAL BIOMECHANICS RESEARCH GROUP, UNIVERSITY OF NSW, AUSTRALIA; J. R. FRISVAD ET AL., ACM SIGGRAPH (2007)

Q AAAS

Who's helping bring the gift of science to everyone?

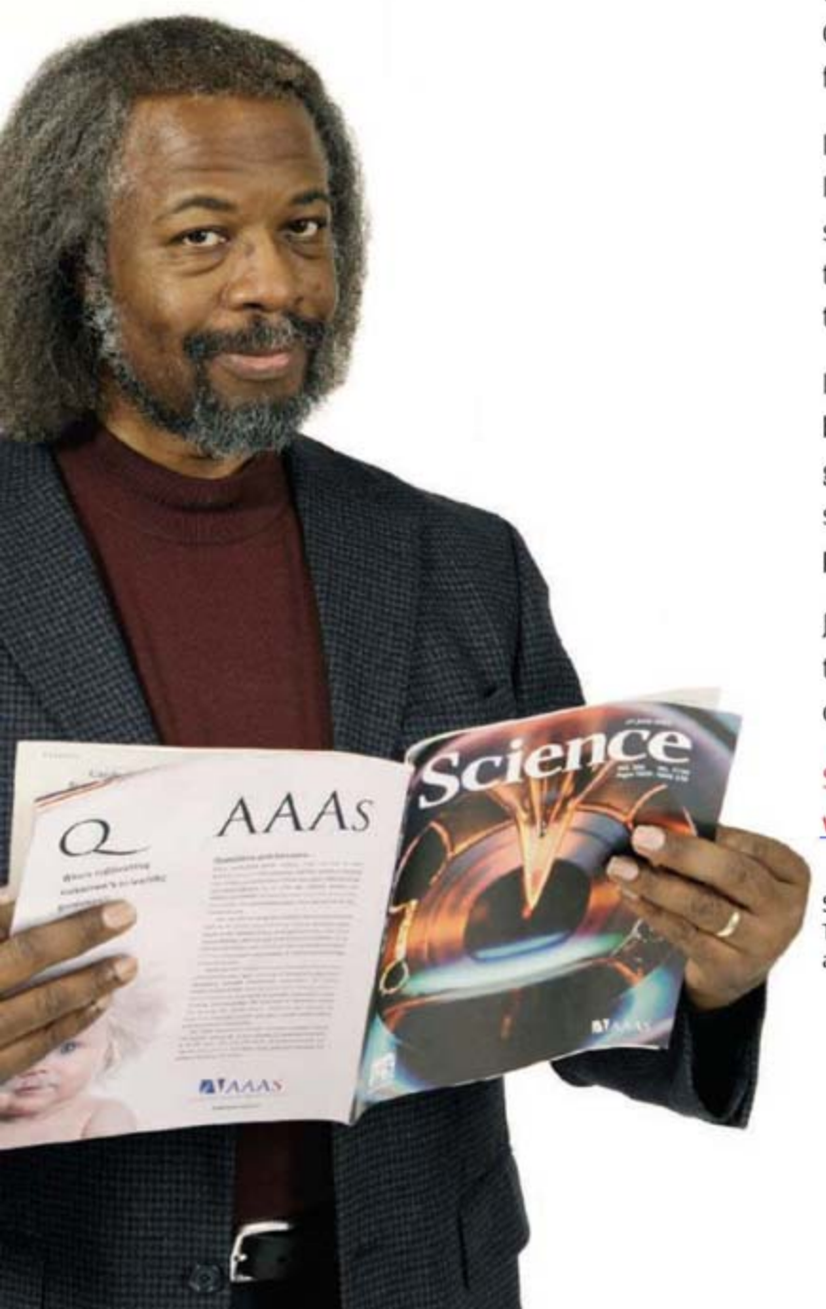

"As a child I got very interested in space travel. When I was six my father gave me some books on rockets and stars. And my universe suddenly exploded in size because I realized those lights in the sky I was looking at were actually places.

I wanted to go there. And I discovered that science and technology was a gift that made this possible. The thrill of most Christmas presents can quickly wear off. But I've found that physics is a gift that is ALWAYS exciting.

I've been a member of AAAS for a number of years. I think it's important to join because AAAS represents scientists in government, to the corporate sector, and to the public. This is very vital because so much of today's science is not widely understood.

I also appreciate getting *Science* because of the breadth of topics it covers. It gives me a great grounding for many activities in my professional life, such as advising government agencies and private corporations."

Jim Gates is a theoretical physicist and professor at the University of Maryland. He's also a member of AAAS.

See video clips of this story and others at www.aaas.org/stories

S. James Gates Jr., Ph.D.
Theoretical physicist
and AAAS member

AAAS
ADVANCING SCIENCE, SERVING SOCIETY

EDITED BY YUDHIJIT BHATTACHARJEE

TWO CULTURES

MACHINE MIND. There are no gondolas or Venetian masks in composer Julian Wagstaff's first opera, which premiered in Edinburgh, U.K., this week. Instead, *The Turing Test* tells the story of two scientists competing to create the ultimate intelligent machine.

Wagstaff was inspired to create the work after a visit to the Massachusetts Institute of Technology's museum in Cambridge, where he was impressed by an exhibit about the English mathematician Alan Turing's test for human intelligence in a computer. He hopes that the opera will convey the challenges involved in creating a computer that meets the Turing test criteria—namely, that you can't tell the computer from a human when you chat with it via a keyboard. "The biggest hurdle is designing a computer that you can imbue with culture and that can produce natural language," says Wagstaff, who has worked as a linguist and a computer programmer.

For the production, Wagstaff collaborated with computer scientists at the University of Edinburgh, where he teaches composition. "It's a highly unusual topic; I can't think of another opera featuring a singing computer," says Gordon Duckett, administrator of the university's School of Informatics, who had several discussions with Wagstaff. "Julian's raising awareness of how far computing has come and questioning what we mean by artificial intelligence."

ON CAMPUS

BIO FALLOUT. A top official at Texas A&M University (TAMU) in College Station has stepped down amid a scandal over biosafety problems that has shut down biodefense research at the school. Richard Ewing, TAMU vice president of research, resigned on 1 August following lapses that have put the school under "tremendous scrutiny," Ewing wrote in a letter to colleagues.

TAMU's problems began with its failure to tell the Centers for Disease Control and Prevention (CDC) in Atlanta, Georgia, that one worker had contracted brucellosis and three others were exposed to Q fever last year. In late June, CDC ordered the school to suspend all research on potential bioweapons pathogens, noting that a *Brucella* aerosol experiment apparently did not have CDC approval. The *Dallas Morning News* has since reported that the infected lab worker didn't have approval to work with the agent. Ewing, a tenured professor, will return to the mathematics department on 31 August.

MONEY MATTERS

CANCER FIGHTER. A billionaire cancer survivor is donating another $700 million to combat the disease.

In 1993, Jon Huntsman Sr. established the Huntsman Cancer Institute at the University of Utah in Salt Lake City with his wife, Karen. Since then, he has gifted more than $225 million to it. The new donation will help expand the institute's treatment efforts and research, which focuses on the genetic causes of cancer.

Huntsman made his fortune developing the polystyrene egg carton and the clamshell Big Mac box. Last month, his current company, the Salt Lake City, Utah–based Huntsman Corp., agreed to a $10.6 billion takeover bid by New York–based Apollo Management.

"One of two men and one of three women [in the United States] will develop cancer at some point in their lives," says Huntsman, 70, who has suffered from mouth, nose, and prostate cancer. "Every family will be affected at some point. There's a great need for money for research."

MOVERS

NOT SO FAST. Sometimes links to one's home institution can get in the way of a once-in-a-lifetime opportunity to do something bigger.

That's what happened to oceanographer Mark Abbott of Oregon State University (OSU), Corvallis, who's changed his mind about leading the geosciences directorate at the National Science Foundation after NSF's lawyers told him that his continuing ties to OSU posed an insurmountable obstacle.

Academics who come to NSF to take up such senior positions typically go on leave from their institution—Abbott is dean of the College of Oceanic and Atmospheric Sciences—and then recuse themselves from all pending decisions on grants and other matters involving their school. But that would have been impractical, says Abbott, given the breadth of NSF funding going to the college. "In the end, there would have been so many geoscience programs involved that I couldn't even be in the room" during discussions, he says. And so NSF will resume its search.

A Life in Science >>

TREASURE TROVE. If you think words like "a total waste of time … will start again" come from the margins of a struggling graduate student's diary, think again. You'll find them—and similar remarks—in the laboratory notebooks of a two-time Nobel laureate and founding father of genomics, Frederick Sanger.

Last week, the British Biochemical Society received a Wellcome Trust award to catalog and preserve the notebooks—35 in all—in which Sanger recorded his groundbreaking research from 1944 to 1981. The books, which the biologist donated to the society in 2005, describe both the first sequencing of a protein (insulin), which earned Sanger his first Nobel Prize in 1958, and the first sequencing of DNA, for which he shared the Nobel Prize with Paul Berg and Walter Gilbert in 1980.

"He was a genius at solving practical problems, finding biochemical tricks to get the answer he was looking for," says Georgina Ferry, who met Sanger while researching her biography of Max Perutz. And yet, "he is the most self-effacing person you could hope to meet." Sanger retired in 1982 and now spends his time gardening at his Cambridgeshire home.

CREDITS (TOP TO BOTTOM): COLIN HATTERSLEY; PETE RIX AND JOE SMITH; WELLCOME IMAGES

Nix on Noah?
886

One man, one Roadmap
887

GRANTS MANAGEMENT

NSF Survey of Applicants Finds a System Teetering on the Brink

A new survey by the National Science Foundation (NSF) offers an inside look into the minds of those seeking funding from the $6 billion agency. It reveals a merit-review system that's bending but not breaking under increased strain.

The survey, conducted for NSF by Booz Allen Hamilton, a consulting firm headquartered in McLean, Virginia, explores the effects of a stressful period (2000–2006) in which the agency boosted the size of grants but held the number of awards steady and had to reject an increasing number of applications. The result has been a lose-lose situation: Program managers and reviewers have had to work harder, and principal investigators have found it tougher to obtain a grant. The good news is that most of the 24,378 scientists who filled out the online survey (a 56% response rate) think the system is thorough and fair.

Sent last fall to everyone who submitted a research proposal to NSF in the past 3 years (more than half were also reviewers), the survey also paints a picture of the typical applicant. He's someone (three-fourths are men) who underestimates his chances of success but would have a go regardless of the odds. He needs the money primarily to keep his lab intact and is prepared to try and try again if his initial application is rejected. He's reviewed up to a half-dozen proposals for NSF in the past 12 months, sometimes cutting corners, and thinks that few contain potentially transformative ideas. Yet he believes his own research, if funded, stands a good chance of shattering the existing paradigm in the field.

NSF officials say the survey results and accompanying report by an internal committee (nsf0745) will help them address the growing burden on the staff and the community without compromising the merit-review process. NSF Director Arden Bement is particularly concerned about what he calls "churn": excellent proposals that keep getting revised and reviewed because funding rates are so low. "They clog up the system," he says, "and they're a burden on everyone: program officers, reviewers, and scientists, who should be doing research rather than rewriting their proposals."

But altering one part of the process has a ripple effect. Responding to complaints that grants were too small, for example, NSF has boosted the size of the average award by 34% since 2000. But those larger grants swallowed up nearly all the 44% growth in NSF's budget over the period. At the same time, the number of applications rose by 47%. With the number of awards holding steady, funding rates plummeted from 30% in 2000 to 21% last year.

That decline, in turn, caused some program managers to limit the number of applications from scientists and/or their institutions. About one-quarter of NSF's 350 funding opportunities now impose some restrictions on applicants; an infrastructure or training initiative might allow only one application per school, for example, and some program solicitations might do likewise for principal investigators. Other programs have begun to require preproposals, with only those that make the cut submitting a full proposal.

The survey found that about one-third of scientists have submitted preproposals, but that the jury is still out on whether the approach saves scientists' time, improves the quality of the final proposal, or curbs the number of applications. Bement doesn't expect the practice to spread but adds that it can be a useful tool. "I think the directorates have been judicious in selecting those limitations that are effective without restricting access," he says.

NSF officials don't know the reason for the increased demand, and the data don't support one pet theory. The budget of the National Institutes of Health (NIH) has basically been flat since a 5-year doubling ended in 2003, and there was speculation that applicants would turn to NSF for help. But that's not the case: The number of submissions to NSF's biology directorate has risen by roughly the same rate through thick and thin NIH budgets. In addition, only 11% of survey respondents said ▶

How low can it go?

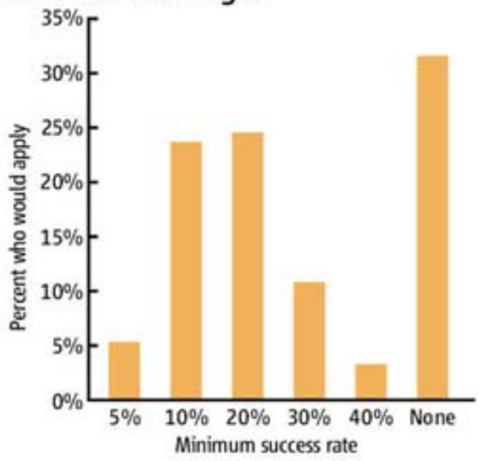

No limits. A plurality of NSF applicants would consider submitting a grant proposal regardless of the expected success rate.

Who's got the brightest ideas?

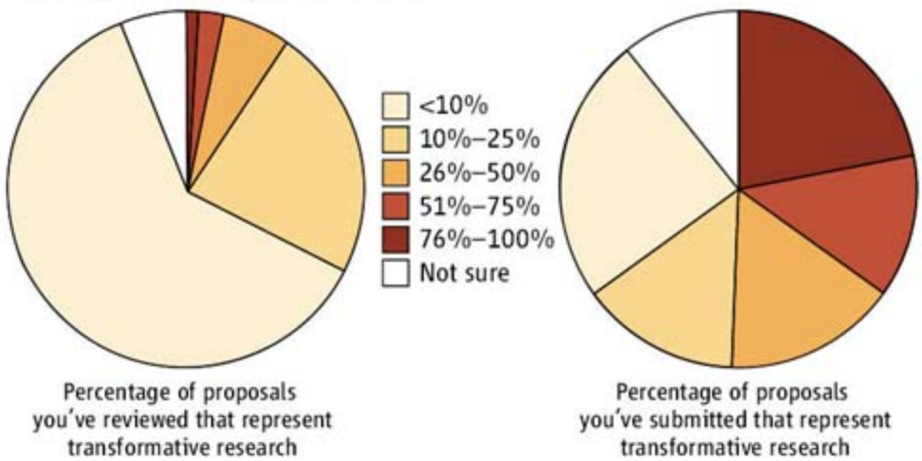

A matter of opinion. Reviewers are much more likely to consider their own proposals pathbreaking.

SOURCE: NSF

From God to ghost bird
888

Jumping junk genes
894

that their decision to seek NSF funding was greatly affected by funding cuts elsewhere.

The survey also found that one in six scientists decline an invitation to review proposals, either by mail or in person at NSF's Arlington, Virginia, headquarters. Nearly two-thirds of those who say no cite a lack of time. Some 70% who said no reported being asked to do more reviews, and 36% say they are devoting less time to each review. But 15% also cite a conflict of interest—perhaps as a potential collaborator—despite the agency's attempt to spot such conflicts ahead of time. In addition, one in six admit that the quality of their reviews has suffered as the number increases.

Bement says that bigger NSF budgets would solve many of these problems, and that he's encouraged by congressional support to date for President George W. Bush's proposal last year to double NSF's budget over 10 years. Otherwise, he says, the situation will only get worse. "My fear is getting into an irreversible downward spiral, with funding rates so low that people stop submitting and we can't find enough reviewers," he says. "Right now we're on the precipice." **–JEFFREY MERVIS**

SOUTH AFRICA

Firing of AIDS Policy Champion Seen as Setback

PRETORIA, SOUTH AFRICA—Last week's dismissal of South Africa's deputy health minister has angered HIV/AIDS treatment activists and exacerbated concerns among researchers and clinicians that the government's commitment to a new 5-year public health strategy on AIDS may be slipping.

Sudden exit. Deputy Health Minister Nozizwe Madlala-Routledge lost her job after traveling to Madrid for a meeting on HIV/AIDS vaccines.

The deputy minister, Nozizwe Madlala-Routledge, had been the most outspoken government advocate of a stronger HIV/AIDS campaign and a champion of a plan, adopted this spring, that calls for cutting in half the HIV infection rate (nearly 19% of the adult population) and quadrupling the number of infected persons receiving antiretroviral (ARV) therapy by 2011. South Africa has the world's largest number of HIV-infected persons, an estimated 5.5 million, of which about a quarter-million now receive ARV therapy. In firing her, President Thabo Mbeki claimed that Madlala-Routledge hadn't been a team player and had made an unauthorized trip.

Pediatric AIDS researcher Hoosen Coovadia of the University of KwaZulu-Natal in Durban said he was concerned about Madlala-Routledge's removal because she had "worked hard at reestablishing trust and confidence with civil society, including its much-derided scientists." AIDS researchers and the government have often been at odds over issues such as the Health Department's long-running support for nonstandard medical remedies. Coovadia and others worry that the deputy minister's departure could endanger the implementation of the HIV/AIDS plan, the result of lengthy negotiations that ended earlier this year (*Science*, 23 March, p. 1651).

Francois Venter, who heads the Southern African HIV Clinicians Society, called the firing "awful" because Madlala-Routledge had convinced activist groups of "a new era of cooperation in tackling a difficult issue." The AIDS and Rights Alliance for Southern Africa, a network of 20 AIDS and human-rights groups in southern Africa, saw the dismissal as "a political reprisal for the deputy minister's outspokenness and truthfulness."

Mbeki's office denied any change in HIV/AIDS policy and made public his dismissal letter to Madlala-Routledge, which expressed his concern about her "inability to work as part of a collective." The president cited her failure to receive prior approval to travel to Madrid in June to attend an International AIDS Vaccine Initiative (IAVI) conference. When the deputy minister learned that her request had been rejected, she flew back to South Africa without attending, explaining later that Mbeki told her that "he believed that politicians have nothing to say in a conference of technocrats and researchers." Even so, several government officials from around the world attended the session. In a statement, IAVI said planners "thought it was important to include a high-level representative of South Africa's health ministry," given the extent of the nation's HIV/AIDS epidemic.

At a fiery news conference in Cape Town last week, Madlala-Routledge expressed hope that her dismissal would not weaken the new strategy: "People are waiting to see if the spirit of unity we had achieved will remain intact. We really do need a united front." Government spokesperson Themba Maseko told *Science* that the dismissal will not impact policy, insisting that the government "reaffirms its commitment to the strategic plan and is doing everything in its power to ensure that we meet its targets."

But many activists were skeptical. Several groups have complained, for example, that after 5 years, South Africa's mother-to-child HIV prevention program has not been expanded beyond 30% coverage. The Health Department counters that it is making progress. Activist groups are planning to review their strategies. Mark Heywood, director of the AIDS Law Project in Johannesburg, says more pressure needs to be exerted "to make sure the AIDS plan is implemented fully." **–ROBERT KOENIG**

CREDIT: GIANLUIGI GUERCIA/AFP/GETTY IMAGES

two phase filter

- Maximum protection against aerosols

- Binds biomolecules

- **ep Dualfilter T.I.P.S.** available in ten sizes

NEW! ep Dualfilter T.I.P.S.®

Stop aerosols!

Unique two-phase filter protection with ep Dualfilter T.I.P.S.®

The new Eppendorf ep Dualfilter T.I.P.S., with their unique two-phase filter, provide the perfect shield against contamination.

The filter consists of two visible phases, each with a different pore size. This two-phase filter protection ensures ultimate absorption of aerosols ❶ and biomolecules ❷, outmatching all conventional filters. Rely on it.

For more information go to
www.eppendorf.com/dualfilter

Features of the ep Dualfilter T.I.P.S.
Double protection provided by the two phase filter

- Provides maximum protection for both pipette and sample
- Ultimate absorption of aerosols and biomolecules
- Free from PCR inhibitor additives
- Patent pending two phase filter technology
- Supplied sterile, Eppendorf PCR clean and pyrogen-free
- IvD conformity
- Batch-related certificates available

eppendorf

In touch with life

Your local distributor: www.eppendorf.com/worldwide · Application Support: +49 180-3 66 67 89
Eppendorf AG · Germany · +49 40 538 01-0 • Eppendorf North America, Inc. 800-645-3050

NEUROSCIENCE

Enzyme Keeps Old Memories Alive

Many substances interfere with memory, as any hung-over partygoer can attest. But although booze and drugs can disrupt the making of new memories (such as the embarrassing antics at last night's party), they leave older memories intact. Neuroscientists think this is because, after a time, memories become wired into the brain in a way that makes them harder to wipe out: Long-term memories, in the generally accepted view, are maintained by structural changes to the synaptic connections between neurons.

A study on page 951 adds to other recent evidence that may challenge, or at least complicate, this view. A team of neuroscientists reports that injecting a drug that blocks an enzyme called protein kinase Mζ (PKMζ) into the cerebral cortex of rats makes the animals forget a meal that made them sick weeks earlier. The findings suggest that the continuing activity of PKMζ is somehow necessary to maintain long-term memory, something that's not predicted by most current hypotheses on the mechanisms of memory. The work also hints at the possibility of future drugs that could tinker with memory—for therapeutic uses or for boosting brainpower.

"This is a somewhat mind-blowing conclusion," says David Glanzman, a neuroscientist at the University of California, Los Angeles. Enzymes similar to PKMζ are known to be important in early stages of memory formation, Glanzman says, but most researchers had thought that these compounds were not needed to sustain memory once synaptic changes—such as the growth of new synapses or the strengthening of existing ones—had occurred.

In the new study, Todd Sacktor of State University of New York Downstate Medical Center in Brooklyn and Reut Shema and Yadin Dudai of the Weizmann Institute of Science in Rehovot, Israel, first gave rats an unsavory meal to remember. They added a novel taste, saccharin, to the rodents' drinking water, then 40 minutes later gave a nausea-inducing injection of lithium. Rats normally avoid saccharin-laced water for weeks after such an experience. But in the days that followed, when the researchers injected the PKMζ-blocking drug, called ZIP, into the insular cortex, where taste memories are thought to reside, rats lost their aversion to saccharin within 2 hours and did not recover it in the 25-day study period. Moreover, giving the injection up to 25 days after the nauseating meal erased the aversion. Yet when given prior to saccharin exposure, ZIP had no effect on the ability to form new memories—the rats still learned to avoid the flavored water.

The findings extend a 2006 study by Sacktor and colleagues that showed that blocking PKMζ in the hippocampus of rats reverses long-term potentiation, a change in neural signaling thought to underlie learning and memory, and causes the animals to forget their fear of a place where they'd previously received a shock (*Science*, 25 August 2006, p. 1141). The new work suggests a broader role for PKMζ as a key component of different types of long-term memories stored in different parts of the brain, Sacktor says.

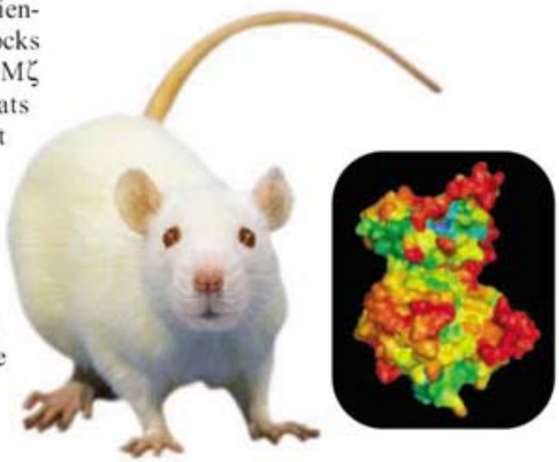

Memory molecule. PKMζ sustains long-term memory in the cerebral cortex of rats.

Going forward, it will be important to figure out how specific ZIP's memory-erasing effects are, says Lynn Nadel, a neuroscientist at the University of Arizona in Tucson. "It's possible that ZIP erases all learning, no matter how old," Nadel says. But if the drug works more selectively, it could one day have clinical applications, he says. For example, researchers and clinicians have been looking for compounds capable of eliminating the painful memories of trauma survivors (*Science*, 2 April 2004, p. 34). The flip side is cognitive enhancement, adds Richard Morris, a neuroscientist at the University of Edinburgh, U.K. "The next step might be to find out whether augmenting the action of PKMζ can help sustain memories for longer than occurs normally." **–GREG MILLER**

CREDITS (LEFT TO RIGHT): NIGEL CATTLIN/VISUALS UNLIMITED; KEVIN BOLDING/SACKTOR LABORATORY

Germany Plans New GM Rules

BERLIN—Proposed new rules governing genetically modified (GM) crops in Germany have disappointed many researchers and farmers. Germany already has one of Europe's strictest laws, and the center-right agriculture minister had raised hopes last year for a reprieve (*Science*, 1 December 2006, p. 1369).

But the new proposal, issued last week, has managed to disappoint both supporters and opponents. GM advocates complain that a new 150-meter buffer zone between GM and conventional crops (300 meters for organic crops) has no scientific basis and will make it impossible to plant GM crops in western Germany's small, patchwork fields. And as before, farmers and researchers would have to pay damages if a neighbor finds stray genes at harvest time. The law also retains the public database of all GM plantings, providing sometimes destructive protesters with a road map. Plant geneticist Frank Ludewig of the University of Cologne, who spent more than a year filing paperwork for a field trial of GM potatoes, says he had expected biotech-friendly changes. "My first thought was, 'No, this can't be true,' " he says. Opponents say they want the buffer zones to be at least 800 meters with no exceptions. A parliamentary vote is expected in September. **–GRETCHEN VOGEL**

Paulson: Edit Out Credit

Before signing a research and science education bill last week (*Science*, 10 August, p. 736), President George W. Bush said he would continue to push for a priority that's not in it: making the corporate "research and development tax credit a permanent part of the tax code." But next door, Treasury Secretary Henry Paulson appears to be less supportive of the idea. Last month, in a white paper, Paulson said that lower corporate taxes and a simpler system could obviate the need for the research credit. The current credit, he said, "creates complexity": time-consuming paperwork and exhaustive audits. "[T]he administrative difficulties erode the positive incentives [for research] the provision provides," the paper said.

Has Paulson jumped ship? No, says IBM lobbyist Linda Evans. "The treasury secretary is looking long term," she says, whereas the White House has more near-term thinking. (A treasury spokesperson did not return calls.) Paulson's ideas are unlikely to get much traction in the Democratic Congress, where a focus is on making the credits permanent; bills that would do that have more than 100 cosponsors between the Senate and House versions, but they've gotten no hearings. **–ELI KINTISCH**

ENDOCRINE DISRUPTERS

Controversy Continues After Panel Rules on Bisphenol A

A federal advisory panel has poured itself the proverbial half-glass of water after digesting the latest studies on the human health risks of an estrogenlike chemical used to make plastics. The chemical industry has proclaimed that the panel's verdict last week confirms its contention that bisphenol A is safe. But environmentalists say the report has been tainted by industry and downplays the risks. Away from the fray, some scientists say the panel's comments about the chemical's effects on the developing brain represent heightened concern compared with previous formal reviews.

Bisphenol A is found in everything from some beverage and baby bottles to the linings of food cans. Small amounts can leach out into food, and most people likely have detectable levels in their blood. These parts-per-billion levels are well below the safe dose set by the Environmental Protection Agency (EPA). In 1997, however, reproductive biologist Frederick vom Saal and others at the University of Missouri, Columbia, found that very low levels fed to pregnant mice could enlarge the prostates of their male offspring. Industry studies couldn't replicate the results, but a review concluded that the results were valid (*Science*, 27 October 2000, p. 695).

How safe? Polycarbonate baby bottles are one source of the controversial chemical bisphenol A.

Since then, other scientists have reported low-dose effects in rodents. Some findings have raised alarms, such as an increase in chromosomal abnormalities in the eggs of mice, discovered after bisphenol A leached from plastic mouse cages (*Science*, 4 April 2003, p. 31). Epidemiology studies have linked bisphenol A and human health problems, such as breast cancer and early puberty. In the first formal U.S. review of bisphenol A, the National Toxicology Program's (NTP's) Center for the Evaluation of Risks to Human Reproduction formed a 12-member expert panel to review more than 500 studies.

Controversy accompanied the first meeting of academic, federal, and industry scientists in March: An environmental group pointed out that the contractor preparing a draft report had done work ▶

MOLECULAR EVOLUTION

Resurrected Proteins Reveal Their Surprising History

It's easy to see evolution's handiwork writ large—just compare a marigold and a musk ox. With a little work, scientists can also pick out subtle differences in the proteins of related organisms. Now researchers in Oregon and North Carolina have gone a step further: retracing the steps by which two proteins diverged from their ancient common ancestor.

In a paper published online in *Science* this week (www.sciencemag.org/cgi/content/abstract/1142819), the researchers report that they resurrected a protein from ancient fish that swam the oceans some 450 million years ago and then worked out the protein's atomic structure. By comparing the protein to more modern versions and doing some deft detective work, they crafted something like a movie of the sequence of key mutations that enabled the ancestral protein to take on new modern functions.

"It's a beautiful piece of work," says David Haussler, a molecular evolution expert at the University of California, Santa Cruz. Haussler says the work underscores how chance mutations that seemingly add little value initially can help set the stage for major evolutionary leaps. "For me, what is so exciting is seeing the dynamics of evolution play out on the molecular level," Haussler says.

The study was led by Joseph Thornton, an evolutionary biologist at the University of Oregon, Eugene. Thornton and his postdoctoral assistant Jamie Bridgham turned to a pair of closely related protein receptors for two steroids, hormones that govern a wide range of metabolic functions in humans and other vertebrates. The first receptor, known as the glucocorticoid receptor (GR), binds to the hormone cortisol, which helps regulate the body's response to stress. The second, called mineralocorticoid (MR), binds to deoxycorticosterone (DOC) in fish and to aldosterone in humans and other tetrapods. The two receptors derived from a common ancestral protein, known as the ancestral corticoid receptor (AncCR), some 450 million years ago.

Last year, Thornton's group reported they had resurrected that ancient protein by comparing the gene sequences of 60 steroid receptors from present-day organisms (*Science*, 7 April 2006, p. 97) and using evolutionary relationships to compute the most likely sequence of the ancestral protein. The team then synthesized a gene for that protein, cloned it into mammalian cells in culture, and regenerated it.

Biochemical tests showed that, like the modern MR protein, it readily bound aldosterone and DOC, and it had a more modest sensitivity to cortisol. "So it's the GR's function that emerged with evolution," Thornton says. That suggested that the gene for the ancient MR protein was duplicated in the ancestral organism—when fish with cartilage-based skeletons were the only vertebrates on Earth—and evolved to become GR, Thornton says.

For its current study, the group set out to unravel those evolutionary steps. They started by teaming up with structural biologist Matthew Redinbo of the University of North Carolina, Chapel Hill, and his postdoctoral assistant Eric Ortlund, who crystallized the AncCR protein and used a powerful x-ray synchrotron to determine its three-dimensional structure, the first of an ancient protein. They then studied precisely how the structure differed from structures of MR and GR.

The researchers worked their way back up the tree of life from AncCR, reconstructing other ancient proteins from ancestral organisms that likely lived around 440 million and 410 million years ago. Whereas the older of these retained the MR-like behavior of AncCR, the more recent protein was found to have a more GR-like function. Comparing

CREDIT: WALLY EBERHART

for chemical companies. NTP fired the contractor.

Amid the scrutiny, the panelists last week stuck with a previous decision to set aside many academic low-dose animal studies that had injected the chemical, because the results failed to account for the detoxifying effects of ingesting bisphenol A. The panel also questioned the relevance of an enlarged prostate because it wasn't shown to be a precursor of cancer, NTP staffers say. The bottom line: On a five-point scale of concern ranging from "negligible" to "serious," the panel had "minimal concern" for potential effects on the prostate during development or accelerated puberty and "negligible concern" that bisphenol A is harming adults.

At the same time, the panel had "some concern" about risks to fetuses and children because of about a half-dozen reports of subtle neurological effects in rodents from minute doses of bisphenol A, including changes in brain structure and a reduced interest among males in exploring their environment. "They're very scattered. No single study has been replicated," but "it raises some flags," says panelist Jane Adams, a neurotoxicologist at the University of Massachusetts, Boston. This area topped a list of research needs from the panel. Some answers could come from the upcoming National Children's Study, said panel chair Robert Chapin of Pfizer.

Vom Saal and others are upset that the panel's conclusions differ from a statement a week earlier by 38 scientists in the online *Reproductive Toxicology* expressing "great cause for concern" about its potential human health risks. In contrast, a European risk assessment in January found no risk to human health at current exposure levels.

Reproductive biologist John Vandenbergh of North Carolina State University in Raleigh, a co-signer of the *Reproductive Toxicology* statement as well as a member of the NTP panel, believes that the latter's lower concern reflects added expertise in epidemiology and human health. "I think there is a human risk. What we're trying to do here is define what the risk is," he says. After receiving public comment, the NTP itself will weigh in on the risks of bisphenol A.

–JOCELYN KAISER

computer models of the likely structures of these two proteins, Thornton's team found 37 amino acid changes. In all modern GRs, the amino acids at five of those sites are always the same—a clue that those mutations are vital to the ancient protein's GR-like function. When the researchers inserted the mutations into AncCR, no single one of them transformed it into a GR-like receptor. But one pair of mutations did turn the ancestral receptor into one that prefers cortisol to aldosterone and DOC. "It didn't get us all of the way there, but it was a huge shift," Thornton says.

Thornton's team suspected that adding the other three conserved mutations into the protein would create a more modern GR. But it didn't happen. Instead, the mutations completely killed the receptor. Reviewing the atomic structures of the ancient and modern proteins, the researchers found another pair of mutations that likely helped reinforce the portions of the protein destabilized by the trio of "killer" mutations. When they added these mutations before the other three highly conserved mutations, they got a protein that works like a modern GR. "That really blew our minds, that we were able to predict the functional effect of these mutations that occurred over 400 million years ago," Thornton says.

The re-creation sheds light on exactly how evolution works at the molecular level, Haussler says. For example, it shows that evolution first made big leaps in changing the AncCR receptor to its GR-like state and then made smaller tweaks in refining its binding abilities. It also shows that mutations having no effect on a protein's function can set the stage for key mutations. If the history of life could be replayed like a movie, Haussler says, such stage-setting mutations probably wouldn't always occur when needed. And that means the movie would likely have a different ending.

–ROBERT F. SERVICE

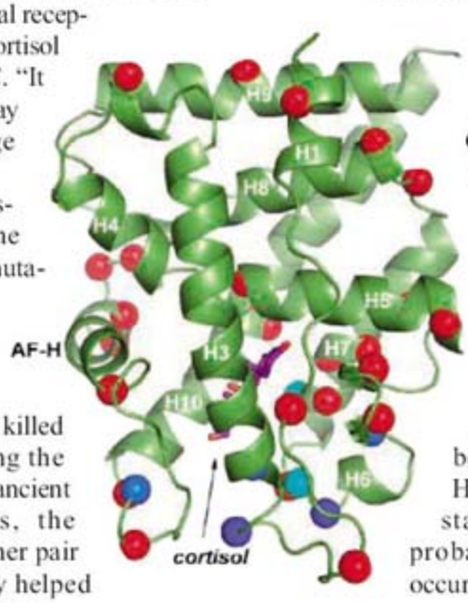

CREDIT: E. A. ORTLUND, *ET AL*./*SCIENCE*

New tricks. Blue spheres mark key mutations that changed an ancient protein's function.

Bank On It

Supporters of biomedical research have hatched a new scheme to boost the flat budget of the National Institutes of Health (NIH): savings bonds. A bill introduced in the House last week by Representative Steve Pearce (R–NM) and two colleagues would create special Treasury "health research" bonds. When the bond is cashed in, the buyer would forfeit 10% of the interest, which would go to the NIH institute of his or her choice. If officials managed to persuade a fifth of U.S. bond buyers to purchase the special securities, NIH would get $158 million a year—a 0.5% drop in the bucket for the $29 billion NIH but far more than the $7 million a year currently raised by a special breast cancer research stamp. The Association of American Medical Colleges has endorsed the bill, which is now in the Ways and Means Committee.

–JOCELYN KAISER

Penny-Pinching at NASA

NASA science chief S. Alan Stern is looking to squeeze more data out of his budget for missions, which is likely to be flat for a while. Before, the Stratospheric Observatory for Infrared Astronomy (SOFIA), for example, was slated for 6 years of extensive tests after it begins flying on a Boeing 747. Now Stern wants SOFIA, which made its first test flight in April, to begin sending back data almost immediately by staggering those tests.

NASA also intends to shorten the Kepler Mission to detect extrasolar planets, with an optional extension. Stern said in a press conference last week that he's considering using extra room on board scheduled missions—a cheaper alternative than building large spacecraft.

–ANDREW LAWLER

Help Wanted

Running California's $3 billion stem cell program should be a plum job, but it's proving tough to fill. Some of the reasons are tough conflict-of-interest requirements and a history of administrative strife. Board chair Robert Klein says there are also "some incredible individuals who were not prepared to give up their laboratories." So to fill the gap left by Zach Hall, the California Institute for Regenerative Medicine (CIRM) has named neuroscientist Richard Murphy, until recently head of the Salk Institute in San Diego and a former member of the CIRM board, as interim president. Murphy says he plans to launch a program for disease-oriented research grants.

–CONSTANCE HOLDEN

MARINE GEOLOGY

Support Is Drying Up for Noah's Flood Filling the Black Sea

It was a hypothesis of biblical proportion: In 1997, two marine geologists proposed that a cataract with the power of 200 Niagaras filled the Black Sea 8400 years ago, driving Neolithic farmers into Western Europe and inspiring the story of Noah's flood (*Science*, 20 February 1998, p. 1132). Now, 10 years later, a torrent of research is still arriving, and almost all of it comes down hard on any Black Sea flood.

The proffered geologic evidence for a catastrophic event was misinterpreted, researchers write in more than 1000 pages of papers, and the raft of data collected around the Black Sea the past 50 years all points to a gradual filling starting thousands of years earlier. Putting it mildly, "the majority wisdom would be against" a flood, says geologist Norm R. Catto of the Memorial University of Newfoundland in St. John's. He is editor-in-chief of *Quaternary International*, where a new collection of papers appears. But a small cadre of researchers maintains that the flood hypothesis is sound and hints that definitive evidence is in the offing.

No flood? Opinion is running against a catastrophic flood through the Bosporus (*above* and *inset*).

The latest surge of research comes in 15 papers in the June issue of *Quaternary International* and 35 papers in a 971-page book, *The Black Sea Flood Question*, published earlier this year by Springer. The new papers agree that the archaeological record shows no sign that people living around the Black Sea 8400 years ago fled from a rapidly advancing sea. "At this point, there just isn't any evidence for something big and catastrophic" in the archaeological record, says archaeologist Allan Gilbert of Fordham University in New York City, an editor of the new book. One apparent piece of supporting evidence—the discovery of the remains of a wood-and-mud house littered about with stone tools 91 meters beneath the Black Sea (*Science*, 22 September 2000, p. 2021)—has not panned out. "It looks peculiar," says Gilbert, but there's no sign it's anything more than a random bunch of rocks and sticks.

Then there's the geologic evidence used to gauge the depth and salinity of the Black Sea over the past 15,000 years. The tools include drowned beach dunes, seismic probing of bottom muds, oxygen isotopes, microscopic fossils, and pollen. Citing such data, the originators of the flood hypothesis—longtime marine geologists William Ryan and Walter Pitman of Lamont-Doherty Earth Observatory in Palisades, New York—have argued that 10,000 years ago, the Black Sea was a modest-sized lake lying perhaps 100 meters below its current level. It was cut off from the salty Mediterranean Sea, they say, because sea level was too low to spill through the Bosporus. When melting glacial ice raised sea level, the Black Sea basin filled up in a geologic instant about 8400 years ago.

But most of the authors of the book consider that scenario "a myth," e-mails another editor of the book, Valentina Yanko-Hombach of the Avalon Institute of Applied Science in Winnipeg, Canada. The Black Sea, she says, was never that low, and it rose gradually over millennia.

Not so fast, says coastal geologist Liviu Giosan of Woods Hole Oceanographic Institution in Massachusetts. Giosan, a native Romanian who studied oceanography in that Black Sea coastal country, has reviewed the new book for *Quaternary Science Reviews* and found it wanting. In particular, he says, the "vast amounts of data" collected around the Black Sea by Soviet scientists and researchers from former communist countries around the Black Sea are suspect. He distrusts much of the carbon-14 dating of lake levels and is frustrated by the traditional lack of access to primary data. As a result, he writes, "many conclusions of studies presented in the book should be considered with a grain of salt" until researchers buttress them with more-direct measures of lake level.

Lately, geologists are in fact looking at more direct sea-level gauges, as well as geologic indicators of past flow through the Bosporus. Richard Hiscott and Ali Aksu of Memorial University of Newfoundland and colleagues have reported several signs that the Black Sea filled slowly and gently. In the *Quaternary International* issue, they describe a core from the shallow Black Sea shelf that contains sediment laid down beneath tens of meters of water when Ryan would have that spot high and dry. On the Black Sea floor just north of the Bosporus, they have mapped old beach ridges and lagoons formed as the lake level slowly rose. And south of the Bosporus, they found a delta built by outflowing waters 10,000 years ago, when Ryan's scenario would have the Black Sea totally cut off.

Ryan and a half-dozen colleagues disagree. "I've found myself following those who criticize the flood," says Ryan, "getting my own data from their sites, and in every case finding a very different story." Where Hiscott and Aksu find a delta built by Black Sea outflow, Ryan and colleagues find a delta formed by a nearby river, as they will soon report in *Marine Geology*. As for the putative beach ridges, Ryan says unpublished coring results show they are actually mud brought in by bottom waters still flowing through the Bosporus today. He also speaks of an as-yet-unpublished description of "an extraordinary debris fan" right where the flood would have dumped its gougings. Erosional features there bear a striking resemblance, he says, to those created by catastrophic outbursts from glacial lakes (*Science*, 20 July, p. 307).

Despite the continuing debate, Giosan, who has worked with Ryan, is guardedly optimistic. "There is momentum toward solving this," he says. "Maybe we'll solve it someday."

–RICHARD A. KERR

CREDITS (TOP TO BOTTOM): JAKE RAJS; NASA-JPL

CREDIT: J. KAISER/SCIENCE

ALAN KRENSKY INTERVIEW

Drawing a Map for the Twenty-Seven Divisions in NIH's Army

BETHESDA, MARYLAND—Alan Krensky should have packed a flak jacket when he moved here. The director of the National Institutes of Health's (NIH's) new planning office says he's already been battered with criticism as he settles into his job, which is to bring more order to the sprawling $29 billion biomedical research agency. "One thing I've learned is, any flag you raise, someone will attack it from one side or the other, and sometimes both sides at the same time," says Krensky, who came to NIH from Stanford University School of Medicine last January.

Yet Krensky seems undaunted. As the official director of the NIH Office of Portfolio Analysis and Strategic Initiatives (OPASI) since 8 July, he faces two main responsibilities. The first is to oversee implementation of the Roadmap, the $483 million set of crosscutting initiatives started 4 years ago by NIH Director Elias Zerhouni that has been criticized as taking money from investigator-initiated grants. Second, OPASI will look across NIH's research portfolio and find better ways to manage it while respecting the turf of its 27 institutes and centers.

Observers say those are formidable challenges. "A lot of this is going to boil down to how well he gets along with institute directors," says former NIH director Harold Varmus, now president of Memorial Sloan-Kettering Cancer Center in New York City, who first called for more central planning at NIH 6 years ago in *Science*.

In an interview, the 55-year-old immunologist talked about his experiences at Stanford, where he headed a $500 million children's health initiative. He also outlined some ideas for OPASI, which will soon become part of a division under Krensky's direction that Congress created to encompass NIH offices such as those on women's health and AIDS.

Krensky is now overseeing midcourse reviews of the Roadmap projects and crafting more rigorous policies, such as time limits, for the next round, which will launch this fall with projects in epigenetics and the microbiome. His edited remarks follow.

–JOCELYN KAISER

Q: What is your response to the claim that the Roadmap takes funding away from investigator-initiated R01s?

I think when people attack it or have concerns, they really misunderstand what it's all about. I don't view the Roadmap as monolithic at all. What attracted me is that it was a new way of looking at things. One term that Elias [Zerhouni] used is a learning laboratory. It's a place to ask questions, a place to do things outside the box.

These are 5-year programs, potentially renewable for 10. And that's what I like. If people don't use it or don't like it, it should disappear. And the idea that it sundowns makes it different from anything else here.

The scale of many of the early projects was very large. I'm not against big projects. If people say, "This has been terrific for my research," it's a success. That being said, I'm very interested in other areas that the Roadmap can do and test. I believe we want more pilots. I believe in small things.

Q: Is OPASI, with its $483 million research fund, essentially a 28th NIH institute?

That is a real problem. Originally, the common fund was a tap from all the institutes and centers. So it was a co-ownership, a co-op essentially. Last year and this year, Congress made it a line item so it now has an income stream like any other [institute].

And so what's central to this is, we're not an [institute], it's about working together. This goes back to what I call cajoling, but we are really working with the entire community—and that's both internally and externally—to develop these programs, and we're much more like the concierge than the bosses.

Q: What is the "fingerprinting" [of individual grants by disease topic] about?

[NIH is] basically building a system that will scan the grants and determine the portfolio [for a particular disease]. Now there are all kinds of ramifications of that. Any number in any [disease] area will be different because it was obtained in a different way. I'm expecting the community and Congress to respond to the numbers, and the communications are going to be very important. The most important part is, if someone else came and ran the same thing, they'd get the same number.

Q: Doesn't Congress want NIH to address redundancies?

In my time here, of all the words that give me the greatest fear, the word "redundancy" comes to the top of the list. The first point made to me is that redundancy is important in science. If you do an experiment once and no one proves that it's correct, it's sort of worthless. So we have to have a certain amount of repetition.

I think redundancy is in the eye of the beholder. For some people it resonates tremendously, for others it is a very worrisome topic. One investigator said to me, "Am I the redundant one?" So in our R01 community, people worry about that.

But at the same time, if people find out they're doing the same thing, they should know about it. I can't prescribe how they respond to that or what they do, but it's of interest.

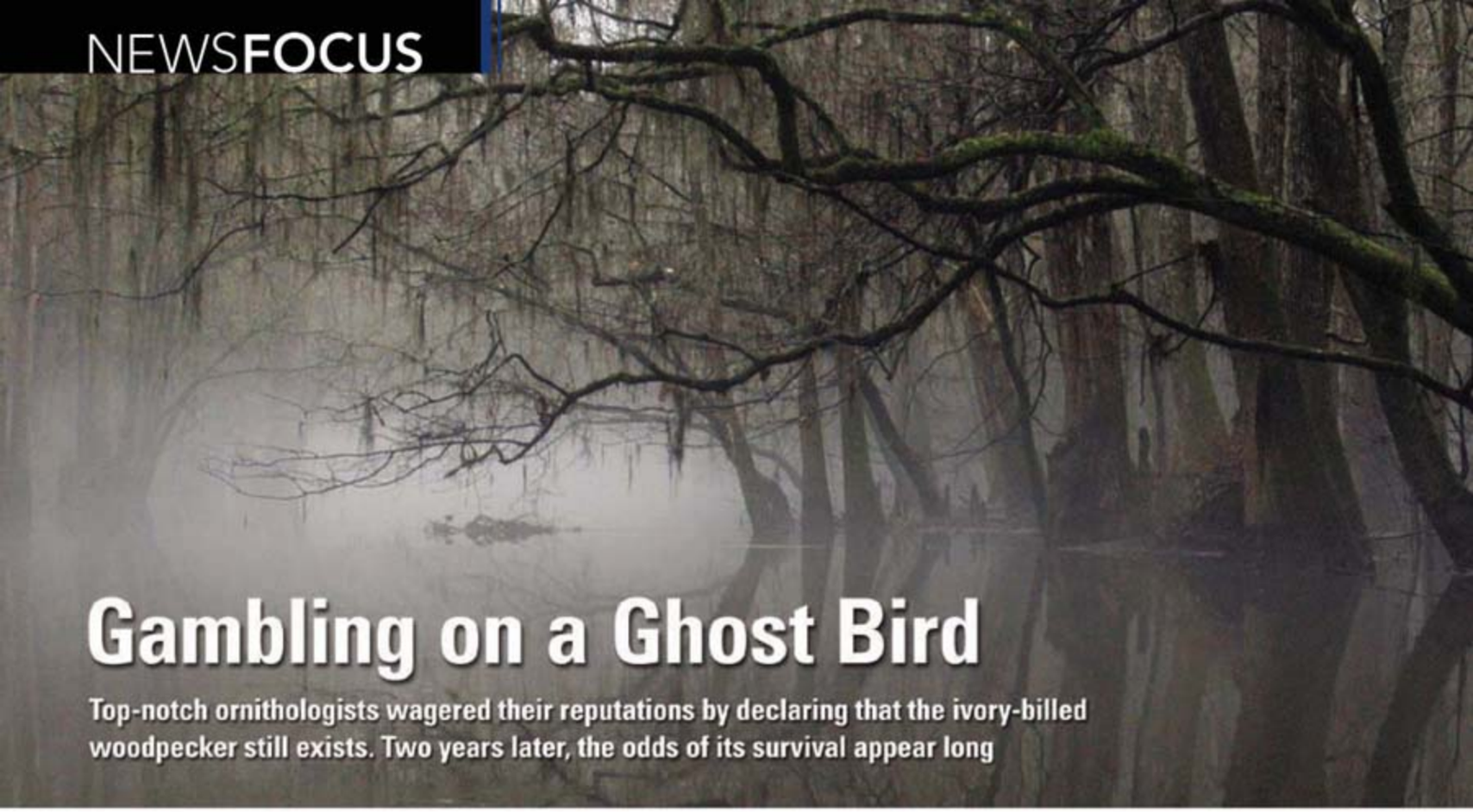

Gambling on a Ghost Bird

Top-notch ornithologists wagered their reputations by declaring that the ivory-billed woodpecker still exists. Two years later, the odds of its survival appear long

ON 28 APRIL 2005, JOHN FITZPATRICK told the world what he had been keeping secret for more than a year. At the headquarters of the Department of Interior in Washington, D.C., flanked by two Cabinet secretaries, Fitzpatrick announced a conservation miracle. The majestic ivory-billed woodpecker—an emblem of southern old-growth forests that was last seen during World War II—still persisted in the Big Woods of Arkansas. "In the world of birding," he said, "nothing could have been more hoped-for than this Holy Grail."

It was an extraordinary claim and a rare piece of good news in conservation. It was also a crowning achievement for Fitzpatrick, director of Cornell University's prestigious Lab of Ornithology, who had fielded probably the most intense search for a bird ever. The 14-month stealth mission yielded several eyewitness sightings, sound recordings, and a video, published online in *Science* that day. "We have conclusive proof that the ivory-billed woodpecker has survived into the 21st century," Fitzpatrick declared in a video released by Cornell. Private donors and federal agencies opened their wallets. The world celebrated a second chance to save the awe-inspiring bird.

And yet after more than 2 years of herculean efforts and sometimes vituperative debate, indisputable evidence of the bird's existence has not emerged. Fitzpatrick still believes his team saw an ivorybill, although he never did himself, in the Big Woods in both 2004 and early 2005, and he speculates that it has either flown elsewhere or died. Skeptics think the mesmerizing ivorybill was never there to begin with and that the Cornell team mistook other woodpeckers and overinterpreted a blurry video. "Why would you announce … one of the biggest things ever in North American ornithology and not have concrete, irrefutable evidence?" asks Mark Robbins of the University of Kansas in Lawrence.

To many critics, this is a story of good intentions gone awry and the power of belief, amplified by secrecy. A top-notch team of scientists was misled by hope, it seems to them, and buoyed by confidence that more searching would bring the definitive photo. Fitzpatrick and his colleagues reject those explanations, defend their objectivity, and say they have no doubts or regrets. Now, as the U.S. Fish and Wildlife Service (FWS) begins to assess the efficacy of the searches it funds, most birders and ornithologists seem resigned that even if an ivorybill was in Arkansas in 2004, the chance to save the species is past. "I want to hope against all odds," says James Bednarz of Arkansas State University in Jonesboro. "But my scientific logic says it's deep in the vortex of extinction."

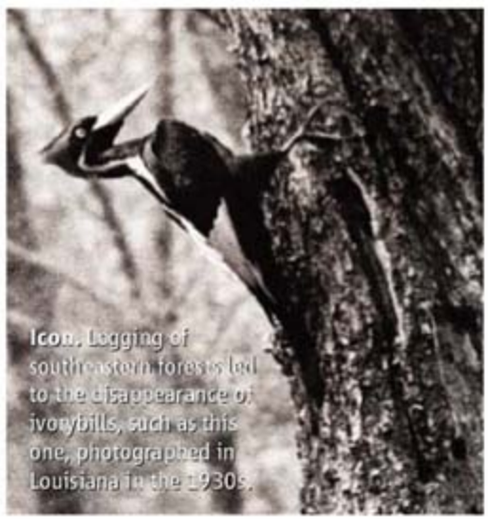

Icon. Logging of southeastern forests led to the disappearance of ivorybills, such as this one, photographed in Louisiana in the 1930s.

CREDITS (TOP TO BOTTOM): MARTJAN LAMMERTINK; JAMES T. TANNER, COURTESY CORNELL LAB OF ORNITHOLOGY

Fleeting glimpses

The largest woodpecker in the United States, the ivorybill (*Campephilus principalis*) lost practically all its old-growth habitat when loggers cut down the bottomland forests of the southeastern United States. As the birds became scarce in the 1880s, ornithologists and birders raced to shoot the survivors for their collections. By the 1960s, most ornithologists were convinced the ivory-billed woodpecker was extinct. Yet every few years, a hunter or birder would announce a sighting. Experts assumed that they were misidentifying a pileated woodpecker (*Dryocopus pileatus*), a large species still abundant in the bottomland forests. In 1966, bird author John Dennis reported seeing an ivorybill in a swamp in east Texas. He swam naked through the water and managed to get a close look, yet no one believed him.

Even a respected scientist caught the fever. George Lowery Jr. of Louisiana State University (LSU) in Baton Rouge, past president of

the American Ornithologists' Union, brought two photographs of ivory-billed woodpeckers to AOU's annual meeting in 1971. Lowery believed that the photos, taken by an acquaintance, were real, but other ornithologists thought the birds looked like posed specimens. His reputation was tarnished. "I wish now that I had said nothing about these birds," he later wrote.

None of this boded well for David Kulivan, a forestry student at LSU. He spotted what he thought were two ivory-billed woodpeckers while turkey hunting near the Pearl River on 1 April 1999 (not an auspicious day of the year to report seeing ivorybills). He recounted the sightings to ornithologist James Van Remsen, curator of birds at LSU's Museum of Natural Science, who was persuaded enough by Kulivan's account to organize a search. Zeiss Sport Optics funded a well-publicized effort in 2002.

Cornell also mounted a small expedition, led by Fitzpatrick. There may have been no one better placed to save the ivory-billed woodpecker than Fitzpatrick, who is shrewd, ambitious, and decisive. "Fitz never goes halfway on anything," says Frank Gill, who retired as chief scientist of the National Audubon Society in New York City. "He can move mountains in a way that no other ornithologist can do." A Harvard graduate who went on to a Ph.D. at Princeton, Fitzpatrick bushwhacked through the Amazon in the 1970s and '80s, discovering seven new species of birds. He made an even bigger mark studying endangered Florida scrub jays and helping to create a national wildlife refuge to save scant remaining habitat. In 1983, as curator of birds at the Field Museum in Chicago, Illinois, he was awarded AOU's highest prize for research.

After a month in the Pearl River, neither group had found anything. Late-night TV comedian Jay Leno mocked the search by reading a newspaper headline: "Researchers fail to find extinct bird." Eventually, the Louisiana Ornithological Society dismissed the Kulivan sighting. Still, the Cornell team won kudos from other researchers for its cautious analysis of their sound recordings, which turned out to have captured gunshots, not the distinctive double-knocks made by ivorybills. Despite heading home empty-handed, the experience fired up Fitzpatrick. "The chance to be there was a dream come true," he says.

Secret mission

Another opportunity arose just 2 years later. Fitzpatrick was in his office at 8:30 a.m. on 1 March 2004 when Tim Gallagher came in, wild-eyed. Gallagher, an avid birder who edits Cornell's *Living Bird* magazine, had just returned from the Cache River National Wildlife Refuge in Arkansas, where he and a friend had seen an ivorybill. Fitzpatrick grilled him for details and finally asked: "What are the chances that the bird you saw was not an ivory-billed woodpecker?" Gallagher replied, "I'm absolutely positive that this bird was an ivory-billed woodpecker."

Fitzpatrick immediately sent Gallagher back to the swamp with a top graduate student. Then in mid-March, he convened a meeting of the Sapsuckers, a crack team of birders from Cornell that competes in the World Series of Birding. Several days later, they were tromping and paddling through the Arkansas swamp. But during that week, the only woodpeckers they saw were pileateds. The team was frustrated, and most of them had to return to their day jobs at the lab.

But Fitzpatrick decided to press ahead, having great confidence in Gallagher's sighting. "I have to put my faith in those people able to separate fact from fiction," he says. He was also convinced that if he didn't act, the bird would truly go extinct. There had been no previous exhaustive searches, he points out. Cornell had the tip, the resources, and the gumption. "Nobody else had the balls to do it," Fitzpatrick says.

He insisted on secrecy—a decision that would later bring the team criticism for being insular and insufficiently skeptical. Fitzpatrick feared that if word of the search got out, "the place would become Coney Island with birders piling in all over the place." Ultimately, some two dozen police officers were ready to protect the habitat after the announcement, but there was no onslaught. The Nature Conservancy, which was involved in the search, had its own concerns. It had been buying land to conserve bottomland hardwood forest and feared that news of the search would drive up prices.

More volunteers arrived, all signing legal confidentiality documents. The cover story for curious locals was that they were doing a biological inventory for The Nature Conservancy. The bird was code-named Elvis. Between 5 and 11 April, there was a flurry of sightings, all by lone, amateur observers. Concerned about the lack of corroboration, Jeffrey Wells of Cornell, the logistical manager, decided to double up the observers. After that, there was just one more sighting. On 25 April, David Luneau—an electrical engineer at the University of Arkansas, Little Rock, who participated in the Pearl River search—and his brother-in-law filmed a 4-second glimpse of a bird fleeing a tree. It has become without doubt the most analyzed bird video in history.

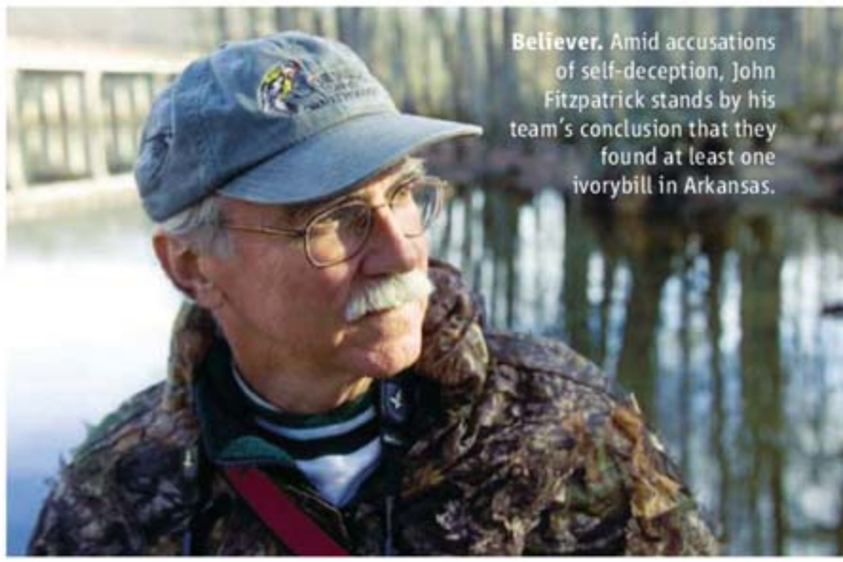

Believer. Amid accusations of self-deception, John Fitzpatrick stands by his team's conclusion that they found at least one ivorybill in Arkansas.

Like the others, Fitzpatrick was initially disappointed by the video's quality. Although the team was convinced from the sightings that the bird was there, and they had intriguing recordings of double knocks and "kent"

CREDIT: JASON KOSKI/CORNELL UNIVERSITY PHOTOGRAPHY

No action. Months of high-quality videotaping failed to catch an ivorybill a second time.

calls, they wanted solid evidence—clear photos or video or a nest hole that would convince skeptics. As Luneau has said, "If you have something like a picture or video or sound recording, … then others are able to make up their minds based on science rather than on their feelings on how much they believe somebody."

With time running out on the 2004–2005 season—the leaves would soon be emerging on the trees and it would be impossible to see anything—Fitzpatrick and the others began planning for the next field season. Fitzpatrick raised about $4 million in cash and pledges for what would become the largest ornithological search in modern times, coupled with a concerted effort to conserve the ivorybill's habitat. As a board member of The Nature Conservancy, Fitzpatrick had rubbed elbows with the likes of Henry Paulson, the former CEO of Goldman Sachs and now U.S. Treasury Secretary. Paulson is an avid birder and, with his wife, donated money to support the search.

At the same time, Fitzpatrick was communicating with the Department of the Interior, where he also had connections. James Tate, science adviser to Secretary Gale Norton, was a former assistant director of the Lab of Ornithology. "We wanted to get as much buy-in from the government to put money into the conservation of this area as we could," Fitzpatrick says. He also decided they would not announce the finding until they had tangible evidence and a paper accepted for publication, probably at the end of the 2005 field season.

To the team's disappointment, nothing better than the video turned up—despite efforts including hoisting observers 25 meters above in a cherry picker. "It became clear that, in all probability, we were not going to obtain any more video evidence anytime soon," says Martjan Lammertink, a woodpecker expert who joined the team that season. By February 2005, Fitzpatrick recalls, he realized that "we need to begin to act as though the Luneau video plus sightings plus sound is going to be enough."

The team went back to the Luneau video. The more they looked, the more convinced they became that it could not be a pileated woodpecker. The wings had a white trailing edge. The wing beats seemed very fast. And the size of the bird, measured as it perched on the tree, was much too big. To bolster their argument, the group took crude models and reenacted the escape flight of the bird, albeit with stiffly flapping wings. They filmed at the exact spot Luneau had taken the video, using the same camera. "The most parsimonious and logical conclusion is that it is probably an ivory-billed woodpecker," Lammertink says. Fitzpatrick e-mailed Don Kennedy, editor-in-chief of *Science*, about submitting a paper. In an editorial published with the paper, Kennedy recalls that he "responded in a New York second!"

The manuscript went out for reviews in early April and was scheduled to be published in mid-May. But on Monday, 25 April, the story leaked. In preparation for an announcement by the Department of the Interior, Tate quickly flew to Florida and drove in a raging rainstorm to meet Fitzpatrick at the Archbold Biological Station to evaluate the evidence. "I'd seen George Lowery and John Dennis have their reputations ruined by naysayers," Tate says. "I did not want that to happen to the secretary, or to me." Tate, who had studied a kind of woodpecker called the yellow-bellied sapsucker, came away convinced.

Field marks. Ivorybills (*right*) superficially resemble pileated woodpeckers (*left*) but are larger and have distinct plumage.

Editors at *Science* rushed the final production of the paper so that it could be published online, along with the video and the recordings, before the news broke in the media. "*Science* wanted to do this with an embargo and make a splash," Fitzpatrick says. It worked: Stories ran in 459 U.S. newspapers, 174 television shows, and 43 radio shows. At the press conference, Interior and the U.S. Department of Agriculture announced joint funding of $10.2 million for the conservation of the ivory-billed woodpecker and its habitat. Fitzpatrick and a few others were whisked back to Cornell on a private jet.

The powder keg explodes

The announcement, Gill recalls, provided a spark that "hit the powder keg of hope and expectations in a way that was just unprecedented. Once it got started, it really got out of control." The town of Brinkley, Arkansas, nearest to the sightings, went wild with promotion. Some 70 experts and officials, including a brigadier general, joined the federal recovery team—a record number. Many scientists were also swayed. At first, "I was completely accepting," recalls Geoffrey Hill of Auburn University in Alabama, who became more skeptical after taking a close look at the video. "It was *Science*, it was the Lab of Ornithology, and it was Fitz."

But others say they looked at the video with dismay. "I was worried right from the start," says Noel Snyder, a retired FWS biologist. He and a few others privately expressed concerns to Fitzpatrick about the strength of the evidence. But they kept quiet, not wanting to rain on a joyful and highly publicized parade.

Jerome Jackson was among the early skeptics. An ornithologist at Florida Gulf Coast University in Fort Myers, Jackson is no stranger to ivorybills, having seen more than 300 museum specimens and written a detailed history called *In Search of the Ivory-Billed Woodpecker*. And in 1986, when FWS convened a meeting to discuss

CREDITS (TOP TO BOTTOM): MARK GODFREY/THE NATURE CONSERVANCY; DAVID ALLEN SIBLEY

declaring the ivory-billed woodpecker extinct, Jackson argued against it and conducted a small search.

Jackson and three other scientists prepared a paper for *PLoS Biology*, arguing that the Luneau video showed a pileated woodpecker. "All we wanted to do was have everyone go, 'Wait a minute!' before any more money got spent," says co-author Robbins. "We didn't want to see precious conservation dollars wasted on something that might not be there."

This made the Cornell team and its sponsors nervous. Not long after *The New York Times* reported the existence of the skeptical but not-yet-published paper, Jackson says, Tate called Jackson on a Saturday night and told him to "back off." Tate denies that and says he just wanted to discuss Jackson's criticisms. "My concern was that the skeptics would destroy our opportunity, destroy that second chance to get the biological information of what the birds needed," Tate says.

Days before publication, and after writing a rebuttal, the Cornell team offered to play the critics additional, unpublished recordings that hadn't been fully analyzed before the submission of the *Science* paper. The recordings convinced co-authors Richard Prum of Yale University and Robbins that at least two ivorybills were living in the Big Woods. They withdrew the paper on 1 August, saying they didn't want to undermine conservation efforts. (In retrospect, now that it's clear the recordings are not solid evidence, they regret the move. "I blinked," Prum says.)

But Jackson, who had been out of town and unreachable, still thought that the doubts needed to be aired. In a long, invited article published in *The Auk* in January 2006, he accused Fitzpatrick's team of "delving into 'faith-based' ornithology and doing a disservice to science." In a March 2006 response in *The Auk*, Fitzpatrick's group charged that the Jackson article was "a series of factual errors and poorly substantiated opinions." Jackson, they implied, was "compromising science with sound bites."

After another round of rebuttals commenced, Fitzpatrick confronted Jackson during an August 2006 meeting in South Carolina and asked him not to publish. Jackson recalls Fitzpatrick heatedly telling him, "You are going to be independently responsible for the extinction of the ivory-billed woodpecker because you are preventing me from raising money for conservation." Shortly thereafter, Fitzpatrick contacted Jackson again and offered co-authorship on a future paper if Jackson would pull his letter. "That's not how I operate," Jackson told him. Fitzpatrick says he wanted to focus on the bird and avoid another unproductive exchange: "It was not my desire to prolong and underscore resentments and personal disagreements."

The tone was much more restrained in a Technical Comment and response published in *Science* on 17 March 2006 (p. 1555). Like the authors of the stillborn *PLoS* paper, David Sibley, who wrote and illustrated *The Sibley Guide to Birds*, thought the Luneau video showed a pileated woodpecker. In the Comment, Sibley and three co-authors argued that the white on the wings is the underside of a pileated's wings, not the trailing edge of an ivorybill's. Moreover, several frames show a black trailing edge, like a pileated's. The white on the back of the torso, which Fitzpatrick had called "clearly evident," was actually "a vague pale blur" of just a few pixels. In addition, they asserted that the size estimate wasn't valid, because what Fitzpatrick identified as a perched bird was instead already in flight.

The Cornell team has stuck to its guns.

Since then, other papers, one published in March in *BMC Biology* and another in *The Wilson Journal of Ornithology* in June, also found the video and acoustic evidence unconvincing. "It's all sort of evaporating," Snyder says. He and others aren't interested in rehashing the Luneau video; they would rather see new evidence. It hasn't arrived. The second massive search, during the 2005–2006 season, also came up dry.

Stalemate

Fitzpatrick and Lammertink say they will remain convinced that the Luneau video shows an ivory-billed woodpecker until they see evidence that a pileated could look and fly like that. "Have we boxed ourselves in? Maybe so, but I don't think it's so unusual in science," Lammertink says.

Skeptics, on the other hand, won't believe in ivory-billed woodpeckers until they see clear proof, such as a roost tree where birds can be repeatedly observed. In the absence of more evidence, the American Birding Association in Colorado Springs, Colorado, continues to list the bird as "probably or actually extinct or extirpated." The majority of birders appear to be agnostic. In an online poll by *Birding* magazine, published in April, 75% responded that the ivorybill might or might not exist.

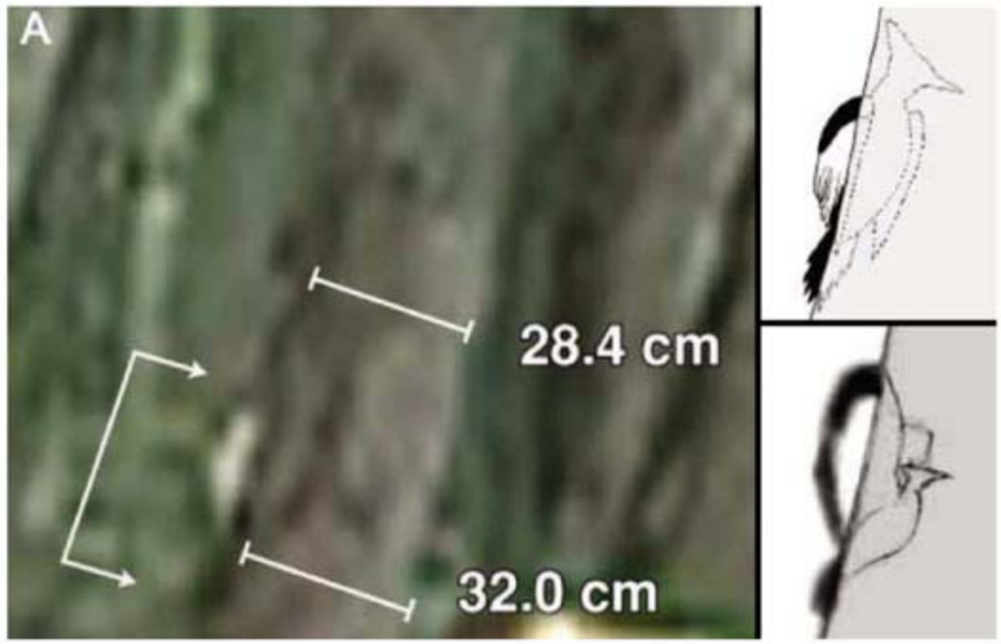

Blurry video. Fitzpatrick's team argues that the bird in this frame was perched (*above, right*), revealing its large size, while Sibley contends it was already in flight (*below, right*).

So what made Cornell so sure? Hill thinks it is the weight they attached to the video. "In retrospect, the Luneau video may loom as one of the most unfortunate things to ever happen to the Laboratory of Ornithology," he writes in his book, *Ivorybill Hunters*. Without it, he speculates, the Cornell team probably would have interpreted the sightings more cautiously. Instead, they threw themselves into a highly involved analysis of murky data. "It was cast as a scientific analysis of these pixels," says Frank Gill. "It had all this pizzazz of technology. That was brilliant on Fitz's part, but it was weird to go to this length."

Jeffrey Walters of Virginia Polytechnic Institute and State University in Blacksburg, who says he was one of the reviewers, says he was swayed by the entire case, including the multiple sightings. He argues that it's unlikely that all the observers were mistaken. But Sibley

CREDITS (TOP TO BOTTOM): SIBLEY *ET AL.*, *SCIENCE* 311, 5767 (2006)

counters that the odds are fairly high—if observers are hoping to see the birds. All the best sightings were from at least 20 meters away and lasted no more than 10 seconds. "It's just a perfect recipe for your brain to fill in the gaps," Sibley says. "You get a brief glimpse and an impression, … and your brain turns it into an ivory-billed woodpecker."

Conducting the analysis in secret compounded the problem, Prum says. "That process of self-convincing took place in isolation from fresh air, from people who didn't report to the boss," says Prum. "Frankly, I think it's antithetical to good science." One solution, Prum suggests, would have been to send the Luneau video to woodpecker experts and ask them to identify the bird without knowing the team's conclusion. Fitzpatrick rejects the charge of groupthink, insisting that the team was as objective as any scientists could be. Both Fitzpatrick and *Science*'s Kennedy defend the decision to publish, noting that the paper was vetted by peer reviewers. "We got more than satisfactorily positive reviews," says Kennedy, who adds that he wasn't fazed by the lack of a clear video. "I thought that it was very important, even if there was some possibility that this might be wrong."

Meanwhile, the search for the bird continues, although it has been scaled back. In the third field season, which concluded in April, Cornell conducted a smaller, mobile search. Rather than focus on a single area, Lammertink and three colleagues spent 5 months, 7 days a week, searching 16 regions by foot and canoe. In addition, FWS also supported searches by other agencies and groups in Texas, Tennessee, Florida, and South Carolina. Again, nothing conclusive turned up. Hill is convinced that he and his team saw ivorybills in 2005 and 2006 along the Choctawhatchee River in Florida, but he admits he can't deliver enough evidence yet.

Lammertink, too, remains optimistic. "There are big areas of unexplored habitat, where on rational grounds you can see that small populations might persist." Fitzpatrick anticipates another year or two of searching at most. "It's just too expensive," he says, noting that it's become harder to raise money. Even if the team quits empty-handed, Lammertink says, it will be difficult to prove the bird is not there. "It may always remain a question mark."

Whether that uncertainty will haunt Cornell remains to be seen. "In some people's minds, the failure to find better evidence in the last couple of years has not been good for the reputation of the Lab of Ornithology," says Russell Charif of Cornell. That specter doesn't worry Fitzpatrick. "I move with the actions that I deem appropriate for the possibility that the birds are there," he says. "And I don't look back."

–ERIK STOKSTAD

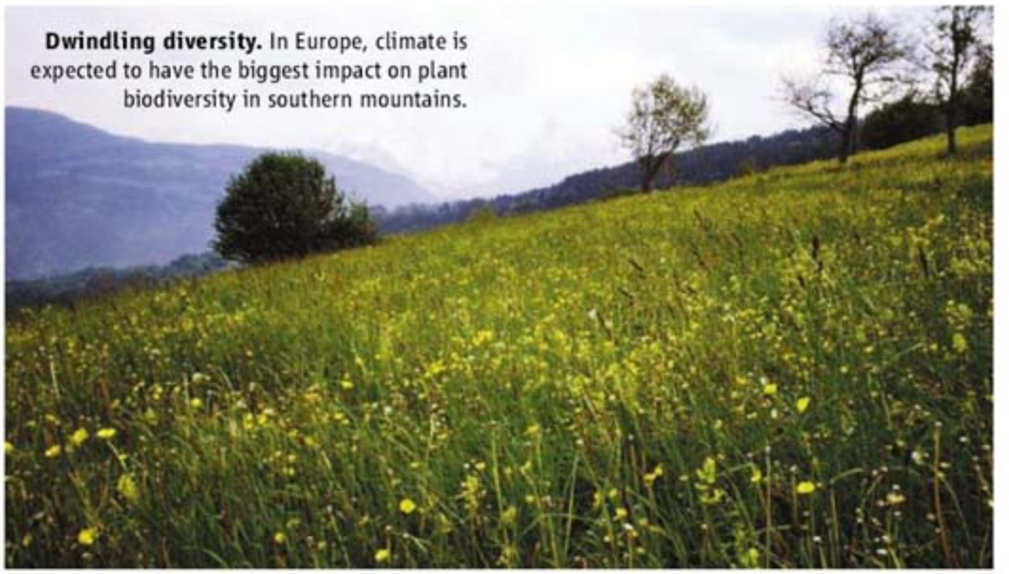

Dwindling diversity. In Europe, climate is expected to have the biggest impact on plant biodiversity in southern mountains.

BIODIVERSITY

Predicting Oblivion: Are Existing Models Up to the Task?

Huge numbers of species may be at risk of extinction from climate change, but coming up with precise estimates is proving tough

The most authoritative guide to today's extinction crisis is a database known as the Red List. Later this month, a group of scientists will gather in England to consider whether the Red List should be opened up to species that, for the moment, show no signs of trouble. Many scientists suspect that the next few decades of global warming could push some species toward oblivion. "The concern," says the meeting's organizer, H. Resit Akçakaya, an ecologist at ecological software company Applied Biomathematics in Setauket, New York, "is that maybe some species that are threatened by climate are not reflected on the Red List." But Akçakaya and others caution that the meeting is unlikely to come up with firm predictions of how many species will become extinct, let alone which ones will be particularly at risk.

The science of predicting extinctions from global warming is only a few years old, and the best models are rife with uncertainties. Experts generally agree that the models may be useful for giving a rough idea of the potential impact of global warming and may also offer guidance for planning preserves. But some scientists are concerned that policymakers will be expecting them to provide more precise estimates than they can deliver. "It's worrying, says Miguel Araújo, an ecologist at the Spanish National Research Council in Madrid.

Much of the current debate over climate-triggered extinctions focuses on what are known as climate-envelope models. Scientists analyze all the places where a species has been recorded and look for features of the climate that those places share. The key factors may be rainfall, for example, or the temperature during the winter.

In the early 2000s, scientists began to look at what happened to these climate envelopes in the scenarios climate scientists have projected for the coming century. "A number of us were noticing that these envelopes seemed to be winking out entirely," says Lee Hannah, chief climate change biologist at the Center for Applied Biodiversity Science at Conservation International, a nonprofit in Arlington, Virginia.

Concerned about the prospect of mass extinctions, an international team of scientists, including Hannah, combined their data into a global analysis. They estimated the size of future climate envelopes, assuming shrinking

CREDIT: JUPITER IMAGES

climate envelopes meant an increased risk of extinction. Their sobering conclusion, published in *Nature* in 2004: Based on a midrange climate-warming scenario for 2050, "15-37% of species in our sample of regions and taxa will be 'committed to extinction.'"

The paper was enormously influential and figures prominently in the Intergovernmental Panel on Climate Change's (IPCC's) upcoming report on the impact of global warming. In a summary for policymakers, the IPCC authors warn that "approximately 20-30% of plant and animal species assessed so far are likely to be at increased risk of extinction if increases in global average temperature exceed 1.5-2.5°C."

Some experts have criticized the IPCC for implying that climate-envelope models are more precise than they actually are. "Simply presenting those numbers as factual, saying this is how many species will go extinct, is misleading," says Richard Pearson, a postdoctoral researcher at the American Museum of Natural History in New York City.

Pearson and other researchers have been testing climate-envelope models for their accuracy and consistency, and they've found some serious causes for concern. Araújo and his colleagues studied the ranges of 116 species of birds in England in the 1970s and 1990s. The red-backed shrike's range shrank dramatically to southeast England in the 1990s, for example, but climate-envelope models based on the 1970s data predicted that the bird's range would stretch all the way to the northern tip of Scotland. "We found that there were lots of uncertainties," he says.

Araújo, Pearson, and other researchers published a study last year in which they compared the projections for a group of plant species in South Africa from several frequently used envelope models. "We found a huge difference between the models," says Pearson. Their projections ranged from a 92% range reduction to a 322% expansion.

Scientists are currently debating how to make better predictions. Climate-envelope models are "simply mapping programs," complains Daniel Botkin, a professor emeritus at the University of California, Santa Barbara. "There's no biology in that."

To improve the performance of these models, Botkin urges researchers to include biological details about species, such as how quickly they disperse and how they interact with other species. Pearson and other modelers have already had some success at doing so, Pearson says. In a paper in press at *Global Ecology and Biogeography*, Pearson and his colleagues report that they can do a much better job of predicting the ranges of owls in Finland if they also factor in where woodpeckers live, as owls make their nests in woodpecker cavities. "In my opinion," says Pearson, the role of biological interactions "is the biggest question out there at the moment, but we're just nibbling on the edges of that."

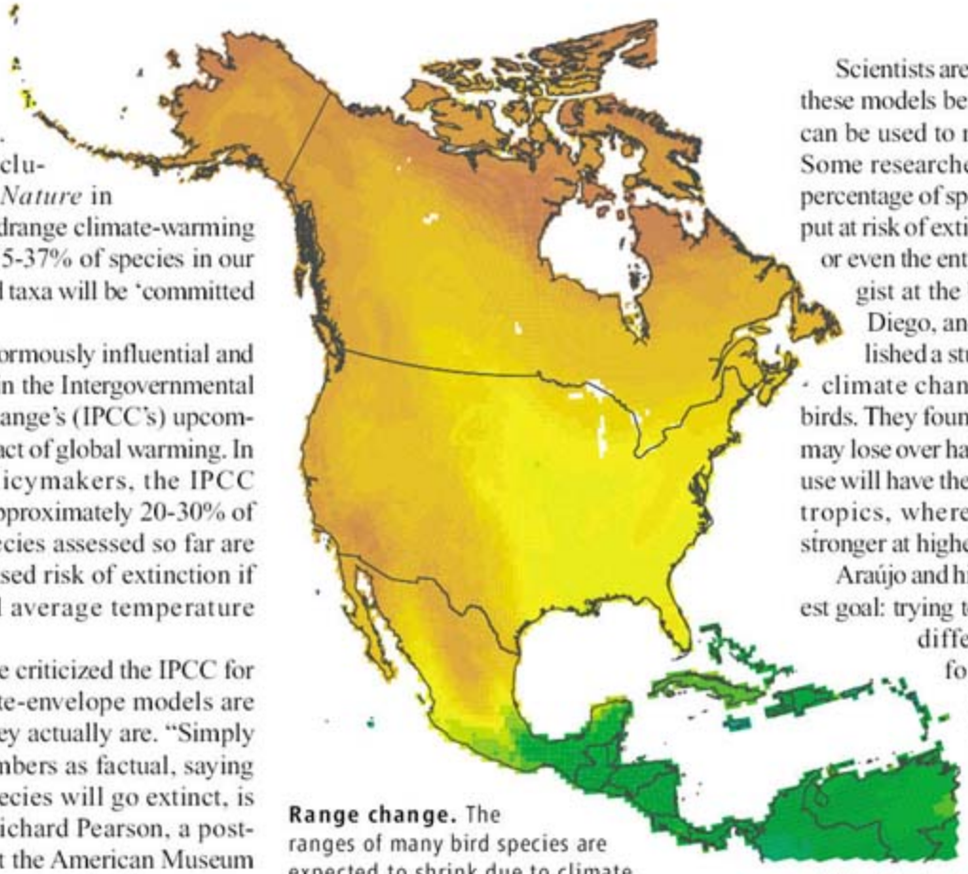

Range change. The ranges of many bird species are expected to shrink due to climate change, Walter Jetz and colleagues reported in 2007 in *PLoS Biology*. This map shows predictions for the average loss in North and Central America (dark green equals 10%, brown equals 60%).

CREDIT: WALTER JETZ/UNIVERSITY OF CALIFORNIA, SAN DIEGO

Other researchers believe that a better strategy is to analyze existing climate-envelope models more effectively. "You have to find automated ways to extract information in intelligent ways from the data you have," says Araújo. He and his colleagues have found that averaging the results of many climate-envelope models provides a more accurate prediction of where species can be found than any one model. "I think that's a much more useful way to go," says Araújo. "This is likely to be a closer match to the truth than anything else we can produce so far."

One problem with these so-called ensemble forecasts, however, is that they are a huge undertaking. Running thousands of models of thousands of species across an entire continent is far beyond the capacity of any existing software. "In the next 2 to 3 years, we won't be able to do it," says Araújo, who is now developing a program he hopes will be up to the task.

Scientists are debating not just how to make these models better but also the best way they can be used to make conservation decisions. Some researchers are trying to estimate the percentage of species that global warming will put at risk of extinction across entire continents or even the entire planet. Walter Jetz, a biologist at the University of California, San Diego, and his colleagues recently published a study of the combined impact of climate change and land-use change on birds. They found that several hundred species may lose over half of their range by 2050. Land use will have the biggest impact on birds in the tropics, whereas climate change will be stronger at higher latitudes.

Araújo and his colleagues have a more modest goal: trying to predict patterns of change in different regions. They've been forecasting which parts of Europe will be particularly vulnerable to losing species through climate change, for instance. They've found that for plants, the mountainous regions in southern Europe will be hit hardest. For amphibians, the arid parts of southwestern Europe are most vulnerable. For now, he suggests, such estimates may be more useful for conservation than a misleadingly precise estimate of a rate of extinction for a particular species.

Identifying these sensitive regions may reveal how existing preserves may change and offer hints about how to design new ones. As the temperature warms, some preserves will no longer have a climate suitable to the species they are supposed to protect.

A number of researchers are using climate-envelope models to study how preserves may have to be altered as species shift their ranges. For instance, existing preserves could be linked by corridors to enable animals and plants to disperse from one habitat to another.

Hannah believes that scientists must move forward with this sort of planning now, even if the models have plenty of room for improvement. "The scary thing for me is that the stuff our models is showing happening decades from now, we're already seeing," he says. He points to the extinction of frogs in the Andes, where researchers suspect that a changing climate may have fostered the spread of a lethal fungus. "These models are the best we've got at the moment, and when we see how the complexity of the world operates, it seems that it may be worse than these models are indicating."

–CARL ZIMMER

Carl Zimmer's latest book, on *E. coli* and the meaning of life, will be published next May.

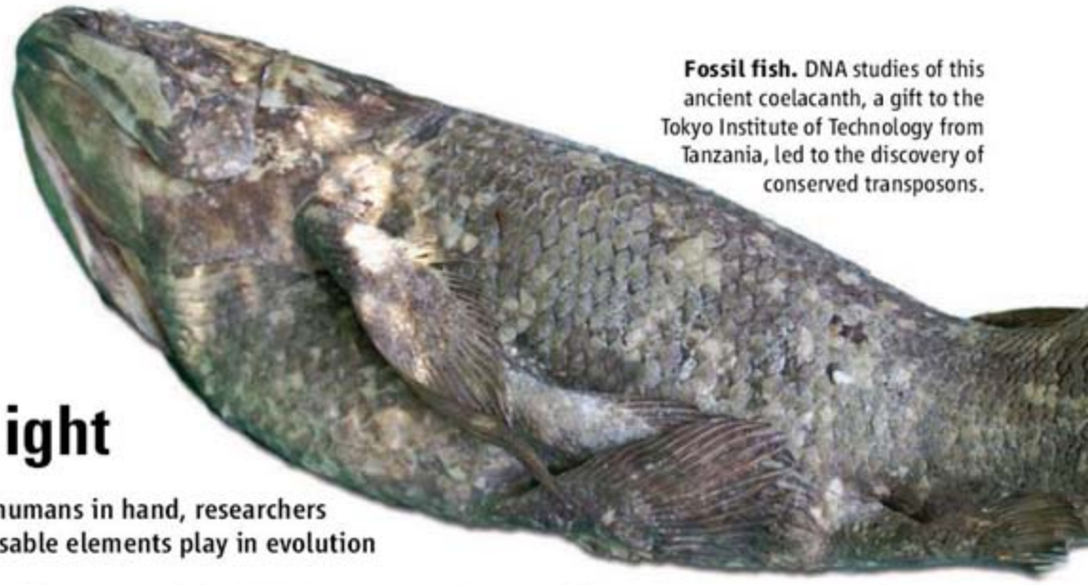

Fossil fish. DNA studies of this ancient coelacanth, a gift to the Tokyo Institute of Technology from Tanzania, led to the discovery of conserved transposons.

EVOLUTION

Jumping Genes Hop Into the Evolutionary Limelight

With genomes from ancient fish to modern humans in hand, researchers are gaining new respect for the role transposable elements play in evolution

Call it a molecular gold rush. Researchers sifting through the supposed junk DNA between genes—a whopping 98% of the human genome—have in the past few years hit a mother lode of functional sequence full of clues about how genomes operate and change through time. And, as junk DNA has gained respect, so have mobile bits of DNA called transposons that are often the source of this genomic clutter.

Most researchers have taken a dim view of transposons, considering them molecular parasites that clog chromosomes with seemingly useless sequence, sometimes disrupting genes. Now, comparative surveys, along with experimental studies of gene regulation, are showing that transposons can influence when, where, and how genes are expressed. These so-called parasites "might be better viewed as symbiotic," says Eric Lander, director of the Broad Institute of Massachusetts Institute of Technology and Harvard University in Cambridge, Massachusetts. David Haussler of the University of California, Santa Cruz, adds that "people are underestimating the impact of transposons" in genome evolution.

Transposons, small packages of DNA that can splice into other sequences, seem to appear suddenly in a genome, copying, cutting, and pasting themselves throughout its chromosomes. Eventually, the genes for making them mobile are disabled by mutations, and the copied sequences themselves mutate until they become indistinguishable from the rest of the genome's junk DNA. But recent studies show that some transposons don't decay. A few have lasted hundreds of millions of years relatively unchanged and are found in the same place in the genomes of many species. To be so highly conserved, they must play a role so important to survival that evolution keeps them intact, weeding out deleterious mutations. One family of transposons, for example, first made its appearance during the evolution of tetrapods; and its descendents are still recognizable, suggesting that they may have helped shape the evolution of that particular group of animals.

Transposons at work. A transposon-activated marker gene was turned on in the developing nervous system of a mouse embryo (*top*) in the same places as a key transcription-factor gene (*bottom*), indicating that the transposon helps control this gene's expression.

Beyond gene boundaries

A few researchers suggested early on that transposons may play important evolutionary roles. Nobel laureate Barbara McClintock called them control elements when she discovered them about 50 years ago, and 2 decades later, Roy Britten and Eric Davidson suggested that they provide fortuitous opportunities for evolutionary innovation. In 1969, they proposed that new branches on the tree of life and ever-more-complex organisms arose at least in part from changes in how genes were regulated. They also argued that these changes were often caused by repetitive elements, many later identified as transposons.

Sets of genes turn on at particular times during development in specific places to specify lungs instead of gills, brain instead of kidney, and so on. Certain regulatory DNA and proteins control these activities and, Britten and Davidson suggested, repetitive elements that copied themselves into different parts of the genome occasionally reconfigured these controls. In the new positions, this mobile genetic material could, for example, corral two independent gene networks and bring them under one regulatory roof, generating new cell types and consequently new structures. "You could have genes that are totally unrelated suddenly getting turned on in the same tissue at the same time," explains Gill Bejerano, a molecular geneticist at Stanford University in Palo Alto, California.

Over the years, this idea lost momentum. "It was untestable," recalls Davidson, a developmental biologist at the California Institute of Technology in Pasadena. But as researchers began comparing genomes rolling off the sequencing machines, it became clear that not all junk DNA was junk, and Davidson and Britten's idea began to look more plausible.

In 2004, Bejerano, then at the University of California, Santa Cruz, and his colleagues described more than 400 stretches of at least 200 bases that were the same in human, rat, mouse, chicken, dog, and, to a lesser extent, fish. Three-quarters of these so-called ultraconserved regions resided outside genes (*Science*, 28 May 2004, p. 1321). Last year, Byrappa Venkatesh of the Institute of Molecular and Cell Biology in Singapore and colleagues compared DNA of elephant sharks and humans, which diverged 530 million years ago. Working with a very sketchy draft of the shark genome, they found 4800 conserved sequences. Like others, they found that these conserved sequences tended to cluster near genes for proteins that regulate transcription and DNA binding.

Greg Elgar of the University of London has found that many conserved elements burst onto the scene between the emergence of lampreys and sharks. The timing suggests

CREDITS (TOP TO BOTTOM): NORIHIRO OKADA/TOKYO INSTITUTE OF TECHNOLOGY (COURTESY OF TAFIRI); G. BEJERANO *ET AL.*, *NATURE* **441**, 87 (2006)

that "the evolution of these sequences [was] key to the establishment of the vertebrate gene-regulatory network for development," Elgar says.

Gradually, researchers began to realize that some of these conserved elements were transposons. The coelacanth, a "living fossil" species that dates back more than 400 million years, led Norihiro Okada of the Tokyo Institute of Technology to a whole conserved superfamily of transposons called short interspersed repetitive elements (SINEs). Okada and his colleagues first found two SINEs in the coelacanth whose sequences looked similar enough to each other to have a common origin; they then searched for the same sequences in genome databases. They found them in salmon, trout, hagfish, dogfish sharks, lancelets, catfish, zebrafish, and the sea urchin, they reported online in *Genome Research* on 22 May 2006. Yet another analysis unearthed 1000 copies of a subset of these SINEs, called AmnSINEs, in both humans and chickens. "It suggests that some of these [transposable elements] had acquired function very early on in evolution, and those functions have been retained," says John Moran, a molecular geneticist at the University of Michigan, Ann Arbor.

When Broad Institute researchers Xiaohui Xie and Michael Kamal trekked through the human genome looking for stretches of DNA that occurred multiple times, they found one that looked quite a bit like the core of a zebrafish transposable element, also part of the SINE family. Eventually, they turned up 123 more copies, some more complete than others. They found this SINE's 180-base core in the same places in other genomes and a few copies in the coelacanth. This work appeared in the 1 August 2006 issue of the *Proceedings of the National Academy of Sciences*. Their SINEs proved to be the same ones that Okada discovered.

When Bejerano took a close look at his ultraconserved sequences, he too discovered the remains of a family of transposable elements. He saw this first in coelacanth DNA, calling it LF-SINE, "LF" for "lobe-finned" fish. He estimates that 10,000 LF-SINEs exist in this fossil fish and, from their sequences, knows they are still active. Through genome comparisons, he and his colleagues found LF-SINE variations in human, chicken, dog, and all the other tetrapod sequences in the public databases.

The conservation of the sequence in similar places in the genomes of all these species suggested they play a key role in genome function. Bejerano tested one that was located 500,000 bases from a gene coding for a transcription factor active in motor neuron development. That's not close enough to be the primary controller of the gene's activity, but Bejerano thought perhaps the transposon could exert a gene-activating effect from afar as a so-called enhancer. He linked the transposon's sequence to a gene that would cause cells expressing that gene to turn blue when stained and put that DNA into fertilized mouse eggs. The marker gene turned developing nervous system tissue blue precisely where Bejerano expected it, he and his colleagues reported 14 May 2006 in *Nature*.

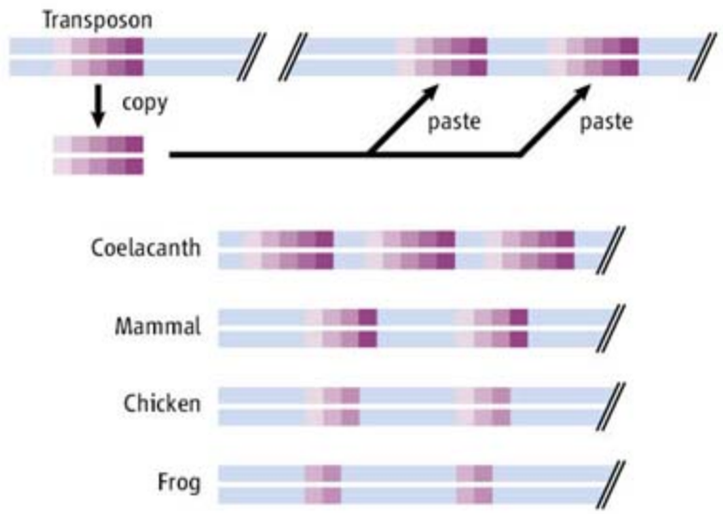

Jumping genes frozen through time. Transposons copy and paste themselves, proliferating throughout a genome. Most slowly mutate beyond recognition, but sometimes they persist, albeit in truncated forms. Those conserved in many species likely serve important functions.

Significant force

No one was sure, however, how frequently transposable elements were co-opted in this way. In theory, the odds are in the transposons' favor. "A transposon has no problem making 50,000 copies and splattering them throughout the genome," Haussler explains. Even if just one or two happen to land where they can be useful, they could still add up to be a powerful force in evolution. Yet "the impression was that there was a case here, a case there, that it was a really interesting fluke," Bejerano says. Now work by Bejerano and others has shown that functional transposable elements are more than a fluke.

Jerzy Jurka of the Genetic Information Research Institute in Mountain View, California, working with Kerstin Lindblad-Toh and Tarjei Mikkelsen, both from the Broad Institute, has found a surprisingly large role for transposons in the evolution of placental mammals. They compared the newly deciphered opossum genome to those of humans and other placental mammals to identify regions that were conserved in placental mammals but not found in this marsupial. These genetic innovations likely underlie the developmental and other differences between the two mammal groups. More than 95% of these innovations in the placental mammals were outside protein-coding genes, and 16% matched up to one of more than a dozen transposon families, the researchers reported in the 10 May issue of *Nature*. They conclude that transposable elements were likely instrumental for regulatory changes underlying features characteristic of placental mammals. "It's such a significant fraction that it can't be dismissed," Lander says.

Overall, Bejerano and his colleagues have just found more than 10,000 conserved transposons in the human genome, many dating back well before the split between placental and marsupial mammals. He and his colleagues first identified these sequences by looking for conserved stretches across a range of vertebrate genomes, including human, and subtracting out any that represented genes. They pinpointed transposon-derived DNA by matching up the shared sequences with known mobile elements in a database. The matches represent more than 5.5% of all the conserved noncoding sequence, he and his colleagues reported online 23 April in the *Proceedings of the National Academy of Sciences*.

At this point, the evidence for a role for most of these partially preserved transposons is circumstantial. Their conservation suggests they have a function; otherwise, they should slowly disappear. But new, more powerful tools for analyzing genomes in silico or for pinpointing where transcription factors bind DNA promise rapid progress toward understanding what these conserved transposons do (*Science*, 25 May, p. 1120). Says Bejerano: "We should have pretty spectacular answers pretty soon."

–ELIZABETH PENNISI

LETTERS

edited by Etta Kavanagh

Biofuels and the Environment

IN HIS EDITORIAL "THE BIOFUELS CONUNDRUM" (27 APRIL, P. 515), Donald Kennedy describes how biofuels, although at first glance a boon for the environment, have hidden costs that could prove environmentally and socially disastrous. His solution is "to abandon this cluttered arena" and to invest in research in plant physiology to overcome biomass recalcitrance for cellulosic conversion. There are several problems with this view. First, it is unlikely that a single approach will suit all circumstances. For example, gasification techniques seem efficient and promising for some feedstocks, but not all. Second, cellulosic conversion demands uniform feedstocks, which translates into high-input and environmentally destructive biofuel monocultures. Such monocultures are unlikely to be sustainable. Third, given the evolutionarily conserved structure of cell walls, it is possible that fooling with it would lead to crops that are prone to structural failure or, more likely, sensitivity to fungal pathogens.

A high-diversity, orchid-rich meadow in the White Carpathian Mountains, which has been mowed almost every year for half a millennium.

More research into plant physiology may help solve some of these problems, but perhaps some of our money is better spent supporting plant ecology. We already know that diverse grasslands can outperform monocultures in biofuels production (*1*). We also know that such grasslands are being lost or degraded worldwide because of a lack of active management. Learning how to use such grasslands sustainably for biofuels will not only reduce greenhouse gas emissions but also promote biodiversity. But we must first move away from a crop-based mentality and rely on expertise from a much broader scientific base than is currently being considered.

MICHAEL W. PALMER

Department of Botany, 104 LSE, Oklahoma State University, Stillwater, OK 74074, USA.

Reference

1. D. Tilman, J. Hill, C. Lehman, *Science* **314**, 1598 (2006).

DONALD KENNEDY'S EDITORIAL "THE BIOfuels conundrum" (27 April, p. 515) is timely and needed. However, we have two concerns. The first is that the suggested use of corn stover as a source for ethanol fuel has serious environmental implications. U.S. agriculture is currently losing topsoil 10 times faster than sustainability (*1*). Removing corn stover and/or leaving the soil unprotected will intensify soil erosion 10-fold or more (*2*). Without the protection of crop residues, soil loss may increase as much as 100-fold (*3*). Increasing soil erosion also intensifies the global warming problem and other problems (*4*, *5*).

Another concern is the fact that green plants collect little solar energy, an average of only 0.1% per year (*6*). Photovoltaics, in contrast, collect 10 to 20% of the solar energy or 100 to 200 times the rate of green plants (*6*).

Crops, forestry, and other green plants collect a total of 53 exajoules of solar energy per year from sunlight (*7*). However, Americans consume more than twice this amount of fossil fuel energy each year (*8*). Some suggest that ethanol produced from corn and cellulosic biomass could replace 30% of the oil used in the United States (*9*). Yet the 20% of the U.S. corn crop now converted into 5 billion gallons of ethanol replaces 1% of U.S. petroleum consumption (*6*). Ethanol yield from sugar is better, as documented in Brazil (Kennedy points this out), but the environmental, economic, and social costs are enormous. Soil erosion associated with sugarcane is greater than any other crop grown in Brazil (*10*).

DAVID PIMENTEL[1] AND RATTAN LAL[2]

[1]Cornell University, Ithaca, NY 14853, USA. [2]President, Soil Science Society of America, and Ohio State University, Columbus, OH 43210, USA.

References

1. NAS, *Frontiers in Agricultural Research: Food, Health, Environment, and Communities* (National Academies Press, Washington, DC, 2003).
2. M. Rasnake, Tillage and Crop Residue Management; see www.ca.uky.edu/agc/pubs/agr/agr99/agr99.htm (1999).
3. D. W. Fryrear, J. D. Bilbro, in *Managing Agricultural Residues*, P. W. Unger, Ed. (Lewis Publishers, Boca Raton, FL, 1994), pp. 7–18.
4. R. Lal, *Geoderma* **123**, 1 (2004).
5. R. Lal, *Soil Sci. Soc. Am.* **52** (no. 50), 12 (2007).
6. D. Pimentel, *Geotimes* **50**, 18 (2005).
7. D. Pimentel, T. Patzek, *Bioscience* **56**, 875 (2006).
8. USBC, *Statistical Abstracts of the United States* (U.S. Bureau of the Census, Washington, DC, 2007).
9. R. D. Perlack *et al.*, Biomass as Feedstock for a Bioenergy and Bioproducts Industry: Technical Feasibility of a Billion-Ton Annual Supply (U.S. Department of Energy Office of Energy Efficiency and Renewable Energy, Office of Biomass Program, and U.S. Department of Agriculture, Oak Ridge, TN, April 2005).
10. G. Sparovek, E. Schung, *Soil Sci. Soc. Am.* **65**, 1479 (2001).

Response

I'M HAPPY THAT PIMENTEL AND PALMER BOTH see the problems with biofuels, and I welcome their departure from that "cluttered space." Pimentel may be right about corn stover; I paired it with wood chips merely to illustrate a distinction and not to advocate its use. By all means, let's focus on other cellulose sources.

CREDIT: MICHAEL W. PALMER

Palmer is, in my view, too discouraged about the capacity of renewed emphasis on plant physiology and biochemistry to produce some solutions in this area. But he's dead right about ecology! Work as promising as Tilman's certainly deserves support.

DONALD KENNEDY

The Tobacco Industry and the Data Quality Act

REGARDING DONALD KENNEDY'S EDITORIAL on the Data Quality Act ("Turning the tables with Mary Jane," 4 May, p. 661), it is important to emphasize that the Data Quality Act is an industry-led initiative that gives private industry access to raw data from federally funded research. The Data Quality Act does not give independent researchers access to industry data to examine the completeness or accuracy of industry-generated research. The Editorial did not mention the leadership role that the Philip Morris Company played in the genesis of the Data Quality Act, as documented by Baba *et al.* (*1*).

In the mid-1990s, after failing to obtain raw data from federally funded researchers by asking for it or suing them, Philip Morris worked to change regulations governing the release of such data. They drafted model data access legislation in 1996 (*1*). In 1997, they met with the Center for Regulatory Effectiveness to seek support for their proposed legislation from the business coalitions that were already fighting the U.S. Environmental Protection Agency's outdoor air regulations (*1*). Part of Philip Morris's strategy was to form a coalition of industry supporters including the American Petroleum Institute, the National Rifle Association, and the Electric Power Research Institute. The Data Access Act was passed in 1998, followed by the Data Quality Act in 2000. Philip Morris then hired lobbyist Jim Tozzi to draft model guidelines for the agencies and meet with major companies to teach them how to use the new regulation to their benefit (*1*). The effects that the tobacco industry has on government regulatory process are still underestimated.

SUZAYNN FRANCINE SCHICK,[1] LISA ANNE BERO,[2] DANIEL M. COOK[3]

[1]Department of Medicine, University of California at San Francisco, San Francisco, CA 94110, USA. [2]Department of Clinical Pharmacy, University of California at San Francisco, San Francisco, CA 94118, USA. [3]School of Public Health, University of Nevada, Reno, NV 89557, USA.

Reference

1. A. Baba, D. M. Cook, T. O. McGarity, L. A. Bero, *Am. J. Public Health* **95** (suppl. 1), S20 (2005).

Explorer XII: Spinning Faster Than Expected

THE ARTICLES IN THE 13 APRIL ISSUE CONcerning sunlight changing the rotation rate of objects in space ("Direct detection of the asteroidal YORP effect," Reports, p. 272; "Spin rate of asteroid (54509) 2000 PH5 increasing due to the YORP effect," Reports, p. 274; "As tiny worlds turn," Perspectives, p. 211) brought back memories of the surprise researchers felt when the rotation rate of the Explorer XII satellite (launched 16 August 1961) did not decrease after launch, but increased instead. The solar paddles were oriented in a propeller fashion, and the effect of solar radiation was soon named the culprit. In this Earth-orbiting satellite, the spin rate increased for six months and decreased for six months.

DAVID H. SCHAEFER

George Mason University, Fairfax, VA 22030, USA. E-mail: Schaefer@gmu.edu

Response

SCHAEFER'S RECOLLECTION IS QUITE CORRECT as regards the unexpected variation in spin rate of Explorer XII (COSPAR designation 1961 ν). The spacecraft was launched into a highly eccentric orbit with an apogee altitude of about 12 Earth radii and a perigee altitude of about 790 km (*1*). Although there was concern about the aerodynamic effects on the spacecraft, the effects of radiation pressure were not anticipated. With the spacecraft spending most of its time well away from the atmosphere, the effects of radiation pressure became dramatically apparent in the increase of the spin rate.

In written and laboratory work (*2*–*4*) done by one of us (Paddack), a small test model was used in a vacuum chamber to show the effects of radiation pressure on a uniformly colored object. Consequently, the Radzievskii effect of variations of color (*5*) and the Crookes radiometer effect (*6*) were removed. By design, the test model had geometry similar to some of the early Explorer spacecraft. Paddack personally knew and consulted with J. V. Fedor, who analyzed and explained the Explorer 12 behavior (*7*).

There were others who contributed to this kind of work in the early years of the launch-

LIFE IN SCIENCE

Stop—Look—Jump

In 1994, I attended the Winter Gordon Conference on Electrochemistry. This meeting was particularly memorable in that the first morning of the conference coincided with the Northridge Earthquake, whose epicenter was about 50 miles away. Like the other attendees, I started my day at about 4:30 that morning. One consequence in the Ventura area was a loss of electrical power for most of that day, but the hotel was prepared with a backup generator. Given the disruption of the main 101 freeway in and out of town, everyone decided to go on with the meeting, as we had power for the slide projector (this is a primitive information transfer… oh, never mind).

Such dedication did not go unrewarded. During the second or third speaker's talk (about 10 a.m.), the first aftershock hit (being chemists, we somehow forgot all about aftershocks). We then noticed that the speaker was directly underneath one of the wonderful chandeliers you seem to see in California hotels and nowhere else—the ones with long, thick hanging glass prisms suspended on what seemed to be the thinnest of threads. This situation was pointed out to the speaker, who looked up, saw the swinging glass overhead, and then proceeded to jump backwards well clear of any danger (such athleticism is normally reserved for the afternoons at Gordon Conferences). Several attendees also noticed that they, too, were under chandeliers, and moved quickly and appropriately. A quick inspection after the shaking stopped revealed a small number of broken prisms on the carpeted floor, at which point heads started shaking instead.

So remember, prisms scatter more than light—they even scatter chemists.

PHIL SZUROMI

EDITOR'S NOTE

This will be an occasional feature highlighting some of the day-to-day humorous realities that face our readers. To prime the pump, we present the following. A group of us were sitting around over drinks at the AAAS Meeting talking about the strange events at lectures we had attended. The following is a gem from a *Science* staff member. Can you top this? Submit your best stories at www.submit2science.org.

CREDIT: PETER HOEY

ing of artificial satellites, including McElvain (*8*) and Clancy and Mitchell (*9*).

STEPHEN J. PADDACK (RETIRED) AND DAVID P. RUBINCAM

NASA Goddard Space Flight Center, Greenbelt, MD 20771, USA.

References

1. See http://nssdc.gsfc.nasa.gov/nmc/tmp/1961-020A-traj.html.
2. S. J. Paddack, *J. Geophys. Res.* **74**, 4379 (1969).
3. S. J. Paddack, Ph.D. dissertation, Catholic University, Washington, DC (1973).
4. S. J. Paddack, J. W. Rhee, *Geophys. Res. Lett.* **2**, 365 (1975).
5. V. V. Radzievskii, *Dokl. Acad. Nauk SSSR* **97** (no. 1), 49 (1954).
6. W. Crookes, *Philos. Trans. R. Soc. London* **166**, 325 (1876).
7. J. V. Fedor, The Effect of Solar Radiation Pressure on the Spin of Explorer XII (NASA TN D-1855, August 1963).
8. R. J. McElvain, in *Guidance and Control (Progress In Astronautics and Rocketry)*, vol. 8, R. E. Roberson, J. S. Farrior, Eds. (Academic Press, New York, 1962), pp. 543–564.
9. T. F. Clancy, T. P. Mitchell, "Effects of radiation forces upon the attitude of an artificial Earth satellite" (Center for Radiophysics and Space Research Report #129, Cornell University, Ithaca, NY, September 1962).

An Update on a Misconduct Investigation

IN THE ARTICLE "TRUTH AND CONSEQUENCES" (News Focus, 1 September 2006, p. 1222), J. Couzin described findings from an investigation at the University of Wisconsin, Madison, that raised questions about three peer-reviewed papers co-authored by Elizabeth Goodwin. In the case of the paper by O. Lakiza *et al.* (*1*), the Editor-in-Chief of *Developmental Biology* said that the authors were reviewing the relevant data. That statement was correct, but the inclusion of an image of a reprint of the paper may have left a negative impression in some readers' minds. Moreover, at the time of the article's publication, the case against Goodwin was not complete and the authors of the three papers were in no position to come to any conclusions about the matter.

The authors of Lakiza *et al.* received a draft of a statement from the University of Wisconsin report by e-mail that suggested a possible problem with two panels out of five in Fig. 1 (one of nine figures in the paper). We identified original data for Fig. 1 and did new experiments with independent methods and reagents to verify the conclusions that the paper reached from data presented in that figure. That process is now complete, and after peer review and scrutiny commensurate with the matter, the results have appeared in *Developmental Biology* (*2*). They verify the original conclusions of Fig. 1 of the paper, i.e., the presence of RNP complexes in vivo and the binding of GLD-1 protein to specific sequences in the 3′UTR of *tra-1*.

The additional validation work was undertaken with support from several labs and would not have been possible without their collective, independent help. Most noteworthy are the young scientists who worked so hard on the paper at early stages of their careers—because they are victims of this unfortunate situation and are doubly victimized if the conclusion the scientific community reaches is that this paper has no merit. Although the scientific results are the most important component of the vindication of the work, I feel strongly that we owe it to our young scientists to draw attention to the verification.

PHILIP M. IANNACCONE

George M. Eisenberg Professor, Deputy Director for Research, Children's Memorial Research Center, Northwestern University Feinberg School of Medicine, 2430 North Halsted Street, Chicago, IL 60614, USA.

References

1. O. Lakiza *et al.*, *Dev. Biol.* **287**, 98 (2005); Epub 29 September 2005.
2. O. Lakiza *et al.*, *Dev. Biol.* **307**, 551 (2007); Epub 19 April 2007.

CORRECTIONS AND CLARIFICATIONS

Reports: "Ultralow friction of carbonate faults caused by thermal decomposition" by R. Han *et al.* (11 May, p. 878). Color traces appeared incorrectly in Fig. 2D; Fig. 3, A, C, and D; and Fig. 4. The corrected figures are shown here.

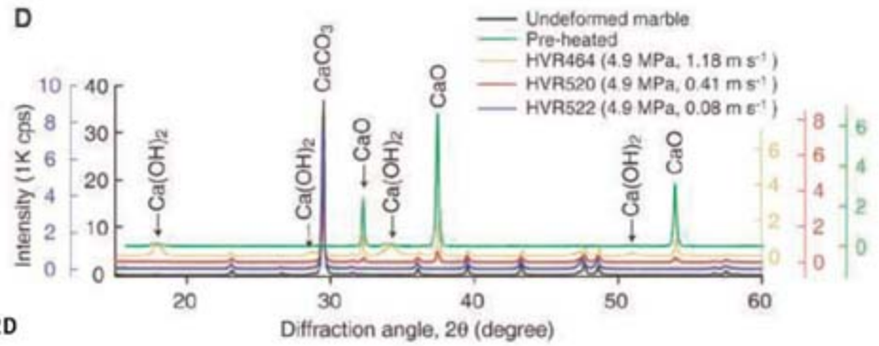

Fig. 2D

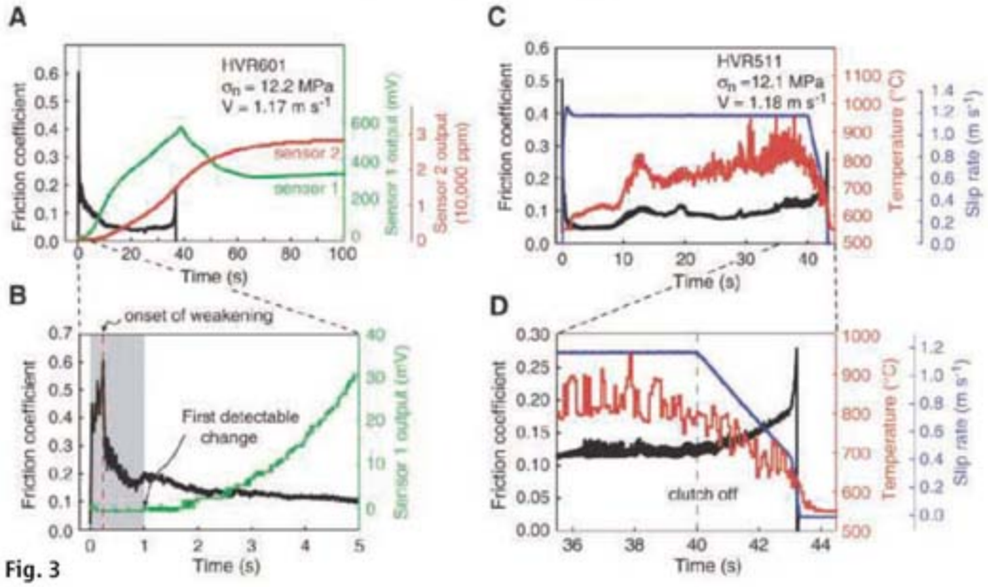

Fig. 3

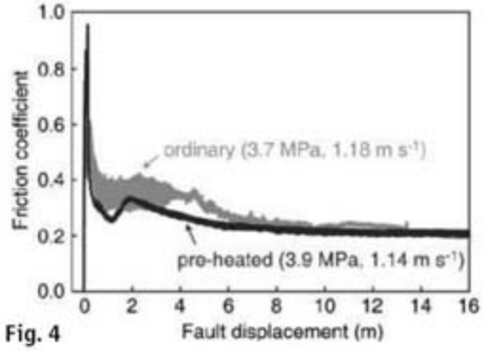

Fig. 4

Letters to the Editor

Letters (~300 words) discuss material published in *Science* in the previous 3 months or issues of general interest. They can be submitted through the Web (www.submit2science.org) or by regular mail (1200 New York Ave., NW, Washington, DC 20005, USA). Letters are not acknowledged upon receipt, nor are authors generally consulted before publication. Whether published in full or in part, letters are subject to editing for clarity and space.

SCIENCE AND SOCIETY

To Arbitrate or to Advocate?

Nathan E. Hultman

Perhaps there was a time when scientists found it easy to maintain a dispassionate separation from the big political questions of their day, toiling with utmost focus on formulating and investigating questions of theoretical importance without being asked by journalists, politicians, bureaucracies, and interest groups to interpret the "broader impact" of their inquiry and discovery. Although the reality of misty visions of past times can be debated, it is clear that present-day issues of science and society—climate change, stem cell research, genetically modified organisms, space research, and biofuels, to name just a few—challenge many scientists to contextualize their research in a wider social matrix. Yet navigating a path of responsible engagement in a loud and contested political context can try the integrity of even the most seasoned researchers; indeed, science is of course sometimes used as a shield for advancing individual political agendas, even by scientists themselves. Moreover, scientists often justify, sometimes under duress, their requests for funding by linking their research to broader societal benefits, even if their research has no such goal. In *The Honest Broker: Making Sense of Science in Policy and Politics*, Roger Pielke Jr. successfully illuminates these challenges to science and scientists. He also poses several reflexive questions that enable researchers to improve their contributions to the public interest.

The Honest Broker
Making Sense of Science in Policy and Politics

by Roger A. Pielke Jr.

Cambridge University Press, Cambridge, 2007. 198 pp. Paper, $29.99. ISBN 9780521694810.

Pielke (a professor in the Environmental Studies Program, University of Colorado) has contributed extensively to debates on climate change science and policy, especially on hurricane and storm damages. His perspectives on the scientific process and climate change also draw on his training as a political scientist, his familiarity with academic views of the role of scientists in policy, and his experience collaborating with his father, Roger Pielke Sr., an atmospheric scientist. The author's background gives him a broad vantage point from which to assess the problems that can arise when bringing scientific expertise into democratic debates.

In formulating his approach, Pielke addresses "scientists who increasingly face everyday decisions about how to position their careers and research in the context of policy and politics." To simplify his argument, he posits four idealized roles for an individual scientist: the disinterested pure scientist; the science arbiter, who provides expertise on narrowly defined, scientifically testable questions; the honest broker, who provides a suite of scientifically informed policy options (in much the same way that a travel guide provides information on restaurants or hotels in unfamiliar territory); and the overt advocate.

Pielke's framework provides a helpful starting point for investigating factors that complicate the science-society relationship. It highlights the question of what role individual scientists should play in a well-functioning democracy: Should a scientist engage in explicit interest-group politics in the Madisonian tradition or provide informed alternatives to politicians and decision-makers? It also illuminates different views of science in society: a linear model, whereby knowledge is created in the lab, packaged by scientific experts, and then handed off to politicians to do what they will; a stakeholder model, in which scientists-as-experts work to understand the interests of different groups and the users of knowledge themselves have some role in its production. Pielke has structured his four types such that the combinations of these two factors span the space of possible roles. The framework also incorporates aspects that explain why some debates tend to become vitriolic—for example, whether the decision at hand is characterized by consensus on values and low uncertainty, whether it is connected to a policy choice, and whether the chosen role of the scientist acts to restrict or expand possible choice for policy-makers. Pielke deftly shows how scientists' selections among these options can affect outcomes.

In making his case, Pielke illustrates possible missteps, focusing on researchers who claim to be acting in a nonpartisan way while simultaneously seeking to reduce society's scope of choices. He notes with obvious regret that "science has come to be viewed as simply a resource for enhancing the ability of groups in society to bargain, negotiate, and compromise in pursuit of their special interests." He also rues that "political battles are played out in the language of science, often resulting in policy gridlock and the diminishment of science as a resource for policy-making." His appropriate distaste for such "stealth issue advocates," however, occasionally strains the framework—in one example, Pielke says that a few well-known scientists "served as Stealth Issue Advocates when they claimed that [Bjørn] Lomborg has gotten his 'science' wrong, and because he has his 'science' wrong then necessarily those who accept his views of 'science' should lose out in political battle." Pielke's emphasis is specifically on the link between political argument and science, but one wishes for more guidance on how scientists might have better engaged in public disagreements over competing scientific approaches.

Government flanked by Magnanimity and Prudence. Detail from Ambrogio Lorenzetti's *Allegory of Good Government*, Palazzo Pubblico, Siena, Italy (1338–39).

CREDIT: ALINARI/ART RESOURCE, NY

Though some of his examples seem peripheral (such as an extended analogy to decision-making under uncertainty within the Bush doctrine of military preemption), Pielke provides useful and thought-provoking metaphors for discussing how best to engage in public debate. Indeed, he urges a more subtle view of this process precisely to improve discussions among the many stakeholders who have an interest in a better world: "The scientific community should … maintain its involvement in

The reviewer is at the Program in Science, Technology, and International Affairs, Georgetown University, Washington, DC 20057, USA. E-mail: neh3@georgetown.edu

contested political issues rather than withdraw, as was historically the case when scientists sought to be 'value free' and removed from practical concerns. It makes no sense to try to return to a bygone—and largely mythical—era when science was thought to be separate from politics." While *The Honest Broker* speaks to the academic literature of science in society—in particular on decision-making under uncertainty and on how scientists themselves can politicize science—the book's direct language and concrete examples convey the concepts to a wide audience. By categorizing different roles in the often vexed but necessary relations between scientists and their social world, Pielke clarifies choices not only for scientists but also for the diverse members of democratic society, for whom scientific perspectives are an essential component of better policy.

10.1126/science.1145781

NEUROSCIENCE

Wittgenstein and the Brain

Barry Dainton

"Whereof one cannot speak, thereof one must be silent." With this now-famous line Ludwig Wittgenstein brought to a close *Tractatus Logico-Philosophicus*, his first great work (*1*). The lines that bring to a close his second great work, *Philosophical Investigations* (*2*), are rather less well known; they include: "The confusion and barrenness of psychology is not to be explained by calling it a 'young science' … in psychology there are experimental methods and conceptual confusion." The alleged confusion stems from certain prevalent ways of thinking about the mental realm that Wittgenstein held to be disastrously misguided. These same ways of thinking are also prevalent, to equally disastrous effect, in contemporary neuroscience, or so philosopher Peter Hacker and neuroscientist Maxwell Bennett argue over the 450 or so Wittgenstein-inspired pages of *Philosophical Foundations of Neuroscience* (*3*). *Neuroscience and Philosophy*, the present (and much briefer) work, is a useful introduction to their position. It contains several extracts from *Foundations*, together with critical surveys by John Searle and Daniel Dennett—derived from an "authors and critics" session at the 2005 American Philosophical Association meeting—and responses from Bennett and Hacker (henceforth "B&H").

Neuroscience and Philosophy
Brain, Mind, and Language

by Maxwell Bennett, Daniel Dennett, Peter Hacker, and John Searle

Columbia University Press, New York, 2007. 227 pp. $25.50, £16. ISBN 9780231140447.

There are several strands to B&H's case, some more contentious than others. Quoting from the like of Blakemore, Crick, Edelman, Frisby, Marr, and Young, they show that neuroscientists commonly talk of subsystems within the brain storing maps, representations, and information; forming hypotheses; or passing "symbols" and "messages" to each other. Much of this talk, they argue, is disguised nonsense. To take just one example, for something to be a map in the ordinary sense of the term, in addition to certain similarities of structure between the map and what it depicts, there are also rules and conventions that allow someone who understands them to know what parts or aspects of the world the map is representing. Because so-called neural maps are typically not associated with such conventions, it is wrong to suppose they "represent" in the way of ordinary maps, although some neuroscientists talk as if they do. Dennett complains that B&H are too conservative by far when it comes to recognizing legitimate and fruitful extensions to the way terms are normally used—such extensions are commonplace in all sciences. He may well be right. But B&H are also right to insist that such extensions must be carefully considered. (Indeed, Dennett's own willingness to ascribe beliefs and intentions to systems as simple as thermostats strikes some as an ill-considered extension of ordinary usage.)

So far so good, but what B&H themselves describe as their main line of argument is more problematic and less obviously of potential use to practicing neuroscientists.

Although Sherrington, Eccles, and Penfield may have subscribed to variants of mind-body dualism, contemporary neuroscientists are generally of the opinion that our mental lives are material in nature and completely dependent upon neural goings-on in our brains. Yet B&H claim that the field remains committed to a pernicious form of dualism. Why so? Because these same neuroscientists hold that brains can think thoughts, have experiences, take decisions, hold grudges, remember past events, and so forth. B&H claim this too is just nonsense. For it is not brains that have thoughts and experiences, it is human beings—i.e., whole human animals. B&H do not deny that our mental lives depend on our brains, but they insist that to ascribe mental powers to brains is as senseless as ascribing mental powers to numbers.

This claim will strike many as bizarre in the extreme. What are their grounds for making it? Their reasoning derives from Wittgenstein, who wrote: "Only of a human being and what resembles (behaves like) a living human being can one say: it has sensations; it sees, is blind; hears, is deaf; is conscious or unconscious." Like Wittgenstein, B&H hold that when it comes to the correct ascription of mental states and processes, it is a subject's capacities for publicly observable behavior that are significant, not what is going on inside the subject (or her or his mind or consciousness). Simplifying only a little, because brains are incapable of the relevant forms of behavior—they can't walk, talk, flinch, point, or run around—it is senseless to ascribe mental attributes to them.

This neobehaviorist conception of the mental is not obviously correct, to say the least. The idea that conscious states possess an inner, subjective and private character—a character that is essential to their being conscious states at all—is a very natural one. As Searle notes in his contribution, Wittgensteinians can plausibly be seen as conflating the external (behavioral) evidence for consciousness with the existence of consciousness. What B&H offer here on these matters is not compelling; they say a good deal more in *Foundations*.

This much-disputed topic aside, B&H's attitude to the brain is vulnerable to a more straightforward objection. I am currently able to think. It seems very plausible to think that I would continue to have this ability if I were reduced to the condition of a healthy living brain (maintained by life-support machinery, say). If I am essentially a human being, as B&H suggest, then I am still a human being in my diminished condition. But because I am now indistinguishable from my brain—we are composed of precisely the same atoms—how can it be senseless to say that brains can think? If there's nothing to distinguish me from my brain, won't my brain be able to do everything I can do?

References

1. L. Wittgenstein, *Tractatus Logico-Philosophicus* (Kegan Paul, Trench, Trübner, London, 1922).
2. L. Wittgenstein, *Philosophical Investigations* (Blackwell, Oxford, 1953).
3. M. R. Bennett, P. M. S. Hacker, *Philosophical Foundations of Neuroscience* (Blackwell, Oxford, 2003).

10.1126/science.1144965

The reviewer is at the Department of Philosophy, University of Liverpool, 7 Abercromby Square, Liverpool L69 7WY, UK. E-mail: bdainton@liv.ac.uk

ENVIRONMENT

Carbon Mitigation by Biofuels or by Saving and Restoring Forests?

The carbon sequestered by restoring forests is greater than the emissions avoided by the use of the liquid biofuels.

Renton Righelato* and Dominick V. Spracklen

Choosing from among the host of strategies for mitigation of anthropogenic carbon emissions is not easy. There are competing environmental priorities, social and economic factors, and commercial and political interests. One strategy that has received extensive attention is the use of biofuels for transport, particularly ethanol from fermentation of carbohydrate crops as a substitute for petrol and vegetable oils in place of diesel fuel. Such an approach would require very large areas of land in order to make a significant contribution to mitigation of fossil fuel emissions and would, directly or indirectly, put further pressure on natural forests and grasslands. There are numerous assessments of the relative merits of different liquid biofuel strategies (e.g., *1*–*3*), but few compare these with other uses of land (*4*).

Two issues need to be addressed before the efficacy of biofuels can be assessed: the net reduction in fossil carbon emissions (avoided emissions) arising from use of agriculturally derived biofuels and the effect of alternative land-use strategies on carbon stores in the biosphere. As land is the limiting resource, the appropriate basis for comparison is a function of land area (Mg C ha^{-1} $year^{-1}$). We use a period of 30 years as a basis for comparing strategies because it is likely to take that much time for carbon-free fuel technologies to be developed and introduced. Estimates of avoided emissions vary widely depending on crop, fuel type, and conversion technology used; some typical examples derived from life-cycle analyses are shown in the figure (right). In these analyses, no allowance has been made for emissions arising from change in land use to produce the fuel crop. In all cases, forestation of an equivalent area of land would sequester two to nine times more carbon over a 30-year period than the emissions avoided by the use of the biofuel. Taking this opportunity cost into account, the emissions cost of liquid biofuels exceeds that of fossil fuels.

Moreover, large areas of land would be needed to make significant quantities of fuel. A 10% substitution of petrol and diesel fuel is estimated to require 43% and 38% of current cropland area in the United States and Europe, respectively (*5*). As even this low substitution level cannot be met from existing arable land, forests and grasslands would need to be cleared to enable production of the energy crops. Clearance results in the rapid oxidation of carbon stores in the vegetation and soil, creating a large up-front emissions cost (*6*) that would, in all cases examined here, outweigh the avoided emissions.

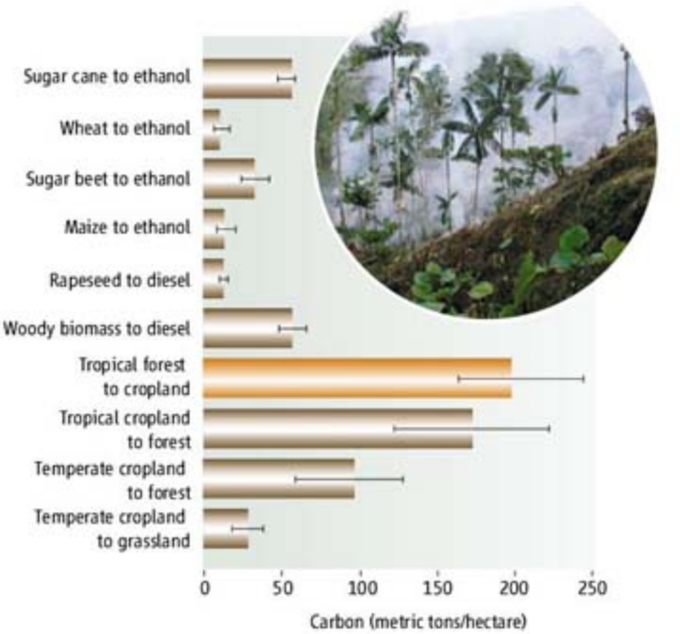

Cumulative avoided emissions per hectare over 30 years for a range of biofuels compared with the carbon sequestered over 30 years by changing cropland to forest and the loss of carbon to the atmosphere by conversion of forest to cropland. Error bars indicate the ranges of values in the literature cited. Details are in the SOM.

Of the biofuel sources shown, only conversion of woody biomass (*1*, *2*, *4*, *7*) may be compatible with retention of forest carbon stocks. Woody biomass can be used directly for fuel or converted to liquid fuels. Although still in a development stage, avoided emissions in temperate zones appear similar to assimilation by forest restoration. Moreover, it may be possible to avoid environmental problems associated with extensive monoculture (*8*) by harvesting from standing forests. In this case, soil and above-ground carbon stocks may be built up in parallel with sustainable harvesting for fuel production.

If the prime object of policy on biofuels is mitigation of carbon dioxide–driven global warming, policy-makers may be better advised in the short term (30 years or so) to focus on increasing the efficiency of fossil fuel use, to conserve the existing forests and savannahs, and to restore natural forest and grassland habitats on cropland that is not needed for food. In addition to reducing net carbon dioxide flux to the atmosphere, conversion of large areas of land back to secondary forest provides other environmental services (such as prevention of desertification, provision of forest products, maintenance of biological diversity, and regional climate regulation), whereas conversion of large areas of land to biofuel crops may place additional strains on the environment. For the longer term, carbon-free transport fuel technologies are needed to replace fossil hydrocarbons.

R. Righelato, World Land Trust, Halesworth, Suffolk, IP19 8AB; D. V. Spracklen, School of Earth and Environment, University of Leeds, Leeds, UK.

*Author for correspondence. E-mail: renton@worldlandtrust.org

References

1. *Well-to-Wheels Analysis of Future Automotive Fuels and Powertrains in the European Context* [European Council for Automotive R&D (EUCAR), European Commission Joint Research Center (JRC), and Conservation of Clean Air and Water in Europe (CONCAWE) joint study, Brussels, May 2006); http://ies.jrc.ec.europa.eu/wtw.html.
2. E. Larson, "A review of LCA studies on liquid biofuels for the transport sector," Scientific and Technical Advisory Panel of the Global Environment Facility (STAP) workshop on Liquid Biofuels, 29 August to 1 September 2005, New Delhi, India; http://stapgef.unep.org/docs/folder.2005-12-07.8158774253/folder.2005-12-08.9446059805/.
3. M. A. Elsayed, R. Mathews, N. D. Mortimer, *Carbon and Energy Balances for a Range of Biofuel Options* (Resources Research Institute, Sheffield Hallam University, Sheffield, UK, 2003).
4. M. U. F. Kirschbaum, *Biomass Bioenergy* **24**, 297 (2003).
5. International Energy Authority, *Biofuels for Transport: An International Perspective* (IEA, Paris, France, 2004), chap. 6; www.iea.org/textbase/nppdf/free/2004/biofuels2004.pdf.
6. R. T. Watson *et al.*, *Land Use, Land-Use Change and Forestry* (Intergovernmental Panel for Climate Change, Geneva, 2001), p 184.
7. D. Tilman, J. Hill, C. Lehman, *Science* **314**, 1598 (2006).
8. S. Raghu *et al.*, *Science* **313**, 1742 (2006).

Supporting Online Material
www.sciencemag.org/cgi/content/full/317/5840/902/DC1

10.1126/science.1141361

PHOTO CREDIT: WORLD LAND TRUST

BIOCHEMISTRY

Getting Into and Through the Outer Membrane

The structures of two related bacterial membrane proteins help to understand protein transport processes in the outer membranes of bacteria, mitochondria, and chloroplasts.

Jan Tommassen

Two membranes surround Gram-negative bacteria, as well as mitochondria and chloroplasts in eukaryotes. Transport of proteins into or through the outer of these membranes usually requires complex molecular machines. Omp85, an evolutionary conserved protein, is the central component of the machine required for folding and inserting outer membrane proteins (OMPs) (*1*). Moreover, some OMPs with sequence similarity to Omp85 are involved in transport processes such as protein secretion in bacteria and protein import into chloroplasts (*2*). In this issue, Kim *et al.* (p. 961) and Clantin *et al.* (p. 957) provide insights into the structures of members of this protein superfamily (*3*, *4*).

The bacterial Omp85 consists of a membrane-embedded β barrel and an amino (N)–terminal periplasmic extension encompassing five polypeptide transport–associated (POTRA) domains. It interacts directly with its substrate proteins (*5*) and is part of a complex that also contains four lipoproteins, YfiO, YfgL, NlpB, and SmpA, of which only one, YfiO, is essential (*6*, *7*). The mitochondrial Omp85 homolog contains only one POTRA domain, which directly interacts with substrate proteins (*8*). The accessory lipoproteins are not found in the mitochondrial system.

Kim *et al.* (*3*) report the structure of a fragment of the Omp85-family member YaeT from *Escherichia coli*. The fragment encompasses four complete POTRA domains and, at the carboxyl (C) terminus, a short segment of the fifth one. Each POTRA domain consists of a three-stranded β sheet and two α helices. In the crystal, the fragment forms a dimer as a result of the augmentation of the β-sheet in POTRA-3 with a β strand formed at the C-terminal end of the other subunit. Although this dimer is a crystallization artifact, the dimer interface may reflect the way in which YaeT interacts with its substrates; this interaction involves a signature motif that forms a β strand at the C termini of these proteins (*5*). Thus, like the POTRA-5 segment in the crystallized YaeT fragment, this signature motif forms a β strand at the C termini of these proteins.

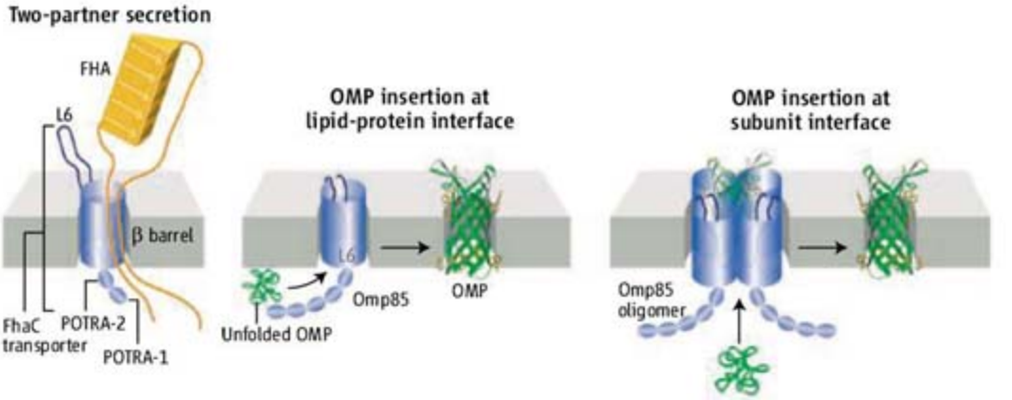

Protein traffic in the outer membrane. (Left) Clantin *et al.* suggest that in two-partner secretion, substrate binding to POTRA-1 opens a channel in the FhaC transporter by displacement of pore-blocking segments (L6). Extracellular folding of the secreted FHA protein into a β helix probably provides energy for transport. **(Middle)** Binding of an OMP to the POTRA domains of an Omp85 protein, such as YaeT studied by Kim *et al.*, results in outer membrane insertion, possibly at the protein/lipid interface. For simplicity, accessory proteins of the Omp85 complex are not shown. **(Right)** A central channel formed by oligomers of Omp85 superfamily members might provide an alternative route for insertion and/or translocation.

Kim *et al.* investigated the possibility that the subunit interface is involved in substrate recognition. Mutations in POTRA-3 that should prevent β augmentation did not interfere with YaeT function but with binding of the YfgL subunit of the machine. Thus, POTRA-3 may bind YfgL by β augmentation. In a series of mutants in which all POTRA domains were deleted one at a time, all deletions severely infringed function. Furthermore, deletion of POTRA-2, -3, -4, and -5 each resulted in loss of YfgL from the machine. Deletion of POTRA-5, which shows the highest sequence conservation of all POTRA domains (*1*), resulted in loss of all accessory lipoproteins.

Clantin *et al.* (*4*) solved the structure of FhaC, a member of the Omp85 superfamily involved in the secretion of filamentous hemagglutinin (FHA) in *Bordetella pertussis* via a pathway known as two-partner secretion. The structure shows a β barrel and an N-terminal extension consisting of an α helix and two periplasmic POTRA domains structurally resembling those of YaeT. The β barrel consists of 16 antiparallel β strands connected by short turns at the periplasmic side and long loops at the cell surface. The channel within the barrel is occluded by loop L6, which folds into the barrel, and by the N-terminal α helix, which spans the channel interior. The residual opening of 3 Å is too narrow to allow for transport of a protein, even in an extended conformation.

However, upon reconstitution of FhaC into planar lipid bilayers and application of a transmembrane potential, much wider channels were revealed with a conductivity of 1200 pS (*9*), corresponding to channel widths of 8 to 10 Å. Thus, the channel appears to be dynamic: Upon binding of FHA to POTRA-1 (*4*), the channel may open by extrusion of the α helix and/or loop L6, thus creating a protein translocation pathway (see the figure, left panel). Previous work indeed showed a topological rearrangement in L6 upon coexpression of FHA (*10*).

What can we learn from the FhaC structure about the C-terminal domain of Omp85 proteins? Omp85 showed much narrower channels in planar lipid bilayers than FhaC. Their conductivity of 120 pS (*5*) could correspond to the closed channels observed in the FhaC crystal structure. Omp85 sequences show a conserved motif that corresponds to the L6 loop of FhaC, but no segment corresponding to the N-terminal helix. Thus, assuming that Omp85 has a similar 16-stranded β barrel as FhaC, another loop besides L6 should contribute to closing the channel.

In the planar lipid bilayer experiments, substrate binding increased the channel activity of Omp85 (*5*), but this increased activity reflected a higher probability for the open state, rather than a widening of the low-conductance chan-

The author is in the Department of Molecular Microbiology and the Institute of Biomembranes, Utrecht University, 3584 CH Utrecht, The Netherlands. E-mail: j.p.m.tommassen@uu.nl

nels. Hence, there is no indication that Omp85 channels can open by displacement of pore-blocking segments. Indeed, it is unlikely that OMPs would insert into the β barrel of Omp85, because it is difficult to envisage how such a barrel could subsequently open laterally to allow for OMP insertion into the membrane. Rather, OMPs will insert at the lipid/protein interface (see the figure, middle panel) or at the subunit interface of an oligomeric complex (see the figure, right panel).

Omp85 forms defined homo-oligomeric complexes in vitro (*5*). Similarly, HMW1B, an FhaC homolog involved in two-partner secretion in *Haemophilus influenzae*, has been purified from the outer membrane as a tetramer (*11*). In liposome-swelling assays, both proteins showed pore sizes of 2.5 to 2.7 nm—much wider than the channel within the FhaC β barrel. Furthermore, electron microscopy has shown that the HMW1B oligomer formed ringlike structures with a central cavity of 2.5 nm (*11*). The possible involvement of these wide channels in protein traffic (see the figure, right panel) needs to be investigated.

The mechanism and the pathway of protein traffic via members of the Omp85 superfamily is still far from understood. Future experiments should focus on the characterization of the oligomeric complexes and on the development of in vitro systems with purified components to study these processes.

References

1. R. Voulhoux, M. P. Bos, J. Geurtsen, M. Mols, J. Tommassen, *Science* **299**, 262 (2003).
2. I. E. Gentle, L. Burri, T. Lithgow, *Mol. Microbiol.* **58**, 1216 (2005).
3. S. Kim *et al.*, *Science* **317**, 961 (2007).
4. B. Clantin *et al.*, *Science* **317**, 957 (2007).
5. V. Robert *et al.*, *PLoS Biol.* **4**, e377 (2006).
6. T. Wu *et al.*, *Cell* **121**, 235 (2005).
7. J. G. Sklar *et al.*, *Proc. Natl. Acad. Sci. U.S.A.* **104**, 6400 (2007).
8. S. J. Habib *et al.*, *J. Cell. Biol.* **176**, 77 (2007).
9. F. Jacob-Dubuisson *et al.*, *J. Biol. Chem.* **274**, 37731 (1999).
10. S. Guédin *et al.*, *J. Biol. Chem.* **275**, 30202 (2000).
11. N. K. Surana *et al.*, *Proc. Natl. Acad. Sci. U.S.A.* **101**, 14497 (2004).

10.1126/science.1146518

CELL BIOLOGY

Aneuploidy in the Balance

An extra chromosome slows yeast cell proliferation, suggesting that aneuploid human cells must overcome this effect during carcinogenesis.

Prasad V. Jallepalli and David Pellman

A central principle of genetics is that cells within an organism contain the same complement of chromosomes. The presence of too many or too few chromosomes, called aneuploidy, is associated with disease, and accounts for the majority of spontaneous miscarriages in humans, as well as hereditary birth defects such as Down syndrome (*1*). Precisely how aneuploidy affects cells is not well understood. Extra chromosomes cause a proportionate increase in gene expression (*2*), potentially altering a cell's dosage of proteins in damaging ways. On the other hand, most cancer cells are aneuploid, suggesting that some patterns of chromosome gain and loss enable cells to escape normal growth restraints and develop into malignant tumors—for example, by acquiring extra copies of an oncogene, or losing a tumor suppressor gene (*3*, *4*). But are the effects of aneuploidy strictly specific to a given over- or underrepresented chromosome, or does aneuploidy evoke a generalized physiological response regardless of what chromosome is affected? A new study by Torres *et al.* (*5*) on page 916 of this issue uncovers characteristics shared by all aneuploid cells, identifying a broad cellular response to aneuploidy that has ramifications for better understanding aneuploidy-linked diseases in humans.

Torres *et al.* analyzed the budding yeast *Saccharomyces cerevisiae*, a well-established and tractable system for studying chromosome segregation errors (*6*). In general, aneuploid yeast cells are at a substantial competitive disadvantage relative to cells with a normal complement of chromosomes (euploids) because they are eventually overtaken by spontaneously arising euploid revertants (*7*, *8*). However, aneuploidy can be beneficial in the presence of strong selective pressure (*9*, *10*). For example, where yeast has two similar genes on different chromosomes, cells in which one of these paralogs is deleted may compensate by the chance gain of an extra copy of the chromosome bearing the other paralog (*10*). Torres *et al.* engineered yeast strains to contain two copies of specific chromosomes (disomes) on an otherwise haploid genetic background. By varying the identity of the extra chromosome, the authors generated disomic strains encompassing 13 of the 16 yeast chromosomes. As expected, genes present on disomic chromosomes were transcribed at about twice their normal levels. However, after correcting for this effect, two groups of genes were coordinately up-regulated in many different aneuploid strains. One cluster, previously characterized as part of the environmental stress response, is also induced in many slow-growing but euploid strains. However, the other cluster, whose expression increased in aneuploid strains independently of growth rate, includes genes involved in ribosome biogenesis. Ribosome biogenesis consumes roughly half of the metabolic energy of a proliferating yeast cell, and it is tightly coupled to signaling pathways that regulate progress through the G_1 phase of the cell division cycle (*11*). Indeed, a substantial fraction of the aneuploid strains examined by Torres *et al.* exhibited a delay in cell cycle entry and an increase in cell size, demonstrating a

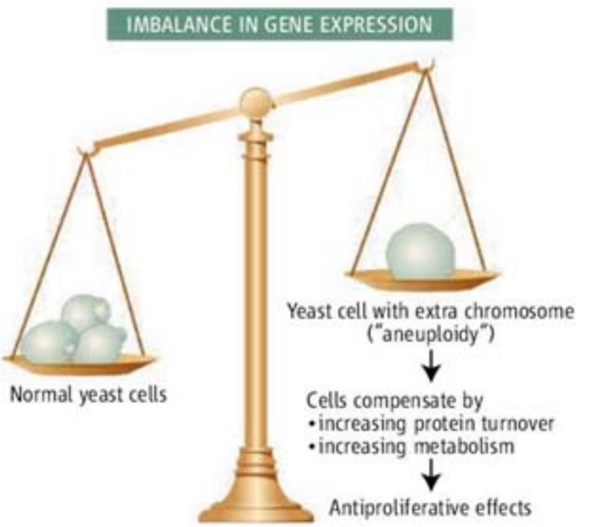

More genes but less fit. Yeast cells that gain an extra chromosome are at a proliferative disadvantage relative to normal cells, regardless of the specific chromosome gained. Aneuploid cells try to compensate for the gene imbalance by increasing protein turnover, which requires more energy and slows down proliferation. Cancer cells somehow overcome the antiproliferative effect of aneuploidy.

CREDIT: P. HUEY/SCIENCE

P. V. Jallepalli is at the Molecular Biology Program, Memorial Sloan-Kettering Cancer Center, New York, NY 10021, USA. E-mail: jallepap@mskcc.org D. Pellman is at the Dana-Farber Cancer Institute, Boston, MA 02115, USA. E-mail: david_pellman@dfci.harvard.edu

functional impact of supernumerary chromosomes on cell proliferation. Identifying the molecular nature of this signal will be of considerable interest.

The authors found that aneuploidy also strongly affects cell metabolism. The aneuploid strains avidly take up glucose, and many also undergo amplification of genes encoding glucose transporters. However, glucose is used less efficiently in these cells, resulting in lower accumulated biomass per unit of glucose. This is intriguing given that many tumor cells exhibit the "Warburg effect" (*12*), in which glycolysis (anaerobic metabolism) is emphasized at the expense of mitochondrial (aerobic) respiration. Although *S. cerevisiae* has a unique physiology that emphasizes fermentation relative to respiration, it will be interesting to determine whether aneuploidy elicits a similar metabolic effect in mammalian cells.

What is the basis for the increased glucose requirement in the yeast aneuploids? Torres *et al*. propose a simple and intuitive explanation. Although transcripts from the disomic chromosome doubled in abundance, steady-state levels of many proteins encoded by these transcripts did not. The aneuploid strains are also sensitive to compounds that inhibit protein translation or block protein degradation by proteasomes. Thus, the gene expression imbalance leads to compensatory proteolysis, which demands more energy (see the figure). Furthermore, analysis of strains harboring large human genomic DNA fragments as yeast artificial chromosomes, which are not expected to be transcribed or translated to any great extent, did not exhibit a growth delay or drug sensitivities associated with authentic yeast disomes, indicating that these phenotypes are triggered by increases in gene expression rather than the presence of extra DNA.

The results of Torres *et al*. and earlier studies of fibroblasts obtained from Down syndrome patients (*13*) indicate that a single extra chromosome can exert a strong antiproliferative effect in both yeast and human cells. If this is the case, then how do aneuploid cancer cells overcome this barrier? There are at least two possibilities. There may be a protective effect of diploidy, as Torres *et al*. found that deleterious consequences of an extra chromosome are less severe in diploid cells than in haploids. This is consistent with previous mathematical analyses showing that increases in the number of sets of chromosomes (ploidy) can buffer the effects of harmful somatic mutations in the short term (*14*). Some cancers may arise through a tetraploid intermediate (*15*), which could enhance this buffering effect. This may explain why yeast tetraploids exhibit high rates of chromosome loss but lack detectable delays in cell cycle progression (*16*). In addition, genes in mammalian cells can be transcriptionally silenced through mechanisms not available in yeast. For instance, most cancer cells exhibit localized chemical modification (hypermethylation) of specific stretches of DNA (CpG islands) in promoter regions of genes (*17*). This could lessen the metabolic impact of aneuploidy by silencing genes on a supernumerary chromosome while preserving expression of other genes on the chromosome that confer a selective clonal advantage. Nonetheless, if at least a portion of the transcriptional and phenotypic response to aneuploidy persists in cancer cells, it may be possible to devise inhibitors that arrest or kill such aneuploid cells selectively, with little or no impact on normal diploid tissues (*18*).

References and Notes

1. T. J. Hassold, P. A. Jacobs, *Annu. Rev. Genet.* **18**, 69 (1984).
2. M. B. Upender *et al.*, *Cancer Res.* **64**, 6941 (2004).
3. M. A. Nowak, *Proc. Natl. Acad. Sci. U.S.A.* **99**, 16226 (2002).
4. H. H. Rajagopalan, C. C. Lengauer, *Nature* **432**, 338 (2004).
5. E. M. Torres *et al.*, *Science* **317**, 916 (2007).
6. M. Brown *et al.*, *Cold Spring Harbor Symp. Quant. Biol.* **56**, 359 (1991).
7. S. K. Waghmare, C. V. Bruschi, *Yeast* **22**, 625 (2005).
8. Y. Zang, M. Garre, K. Gjuracic, C. V. Bruschi, *Yeast* **19**, 553 (2002).
9. M. J. Dunham *et al.*, *Proc. Natl. Acad. Sci. U.S.A.* **99**, 16144 (2002).
10. T. R. Hughes *et al.*, *Nat. Genet.* **25**, 333 (2000).
11. P. Jorgensen *et al.*, *Genes Dev.* **18**, 2491 (2004).
12. O. Warburg, *Science* **123**, 309 (1965).
13. D. J. Segal, E. E. McCoy, *J. Cell Physiol.* **83**, 85 (1974).
14. H. A. Orr, *Genetics* **139**, 1441 (1995).
15. Z. Storchova, D. Pellman, *Nat. Rev. Mol. Cell Biol.* **5**, 45 (2004).
16. Z. Storchova *et al.*, *Nature* **443**, 541 (2006).
17. M. Esteller, *Nat. Rev. Genet.* **8**, 286 (2007).
18. P. V. Jallepalli, C. Lengauer, *Nat. Rev. Cancer* **1**, 109 (2001).

19. Work in the laboratories of P.V.J. and D.P. is supported by NIH grants CA107342 (P.V.J.) and CA098537 and GM061345 (D.P.).

10.1126/science.1146857

GEOPHYSICS

The Need to Study Speed

Shamita Das

Rapid ruptures can cause more earthquake damage than slow ones. Lessons from past events indicate which faults may be most dangerous.

The damage earthquakes cause to society depends in part on how fast rock ruptures (*1*). During the 1960s, owing partly to limited observation and partly to inadequate theory, researchers believed that ruptures could not propagate faster than about 3 km/s, the speed of a transvere (shear) wave moving in rock. Several theoretical studies in the 1970s found that some ruptures could exceed this speed, perhaps reaching 5 km/s (*2*). Recently, Bhat *et al*. reported field observations showing that an earthquake in Tibet ruptured faster than the shear wave speed (*3*). Given the potential for increased destruction, we must take such information into account when planning earthquake-resistant construction worldwide.

The first earthquake that ruptured faster than the shear speed was the 1979 Imperial Valley, California, event (*4*). No other example was found for two decades, supporting those who resisted the idea of supershear rupture speeds. However, starting in 1999, researchers began to measure fast rupture speeds (*5, 6*) in the laboratory. The improvement in quality and quantity of seismometers worldwide also led to new reports of supershear rupture speeds (*7*). Yet, because these reports were based on analysis of very few seismograms, few accepted the possibility of supershear rupture speeds.

Then in 2003, Bouchon and Vallée reported convincing evidence of supershear rupture speed for the 2001 Kunlunshan, Tibet, earthquake (magnitude M_w = 7.8) (*8*). This earthquake, in which the net slip was in the direction of the surface path of the fault (a strike-slip fault), ruptured a segment longer than 400 km, the longest strike-slip fault rupture (both on land and under water) since the 1906 California earthquake. Robinson *et al*. (*9*) showed that the rupture started slowly, accelerated to a supershear wave speed, and then propagated over more than 100 km at a speed of nearly 6 km/s, before slowing and stopping (see the figure, left panel). The region of very high rupture speed coincided with the region of highest earthquake displacement, highest fault slip-rate, and highest stress release and occurred on a very straight portion of the fault.

The author is in the Department of Earth Sciences, University of Oxford, Parks Road, Oxford OX1 3PR, UK. E-mail: das@earth.ox.ac.uk

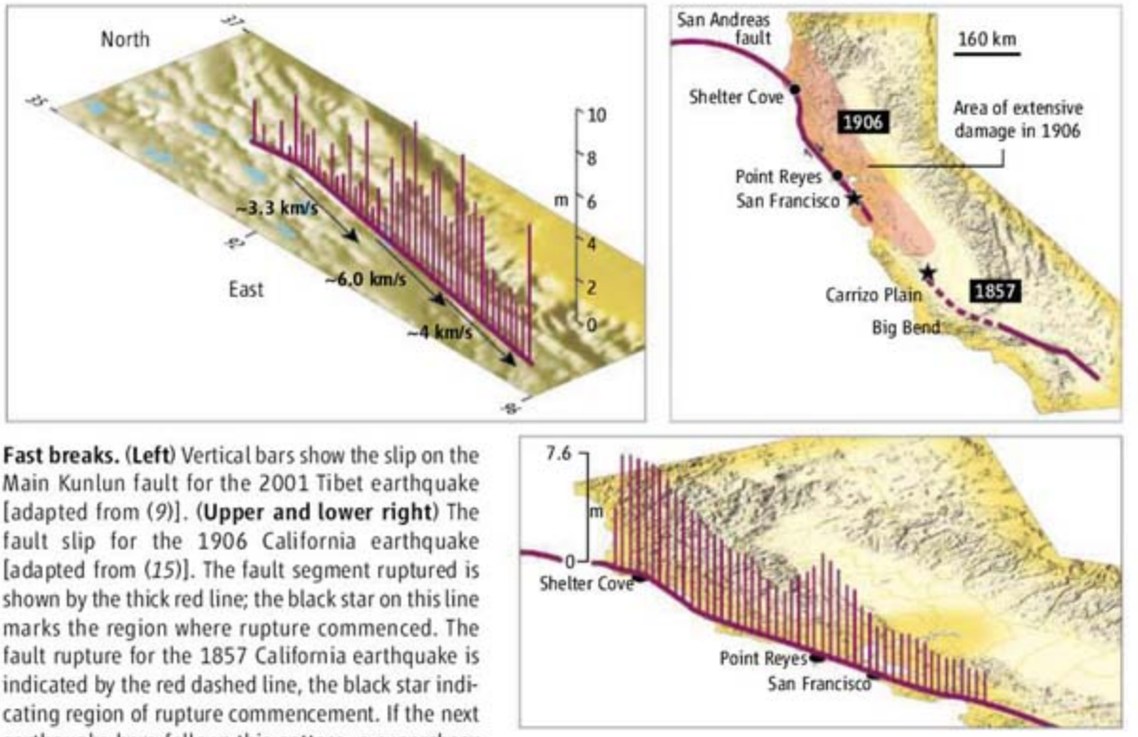

Fast breaks. (Left) Vertical bars show the slip on the Main Kunlun fault for the 2001 Tibet earthquake [adapted from (*9*)]. **(Upper and lower right)** The fault slip for the 1906 California earthquake [adapted from (*15*)]. The fault segment ruptured is shown by the thick red line; the black star on this line marks the region where rupture commenced. The fault rupture for the 1857 California earthquake is indicated by the red dashed line, the black star indicating region of rupture commencement. If the next earthquake here follows this pattern, a supershear rupture propagating southward would strongly focus shock waves on Santa Barbara and Los Angeles.

High slip rate (the relative speed of the two sides of the fault) may drastically lower the friction on the fault (*10, 11*), allowing much higher rupture speed (the speed at which the two sides separate at the leading edge of the fault). In the Kunlun earthquake, the region of large displacement has been separately confirmed from satellite measurements (*12*). In addition, field observations, made several months later by Bhat *et al*., showed a ~25-km-wide region to the south of the supershear rupture section of the fault with many off-fault open cracks (*3*). Calculations show that as the rupture moves from sub- to supershear speeds, large perpendicular stresses develop in the off-fault regions, as the shock wave passes through, which could explain these cracks (*3*). These off-fault open cracks are seen in only that portion of the fault that was found to have the very high rupture speed (*9*). This is independent corroboration that the earthquake did actually reach supershear speeds in this long, straight section of the fault, the first earthquake for which such direct evidence is available.

The Tibet earthquake suggests that long, straight strike-slip faults are necessary for ruptures to propagate at supershear speeds. Re-examination of earlier reports of supershear rupture also show that such speeds generally occur on the straight section of faults (*7, 13*), although not all straight portions of faults reach supershear speeds. Thus, straightness of the fault is only a necessary (but not sufficient) condition for very fast rupture. Fracture mechanics studies show that long, straight faults are more likely to reach the high rupture speeds. The faults start from rest, accelerate to the maximum permissible speed, and continue at this speed provided there are no obstacles along the way and fault friction is low (*2*).

What can the 2001 Tibet earthquake teach us about, for example, the 1906 and the 1857 California earthquakes? Any repeats of these events may lead to fewer deaths but will certainly produce greater financial cost than the 2004 Sumatra-Andaman earthquake and tsunami. The 2001 Tibet earthquake is very similar to the 1906 San Francisco earthquake, both being vertical strike-slip faults and having similar magnitude, fault length and width, and hence similar average slip and average stress drop.

The 1906 earthquake rupture started south of San Francisco (see the figure, upper right panel) and propagated both to the northwest and to the southeast. Geodetic measurements (*14*) show that the largest displacements were to the north of San Francisco, which is in agreement with results obtained by inversion of available seismograms (*15*). This northern segment may have reached supershear rupture speeds (*16*). The fact that the high fault-displacement region is also here, where the fault is very straight, would provide additional support for this notion, assuming the 1906 and the 2001 earthquakes behaved similarly. Unfortunately, due to heavy rains and rapid rebuilding following the 1906 earthquake, no information is available on whether off-fault cracks appeared in this region. Fortunately, the cold desert climate of Tibet had preserved the off-fault open cracks from the 2001 earthquake, uneroded during the winter months, until the scientists visited.

Of course, no seismograms are available for the 1857 Fort Tejon earthquake (see the figure, upper right panel), which was a strike-slip earthquake with a rupture length greater than 300 km. Trenching across the fault revealed that the largest slip occurred in the Carrizo Plain, where the fault is very straight (*17*). One can speculate that the 1857 earthquake may have propagated at supershear speeds in the Carrizo Plain, and slowed as it went around the "Big Bend," just as the 2001 Tibet earthquake slowed at a bend in the fault strike.

The 1857 and 1906 California earthquakes may have propagated faster than was believed. If so, we need to apply the same analysis to other great strike-slip faults around the world, such as the more than 10,000-km-long Himalayan-Alpine seismic belt. We also need to develop a measure of the "straightness" of faults and the length of the straight portion required for such fast rupture speeds. Observations of off-fault open cracks can be used as a diagnostic tool for supershear rupture, and it would be useful to search for and document them.

References and Notes

1. R. Madariaga, *Ann. Geophys.* **1**, 17 (1983).
2. B. V. Kostrov, S. Das, in *Principles of Earthquake Source Mechanics* (Cambridge Univ. Press, New York, 1988), p. 286.
3. H. S. Bhat *et al*., *J. Geophys. Res.* **112**, B06301 (2007).
4. R. Archuleta, *J. Geophys. Res.* **89**, 4559 (1984).
5. A. J. Rosakis, O. Samudrala, D. Coker, *Science* **284**, 1337 (1999).
6. K. Xia, A. J. Rosakis, H. Kanamori, J. R. Rice, *Science* **308**, 681 (2005).
7. M. Bouchon *et al*., *Geophys. Res. Lett.* **28**, 2723 (2001).
8. M. Bouchon, M. Vallée, *Science* **301**, 824 (2003).
9. D. P. Robinson, C. Brough, S. Das, *J. Geophys. Res.* **111**, B08303 (2006).
10. R. Han, T. Shimamoto, T. Hirose, J.-H. Ree, J. Ando, *Science* **316**, 878 (2007).
11. R. Madariaga, *Science* **316**, 842 (2007).
12. C. Lasserre *et al*., *J. Geophys. Res.* **110**, B12408 (2005).
13. E. Dunham, R. J. Archuleta, *Bull. Seismol. Soc. Am.* **94**, S256 (2004).
14. http://earthquake.usgs.gov/regional/nca/1906/18april/offset.php, based on (*18*).
15. D. J. Wald, H. Kanamori, D. V. Helmberger, *Bull. Seismol. Soc. Am.* **83**, 981 (1993).
16. S. Song, G. C. Beroza, P. Segall, *Eos Trans. AGU* **86** (Fall Meet. Suppl.), abstract S12A-05 (2005).
17. K. Sieh, *Bull. Seismol. Soc. Am.* **68**, 1421 (1978).
18. W. Thatcher, G. Marshal, M. Lisowski, *J. Geophys. Res.* **102**, 5353 (1997).

10.1126/science.1142143

NEUROSCIENCE

Synapses Here and Not Everywhere

Local degradation of synaptic proteins determines which neuronal connections persist and which are eliminated during development.

David M. Miller

Brain function depends on a vast array of synapses, or connections, between neurons. The overall architecture of these networks is defined by the creation of specific synapses as well as by the removal or pruning of excess connections. Pruning is particularly dramatic in the human brain, in which an estimated 40% of synapses generated during postnatal growth are eliminated by adulthood (*1*). The scope of this phenomenon argues for robust mechanisms that select synapses for preservation or destruction, but the molecular details are obscure. For instance, how is this choice regulated in a single neuron that initially synapses with multiple partners? On page 947 of this issue, Ding *et al.* (*2*) provide an intriguing model of this process in which the creation of adult synapses triggers the destruction of developmentally transient synapses forged by the same neuron.

These findings are derived from studies of a motor neuron circuit that regulates egg laying in the nematode *Caenorhabditis elegans*. The hermaphrodite-specific neuron (HSNL) synapses with muscles and with VC-class motor neurons adjacent to the vulva, an opening through which fertilized embryos are expelled from the uterus (see the figure). Specialized structures assemble at these synapses for the release of neurotransmitter signals from the presynaptic membrane to stimulate receptors at the postsynaptic surface. Ding *et al.* expressed presynaptic proteins (labeled with green fluorescent protein) in nematodes and observed that HSNL synapses near the vulva in the primary synapse region are accompanied by a distal set of HSNL connections in the secondary synapse region during larval development. However, by the adult stage, these secondary synapses were removed as the primary synapse region matured. The authors propose that a local cue directs the maturation and elimination events simultaneously, and that synapse removal results from the destruction of presynaptic proteins by the ubiquitin-proteasome system.

The ubiquitin-proteasome system uses the enzyme E3 ubiquitin ligase to attach the peptide ubiquitin to specific protein substrates. These ubiquitin-labeled targets are dismembered in a barrel-shaped structure called the proteasome. The SCF (Skp1–Cullin–F-box) type of E3 ubiquitin ligase is composed of multiple subunits and achieves target selectivity with an interchangeable set of F-box adaptor proteins (*3*).

Earlier work by Shen and colleagues revealed that intercellular contact between a pair of immunoglobulin membrane proteins, SYG-1 and SYG-2, directs assembly of the primary synapse region (*4*, *5*). Remarkably, SYG-2, the instructive signal that stimulates synapse formation in this location, is presented by a nearby epithelial cell (guidepost cell) rather than by postsynaptic vulval muscle or VC motor neurons. Complementary expression of SYG-1 in the HSNL neuron tethers presynaptic components to this spot.

In addressing the mechanism underlying this process, Ding *et al.* discovered that the intercellular domain of SYG-1 directly interacts with SKR-1, a *C. elegans* homolog of a core component (Skp1) of the SCF complex. This result must have induced some head-scratching at first, because contact with the SCF complex is typically a death sentence for targeted proteins. But SYG-1 is clearly not degraded, and the primary synapse region remains intact. The key to this mystery was suggested by experiments showing that SYG-1 blocks SKR-1 binding to a specific F-box adaptor protein, SEL-10. Thus, Ding *et al.* reasoned that SYG-1–SKR-1 interaction in the HSNL neuron effectively disrupts local ubiquitination activity by the SCF com-

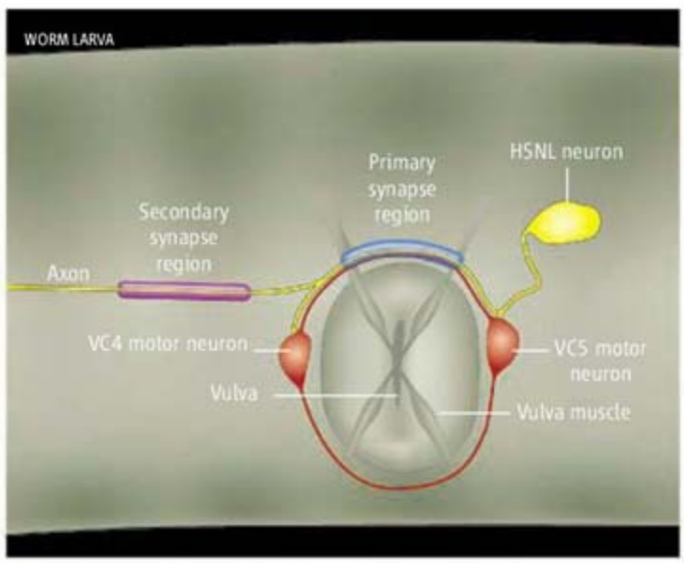

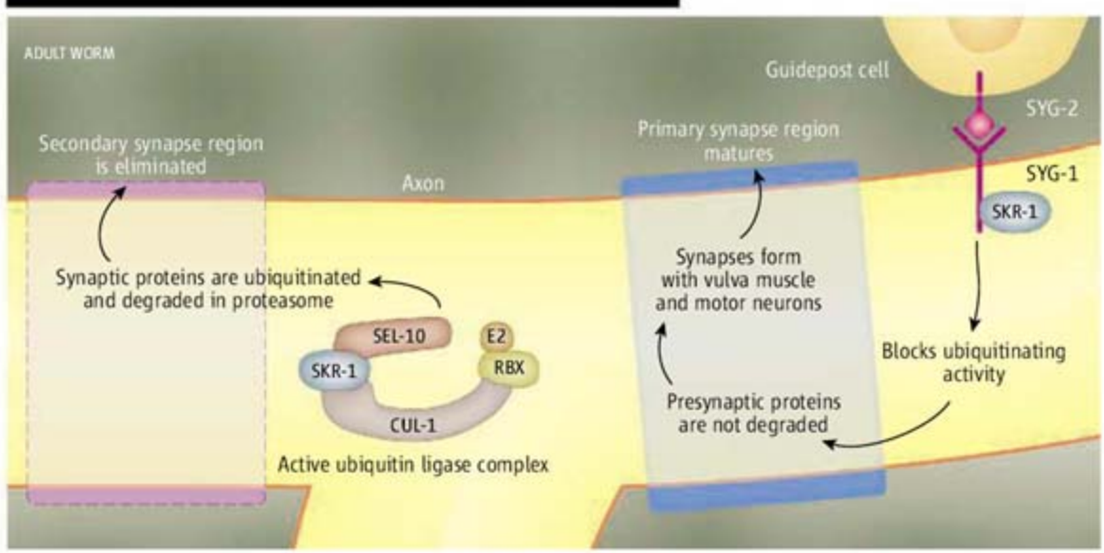

Disconnections. (**Top**) The developing HSNL motor neuron initially forms synapses with vulval muscles and motor neurons in two locations. (**Bottom**) The protein SYG-1 blocks proteolysis of synaptic proteins at primary synapses but allows destruction of secondary synapses. E2, E2 ubiquitin conjugating enzyme; RBX, Ring finger protein.

The author is in the Department of Cell and Developmental Biology, Vanderbilt University, 465 21st Avenue South, Nashville, TN 37232–8240, USA. E-mail: david.miller@vanderbilt.edu

plex, and thereby protects primary synapses from destruction. This model is supported by genetic experiments showing that primary synapses are unstable in nematodes lacking SYG-1 (*syg-1* mutants) and that synapse removal requires components (SKR-1 and SEL-10) of the SCF complex.

But herein lies a paradox. In addition to protecting the primary synapse region from destruction, SYG-1 also triggers the demise of the secondary synapse region. Indeed, secondary synapses are preserved in *syg-1* mutants, whereas primary synapses are not. How does SYG-1 direct the remote destruction of the secondary synapse region? The authors show that the ubiquitin-proteasome system is required to remove secondary synapses during normal development. Thus, SYG-1 localization to the primary synapse region somehow stimulates proteolytic activity in the secondary synapse region. To explain this effect, Ding *et al.* propose that the SCF complex is limiting in the HSNL neuron. In this model, high SCF activity in the primary synapse region (for example, in mutant worms lacking SYG-1) indirectly protects the secondary synapse region from destruction. Conversely, when active SCF is excluded from the primary synapse region (as in the wild-type worms), more SCF is available to "attack" target proteins in the secondary synapse region. Although this model is pleasingly elegant and supported by additional experiments (artificial elevation of SCF activity in the HSNL neuron removes both primary and secondary synapses), Ding *et al.* acknowledge that SYG-1 could also act through unknown alternative signaling pathways to eliminate secondary synapses.

Additional specific information about the mechanism proposed by Ding *et al.* is needed to build a detailed biochemical model of the process. For example, which of the presynaptic components in the HSNL neuron is directly targeted by the SCF complex? Liprin-alpha is an attractive candidate, as its removal is predicted to destabilize presynapse assembly (*6*, *7*). Another question is whether the postsynaptic apparatus—the organization of proteins in the cells receiving stimulation by the HSNL neuron—is disassembled in concert with the presynapse. If so, how are these events coordinated?

Earlier studies have firmly established roles for the ubiquitin-proteasome system in axon guidance and synaptogenesis in disparate species. Learning and memory—higher-order functions that originate with synaptic plasticity—also depend on regulated proteolysis (*3*). Ding *et al.* have now provided an exciting example of how this degradation system can be marshaled to control the placement of specific synapses in *C. elegans*. The evolutionary conservation of the components of this mechanism suggests that additional work in this genetically tractable model organism may reveal fundamental secrets of human brain development.

References

1. P. R. Huttenlocher, C. de Courten, *Hum. Neurobiol.* **6**, 1 (1987).
2. M. Ding, D. Chao, G. Wang, K. Shen, *Science* **317**, 947 (2007); published online 12 July 2007 (10.1126/science.1145727).
3. A. N. Hegde, *Prog. Neurobiol.* **73**, 311 (2004).
4. K. Shen, R. D. Fetter, C. I. Bargmann, *Cell* **116**, 869 (2004).
5. K. Shen, C. I. Bargmann, *Cell* **112**, 619 (2003).
6. M. R. Patel *et al.*, *Nat. Neurosci.* **9**, 1488 (2006).
7. Y. Dai *et al.*, *Nat. Neurosci.* **9**, 1479 (2006).

10.1126/science.1147570

OCEANS

A Change in Circulation?

Measurements with a new observational array have revealed surprisingly large variations in ocean circulation in the North Atlantic.

John A. Church

Earlier this year, the Intergovernmental Panel on Climate Change (IPCC) reported unequivocal evidence that climate change is happening now (*1*). One public image of climate change is a rapid and dramatic collapse of the northward flow of warm water to high latitudes, with possible serious implications for North American and European climate. So, has the northward flow of warm water changed? How would we know if it had, and how can we monitor it in the future? A remarkable new observational program has begun to address these questions. In this issue, Kanzow *et al.* on page 938 (*2*) and Cunningham *et al.* on page 935 (*3*) report initial results from the program.

Warm water emerges from the Florida Strait and flows northward along the east coast of America as the Gulf Stream (see the figure). After leaving the coast of North America, the warm water flows northeastward before it diverges, with some water continuing northward beyond Iceland and the remainder returning in the broad southward flow of the subtropical gyre in the upper kilometer or so of the ocean.

Throughout its northward journey, the warm water loses heat to the atmosphere and becomes denser. The colder, denser water sinks at high latitudes and returns southward at depths of 2 to 5 km. This northward flow of near-surface, warm water and southward flow of cold, deep water is known as the North Atlantic meridional overturning circulation. The northward flow is controlled by a combination of surface winds and density gradients, with warmer, saltier, lighter water at low latitudes and colder, fresher, denser water at higher latitudes.

Two processes can prevent high-latitude water from sinking: surface warming and decreased salinity caused by freshwater runoff from rain and meltwater from glaciers and the Greenland Ice Sheet. This would disrupt the meridional overturning circulation. Observations indicate that there has indeed been a freshening of the North Atlantic (*4*). Climate change models (*5*) in which the CO_2 concentrations quadruple over 140 years project a decrease in the meridional overturning circulation by 10 to 50%.

Bryden *et al.* (*6*) analyzed five sets of ship-based, full-depth temperature and salinity measurements across the North Atlantic near 25°N, completed between 1957 and 2004. From these data, they estimated that the overturning circulation had decreased by 30% and the northward heat transport decreased by over 20%, as a result of an inferred decrease in the southward transport of the coldest, densest water and an increase in southward transport of the warmer water in the upper kilometer of the ocean. This decrease in the meridional overturning circulation is much larger than suggested by climate model simulations of the 20th century, and more akin to the up to 50% decrease projected for the end of the 21st century (*5*, *7*). Are the models not responding rapidly enough to greenhouse gas changes, or was the observed change—as Bryden *et al.* cautioned—uncomfortably close to the uncertainties in previous observational estimates?

In a bold new initiative led by the UK

The author is in the CSIRO Marine and Atmospheric Research and Antarctic Climate and Ecosystems CRC, GPO Box 1538, Hobart, Tasmania 7001, Australia. E-mail: john.church@csiro.au

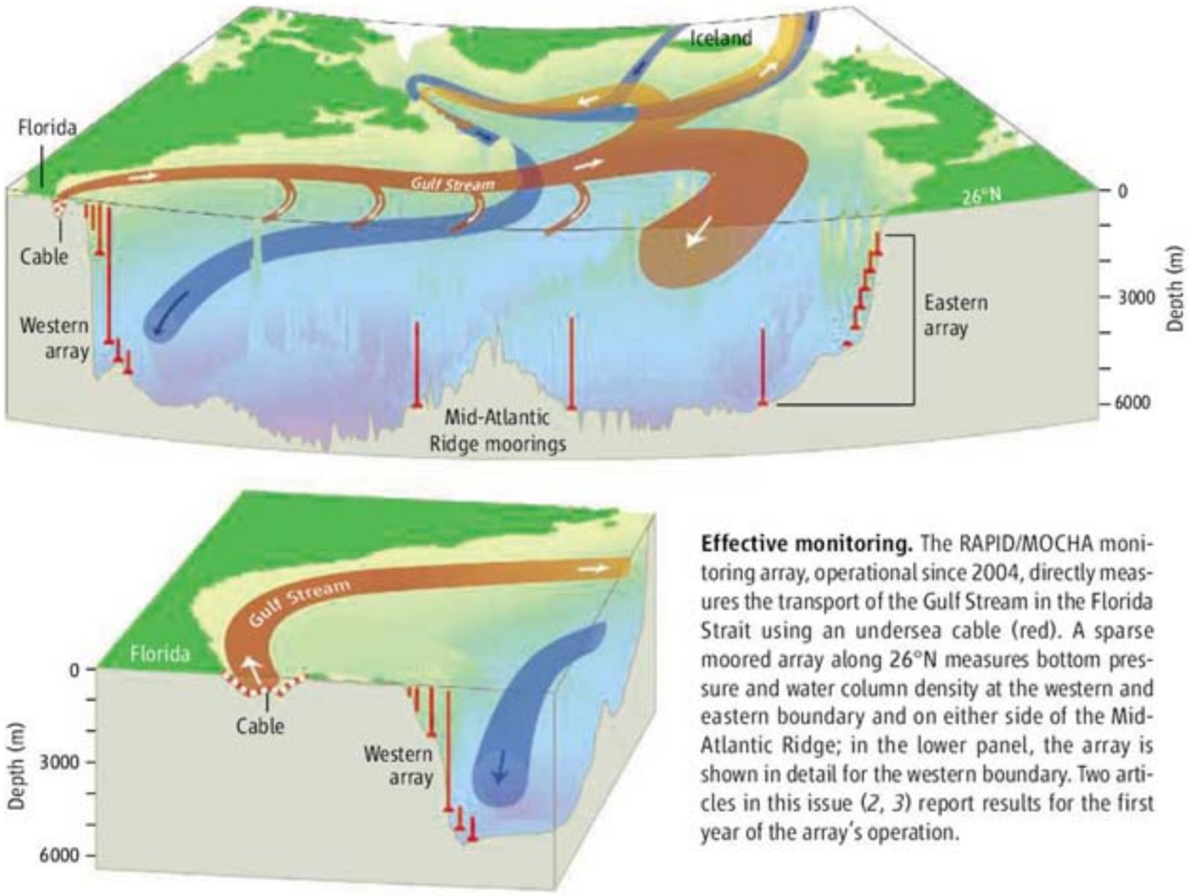

Effective monitoring. The RAPID/MOCHA monitoring array, operational since 2004, directly measures the transport of the Gulf Stream in the Florida Strait using an undersea cable (red). A sparse moored array along 26°N measures bottom pressure and water column density at the western and eastern boundary and on either side of the Mid-Atlantic Ridge; in the lower panel, the array is shown in detail for the western boundary. Two articles in this issue (*2*, *3*) report results for the first year of the array's operation.

CREDIT: LOUISE BELL AND NEIL WHITE/CSIRO

National Environmental Research Council (with support from U.S. agencies), the RAPID/MOCHA (Rapid Climate Change/Meridional Overturning Circulation and Heat Flux Array) array was deployed in March 2004 to continuously monitor the meridional overturning circulation at 26°N. These observations are a component of a larger set of activities of the World Climate Research Programme's CLIVAR (Climate Variability and Predictability) Project to monitor the North Atlantic meridional overturning circulation.

The inexpensive array along 26°N consists of instruments measuring the variations in the bottom pressure, and temperature and salinity (and thus density), throughout the water column near the western and eastern boundaries and on either side of the Mid-Atlantic Ridge (see the figure). These measurements can be combined to estimate variations in the horizontal pressure difference between the western and eastern boundary throughout the water column. The pressure differences are directly proportional to variations in the horizontally integrated northward flow. The ocean-interior measurements are complemented by estimates of the northward flow of the Gulf Stream through the Florida Strait by an undersea cable and satellite measurements of the wind stress and hence of the surface-wind–driven transport.

On time scales of 15 days and longer, the sum of transports into the North Atlantic should be about zero. Indeed, the observations reported by Kanzow *et al.* indicate that the sum varies with a root-mean-square value of only 3.4 Sv (1 Sv = 10^6 m^3/s), slightly larger than the expected measurement errors of 2.7 Sv, thus demonstrating the remarkable effectiveness of the array. The fact that the observed sum varies slightly more than the expected measurement errors presumably reflects deficiencies in the method, such as the unobserved flow deeper than the deepest part of the array and the impact of the Mid-Atlantic Ridge.

Cunningham *et al.* report a year-long average meridional overturning circulation of 18.7 ± 5.6 Sv (*3*), but with large variability ranging from 4.4 to 35.3 Sv over the course of the year. This range includes all five meridional overturning circulation values estimated from the snapshots analyzed by Bryden *et al.*; thus, the apparent long-term decrease inferred by these authors may merely be a result of large intra-annual variability.

Cunningham *et al.* estimate that they can measure the annual average overturning to a resolution of 1.5 Sv. This would be sufficient to detect any large abrupt transition of the meridional overturning circulation. An assessment of the current generation of climate models indicates that such a large abrupt transition is very unlikely during the 21st century (*6*), but verification of these projections and continuing assessment of the stability of the meridional overturning circulation remains a priority.

It remains unclear how much the meridional overturning circulation varies from year to year. Understanding this variability will be critical to improving models, thus allowing more reliable projections of climate change. This variability will determine how long a record will be required to determine a trend in the meridional overturning circulation. A recent coupled ocean atmosphere model study (*8*) suggests that it would take several decades of observations to detect such a trend. Similarly, it will take decades of monitoring to determine which (if any) of the models analyzed by the IPCC (*7*) most accurately reflects reality.

The effectiveness and the inexpensive nature of the RAPID/MOCHA array should allow long-term monitoring of an important element of the global climate system. Equivalent observational schemes for the Southern Ocean limb of the meridional overturning circulation, where decadal water-mass changes have also been observed (*9*), remain to be designed.

References and Notes

1. Intergovernmental Panel on Climate Change, *Climate Change 2007: The Physical Science Basis. Contribution of Working Group I to the Fourth Assessment Report of the Intergovernmental Panel on Climate Change*, S. Solomon *et al.*, Eds. (Cambridge Univ. Press, Cambridge, UK, and New York, 2007).
2. T. Kanzow *et al.*, *Science* **317**, 938 (2007).
3. S. A. Cunningham *et al.*, *Science* **317**, 935 (2007).
4. R. Curry, C. Mauritzen, *Science* **308**, 1772 (2005).
5. J. Gregory *et al.*, *Geophys. Res. Lett.* **32**, L12703 (2005).
6. H. L. Bryden, H. R. Longworth, S. A. Cunningham, *Nature* **438**, 655 (2005).
7. G. A. Meehl *et al.*, in (*1*), Chapter 10.
8. S. S. Drijfhout, W. Hazeleger, *J. Clim.* **20**, 1571 (2007).
9. S. R. Rintoul, *Geophys. Res. Lett.* **34**, L06606 (2007)
10. This paper is a contribution to the CSIRO Climate Change Research Program and the CSIRO Wealth from Oceans Flagship and was supported by the Australian Government's Cooperative Research Centres Programme through the Antarctic Climate and Ecosystems Cooperative Research Centre. The author was part-funded by the Australian Climate Change Science Program.

10.1126/science.1147796

Plant Speciation

Loren H. Rieseberg[1,2*] and John H. Willis[3]

Like the formation of animal species, plant speciation is characterized by the evolution of barriers to genetic exchange between previously interbreeding populations. Prezygotic barriers, which impede mating or fertilization between species, typically contribute more to total reproductive isolation in plants than do postzygotic barriers, in which hybrid offspring are selected against. Adaptive divergence in response to ecological factors such as pollinators and habitat commonly drives the evolution of prezygotic barriers, but the evolutionary forces responsible for the development of intrinsic postzygotic barriers are virtually unknown and frequently result in polymorphism of incompatibility factors within species. Polyploid speciation, in which the entire genome is duplicated, is particularly frequent in plants, perhaps because polyploid plants often exhibit ecological differentiation, local dispersal, high fecundity, perennial life history, and self-fertilization or asexual reproduction. Finally, species richness in plants is correlated with many biological and geohistorical factors, most of which increase ecological opportunities.

Plants provide extraordinary opportunities for studying speciation. Flowering plants are especially speciose, trailing only insects in named species diversity. Much of this diversification has occurred recently, creating spectacular examples of adaptive radiation and of speciation in action (table S1). Plants are mostly sessile but vary dramatically in mating system, ploidy level, mode of dispersal, and life history, aiding efforts to understand the contribution of various ecological and evolutionary factors to speciation.

What Is a Plant Species?

The definition of a species in plants has been a major impediment to botanical studies of speciation; botanists have often expressed doubt that plant species even exist, because of frequent reports of interspecific hybrids (*1*) and because phenotypic variation in some plant groups does not assort readily into discrete categories (*2*). These concerns were amplified by claims that gene flow within many plant species was so low that populations rather than species were the most inclusive reproductive units (*2*, *3*).

Recent work allays these concerns. Analyses of morphometric data from more than 200 plant genera indicate that discrete clusters of morphologically similar individuals occur within most sexual plant lineages, that these clusters correspond closely to groups with significant postpollination reproductive isolation, and that interspecific hybridization is not the primary cause of poorly defined species boundaries (*4*). Molecular population genetic studies imply that migration rates within plant species are higher than earlier direct estimates and do not differ, on average, from those of animals (*5*). Theoretical (*6*) and empirical work further indicates that even in species with low gene flow, populations may evolve in concert through the spread of advantageous alleles (*7*).

Although many plant species are held together by gene flow and kept apart from other species by reproductive barriers, there are exceptions. For example, some plants reproduce without sex. These asexual taxa are composed of clonal hybrid genotypes that fill the phenotypic space between their sexual parental species (table S1). Because sexual reproduction is infrequent in such species, it is difficult to discuss their evolution in terms of sexual isolation and speciation. In contrast, self-fertilizing (selfing) species often maintain genetic and phenotypic cohesion (*4*) because they have higher within-species gene flow than previously hypothesized (*8*), and their restricted outcrossing (exchange of pollen between individuals) impedes interspecific hybridization. Reproductive isolation between species may be incomplete, however, particularly in groups that have recently undergone multiple speciation events or those that have long generation times. This incomplete isolation may result in some gene flow between groups that are otherwise well-defined species (table S1).

Reproductive Isolation

Reproductive isolation is not the proximal cause of diversification; this is the province of diversifying selection and genetic drift. However, reproductive isolation can facilitate the accumulation of genetic differences between groups of populations, thereby sharpening boundaries between them and permitting adaptive traits to move closer to their fitness optima. This does not require absolute isolation. Rather, any reduction in the effective migration rate facilitates divergence, which reduces effective migration rates even further. The resulting feedback loop, given enough time, usually leads to complete genetic isolation.

Multiple reproductive barriers isolate most plant species. These include prepollination barriers that limit the transfer of pollen from individuals of one species to stigmas of other species. Several prepollination barriers—ecogeographic, mechanical, and temporal—are found in animal species, whereas pollinator isolation is exclusively associated with plant speciation. Other barriers, such as an advantage of conspecific pollen in fertilizing eggs compared with nonconspecific pollen (conspecific pollen precedence) and the failure of nonconspecific pollen to fertilize eggs (gametic incompatibilities), act after pollination but before fertilization, resulting in postpollination, prezygotic isolation. A final set of barriers, also found in animals, act after

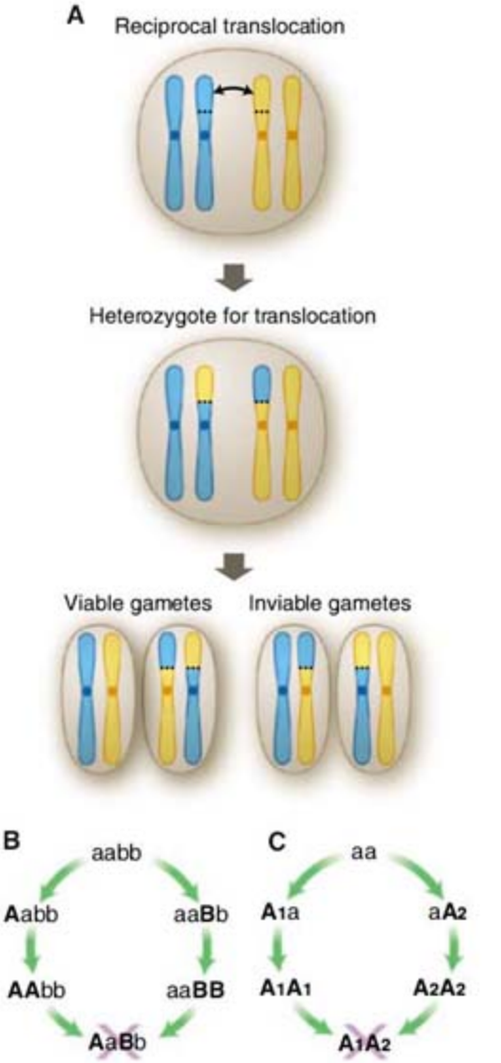

Fig. 1. Genetics of hybrid incompatibilities. (**A**) Example of a typical chromosomal rearrangement in plants, showing loss of fertility in heterozygotes because 50% of gametes are unbalanced genetically and inviable. (**B**) Classic two-locus BDM incompatibility in which new mutations are established at alternate loci and without loss of fitness in geographically isolated populations, but which are incompatible in hybrids. (**C**) Single-locus BDM incompatibility in which new mutations are established at the same locus and without loss of fitness in geographically isolated populations, but which are incompatible in hybrids.

[1]Department of Botany, University of British Columbia, Vancouver, BC V6T 1Z4, Canada. [2]Department of Biology, Indiana University, Bloomington, IN 47405, USA. [3]Department of Biology, Duke University, Durham, NC 27708, USA.

*To whom correspondence should be addressed. E-mail: Lriesebe@interchange.ubc.ca

fertilization: hybrid inviability, sterility, and the failure or reduction in successful reproduction in subsequent generations (hybrid breakdown). These postzygotic barriers may be a by-product of changes in the internal genetic environment (intrinsic isolation) or in the external ecological environment (extrinsic isolation). Current challenges are to estimate the relative contribution of different reproductive barriers in limiting gene flow among contemporary populations and to determine the order and speed with which they arose.

All else being equal, early-acting reproductive barriers will contribute more to isolation than late-acting barriers (*9*). For example, the production of hybrid seeds in artificial crosses and reductions in the fertility of first-generation hybrids are commonly tested in the greenhouse. Cross-compatibility data (*4*) reveals that hybrid fertility reduction is the slightly stronger of the two barriers. However, because hybrid seed production acts before reductions in fertility, reduced hybrid seed production actually would be expected to contribute about 75% and hybrid sterility just 25% of the total isolation caused by these two barriers.

Unfortunately, only a few studies provide comprehensive estimates of isolation between pairs of sibling species (table S1). In these, the cumulative effects of many reproductive barriers lead to almost complete isolation. Early-acting reproductive barriers such as ecogeographic, pollinator, and mating system isolation are most important (table S1 and fig. S1), whereas late-acting postzygotic barriers contribute very little to isolation. Ecogeographic isolation has long been viewed as the most important reproductive barrier in plants (*10*), and its preeminence has been confirmed by numerous reciprocal transplant studies showing differences in habitat preferences among closely related species or subspecies (Table 1). Pollinator and mating system isolation are less frequent, with the former arising when the focal species is numerically dominant but does not fully use the array of available animal pollinators (*11*).

It is difficult to determine the order of reproductive barrier evolution. Indirect evidence from analyses of patterns of reproductive isolation suggests that prepollination barriers often arise first. For example, 19% of 1234 interspecific cross combinations (most from rapidly radiating lineages isolated by ecological barriers) failed to show evidence of cross-incompatibility or intrinsic postzygotic isolation (*4*). Intrinsic postzyotic barriers may arise first in polyploid species that are intersterile with their diploid progenitors but that fail to exhibit ecological differences (table S1). Likewise, intrinsic postzygotic barriers may sometimes arise before ecological barriers (other than mating system isolation) in selfing species (Table 1).

We know surprisingly little about the speed of plant speciation, although studies of contemporary evolution imply that reproductive barriers can arise rapidly. For example, grass populations exposed to different fertilizer treatments or to mine tailings exhibit both temporal (flowering time) and habitat isolation (seeds transplanted between sites have reduced survival) (table S1). Interestingly, flowering time divergence is greatest at the boundary between habitats in both experiments, a pattern suggestive of reinforcement, where selection against unfit hybrids has enhanced prezygotic isolation. These studies of speciation in action illustrate the plausibility of reinforcement and sympatric speciation, both of which are increasingly well supported by theory (*12*) and empirical work (table S1).

Although individual reproductive barriers can arise rapidly, most plant species remain separated by numerous barriers, which implies that complete speciation typically requires many thousands of generations. The main exceptions to this are hybrid and polyploid speciation. Fully isolated polyploid species may arise in one or two generations, and diploid or homoploid hybrid species may achieve isolation in as few as 60 generations (*13*).

Genetics of Isolation

Genetic analyses provide information on the numbers and kinds of genetic changes underlying reproductive barriers, as well as on the evolutionary forces responsible for their origin. Studies of pollinator isolation have shown, for example, that major quantitative trait loci (QTLs) sometimes underlie shifts in the animals that pollinate plants (pollination syndrome) (table S1) and changes in pollinator preferences in the field (Table 1). In contrast, two studies of mating system isolation detected many smaller genetic changes (table S1). These different architectures might be explained by the fact that many intermediate pollinator syndromes are maladaptive (e.g., red flowers lacking a nectar reward are unattractive to both birds and bees) and favor larger genetic steps, whereas small increases in selfing rates may be favored if inbreeding depression costs are not prohibitive (*14*). Analyses of the direction of QTL effects imply that most traits contributing to prepollination isolation diverged through directional selection; as predicted for adaptive phenotypes, QTL effects for these traits are mostly in the same direction as the parental differences (*15*). QTL effects are predicted to vary in direction (i.e., have opposing effects) for traits not under consistent directional selection (*16*).

Recent genetic analyses of prezygotic and extrinsic postzygotic barriers associated with discrete habitat differences are particularly informative because many of the studies have been performed in the field. This makes it possible to estimate the

Table 1. Case studies of plant speciation.

Topic	Taxa studied	Conclusions	Ref.
Reproductive isolation	*Gilia capitata* ssp. *capitata* and *G. c.* ssp. *chamissonis*	Local adaptation of interfertile subspecies to different habitats restricts successful migration and gene flow.	(*48*)
	Arctic *Draba*	Three self-fertilizing morphological species each appears to comprise thousands of cryptic biological species.	(*49*)
Genetics of isolation	*Mimulus lewisii* and *M. cardinalis*	Allele increasing petal carotenoid concentration reduced bee visitation by 80%; allele increasing nectar production doubled hummingbird visitation.	(*50*)
	Lycopersicon hirsutum and *L. pimpinellifolium*	Tomato lines with resistance gene (*Cf-2*) from *L. pimpinellifolium* exhibit autonecrosis of mature leaves, but no autonecrosis observed when complementary gene (*RC3*) from *S. pimpinellifolium* also introduced.	(*51*)
Hybrid and polyploid speciation	*Helianthus anomalus*, *H. deserticola*, and *H. paradoxus*	Three diploid species arisen via hybridization from same two parental species. Karyotypically divergent hybrids colonized extreme habitats through selection on transgressive traits (Fig. 2).	(*52*)
	Brassica napus	Chromosomal rearrangement after polyploidization responsible for flowering time divergence among synthetic polyploid lineages.	(*53*)
Factors affecting species richness	Angiosperms	Acquisition of nectar spurs in wide variety of plants correlated with increased species diversity.	(*44*)
	Andean *Lupinus*	Most rapid species radiation in plants driven by ecological opportunities afforded by uplift of Andes.	(*54*)

strength of selection on traits and QTLs that contribute to habitat isolation. Studies have shown, for example, that the strength of selection on QTLs that contribute to habitat isolation is sufficient to permit speciation in the presence of gene flow, that hybrid inviability may arise as a by-product of habitat selection, and that interspecific hybridization can facilitate the exchange of adaptive alleles between species (table S1).

Genetic studies of postpollination, prezygotic isolation have focused on the relationship between self-incompatibility (SI) mechanisms, which enforce outcrossing in many hermaphroditic plants, and interspecific incompatibility. This interest stems from early observations that self-compatible species are more compatible in interspecific crosses than are SI species, implying that SI may contribute to both intra- and interspecific incompatibilities. This was confirmed by detection of a QTL for interspecific incompatibility that colocalizes with the SI locus, as well as observations that crosses between self-compatible species fail after transformation with a SI gene from a self-incompatible species (table S1). Diversification of genes that contribute to SI appears to result from frequency-dependent selection (*17*). Interestingly, other plant reproductive proteins appear to be under positive selection as well, including candidates for species-specific recognition between pollen and stigma (table S1).

Intrinsic postzygotic barriers offer special challenges to genetic analyses because the phenotypes of interest (hybrid sterility and inviability) impede genetic study and lack obvious candidate genes for functional analyses (see below, however). Intrinsic postzygotic isolation may be caused by chromosomal rearrangements and/or changes in genes (Fig. 1). Population genetic theory minimizes the importance of strongly underdominant chromosomal rearrangements (those that reduce the fitness of heterozygotes) because their negative effects on fitness should prevent them from becoming established, except in small, inbred populations. Weakly underdominant rearrangements are more easily established but contribute little to reproductive isolation. In contrast, the Bateson-Dobzhansky-Muller (BDM) model accounts for the accumulation of interspecific incompatibilities in genes without loss of fitness (Fig. 1). Briefly, as a lineage diverges, geographically isolated or neighboring allopatric populations may accumulate independent mutations. These mutations are compatible with the ancestral genotype but are incompatible when combined. BDM incompatibilities generally involve two or more loci, although it is theoretically possible for BDM incompatibilities to result from the allopatric accumulation of independent mutations at a single locus (Fig. 1).

Despite theoretical doubts about their importance in speciation, chromosomal rearrangements often contribute to the sterility of hybrid plants (*18, 19*). Unlike *Drosophila* (in which hybrid sterility is mostly due to BDM incompatibilities), sterile plant hybrids often recover fertility after chromosomal doubling (*18*). This is expected if chromosomal rearrangements are the cause of sterility, because chromosomal doubling furnishes an exact homolog for each chromosome, whereas doubling should not affect BDM incompatibilities. Microchromosomal rearrangements such as the gain and loss of duplicate genes are more frequent than previously suspected and may lead to hybrid incompatibilities with no loss of fitness in the diverging lineages (*20*). Finally, hybrid sterility in plants frequently maps to chromosomal rearrangements (*21*), although whether the cause is chromosomal underdominance or BDM loci that have accumulated within the rearrangements is often unclear. The reduced recombination associated with chromosomal rearrangements can facilitate the accumulation of hybrid incompatibilities in these regions (*19, 22*) or expedite the establishment of rearrangements in the first place (*23*).

BDM hybrid sterility in plants may be under simple or complex genetic control. However, fewer loci contribute to hybrid sterility in plants than in *Drosophila*, and there appears to be no difference in the numbers of pollen (male) versus seed (female) incompatibilities, perhaps because plants largely lack differentiated sex chromosomes (*24*). In addition, cytoplasmic male sterility (CMS), which results from an incompatibility between the plant's nuclear genome and its cytoplasm, is frequently reported in intra- and interspecific plant hybrids, but not in animal hybrids (*25*). CMS is under frequency-dependent selection in hermaphrodite-biased populations, which predominate in plants, but under strong negative selection if there are separate male and female sex morphs. CMS is caused by aberrant, frequently chimeric, mitochondrial genes in all examples characterized at the molecular level (*26*). CMS phenotypes are rescued by nuclear-encoded, mitochondrial-targeted genes that restore fertility (*Rf* genes). With the exception of *Rf2* from maize, all cloned *Rf* genes are members of the pentatricopeptide repeat gene family (PPR), an unusually large gene family in plants (441 genes in *Arabidopsis*) that controls organelle gene expression. Although the molecular evolution of *Rf* genes is unknown, they are likely to be involved in coevolutionary chases with CMS as a result of genetic conflict between cytoplasmic and nuclear genes. These evolutionary dynamics may reduce the long-term effectiveness of CMS as a species barrier, because the same evolutionary forces that cause the spread of CMS within species could facilitate the introgression of CMS and restorers across species boundaries.

BDM factors also can cause hybrid weakness or inviability. Hybrid weakness is often manifested as necrosis in developing seedlings or adult plant tissue, similar to the phenotype of pathogen attacks (*27*). These observations imply that hybrid weakness may result from changes in pathogen resistance genes (Table 1), which diverge in response to selection pressure exerted by pathogens. More studies are needed to determine the frequency of this mechanism for hybrid weakness in interspecific crosses and to elucidate other mechanisms of hybrid inviability.

A final emerging difference between plants and animals (or at least *Drosophila*) is that most BDM incompatibilities characterized in plants are polymorphic within species (*27–29*) (Table 1). This is consistent with an origin of BDM incompatibilities through frequency-dependent selection, local adaptation, or drift. However, it also implies that BDM incompatibilities are

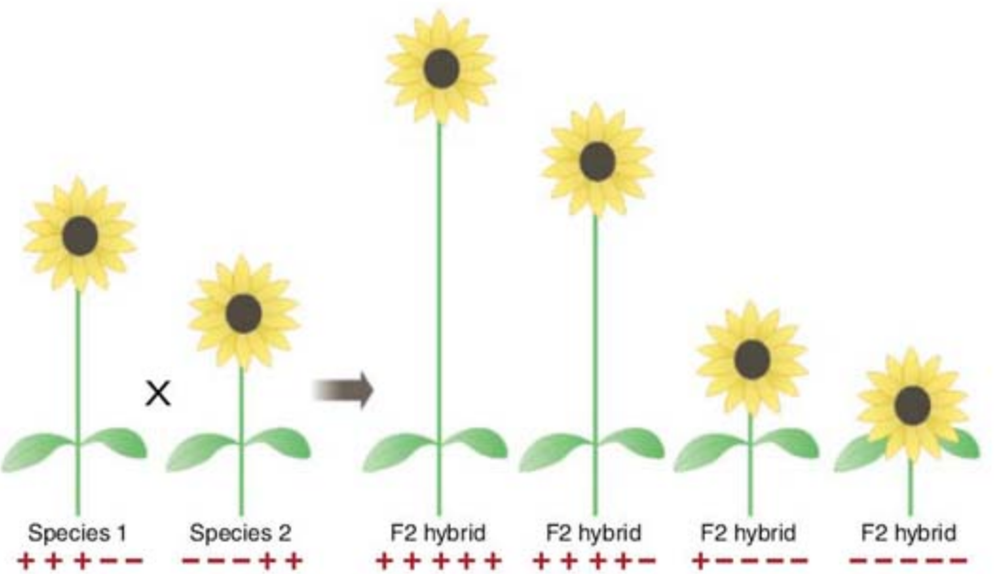

Fig. 2. Genetic basis of transgressive segregation showing how segregating hybrids can combine plus and minus alleles from parental species, thereby generating extreme phenotypes or adaptations to extreme habitats.

rarely the cause of speciation in plants, because they correlate poorly with species boundaries and typically make small contributions to total isolation.

Hybrid and Polyploid Speciation

Although most studies of speciation focus on how lineages diverge, speciation is not always about divergence. Indeed, a substantial fraction of speciation events in plants involves the reunion of divergent genes and genomes through sexual hybridization. There are two kinds of hybrid speciation: homoploid and polyploid. Homoploid hybrid speciation refers to the origin of a new hybrid lineage without a change in chromosome number, whereas polyploid hybrid speciation involves the full duplication of a hybrid genome (allopolyploidy). Polyploids not of hybrid origin are autopolyploids.

Homoploid hybrid speciation is rarer than polyploid speciation for two reasons. First, homoploid hybrid species have strongly reduced fitness in early generation hybrids as selection eliminates incompatibilities. In contrast, polyploid species need not have low fertility during intermediate stages. Second, genome duplication protects the genetic integrity of newly derived polyploids, but no such barrier prevents homoploid hybrids from back-crossing with their parental species. In addition to these biological difficulties, homoploid hybrid species are technically challenging to detect because they often lack diagnostic features, such as a change in chromosome number. So far, there are 15 to 20 good examples in the literature (*30*), but more are likely to be discovered with the widespread application of genomic tools to natural plant populations (*31*).

Homoploid hybrid species may become reproductively isolated by rapid karyotypic evolution, ecological divergence, and spatial isolation of the new hybrid lineage. Simulation studies indicate that although strong ecological selection promotes hybrid speciation, without chromosomal or spatial isolation the hybrid population forms a steep step in a cline between the parental species (*32*). Karyotypic divergence and spatial isolation both reduce the probability that hybrid species will be generated but will enhance the evolutionary independence of hybrid lineages once they arise.

As hypothesized, all plant homoploid hybrid species are ecologically diverged and exhibit some degree of ecogeographic isolation, and roughly half have differing karyotypes (*30*). Most commonly, the hybrid species are adjacent to one or both parental species, although there are examples of long-distance dispersal as well (table S1). Some hybrids occupy habitats that are intermediate between the parental species, whereas others have colonized an extreme habit by combining QTLs with effects in the same direction from both parental species (Table 1 and Fig. 2). Homoploid hybrid species are easily recreated in the greenhouse, perhaps explaining why many are multiply derived in the wild (table S1).

In contrast to homoploid hybrid species, polyploid species are easily diagnosed because of chromosome number changes associated with genome doubling. However, the frequency of polyploid speciation remains controversial. When there are multiple polyploid species within a genus, it is difficult to determine whether there was a single transition to the new ploidal level followed by divergent speciation or whether each polyploid species arose independently. Recent model-based estimates (*33*) assume a single transition to a new ploidal level within a genus and provide a lower bound of the polyploid speciation rate: 2 to 4% in flowering plants and 7% in ferns. This contrasts with Stebbins' (*34*) estimate of 30 to 35% for flowering plants, which assumes that all polyploid species within a genus are independently derived. Because many polyploid species are themselves multiply derived (Table 1), Stebbins' estimate is probably closer to the true polyploid speciation rate. However, neither of these estimates (*33*, *34*) includes intraspecific ploidal variation. At least 8 to 9% of named plant species vary in ploidal level, and this might be the tip of the iceberg (*35*). If each ploidal level (cytotype) is viewed as a cryptic biological species, then the contribution of polyploidy to biological species diversity is even higher than previously surmised. In addition, there has been confusion between estimates of the proportion of species that are polyploid and the rate of polyploid speciation. Analyses of the age distribution of duplicate genes in diverse flowering plants (*36*) indicate that essentially all may be paleopolyploids, but this should not be equated with the polyploid speciation rate.

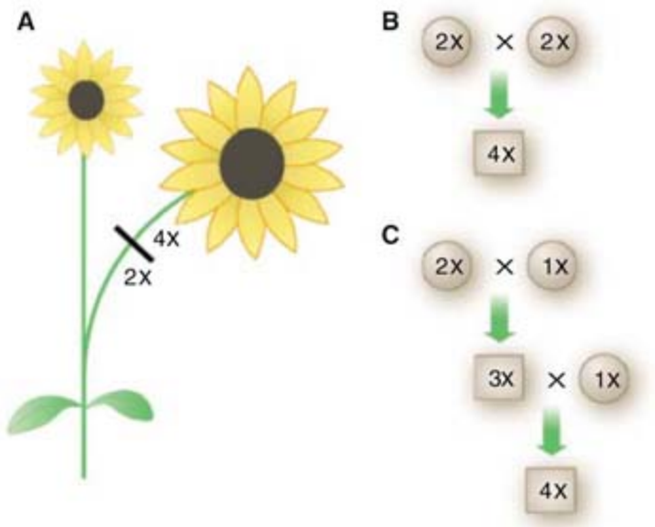

Fig. 3. Mechanisms by which polyploids can arise. (**A**) Somatic doubling, in which chromosome number is doubled in vegetative tissue that gives rise to reproductive organs. (**B**) Fusion of unreduced gametes that are produced when cell walls fail to form in the final stage of meiosis. (**C**) A triploid bridge, in which unreduced and reduced gametes form triploids. If the triploids also produce unreduced gametes, the triploid gametes may fuse with reduced gametes from diploid individuals to generate stable tetraploids.

Polyploids can arise by somatic doubling, by the fusion of unreduced gametes, and by means of a triploid bridge (Fig. 3). Unreduced gametes are common in plants and likely represent the most frequent route to polyploidy (*37*). However, most newly arisen polyploids fail to become established because of meiotic abnormalities and/or the paucity of appropriate mates (*38*). The establishment of polyploids is favored by differential niche preference, low dispersal, a selfing or asexual mating system, high fecundity, and a perennial life history (*39*, *40*). Niche separation, low dispersal, and selfing increase the probability of successful matings during early stages of polyploid species establishment; otherwise most matings will be with the diploid progenitors (*40*, *41*). Stochastic events due to a small number of polyploid colonizers decrease the chance of establishment, but this barrier is minimized by high fecundity and a perennial life history, which allows plants to reproduce at multiple times over their life cycle (*39*).

Because intraspecific matings are far more common than interspecific matings in natural populations of plants, autopolyploids must arise at a much higher rate than allopolyploids (*37*). However, named species are more likely to be allopolyploids (*42*), which implies that allopolyploids are more easily established in nature, easier to find, and/or more readily recognized by taxonomists. Establishment of allopolyploids is favored because of greater niche separation from their diploid progenitors (*43*), and taxonomists appear reluctant to name phenotypically cryptic autopolyploid species.

Recent attention has been given to changes in gene expression, genome content, and DNA methylation that accompany hybrid and polyploid speciation, but these genomic alterations only rarely have been linked to changes in ecology or mating system that affect polyploid establishment (Table 1). Indeed, many described genomic changes appear to be maladaptive by-products of reuniting divergent genomes. However, maladaptive changes in gene expression in first-generation interspecific hybrids may be reduced by genome doubling, and elimination of DNA sequences may help restore fertility in polyploids (table S1).

Factors Affecting Speciation or Extinction Rates

Recent advances in comparative methods have made it possible to identify biological or geo-

historical factors affecting speciation or extinction rates. The most rigorous approach compares species richness of multiple sister clades that differ in the presence or absence of a given trait (*44*). A significant association may result from either increased speciation or reduced extinction. Traits associated with increased species richness in plants include resin canals, nectar spurs, biotic pollination, herbaceous growth form, abiotic dispersal, increased neutral evolution, bilateral symmetry of flowers, twig epiphytism, and polyploidy (*45*) (table S1). Many of these examples involve biotic interactions, leading to suggestions that coevolution may drive speciation in many plant groups or that niche space may be less constrained in biotic than abiotic interactions (*46*). The most rapid diversification rates in plants are associated with ecological opportunities created by major geological changes such as the uplift of the Andes or island formation (Table 1), which implies that mechanisms that expand niche diversity often increase species diversification (or reduce extinction). Unfortunately, the factors listed above do not fully account for the most striking trend in species richness—the negative correlation with latitude—which appears to have a pluralistic explanation (*47*) (table S1).

Concluding Remarks

The field of plant speciation is in for an exciting decade. The wide availability of genomic tools and resources for crop and noncrop species, from green algae to mosses to angiosperms, will accelerate our understanding of the genetic and ecological bases of speciation. These resources not only will facilitate the cloning and functional characterization of genes underlying reproductive barriers but also will make it possible to quantify the effects of individual mutations or alleles on reproductive isolation or fitness in natural populations (Table 1). Likewise, the widespread application of molecular phylogenetic approaches simplifies comparative study.

We expect to see rapid progress in each of the areas highlighted in our review. For example, studies of the geography of selective sweeps should provide an objective method for evaluating the importance of different kinds of reproductive barriers and geohistorical processes in speciation. Our understanding of reproductive isolation will also be enhanced by additional field-based estimates of isolation across all life history stages. With the cloning of BDM incompatibilities in plants, the next step is molecular evolutionary studies of these genes to identify the forces that drive their evolution. Finally, comparative analyses of the effects of different kinds of reproductive barriers on species richness should allow us to determine whether reproductive barriers themselves increase speciation rates.

References and Notes

1. M. L. Arnold, *Natural Hybridization and Evolution* (Oxford Univ. Press, Oxford, 1997).
2. B. D. Mishler, M. J. Donoghue, *Syst. Zool.* **31**, 491 (1982).
3. P. R. Ehrlich, P. H. Raven, *Science* **165**, 1228 (1969).
4. L. H. Rieseberg, T. E. Wood, E. J. Baack, *Nature* **440**, 524 (2006).
5. C. L. Morjan, L. H. Rieseberg, *Mol. Ecol.* **13**, 1341 (2004).
6. M. C. Whitlock, *Genetics* **164**, 767 (2003).
7. S. F. McDaniel, A. J. Shaw, *Mol. Ecol.* **14**, 1121 (2005).
8. E. G. Bakker *et al.*, *Mol. Ecol.* **15**, 1405 (2006).
9. J. Ramsey, H. D. Bradshaw, D. W. Schemske, *Evolution Int. J. Org. Evolution* **57**, 1520 (2003).
10. G. L. Stebbins, *Variation and Evolution in Plants* (Columbia Univ. Press, New York, 1950).
11. R. D. Sargent, S. P. Otto, *Am. Nat.* **167**, 67 (2006).
12. S. Gavrilets, A. Vose, *Mol. Ecol.* **16**, 2910 (2007).
13. M. C. Ungerer, S. J. E. Baird, J. Pan, L. H. Rieseberg, *Proc. Natl. Acad. Sci. U.S.A.* **95**, 11757 (1998).
14. L. Fishman, A. J. Kelly, J. H. Willis, *Evolution Int. J. Org. Evolution* **56**, 2138 (2002).
15. L. H. Rieseberg, S. Church, C. L. Morjan, *New Phytol.* **161**, 59 (2004).
16. H. A. Orr, *Genetics* **149**, 2099 (1998).
17. B. Igic, J. R. Kohn, *Proc. Natl. Acad. Sci. U.S.A.* **98**, 13167 (2001).
18. G. L. Stebbins, *Adv. Genet.* **9**, 147 (1958).
19. L. H. Rieseberg, *Trends Ecol. Evol.* **16**, 351 (2001).
20. C. R. Werth, M. D. Windham, *Am. Nat.* **137**, 515 (1991).
21. Z. Lai *et al.*, *Genetics* **171**, 291 (2005).
22. M. A. F. Noor, K. L. Grams, L. A. Bertucci, J. Reiland, *Proc. Natl. Acad. Sci. U.S.A.* **98**, 12084 (2001).
23. M. Kirkpatrick, N. Barton, *Genetics* **173**, 419 (2006).
24. L. C. Moyle, E. B. Graham, *Genetics* **169**, 355 (2005).
25. L. Fishman, J. H. Willis, *Evolution Int. J. Org. Evolution* **60**, 1372 (2006).
26. J. D. Gillman, S. Bentolila, M. R. Hanson, *Plant J.* **49**, 217 (2007).
27. K. Bomblies, D. Weigel, *Nat. Rev. Genet.* **8**, 382 (2007).
28. P. Christie, M. R. Macnair, *Evolution Int. J. Org. Evolution* **41**, 571 (1987).
29. A. L. Sweigart, A. R. Mason, J. H. Willis, *Evolution Int. J. Org. Evolution* **61**, 141 (2007).
30. B. L. Gross, L. H. Rieseberg, *J. Hered.* **96**, 241 (2005).
31. M. J. Hegarty, S. J. Hiscock, *New Phytol.* **165**, 411 (2005).
32. C. A. Buerkle, R. J. Morris, M. A. Asmussen, L. H. Rieseberg, *Heredity* **84**, 441 (2000).
33. S. P. Otto, J. Whitton, *Annu. Rev. Genet.* **34**, 401 (2000).
34. G. L. Stebbins, *Chromosomal Evolution in Higher Plants* (Edward Arnold, London, 1971).
35. D. E. Soltis *et al.*, *Taxon* **56**, 13 (2007).
36. L. Cui *et al.*, *Genome Res.* **16**, 738 (2006).
37. J. Ramsey, D. W. Schemske, *Annu. Rev. Ecol. Syst.* **29**, 467 (1998).
38. D. A. Levin, *Taxon* **24**, 35 (1975).
39. D. J. Rodriguez, *Am. Nat.* **147**, 33 (1996).
40. E. J. Baack, *Heredity* **94**, 538 (2005).
41. J. H. Rausch, M. T. Morgan, *Evolution Int. J. Org. Evolution* **59**, 1867 (2005).
42. J. Mallet, *Nature* **446**, 279 (2007).
43. D. A. Levin, *Am. Nat.* **122**, 1 (1983).
44. S. A. Hodges, M. L. Arnold, *Proc. R. Soc. London B. Biol. Sci.* **262**, 343 (1995).
45. J. A. Coyne, H. A. Orr, *Speciation* (Sinauer Assoc., Sunderland, MA, 2004).
46. K. Bolmgren, O. Eriksson, H. P. Linder, *Evolution Int. J. Org. Evolution* **57**, 2001 (2003).
47. G. G. Mittelbach *et al.*, *Ecol. Lett.* **10**, 315 (2007).
48. E. S. Nagy, K. J. Rice, *Evolution Int. J. Org. Evolution* **51**, 1079 (1997).
49. H. H. Grundt *et al.*, *Proc. Natl. Acad. Sci. U.S.A.* **103**, 972 (2006).
50. D. W. Schemske, H. D. Bradshaw, *Proc. Natl. Acad. Sci. U.S.A.* **96**, 11910 (1999).
51. J. Kruger *et al.*, *Science* **296**, 744 (2002).
52. L. H. Rieseberg *et al.*, *Science* **301**, 1211 (2003).
53. J. Wang, L. Tian, H. S. Lee, Z. J. Chen, *Genetics* **173**, 965 (2006).
54. C. Hughes, R. Eastwood, *Proc. Natl. Acad. Sci. U.S.A.* **103**, 10334 (2006).

55. We thank the great botanical naturalists of the 20th century who provided the foundation for current studies of plant speciation. These include the founding fathers of ecological genetics (J. Clausen, D. Keck, and W. Hiesey), the grand synthesizers (G. L. Stebbins and Verne Grant), and the hybridization enthusiast, Edgar Anderson. We also thank members of the Rieseberg and Willis laboratories and three referees for useful comments on an earlier version of this paper. The authors' research on speciation has been supported by NSF, NIH, USDA, and the National Sciences and Engineering Research Council of Canada.

Supporting Online Material

www.sciencemag.org/cgi/content/full/317/5840/910/DC1
Fig. S1
Table S1
References

10.1126/science.1137729

Human Genome Ultraconserved Elements Are Ultraselected

Sol Katzman,[1]* Andrew D. Kern,[2]* Gill Bejerano,[2]† Ginger Fewell,[3] Lucinda Fulton,[3] Richard K. Wilson,[3] Sofie R. Salama,[2,4] David Haussler[1,2,4]‡

Unexpectedly long regions of extremely conserved DNA, known as ultraconserved elements, were first found by comparing the human, mouse, and rat genomes (*1*).

Although the DAF spectrum of the nonsynonymous sites is consistent with that observed previously, the spectrum for the ultraconserved sites is qualitatively different (Fig. 1). Large fractions of DAF is likely to show a difference between the reference human genome and the reference genomes of mouse and rat and hence be excluded from study. Our probability model compensates for such bias (fig. S1), which also applies to polymorphism studies of other conserved regions. In addition, a separate analysis shows that our results are not influenced by different strengths of linkage between sites within the separate classes analyzed (*6*). We can rule out other regional effects because the bases immediately flanking the ultraconserved regions have a much lower mean selection coefficient (fig. S3).

Previous studies have indicated that conserved noncoding regions can exhibit selection coefficients comparable to those of protein-coding regions (*7*). Our analysis shows that selection in the vertebrate-specific ultraconserved noncoding regions is in fact much stronger. These data argue that ultraconserved elements are currently, as well as historically, strongly constrained functional elements.

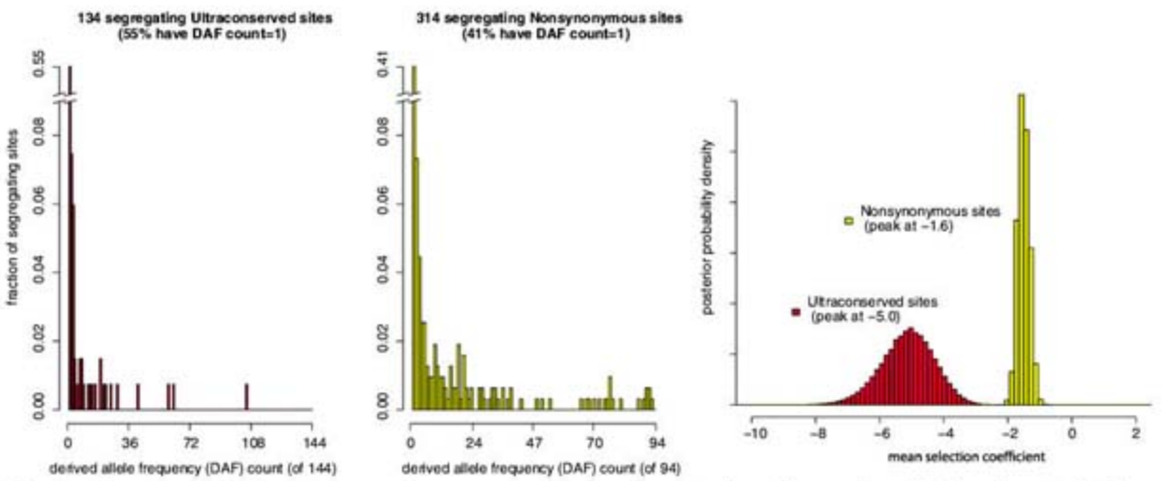

Fig. 1. Ultraconserved elements are under stronger selection than protein-coding regions. (**Left** and **center**) Histograms of the derived allele frequency counts for segregating sites in the indicated categories. In each histogram the first bar, corresponding to singleton heterozygotes (DAF count = 1), is truncated. (**Right**) The Bayesian posterior distributions for the mean selection coefficient. The *x* axis is given in units of $\alpha = 2N_e s$, where N_e is the effective population size and *s* is the fitness parameter.

Most are non–protein-coding regions, unique to vertebrates, and have undergone little or no evolutionary change since mammal and bird ancestors diverged about 300 million years ago. Many may function as distal enhancers for neighboring developmental genes (*2*). However, the reason for their extreme conservation remains a mystery. They could be unusually large patches of sites under weak levels of negative selection (*3*, *4*) or simply mutational cold spots.

We measured the derived (new) allele frequency (DAF) spectrum for the segregating human polymorphisms in the ultraconserved regions. It is markedly shifted toward rare derived alleles, as is characteristic of regions under negative selection in which introduced mutations are unlikely to spread to high frequencies within populations.

We analyzed genomic DNA sequences in 72 individuals (a mixture of European Americans and African Americans) spanning 315 of the ultraconserved elements and found 134 segregating sites. We compared the DAFs for these sites with those in 314 segregating nonsynonymous sites in 211 genes obtained from 47 individuals of similar background available from the SeattleSNPs consortium (*5*).

both the segregating ultraconserved sites (55%) and the nonsynonymous sites (41%) are present in only one allele in one sample. However, only 3% of the segregating ultraconserved sites exhibit DAFs of more than 25%, compared with 14% of the segregating nonsynonymous sites (χ^2 *P* value of 0.002), even after performing a normalization to a common sample size of 80 chromosomes (*6*).

To estimate the distribution of selection coefficients from these DAF spectra, we applied a hierarchical Bayesian model in which the mean selection coefficient for a set of bases is a random variable whose distribution we estimate via Markov chain Monte Carlo (MCMC) methods (*6*). Negative values imply that derived alleles are deleterious. A comparison of the posterior distributions (Fig. 1) shows that the ultraconserved sites are, on average, under purifying selection that is three times greater than that acting on nonsynonymous sites. The 95% credible intervals do not overlap at all.

Such estimates are subject to ascertainment bias, both in the selection of segregating sites (a bias we avoid by completely resequencing the entire region) and implicit in the definition of the ultraconserved regions themselves. A region of the genome containing a segregating site with high

References and Notes

1. G. Bejerano *et al.*, *Science* **304**, 1321 (2004); published online 6 May 2004 (10.1126/science.1098119).
2. L. A. Pennacchio *et al.*, *Nature* **444**, 499 (2006).
3. P. D. Keightley, M. J. Lercher, A. Eyre-Walker, *PLoS Biol.* **3**, e42 (2005).
4. G. V. Kryukov, S. Schmidt, S. Sunyaev, *Hum. Mol. Genet.* **14**, 2221 (2005).
5. J. M. Akey *et al.*, *PLoS Biol.* **2**, e286 (2004).
6. Materials and methods are available on *Science* Online.
7. J. A. Drake *et al.*, *Nat. Genet.* **38**, 223 (2006).
8. We thank J. Kent, M. Diekhans, D. Thomas, K. Pollard, C. Lowe [University of California Santa Cruz (UCSC)], J. Reed, S. Scott (Genome Sequencing Center), W. Schackwitz, J. Martin, L. Pennacchio (U.S. Department of Energy Joint Genome Institute), P. Robertson (SeattleSNPs), the UCSC Genome Browser group, and anonymous reviewers. Funding was provided by NIH National Human Genome Research Institute (S.K., A.D.K., G.B., D.H., and R.K.W.) and Howard Hughes Medical Institute (S.R.S. and D.H.).

Supporting Online Material

www.sciencemag.org/cgi/content/full/317/5840/915/DC1
Materials and Methods
Figs. S1 to S3
Reference

12 March 2007; accepted 28 June 2007
10.1126/science.1142430

[1]Department of Biomolecular Engineering, University of California, Santa Cruz, CA 95064, USA. [2]Center for Biomolecular Science and Engineering, University of California, Santa Cruz, CA 95064, USA. [3]Genome Sequencing Center, Washington University School of Medicine, St. Louis, MO 63108, USA. [4]Howard Hughes Medical Institute, University of California, Santa Cruz, CA 95064, USA.

*These authors contributed equally to this work.
†Present address: Department of Developmental Biology and Department of Computer Science, Stanford University, Stanford, CA 94305, USA.
‡To whom correspondence should be addressed. E-mail: haussler@soe.ucsc.edu

Effects of Aneuploidy on Cellular Physiology and Cell Division in Haploid Yeast

Eduardo M. Torres,[1] Tanya Sokolsky,[1]* Cheryl M. Tucker,[2] Leon Y. Chan,[1] Monica Boselli,[1] Maitreya J. Dunham,[2] Angelika Amon[1]†

Aneuploidy is a condition frequently found in tumor cells, but its effect on cellular physiology is not known. We have characterized one aspect of aneuploidy: the gain of extra chromosomes. We created a collection of haploid yeast strains that each bear an extra copy of one or more of almost all of the yeast chromosomes. Their characterization revealed that aneuploid strains share a number of phenotypes, including defects in cell cycle progression, increased glucose uptake, and increased sensitivity to conditions interfering with protein synthesis and protein folding. These phenotypes were observed only in strains carrying additional yeast genes, which indicates that they reflect the consequences of additional protein production as well as the resulting imbalances in cellular protein composition. We conclude that aneuploidy causes not only a proliferative disadvantage but also a set of phenotypes that is independent of the identity of the individual extra chromosomes.

The cell division cycle is a highly controlled process that generates two daughter cells of identical genetic makeup. Surveillance mechanisms known as checkpoints ensure that this process occurs with high fidelity. However, despite these surveillance mechanisms, chromosome missegregation occurs once every 5×10^5 cell divisions in yeast (*1*) and on the order of once every 10^4 to 10^5 divisions in mammalian cells (*2*), producing a condition known as aneuploidy.

More than a century ago, aneuploidy was postulated to be a common characteristic of cancer cells (*3*). Since then, it has been proposed that aneuploidy contributes to tumorigenesis by providing a mechanism by which oncogenes are gained or tumor suppressor genes are lost (*4*). Studies examining the effects of aneuploidy on cell proliferation in *Schizosaccharomyces pombe* (*5*) and *Drosophila* (*6*) and the effects of trisomy on cell proliferation in humans (*7*) suggest that aneuploidy can also interfere with cell proliferation. To address how aneuploidy affects the proliferation and physiology of normal cells, we generated a set of yeast strains in which each strain bears an extra copy of one or more of almost all of the yeast chromosomes. Their characterization represents a comprehensive analysis of the effects of aneuploidy on cellular physiology. We found that in addition to chromosome-specific phenotypes, aneuploid strains share a number of traits, pointing toward the existence of a general cellular response to aneuploidy.

Generation of aneuploid yeast strains. To create yeast cells that contain an additional chromosome, we used a chromosome transfer strategy. During mating, if one of the mating partners lacks the karyogamy gene *KAR1*, nuclear fusion does not occur (*8*). However, occasionally individual chromosomes are transferred from one nucleus to the other during these abortive matings (*8*, *9*). When the two mating partners carry different selectable markers at the same genomic location, these rare chromosome transfers can be selected for (fig. S1). Using this technique, we generated 13 of the 16 possible disomic strains (tables S1 and S2) (*10*).

To ensure that strains with the correct marker combination were indeed disomic for the entire chromosome, we performed comparative genomic hybridization, which allows for the quantification of gene copy number on a genome-wide scale. This analysis also revealed that some of the strains obtained from the chromosome transfer procedure carried one or two extra chromosomes in addition to the one we selected for (fig. S2A). Although the second chromosome cannot be selected for, these strains were karyotypically stable enough to conduct a phenotypic characterization.

Aneuploidy causes a transcriptional response. To characterize the effects of aneuploidy on gene expression, we grew each aneuploid yeast strain to mid-log phase in batch culture and measured genome-wide gene expression relative to the wild-type strain with the use of DNA microarrays. An approximate doubling of gene expression was observed along the entire length of the disomic chromosomes, indicating that most if not all genes are expressed proportionally to the number of DNA copies in the cell (Fig. 1A). A similar result has been reported for a smaller data set (*11*).

To reveal more subtle correlations masked by the strong chromosome-specific signals (fig. S3A), we applied a clustering program that allows the assignment of a reduced weight to genes on disomic chromosomes (*10*) (Fig. 1B). This analysis showed that many aneuploid yeast strains—particularly strains disomic for chromosomes IV, XIII, XV, and XVI and strains with multiple extra chromosomes—exhibited a gene expression signature characteristic of the yeast environmental stress response (ESR). Of the 870 genes identified by Gasch *et al.* to constitute the ESR cluster, 615 also showed the same transcriptional change in yeast strains with additional chromosomes (Fig. 1B) (*12*). These same expression changes are also observed in yeast strains growing at slower growth rates (*13*). Mutants defective in cell proliferation, such as temperature-sensitive *cdc28-4* or *cdc23-1* grown at the permissive temperature (*cdc28-4* mutants exhibit a G_1 delay; *cdc23-1* mutants exhibit a metaphase delay), also exhibited some of the same changes in gene expression (Fig. 1B), raising the possibility that defects in cell proliferation could also cause this transcriptional response.

All aneuploid strains that we examined proliferated more slowly than did wild-type cells (fig. S4, A, B, F, and G). Gene expression patterns that are linked to growth rates could thus mask gene expression patterns common to all aneuploid strains. To eliminate differences in gene expression caused by differences in doubling time, we grew all aneuploid strains and the wild type at the same growth rate in the chemostat under conditions where phosphate was limiting. Because the set doubling time of ~6 hours was longer than the doubling time of each strain in batch growth, all strains grew at the same rate. When cells reached steady state, samples for gene expression were harvested for microarray analysis. Slow-growing strains carrying the *cdc28-4* and *cdc23-1* mutations were also grown under the same conditions. The gene expression changes that correlated with growth rate differences were not present in any of the chemostat-grown samples. The remaining gene expression changes included a transcription pattern shared by most of the aneuploid strains and not detectable or not present in exponentially growing cultures, nor in wild-type cells or *cdc28-4* and *cdc23-1* mutants grown in the chemostat under phosphate-limiting conditions (Fig. 1C and fig. S3B).

Of the 4963 genes whose expression change was greater than the control threshold (factor of 1.3) in at least one strain, 397 genes showed changed expression in 10 or more of the 14 aneuploid strains. We used the program GO Term Finder, available from the *Saccharomyces* Genome Database (*14*), to identify the functional categories enriched in each gene set. The group that showed increased expression was enriched

[1]Center for Cancer Research, Howard Hughes Medical Institute, Massachusetts Institute of Technology, E17-233, 40 Ames Street, Cambridge, MA 02139, USA. [2]Lewis-Sigler Institute for Integrative Genomics, Princeton University, Princeton, NJ 08544, USA.

*Present address: Applied Biosystems, 500 Cummings Center, Beverly, MA 01915, USA.

†To whom correspondence should be addressed. E-mail: angelika@mit.edu

in ribosomal biogenesis genes, particularly those related to ribosomal RNA processing (Fig. 1D and table S4). Genes with annotations related to nucleic acid metabolism were also enriched (table S4). The more variable set of genes whose expression was decreased was enriched for genes involved in carbohydrate metabolism (Fig. 1D and table S4). We conclude that aneuploid strains, when normalized for growth rate in phosphate-limited chemostats, are somehow perturbed with respect to ribosomal biogenesis and energy production.

Most aneuploid yeast strains exhibit a G_1 delay. To determine how aneuploidy affects cell physiology, we characterized the proliferation properties of strains carrying one or several extra chromosomes. The doubling time and cell size were slightly increased in most aneuploid strains in complete medium [yeast extract, peptone, and dextrose (YPD); fig. S4A] and synthetic medium that selects for the presence of the disome (–His+G418; fig. S4B). Even disomic strains that did not exhibit a proliferation delay, such as cells disomic for chromosomes I or II, showed decreased proliferative capacity relative to wild-type cells when the strains were cocultured (fig. S4, F and G). Furthermore, some of the aneuploids, such as strains disomic for chromosomes IV, XI, or XIII, also exhibited poor viability as judged by their inability to form colonies on plates (fig. S4E). The proliferative disadvantage and increase in cell size were also observed in diploid cells carrying an extra chromosome (fig. S4, C and D), indicating that the gain of an extra chromosome interferes with cell proliferation of both haploid and diploid cells. Thus, contrary to what we would have expected from studies on cancer cells, where aneuploidy is thought to bring about a proliferative advantage (*4*), aneuploidy causes a proliferative disadvantage in yeast.

To determine in which stage of the cell cycle the aneuploid yeast strains were delayed, we examined cell cycle progression after release from a pheromone-induced G_1 phase arrest. Entry into the cell cycle, as judged by bud formation (Fig. 2A) and DNA replication (Fig. 2B), was delayed in 16 of 20 aneuploid strains. With the exception of cells disomic for chromosomes I, II, V, or IX, all aneuploid strains exhibited a delay in entry into the cell cycle (fig. S5 and table S1), with most strains (disome VIII, X, XI, XII, XIII, XIV, V+IX, VIII+XV, and XI+XV strains) showing a delay ranging from 10 to 20 min. Cells disomic for multiple chromosomes (disome V+VII, VIII+XIV, XI+XVI, and I+VI+XIII strains), as well as cells disomic for chromosome IV or XVI, exhibited a G_1 delay of 25 min or more. Aneuploids exhibited few other cell cycle delays. The metaphase to anaphase transition was delayed in only 2 of the 20 aneuploid strains (fig. S5 and table S1), and only 7 of 20 exhibited a delay in entry into mitosis (as determined by a delayed appearance of cells with metaphase spindles) (Fig. 2C, table S1, and fig. S5). We conclude that most aneuploid strains are delayed in G_1 phase. In general, the delay appears to be larger in strains carrying an extra copy of a large chromosome or extra copies of multiple chromosomes (fig. S6), which suggests that the amount of additional yeast DNA may contribute to determining the length of the G_1 delay.

The molecular events underlying the G_1 to S phase transition are well characterized in *S. cerevisiae*. The cyclin-dependent kinase (CDK) Cdc28 associated with the cyclin Cln3 inhibits Whi5, an inhibitor of the transcription factor complex SBF (*15*, *16*). SBF in turn induces the transcription of genes encoding two other cyclins, *CLN1* and *CLN2*, which, when complexed with Cdc28, promote entry into the cell cycle (*17*). We analyzed the abundance of *CLN2* RNA and Cln2 protein in strains disomic for chromosomes IV, XIII, or VIII+XIV. Accumulation of *CLN2* RNA and Cln2 protein was delayed and paralleled the delay in bud formation and DNA replication (Fig. 2, D and E). Our results indicate that in the strains that we analyzed, aneuploidy interferes with the G_1 to S phase transition upstream of *CLN2* transcription. How the presence of additional yeast chromosomes prevents Cln2 accumulation remains to be determined. Cln3-CDKs promote *CLN2* accumulation and are the target of events such as cell growth that control the G_1 to S phase transition (*18*, *19*). Thus, the presence of extra chromosomes might affect Cln3-CDK function.

Aneuploids exhibit increased glucose uptake. To further investigate the effects of aneuploidy on cell proliferation, we examined the kinetics with which aneuploid cells enter stationary phase. Most aneuploids reached saturation at a smaller population size [as measured by optical density at 600 nm (OD_{600})] (Fig. 3, A and B) and lost viability upon prolonged culturing in stationary phase (Fig. 3C). In general, the maximum OD_{600} was lower in strains carrying two copies of large chromosomes or two copies of multiple chromosomes (Fig. 3, A and B). Thus, biomass accumulation appears to be inversely correlated with the amount of additional yeast DNA present in the aneuploid strains and the severity of their proliferation defects.

To determine whether the lower OD_{600} at which aneuploids enter stationary phase was due to nutrient depletion, we simultaneously measured glucose uptake and accumulation of biomass. This comparison revealed that wild-type cells generated more biomass per internalized glucose molecule than did aneuploid cells. Whereas wild-type cells reached cell densities of OD_{600} = 9, having taken up 75% of the glucose in the medium, cells disomic for chromosome IV only reached a cell density of OD_{600} of less than 4 (Fig. 3D). The increase in glucose uptake correlated with the severity of the cell cycle delay, with strains with a shorter doubling time accumulating more biomass per glucose molecule (Fig. 3E).

Consistent with the idea that aneuploids take up more glucose, we observed that the gene loci encoding the high-affinity glucose transporters Hxt6 and Hxt7 were amplified (fig. S2B) and more highly expressed (Fig. 1 and fig. S2B) in most of the aneuploid strains we generated (n = 42). Strains that did not show this amplification and increased expression were those that carried an extra copy of chromosome VIII, which carries three genes encoding other high-affinity glucose transporters. Together with the microarray experiments indicating changes in gene expression relating to carbohydrate metabolism, our results suggest that aneuploids require more carbohydrates or energy (or both) for cell survival and proliferation than do wild-type cells.

Most genes on the aneuploids' extra chromosomes are expressed. Why would aneuploids need additional glucose? Because an estimated 60 to 90% of the intracellular chemical energy is devoted to protein production (*20*), we hypothesized that macromolecule biosynthesis from the additional chromosome present in aneuploid strains could be one reason. Indeed, our expression profile analysis of aneuploids showed that most genes present on the additional chromosomes were transcribed: 93% of genes carried on the chromosome that was present in two copies were overexpressed by a factor of at least 1.3 over the wild type, and expression of 83% of genes went up by a factor of 1.5 or more (Fig. 1, A and C). To determine whether the transcripts produced from the extra chromosomes were also translated, we measured the amounts of a small number of proteins. The amounts of Arp5, Tcp1, and Cdc28 protein were increased in strains disomic for the chromosomes containing the genes encoding these proteins (Fig. 4A). Our results suggest that at least some of the genes present on the additional chromosomes are not only transcribed but also translated.

Interestingly, most of the proteins (13 of 16) that we analyzed showed no change in abundance, even though the amount of transcript was increased in accordance with the increase in gene copy number (Fig. 4A and fig. S7). With the exception of Leb4 and Fcy1 (for which it is not known whether they are components of protein complexes), all 13 proteins analyzed are components of protein complexes. Rpa1 is a component of the replication machinery, Mre11 of the RMX complex, Rps2 and Rpl32 of the ribosome, Rpt1 of the proteasome, Nop1 of the nucleolus, histone H3 of the nucleosome, Yaf9 and Eaf3 of the NuA4 histone H4 acetyltransferase complex, and Elp3 of the elongator complex. These findings indicate that many proteins synthesized from the additional chromosomes are either not translated or, more likely, degraded shortly after synthesis (*21*).

Consistent with the idea that increased protein degradation occurs in aneuploid yeast strains, the proliferation of a number of aneuploid strains (IV, XII, XIII, XIV, and XVI) was inhibited by concentrations of the proteasome inhibitor MG132 at which wild-type cells grow, as judged by their ability to form colonies on plates containing the

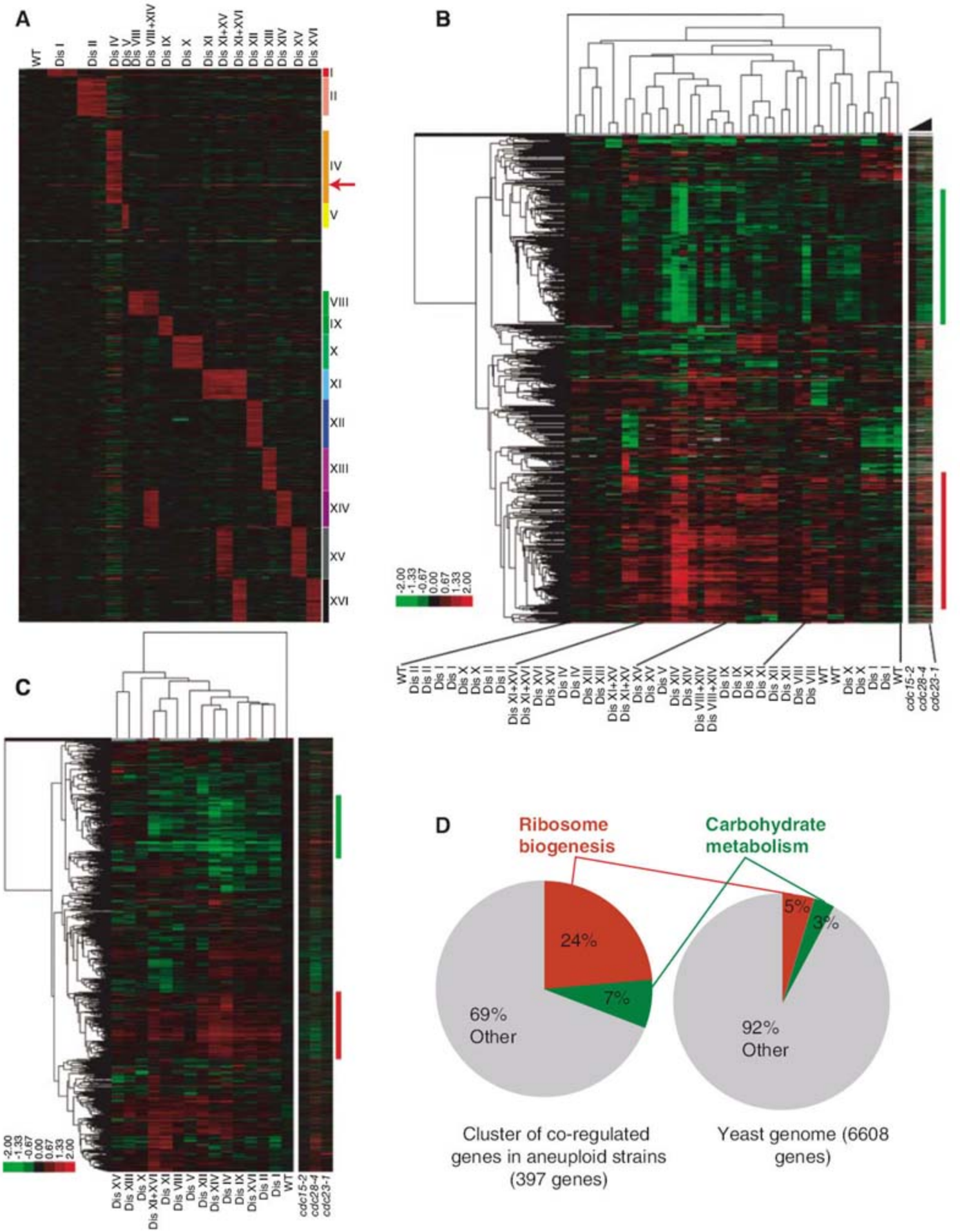
A
WT
Dis I
Dis II
Dis IV
Dis V
Dis VIII
Dis VIII+XIV
Dis IX
Dis X
Dis XI
Dis XI+XV
Dis XI+XVI
Dis XII
Dis XIII
Dis XIV
Dis XV
Dis XVI
I
II
IV
V
VIII
IX
X
XI
XII
XIII
XIV
XV
XVI
B
-2.00
-1.33
-0.67
0.00
0.67
1.33
2.00
C
D
Ribosome biogenesis
Carbohydrate metabolism
24%
7%
69% Other
5%
3%
92% Other
Cluster of co-regulated genes in aneuploid strains (397 genes)
Yeast genome (6608 genes)

Fig. 1. Effects of aneuploidy on gene expression. (**A**) Gene expression of wild-type and aneuploid strains grown in batch cultures, ordered by chromosome position. Experiments (columns) are ordered by the number of the chromosome that is present in two copies. The expression patterns of aneuploid strains were compared to those of wild-type cells (A11311) grown under the same conditions. Data were renormalized to account for the disome. The arrow points to the genomic location of *HXT6* and *HXT7*. The data are provided in table S5. Strain order [note that the number after each strain number denotes the experiment number; the same nomenclature is used in (B)]: A11311 #1, A11311 #2, A11311 #3, A11311 #4, A12683 #1, A12683 #2, A6863 #1, A6863 #2, A12685 #1, A12685 #2, A6865 #1, A6865 #2, A12687 #1, A12687 #2, A14479 #1, A13628 #1, A13628 #2, A15615 #1, A15615 #2, A13975 #1, A13975 #2, A12689 #1, A12689 #2, A6869 #1, A6869 #2, A13771 #1, A13771 #2, A12691 #1, A12691 #2, A12699 #1, A12699 #2, A12693 #1, A12693 #2, A12695 #1, A12695 #2, A13979 #1, A13979 #2, A12697 #1, A12697 #2, A12700 #1, A12700 #2. (**B**) Hierarchically clustered gene expression data obtained from strains grown in batch cultures. Data from (A) were filtered for genes changing by a factor of >1.8 on at least two arrays. Genes present on chromosomes in two copies were downweighted and all data were clustered using the program WCluster. Clustering with all genes weighted equally is shown in fig. S3A. Gene expression for strains, ordered by increasing doubling time, carrying a *cdc15-2*, *cdc28-4*, or *cdc23-1* mutation compared to a matched wild type (A2587) grown at 23°C is shown adjacent to the main cluster. The columns labeled WT are biological replicates. Note that *cdc15-2* mutants do not show the ESR expression profile, which is consistent with the fact that *cdc15-2* mutants show only a slight proliferation defect at 23°C. Green and red bars correspond to putative clusters associated with ESR or growth rate that are down- and up-regulated, respectively. Replicates for each strain were more related to each other than to any other strains, indicating that the expression arrays were highly reproducible. Strain order: A11311 #4, A12685 #2, A12685 #1, A12683 #2, A12683 #1, A12689 #2, A12689 #1, A6865 #2, A6865 #1, A12699 #2, A12699 #1, A12700 #2, A12700 #1, A12687 #2, A12687 #1, A12695 #2, A12695 #1, A12691 #2, A12691 #1, A12697 #2, A12697 #1, A14479 #1, A13979 #2, A13979 #1, A15615 #2, A15615 #1, A13975 #2, A13975 #1, A13771 #2, A13771 #1, A12693 #2, A12693 #1, A13628 #2, A13628 #1, A11311 #3, A11311 #2, A6869 #2, A6869 #1, A6863 #2, A6863 #1, A11311 #1, A2596, A2594, A755. (**C**) Hierarchically clustered gene expression data obtained from strains grown in a chemostat under phosphate-limiting conditions. The expression patterns of aneuploid strains were compared to wild-type cells (A11311) grown under the same conditions. Data were renormalized, filtered for genes changing by at least a factor of 1.3 in at least one experiment, and clustered with genes present on chromosomes present in two copies downweighted. Clustering with all genes weighted equally is shown in fig. S3B. Gene expression for strains carrying a *cdc15-2* (A2596), *cdc28-4* (A2594), or *cdc23-1* (A755) mutation as compared to a matched wild type (A2587) grown at 23°C is shown adjacent to the main cluster. Green and red bars indicate putative common transcriptional responses that are down- and up-regulated in aneuploid strains, respectively. The data are provided in table S5. Strain order: A12697, A12695, A12689, A12699, A13771, A13628, A14479, A12693, A13979, A12687, A13975, A12700, A12685, A12683, A11311, A2596, A2594, A755. (**D**) Pie-chart representation of genes changing expression significantly in at least 10 of 14 disomic strains grown under phosphate-limiting conditions grouped by GO terms. Full GO results, including genes annotated to each term, can be found in table S4.

drug (Fig. 4F; note that strains with multiple additional chromosomes could not be tested because of the need to delete *PDR5* to test the effects of MG132) (*22*, *23*). Furthermore, proliferation of all aneuploid strains was hampered by the protein synthesis inhibitor cycloheximide (Fig. 4C), which can be a sign of ubiquitin depletion (*24*). Several proteins such as α-tubulin and histones, which are components of multiprotein complexes, are degraded if they are overexpressed or their binding partners are missing (*25*, *26*). Such a mechanism might regulate the amounts of the proteins that did not increase in abundance, in accordance with gene dosage in the aneuploid strains. Thus, transcription, translation, and degradation of proteins produced from the additional chromosomes present in aneuploids may contribute to the increased glucose uptake of these cells.

Proliferation of aneuploids is inhibited by protein synthesis inhibitors and high temperature. To determine whether the synthesis of proteins from the additional chromosomes and their presence in the cell represents an increased burden on the cell's protein production machinery, we examined the ability of aneuploid strains to grow under conditions that interfere with transcription, protein synthesis, and protein folding. Proliferation of all aneuploids, with the exception of strains disomic for chromosomes I, X, or XIV, was inhibited by a high (20 μg/ml) concentration of the RNA polymerase inhibitor thiolutin (Fig. 4B). At low concentrations of the RNA polymerase inhibitor (5 μg/ml to 15 μg/ml), proliferation of only a subset of strains was impaired (fig. S8H). However, all aneuploid strains showed decreased proliferation when exposed to the protein synthesis inhibitor cycloheximide at concentrations of 0.1 and 0.2 μg/ml, and proliferation of most strains was impaired at a concentration of 0.05 μg/ml (Fig. 4C). With the exception of strains disomic for chromosomes I, II, or IX, aneuploid strains also showed increased sensitivity to the protein synthesis inhibitors hygromycin and rapamycin (Fig. 4D; cells disomic for chromosome X were not sensitive to rapamycin, perhaps because *TOR1* is located on this chromosome). The proliferation-inhibitory effects of protein synthesis inhibitors on aneuploids was not a consequence of the proliferation defect of aneuploids, because *cdc28-4* and *cdc23-1* mutants, which are severely impaired in cell division even at 23°C, did not exhibit increased sensitivity to cycloheximide or rapamycin (Fig. 4, C and D).

Proliferation of aneuploids was also decreased under conditions that led to the accumulation of unfolded proteins. All strains carrying an extra chromosome, with the exception of cells disomic for chromosome I, showed impaired proliferation at increased temperatures (37°C; Fig. 4E) and were modestly sensitive to the Hsp90 inhibitor geldanamycin (except cells disomic for chromosome X; Fig. 4F).

Aneuploids did not exhibit increased sensitivity to any toxic agents. Aneuploids formed colonies as well as did wild-type cells on medium containing the DNA replication inhibitor hydroxyurea (fig. S8B) or medium containing the proline analog azetidine 2-carboxylic acid (AZC; fig. S8E) or 6-azauracil (AZA; fig. S8I), which interferes with uridine triphosphate and guanosine triphosphate biosynthesis. None of the aneuploids showed altered proliferation in the presence of the autophagy inhibitor chloroquine (fig. S8D) or hydrogen peroxide (fig. S8G). Strains were also respiration-proficient as judged by their ability to grow on the nonfermentable carbon source glycerol (fig. S8, C and I) and did not exhibit increased sensitivity to the F1F0 adenosine triphosphate synthase inhibitor oligomycin (fig. S8I). About half of the aneuploid strains analyzed exhibited increased sensitivity to the microtubule-depolymerizing drug benomyl (fig. S8F), the basis of which warrants further investigation. Our results indicate that the proliferation of aneuploid strains is specifically impaired under conditions interfering with transcription, translation, and protein folding.

The phenotypes shared by aneuploid yeast strains are due to the presence of additional yeast genes. The phenotypes shared by aneuploids might result from the mere presence of additional DNA or from the RNAs and proteins synthesized from these chromosomes. Thus, we tested the effects of seven yeast artificial chromosomes (YACs) containing human or mouse DNA inserts ranging from ~350 kb to 1.6 Mb in size (table S3). Although we cannot exclude the possibility that some transcription and translation occurs from the mammalian DNA in yeast, the YACs do not produce yeast proteins, and it is highly likely that the amount of transcription and translation from the YACs is less than that occurring from yeast chromosomes, which are densely packed with mostly intronless genes.

The gene expression profile shared by aneuploid strains grown under phosphate-limiting chemostat conditions was also observed in YAC-carrying strains (Fig. 5A), which suggests that the mere presence of extra DNA is mainly responsible for this gene expression pattern. The other phenotypes observed in aneuploids were not shared by the YAC-bearing strains. With the exception of a minor (5 min) delay observed in cells carrying the largest YAC (YAC-1; 1.6 Mb),

none of the YAC-bearing strains exhibited delays in entry into the cell cycle (Fig. 5C). Nor was progression through other cell cycle stages affected, as judged by DNA content analysis (Fig. 5D). Furthermore, YAC-bearing strains did not exhibit increased sensitivity to thiolutin, cycloheximide, rapamycin, or high temperature (Fig. 5B). Curiously, the strain bearing the largest YAC exhibited increased sensitivity to hygromycin, the basis of which is at present unclear. We conclude that at least two aspects of aneuploidy may contribute to the phenotypes shared by aneuploid strains: (i) The expression signature shared by aneuploid strains appears to be elicited by the presence of extra DNA, and (ii) the cell cycle delays and proliferation defects under conditions interfering with protein synthesis and folding are in large part due to yeast transcripts and yeast proteins generated from extra chromosomes.

Discussion. Our analysis of aneuploid yeast strains was, by virtue of the way they were isolated, limited to aneuploid strains that are viable. Thus, most strains we characterized contained one additional chromosome, a few carried two, and one carried three. Strains with many additional chromosomes were not obtained, likely because they are inviable. The characterization of the 20 viable aneuploids that we analyzed nonetheless revealed that in addition to phenotypes that are chromosome-specific (for example, several aneuploid strains exhibit cell cycle defects in addition to the G_1 delay observed in most strains), these strains share several phenotypes.

Diploid yeast cells do not exhibit the phenotypes shared by the aneuploid strains we analyzed (figs. S4 and S8A). This result shows that the duplication of the entire genome is not nearly as deleterious as the duplication of a subset of chromosomes; moreover, it indicates that the genomic imbalance that results from aneuploidy is responsible for the phenotypes we observed. The finding that the severity of the phenotypes shared by aneuploids is generally greater in strains disomic for large or multiple chromosomes supports this idea. Our data further suggest that an increase in ploidy buffers the detrimental effects of the imbalances caused by aneuploidy. The phenotypes shared by aneuploids were generally less severe in trisomic than in disomic cells.

Our analysis of strains carrying YACs with mammalian DNA inserts suggests that most phenotypes common to aneuploids are caused by the additional yeast gene products. Only the gene expression pattern of aneuploids observed under phosphate-limiting conditions is also seen in the YAC-carrying strains, which suggests that the mere presence of extra DNA elicits this gene expression response. The cell cycle delay and impaired proliferation in the presence of transcription antagonists, translation inhibitors, or high temperatures were not observed in YAC-bearing strains. Most of the phenotypes shared by aneuploids—such as the increase in glucose uptake, the gene expression pattern observed in logarithmically growing cells, impaired proliferation in the presence of proteasome inhibitors, and G_1 delay—appear to correlate with the number of additional yeast genes. In the case of other phenotypes, such as increased sensitivity to protein synthesis inhibitors and conditions requiring increased protein folding activity, the correlation is not as striking. These findings, together with the observation that disomy for the small chromosome VI is lethal (*10*), indicate that the total amount of additional RNA and protein produced by aneuploids, the cellular imbalances caused by these extra proteins, and specific gene products present on individual chromosomes all

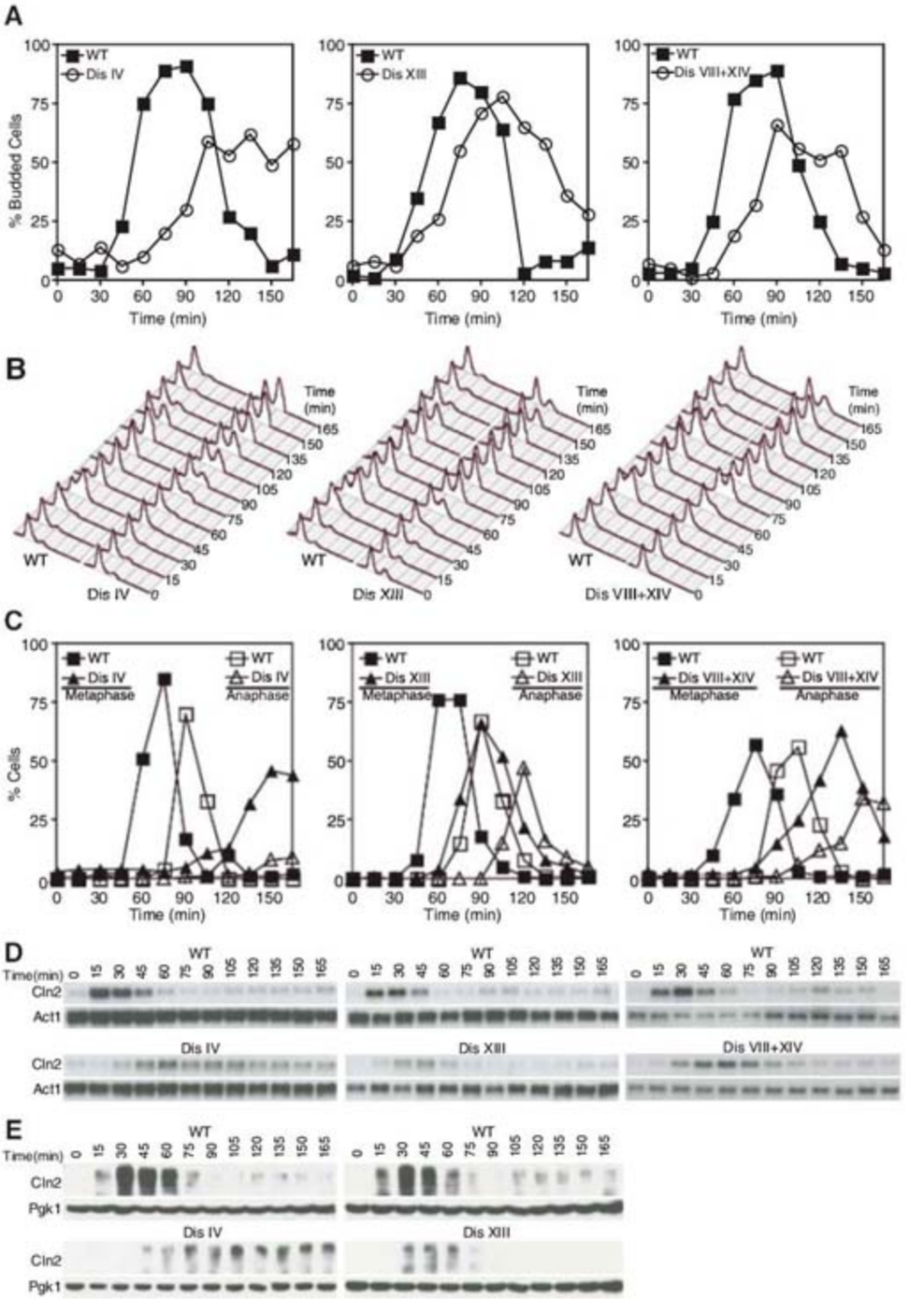

Fig. 2. Delay in G_1 of the cell cycle in aneuploid cells. Wild-type cells (A11311), cells disomic for chromosome IV (A12687), disomic for chromosome XIII (A12695), and disomic for chromosomes VIII and XIV (A15615), all carrying a *CLN2-HA* fusion with the exception of strain A15615, were arrested in G_1 with α-factor pheromone and released from the block as described (*10*). Samples were taken at indicated times to determine the percentage of budded cells (**A**), DNA content (**B**), the percentage of cells with metaphase and anaphase spindles (**C**), and the amount of *CLN2* RNA (**D**) and Cln2 protein (**E**). *ACT1* was used as a loading control in Northern blots (D). Pgk1 was used as loading control in Western blots (E). In strain A15615, we only examined *CLN2* RNA levels because chromosome XIV is not marked in this strain and we were therefore not able to select for the presence of two copies of this chromosome when introducing the Cln2-HA allele.

likely contribute to the phenotypes shared by aneuploids.

Striking among the phenotypes shared by aneuploid yeast strains are those indicative of protein degradation and folding distress. These observations suggest that proteins synthesized from the additional chromosomes disrupt cellular physiology, interfering with metabolic pathways and other basic cellular processes. We propose that the cell responds to this state of imbalance in a multilayered fashion not dissimilar to that of a stress response. The cell's attempt to restore wild-type physiology is reflected by the fact that although most genes present on the additional chromosomes are transcribed, the amounts of many proteins are not increased. The decrease in biomass produced per glucose molecule may be an indicator that more energy is being used to degrade proteins and induce mechanisms that shield the cell from the effects of excess proteins or compensate for their effects. Even the delay in G_1 might be a reflection of basic cellular pathways (such as growth) being slowed down.

Cancer cells, most of which are aneuploid, share several properties with yeast cells carrying additional chromosomes. Proliferation of both types of cells is impaired in the presence of protein synthesis inhibitors (*27*) and geldanamycin (*28*), and both exhibit increased glucose uptake (*29*). These parallels between tumor cells and aneuploid yeast strains raise the possibility that some phenotypes exhibited by tumor cells are elicited by their aneuploid state. Thus, the phenotypes exhibited by aneuploid yeast strains could be the starting point to determine whether aneuploid mammalian cells also share a set of phenotypes. These shared properties would be ideal targets for chemotherapeutics.

Our analysis shows that aneuploidy causes a proliferative disadvantage in yeast. The same could be true in human cells, not only because of the high degree of conservation of basic cellular processes among eukaryotes but also because trisomy 21 foreskin fibroblasts proliferate more

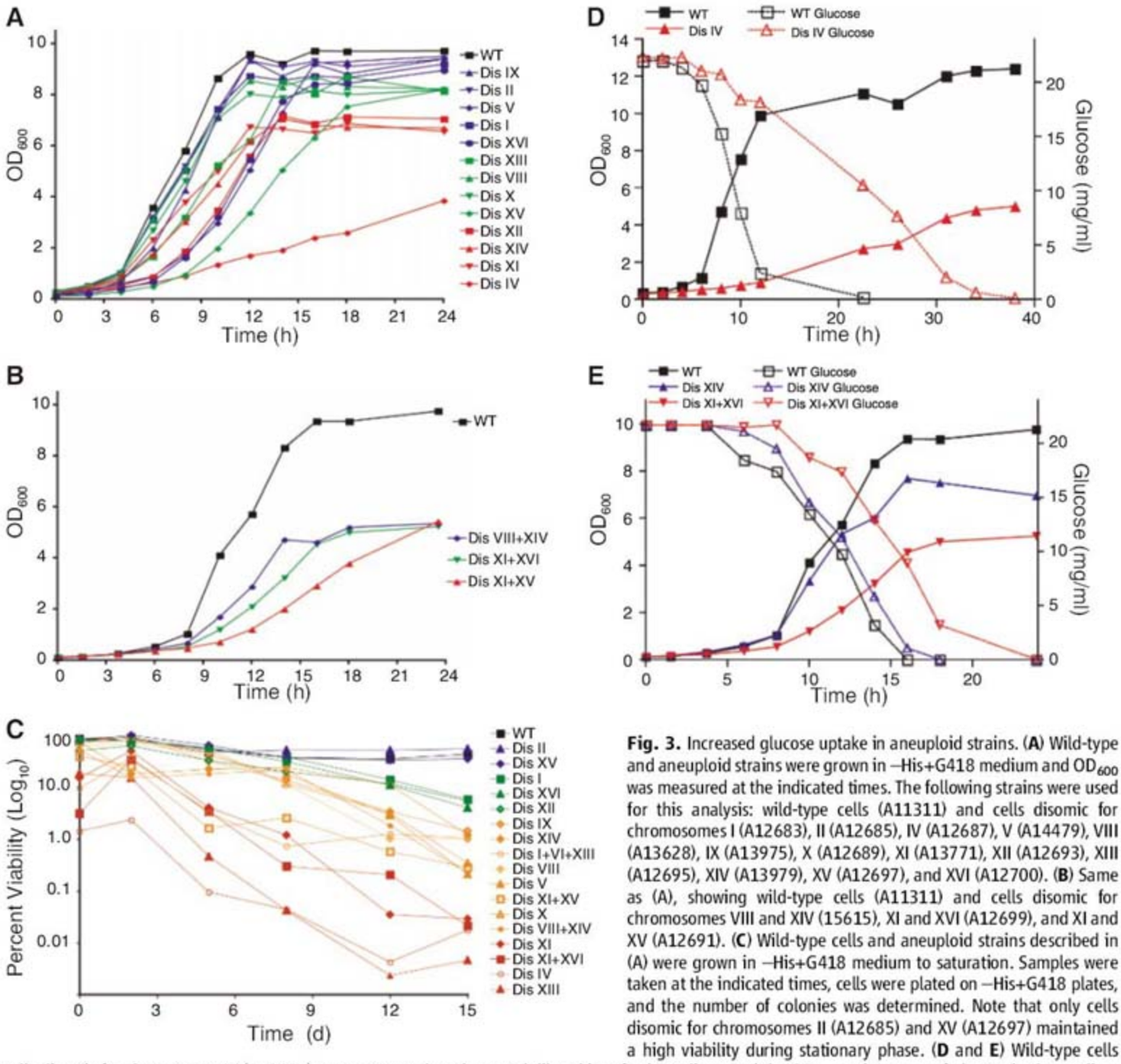

Fig. 3. Increased glucose uptake in aneuploid strains. (**A**) Wild-type and aneuploid strains were grown in −His+G418 medium and OD_{600} was measured at the indicated times. The following strains were used for this analysis: wild-type cells (A11311) and cells disomic for chromosomes I (A12683), II (A12685), IV (A12687), V (A14479), VIII (A13628), IX (A13975), X (A12689), XI (A13771), XII (A12693), XIII (A12695), XIV (A13979), XV (A12697), and XVI (A12700). (**B**) Same as (A), showing wild-type cells (A11311) and cells disomic for chromosomes VIII and XIV (15615), XI and XVI (A12699), and XI and XV (A12691). (**C**) Wild-type cells and aneuploid strains described in (A) were grown in −His+G418 medium to saturation. Samples were taken at the indicated times, cells were plated on −His+G418 plates, and the number of colonies was determined. Note that only cells disomic for chromosomes II (A12685) and XV (A12697) maintained a high viability during stationary phase. (**D** and **E**) Wild-type cells and cells disomic for chromosome IV (A12687) were grown to log phase and diluted into fresh medium, and the OD_{600} and amount of glucose in the medium were determined at the indicated times. (E) Same as (D) for wild-type cells and cells disomic for chromosome XIV (A13979) or XI+XVI (A12699).

slowly than normal diploid fibroblasts (*7*). Is it thus possible that aneuploidy does not contribute to carcinogenesis but rather antagonizes it? Aneuploidy provides a means of gaining additional copies of oncogenes or losing tumor suppressor genes (*4*, *30*), and the cellular imbalances caused by aneuploidy could create a selective stress that could promote the accumulation of growth and proliferation-promoting genomic alteration. Under selective conditions, even in yeast, certain aneuploidies may be advantageous (*31*). However, our data show that aneuploidy in itself results in a proliferative disadvantage for the cell. Clearly, this disadvantage must be overcome during tumor formation through the acquisition of mutations that allow cells to tolerate aneuploidy. The aneuploid yeast strains described here could provide the opportunity to identify such genes.

References and Notes

1. L. H. Hartwell, S. K. Dutcher, J. S. Wood, B. Garvik, *Rec. Adv. Yeast Mol. Biol.* **1**, 28 (1982).
2. M. J. Rosenstraus, L. A. Chasin, *Genetics* **90**, 735 (1978).

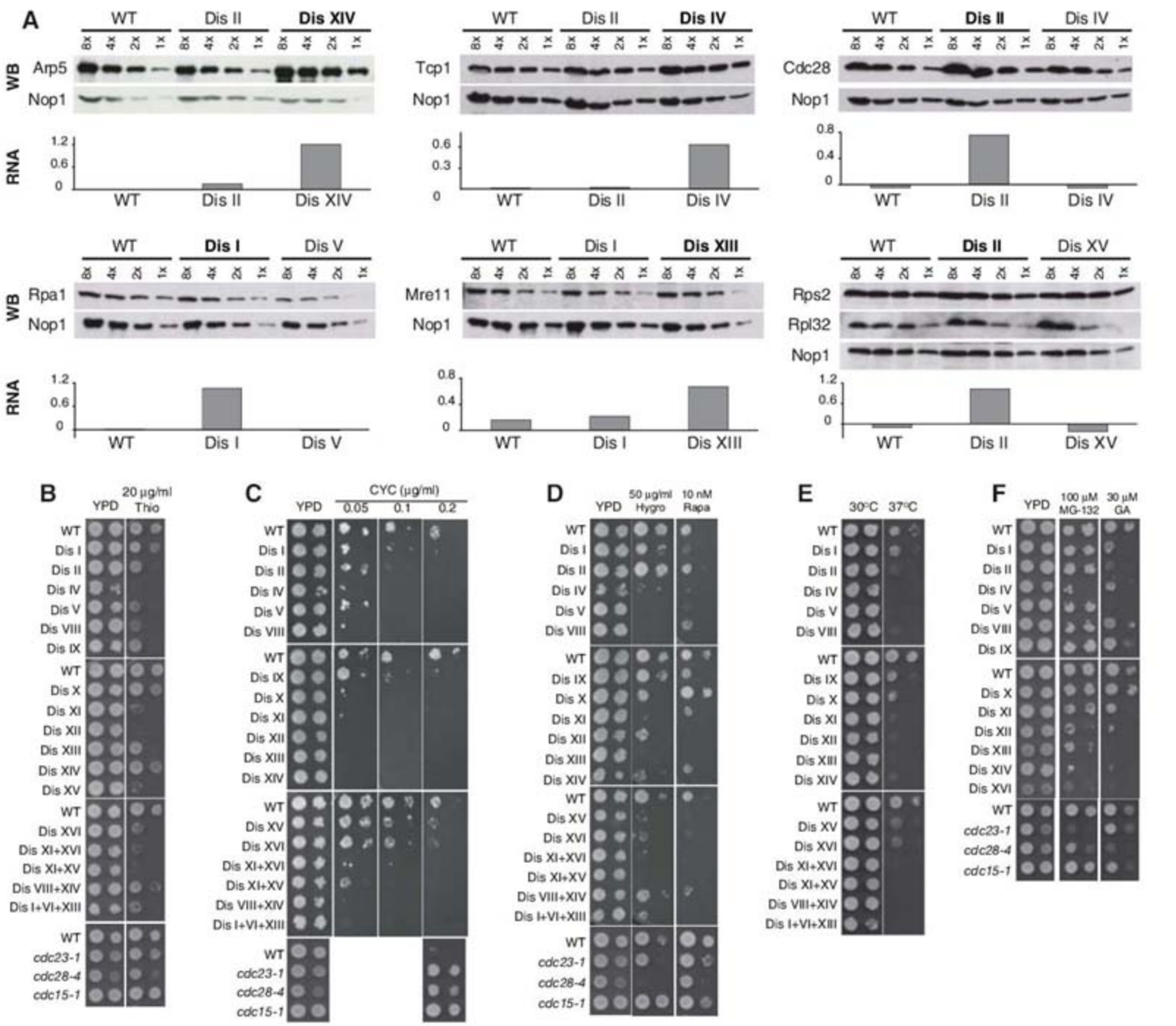

Fig. 4. Increased sensitivity of aneuploid strains to conditions interfering with protein synthesis and folding. (**A**) Examples of effects of increased gene dosage on protein abundance. Arp5, Tcp1, Cdc28, Rpa1, Mre11, Rps2, and Rpl32 proteins were examined in wild-type cells; in cells disomic for the chromosome on which the encoding gene is located; and in cells disomic for a different chromosome by Western blot analysis. Boldface type indicates the disome on which the encoding gene of interest is located. RNA levels of the gene product of interest are shown as a $\log_2$ ratio of wild type of an average of two microarray analyses below the blot. Nop1 was used as a loading control; 50 µg (8×), 25 µg (4×), 13 µg (2×), and 6 µg (1×) of extract were loaded. Arp5 protein and RNA levels were analyzed in wild-type (WT) (A11311), Dis II (A12685), and Dis XIV (A13979); Tcp1 in WT (A11311), Dis II (A12685), and Dis IV (A12687); Cdc28 in WT (A11311), Dis II (A12685), and Dis IV (A12687); Rpa1 in WT (A11311), Dis I (A12683), and Dis V (14479); Mre11 in WT (A11311), Dis I (A12683), and Dis XIII (A12695); and Rps2 and Rpl32 in WT (A11311), Dis II (A12685), and Dis XV (A12697). (**B** to **F**) Proliferative capability of disomes in the presence of thiolutin (B), cycloheximide (C), hygromycin and rapamycin (D), high temperature (37°C) (E), and MG132 and geldanamycin (F); 10-fold dilutions are shown. Strains (from the top): A11311, A12683, A12685, A12687, A14479, A13628, A13975, A12689, A13771, A12693, A12695, A13979, A12697, A12700, A12699, A12691, A15615, A15614, A11311, A755, A2594, and A2595. In (F), the order is A15548, A15550, A15552, A15554, A15556, A15558, A15560, A15562, A15564, A15566, A15567, A15568, A15572, A11311, A755, A2594, and A2595.

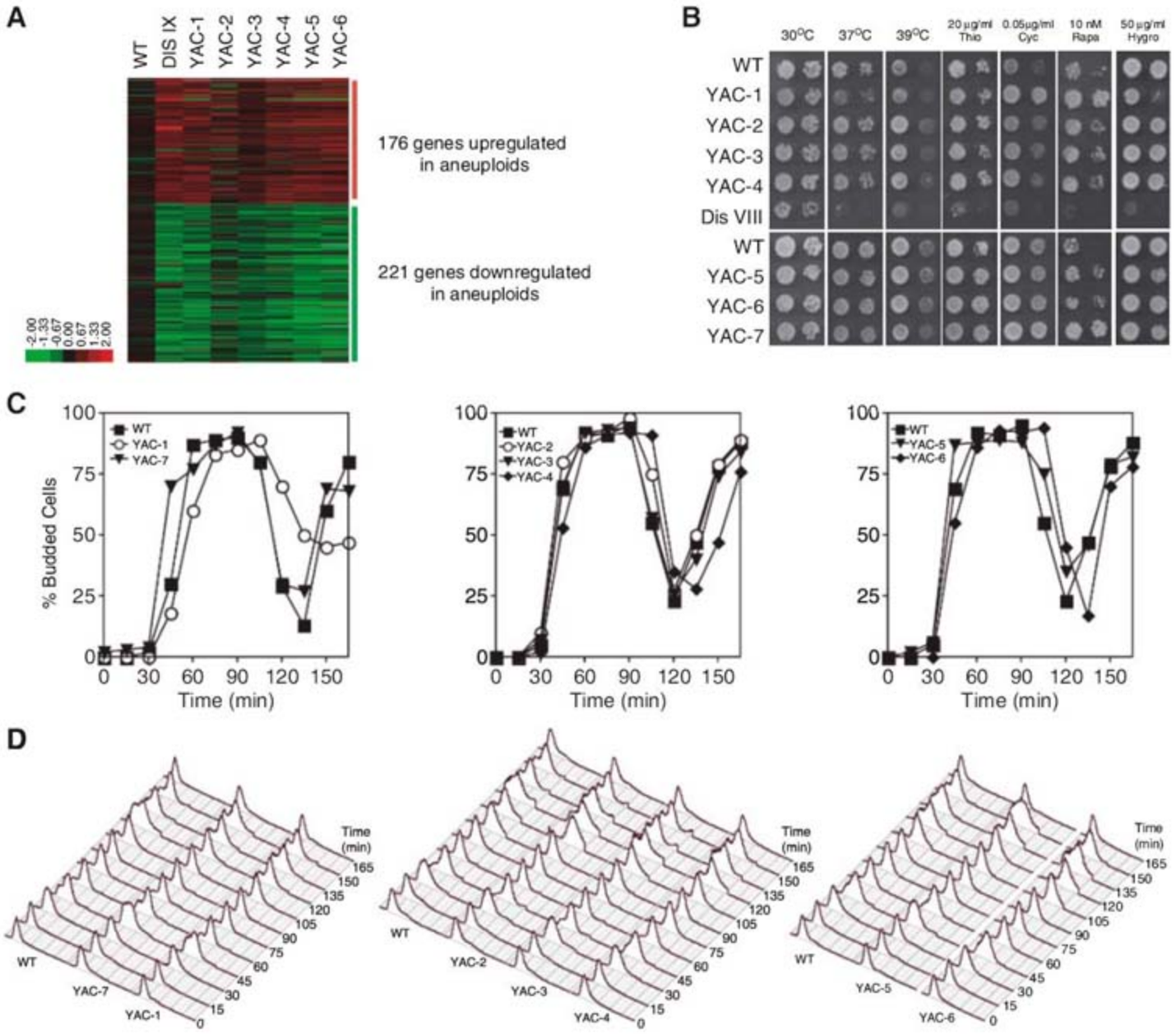

Fig. 5. Effects of human and mouse DNA on yeast. (**A**) Gene expression of YAC-containing strains grown under phosphate-limiting conditions. The gene expression pattern is shown for the 397 genes identified as changed in aneuploid strains grown under phosphate-limiting conditions. Genes increasing in expression in the aneuploid strains are marked by the red bar, and genes decreasing in expression by the green bar. Data for wild-type cells and cells disomic for chromosome IX are from Fig. 1C and are shown for comparison. Data are provided in table S5. Order of strains (from the left): A11311, A13975, A16854 (this strain contains a truncated version of YAC-1), A17392, A17393, A17394, A17397, A16851. (**B**) Behavior of YAC-carrying strains and aneuploid strains in the presence of high temperature (37°C, 39°C), thiolutin, cycloheximide, rapamycin, and hygromycin. Strains (from the top): A11311, A16850, A17392, A17393, A17394, A13628, A11311, A17396, A17397, and A16851. (**C** and **D**) Wild-type cells (A11311) and cells carrying YAC-1 (A16850), YAC-7 (A16851), YAC-2 (A17392), YAC-3 (A17393), YAC-4 (A17394), YAC-5 (A17396), or YAC-6 (A17397) were released from a pheromone-induced G_1 arrest as described in Fig. 2. At the indicated times, samples were taken to determine the percentage of budded cells (C) and DNA content (D).

3. T. Boveri, *Neu Folge* **35**, 67 (1902).
4. C. Lengauer, K. W. Kinzler, B. Vogelstein, *Nature* **396**, 643 (1998).
5. O. Niwa, Y. Tange, A. Kurabayashi, *Yeast* **23**, 937 (2006).
6. D. L. Lindsley *et al.*, *Genetics* **71**, 157 (1972).
7. D. J. Segal, E. E. McCoy, *J. Cell. Physiol.* **83**, 85 (1974).
8. J. Conde, G. R. Fink, *Proc. Natl. Acad. Sci. U.S.A.* **73**, 3651 (1976).
9. T. Nilsson-Tillgren, J. G. Litske, S. Holmberg, M. C. Kielland-Brandt, *Carlsberg Res. Commun.* **45**, 113 (1980).
10. See supporting material on *Science* Online.
11. T. R. Hughes *et al.*, *Nat. Biotechnol.* **19**, 342 (2001).
12. A. P. Gasch *et al.*, *Mol. Biol. Cell* **11**, 4241 (2000).
13. B. Regenberg *et al.*, *Genome Biol.* **7**, R107 (2006).
14. E. I. Boyle *et al.*, *Bioinformatics* **20**, 3710 (2004).
15. M. Costanzo *et al.*, *Cell* **117**, 899 (2004).
16. R. A. de Bruin, W. H. McDonald, T. I. Kalashnikova, J. Yates 3rd, C. Wittenberg, *Cell* **117**, 887 (2004).
17. C. Wittenberg, K. Sugimoto, S. I. Reed, *Cell* **62**, 225 (1990).
18. L. Dirick, T. Bohm, K. Nasmyth, *EMBO J.* **14**, 4803 (1995).
19. D. Stuart, C. Wittenberg, *Genes Dev.* **9**, 2780 (1995).
20. A. L. Lehninger, D. L. Nelson, M. M. Cox, *Principles of Biochemistry* (Worth, New York, ed. 2, 1993).
21. U. Schubert *et al.*, *Nature* **404**, 770 (2000).
22. E. Balzi, M. Wang, S. Leterme, L. Van Dyck, A. Goffeau, *J. Biol. Chem.* **269**, 2206 (1994).
23. P. H. Bissinger, K. Kuchler, *J. Biol. Chem.* **269**, 4180 (1994).
24. J. Hanna, D. S. Leggett, D. Finley, *Mol. Cell. Biol.* **23**, 9251 (2003).
25. W. Katz, B. Weinstein, F. Solomon, *Mol. Cell. Biol.* **10**, 5286 (1990).
26. A. Gunjan, A. Verreault, *Cell* **115**, 537 (2003).
27. J. B. Easton, P. J. Houghton, *Oncogene* **25**, 6436 (2006).
28. L. Whitesell, S. L. Lindquist, *Nat. Rev. Cancer* **5**, 761 (2005).
29. R. A. Gatenby, R. J. Gillies, *Nat. Rev. Cancer* **4**, 891 (2004).
30. B. A. Weaver, D. W. Cleveland, *Curr. Opin. Cell Biol.* **18**, 658 (2006).
31. M. J. Dunham *et al.*, *Proc. Natl. Acad. Sci. U.S.A.* **99**, 16144 (2002).

32. We thank D. Koshland, B. Brewer, J. Warner, and B. Adamson for reagents; C. Huttenhower, M. Hibbs, and O. Troyanskaya for use of the WCluster program; C. DeSevo for technical assistance; and D. Pellman, A. Hochwagen, F. Solomon, and members of the Amon

lab for suggestions and critical reading of this manuscript. A.A. thanks I. Hershkovitz for encouragement. Supported by NIH grant GM56800 and a David Koch Research Award (A.A.) and NIH grant GM071508 to the Lewis-Sigler Institute. A.A. is an Investigator of the Howard Hughes Medical Institute. All microarray data are available in final processed form in table S5, and as raw data through the Princeton University MicroArray Database (puma.princeton.edu) and the Gene Expression Omnibus (GEO, www.ncbi.nlm.nih.gov/geo) under accession number GSE7812.

Supporting Online Material
www.sciencemag.org/cgi/content/full/317/5840/916/DC1

Materials and Methods
Figs. S1 to S8
References

7 March 2007; accepted 19 June 2007
10.1126/science.1142210

Detection of Circumstellar Material in a Normal Type Ia Supernova

F. Patat,[1]* P. Chandra,[2] R. Chevalier,[2] S. Justham,[3] Ph. Podsiadlowski,[3] C. Wolf,[3] A. Gal-Yam,[4] L. Pasquini,[1] I. A. Crawford,[5] P. A. Mazzali,[6,7] A. W. A. Pauldrach,[8] K. Nomoto,[9] S. Benetti,[10] E. Cappellaro,[10] N. Elias-Rosa,[6,11] W. Hillebrandt,[6] D. C. Leonard,[12] A. Pastorello,[13] A. Renzini,[10] F. Sabbadin,[10] J. D. Simon,[4] M. Turatto[10]

Type Ia supernovae are important cosmological distance indicators. Each of these bright supernovae supposedly results from the thermonuclear explosion of a white dwarf star that, after accreting material from a companion star, exceeds some mass limit, but the true nature of the progenitor star system remains controversial. Here we report the spectroscopic detection of circumstellar material in a normal type Ia supernova explosion. The expansion velocities, densities, and dimensions of the circumstellar envelope indicate that this material was ejected from the progenitor system. In particular, the relatively low expansion velocities suggest that the white dwarf was accreting material from a companion star that was in the red-giant phase at the time of the explosion.

As a result of their extreme luminosities and high homogeneity, type Ia supernovae (SNe Ia) have been used extensively as cosmological reference beacons to trace the evolution of the universe (*1*, *2*). However, despite recent progress, the nature of the progenitor stars and the physics that govern these powerful explosions remain poorly understood (*3*, *4*). In the presently favored single-degenerate model, the supernova (SN) progenitor is a white dwarf that accretes material from a nondegenerate companion star in a close binary system (*5*); when it approaches the Chandrasekhar limit, the white dwarf explodes in a thermonuclear blast. A direct method for investigating the nature of the progenitor systems of SNe Ia is to search for signatures of the material transferred to the accreting white dwarf in the circumstellar material (CSM). Previous attempts have aimed at detecting the radiation that would arise from the interaction between the fast-moving SN ejecta and the slow-moving CSM in the form of narrow emission lines (*6*), radio emission (*7*), and x-ray emission (*8*). The most stringent upper limit to the mass-loss rate set by radio observations is as low as 3×10^{-8} solar masses per year ($M_\odot$ year^{-1}) for an assumed wind velocity of 10 km s^{-1} (*7*). Two notable exceptions are represented by two peculiar SNe Ia, SN 2002ic and SN 2005gj, which have shown extremely pronounced hydrogen emission lines (*9*, *10*) that have been interpreted as a sign of strong ejecta-CSM interaction (*11*). However, the classification of these supernovae as SNe Ia has recently been questioned (*12*), and even if they were SNe Ia, these supernovae are unlikely to account for normal SNe Ia explosions (*7*) that, of those observed so far, lack any signature of mass transfer from a hypothetical donor. Here we report direct evidence of CSM in a SN Ia that has shown normal behavior at x-ray, optical, and radio wavelengths.

SN 2006X was discovered in the Virgo cluster spiral galaxy NGC 4321 (*13*). A few days

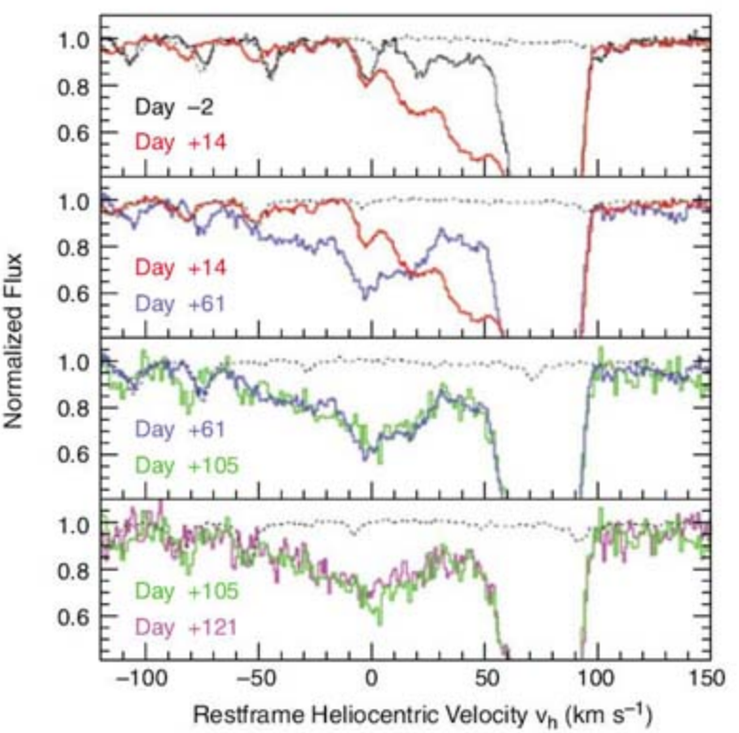

Fig. 1. Time evolution of the Na D_2 component region as a function of elapsed time since *B*-band maximum light. We corrected the heliocentric velocities to the rest-frame using the host galaxy recession velocity. All spectra have been normalized to their continuum. In each panel, the dotted curve traces the atmospheric absorption spectrum.

[1]European Southern Observatory (ESO), Karl Schwarzschild Strasse 2, 85748, Garching bei München, Germany. [2]University of Virginia, Department of Astronomy, Post Office Box 400325, Charlottesville, VA 22904, USA. [3]Department of Astrophysics, University of Oxford, Oxford OX1 3RH, UK. [4]Astronomy Department, MS 105-24, California Institute of Technology, Pasadena, CA 91125, USA. [5]School of Earth Sciences, Birkbeck College London, Malet Street, London WC1E 7HX, UK. [6]Max-Planck-Institut für Astrophysik, Karl Schwarzschild Strasse 1, 85748, Garching bei München, Germany. [7]Istituto Nazionale di Astrofisica (INAF)–Osservatorio Astronomico, via Tiepolo 11, 34131 Trieste, Italy. [8]Institut für Astronomie und Astrophysik der Ludwig-Maximilians-Universität, 81679 Munich, Germany. [9]Department of Astronomy, University of Tokyo, Bunkyo-ku, Tokyo 113-0033, Japan. [10]INAF-Osservatorio Astronomico, vicolo Osservatorio 5, 35122 Padova, Italy. [11]Universidad de La Laguna, Avenida Astrofísico Francisco Sánchez s/n, E-38206, La Laguna, Tenerife, Spain. [12]Department of Astronomy, San Diego State University, San Diego, CA 92182, USA. [13]Astrophysics Research Centre, Queen's University Belfast, BT7 1NN, UK.

*To whom correspondence should be addressed. E-mail: fpatat@eso.org

after its detection, the object was classified as a normal SN Ia event occurring 1 to 2 weeks before maximum light, which was affected by substantial extinction (*14*). Prompt observations with the Very Large Array (VLA) telescope have shown no radio source at the SN position (*15*), establishing one of the deepest and earliest limits for radio emission from a SN Ia and implying a mass-loss rate of less than a few 10^{-8} $M_{\odot}$ year^{-1} (for a low wind velocity of 10 km s^{-1}). The SN was not visible in the 0.2-to-10 keV x-ray band down to the detection limit of the Swift satellite (*8*).

We have observed SN 2006X with the Ultraviolet (UV) and Visual Echelle Spectrograph mounted at the ESO 8.2-m Very Large Telescope. Observations were carried out on four different epochs, which correspond to days −2, +14, +61, and +121 with respect to *B*-band maximum light. Additionally, a fifth epoch (day +105) was covered with the High Resolution Echelle Spectrometer mounted at the 10-m Keck telescope (*16*). The most notable finding from our data is the clear evolution seen in the profile of the Na I D doublet lines (5889.95, 5895.92 Å). Indeed, besides a strongly saturated and constant component arising in the host galaxy disk [supporting online material (SOM) text S2 and fig. S1], a number of features spanning a velocity range of about 100 km s^{-1} appear to vary substantially with time (Fig. 1 and fig. S2). SN 2006X is projected onto the receding side of the galaxy, and the component of the rotation velocity along the line of sight at the apparent SN location is about +75 km s^{-1} (*17*), which coincides with the strongly saturated Na I D component, the saturated Ca II H&K lines, and a weakly saturated CN molecular vibrational band (0-0) (Fig. 2 and fig. S1). This and the lack of time evolution prove that the deep absorption arises within the disk of NGC 4321 in an interstellar molecular cloud (or system of clouds) that is responsible for the bulk of the reddening suffered by SN 2006X (SOM text S2).

In contrast, the relatively blue-shifted structures of the Na I D lines show a rather complex evolution. The number of features, their intensity, and their width are difficult to establish. Nevertheless, for the sake of discussion, four main components, which we will indicate as "A," "B," "C," and "D," can be tentatively identified in the first two epochs (Fig. 2). Components B, C, and D strengthen between day −2 and day +14 while component A remains constant during this time interval. The situation becomes more complicated on day +61: Components C and D clearly start to decrease in strength, but component B remains almost constant, and component A becomes deeper and is accompanied by a wide absorption that extends down to a rest-frame heliocentric velocity $v_h \cong -50$ km s^{-1} (Fig. 1 and fig. S2). After this epoch, there is no evidence of evolution, and component A remains the most intense feature up to the last phase covered by our observations, more than 4 months after the explosion.

Variable interstellar absorption on comparably short time scales has been claimed for some gamma-ray bursts (GRBs), and it has been attributed by some authors to line-of-sight geometrical effects, resulting from the fast GRB expansion coupled to the patchy nature of the intervening absorbing clouds (*18*). Our data clearly show that despite the marked evolution in the Na I D lines, Ca II H&K components do not change with time (Fig. 2, fig. S3, and SOM text S3 and S4). Therefore, in the case of SN 2006X, transverse motions in the absorbing material and line-of-sight effects due to the fast SN photosphere expansion (typically 10^4 km s^{-1}) can be definitely excluded, because they would cause variations in all absorption features.

For this reason, we conclude that the Na I features seen in SN 2006X, arising in a number of expanding shells (or clumps), evolve because of changes in the CSM ionization conditions induced by the variable SN radiation field. In this context, the different behavior that is seen in the Na I and Ca II lines is explained in terms of (i) the lower ionization potential of Na I (5.1 eV, corresponding to 2417 Å) with respect to Ca II (11.9 eV, corresponding to 1045 Å), (ii) their different recombination coefficients, and (iii) their photoionization cross sections coupled to a UV-deficient radiation field (SOM text S4). Regrettably, not much is known about the UV emission of SNe Ia shortward of 1100 Å (*8*, *19*). Theoretically, a severe UV line blocking, by heavy elements such as Fe, Co, and Mg, is expected (*20*). An estimate of the Na I ionizing flux, S_{UV}, can be derived from a synthetic spectrum of a SN Ia at maximum light (*21*), which turns out to be $S_{UV} \sim 5 \times 10^{50}$ photons s^{-1}. One can verify that this flux is largely sufficient to fully ionize Na I up to rather large distances (~5×10^{18} cm).

Nevertheless, because the recombination time scale τ_r must be of the order of 10 days, this requires an electron density n_e as large as 10^5 cm^{-3} (SOM text S4). Given the low abundance of any other element besides hydrogen, such a high electron density can be produced only by partial hydrogen ionization. As a result of the severe line blocking suffered by SNe Ia (*20*), the flux of photons capable of ionizing H is very small (~4×10^{44} photons s^{-1}), and this requires that the gas where the Na I time-dependent absorptions arise must be confined within a few 10^{16} cm from the SN (SOM text S4). In a SN of this type, the flux in the 1120-to-2640 Å band decreases by a factor of 10 in the first 2 weeks after maximum light (*8*, *19*). Because, at a distance of ~10^{16} cm from the SN, the ionization time scale τ_i for Na I is much shorter than τ_r, the ionization fraction grows with time following the increase of the UV flux during the pre-maximum phase, whereas, after the maximum phase, the ionization fraction decreases following τ_r. This result would explain the overall growth of the blue components' depth, as shown by our data, in terms of an increasing fraction of neutral Na, whereas the different evolution of individual components would be dictated by differences in the densities and distances from the SN. Moreover, once all the Na II has recombined [which should happen within a few τ_r (i.e., ~1 month)], there should be no further evolution, which is in qualitative agreement with the observations. Additionally, because the flux of photons that can ionize Ca II is more than four orders of magnitude less than that of Na I (SOM text S4), the corresponding ionization fraction is expected to be only a few percent. Therefore, the recombination of Ca III to Ca II does not produce measurable effects on the depth of the Ca II H&K lines, as is indeed observed (SOM text S3).

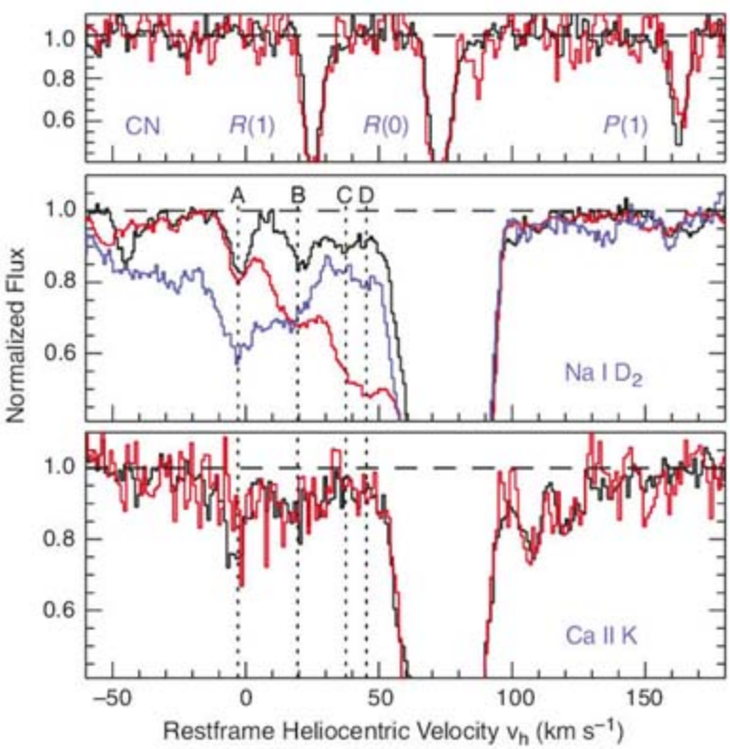

Fig. 2. Evolution of the Na I D_2 and Ca II K line profiles between day −2 (black), day +14 (red), and day +61 (blue, Na I D_2 only). The vertical dashed lines mark the four main variable components at −3 ("A"), +20 ("B"), +38 ("C"), and +45 ("D") km s^{-1}. For comparison, the upper panel shows the *R*(0), *R*(1), and *P*(1) line profiles of the (0-0) vibrational band of the CN $B^2\Sigma - X^2\Sigma$. The velocity scale refers to the *R*(0) transition (3874.608 Å).

The H mass [M(H)] contained in the shells generating the observed absorptions can be estimated from our observations after some conservative assumptions are made. The Na I column density N(Na I) deduced from the most intense feature (component D, day +14) is N(Na I) $\cong 10^{12}$ cm^{-2}. Assuming that the material generating this component is homogeneously distributed in a thin spherical shell with radius 10^{17} cm, a solar Na/H ratio (log Na/H = −6.3), and complete Na recombination, an upper limit to the shell mass can be estimated as $M(\mathrm{H}) \leq 3 \times 10^{-4}\ M_{\odot}$ (this value is reduced by a factor of 100 for material at about 10^{16} cm, the most likely distance for components C and D). Even in the case of complete ionization, such a H mass would produce an Hα luminosity of $\sim 4 \times 10^{34}$ erg s^{-1}, which is two orders of magnitude below the 3-σ upper limits set by our observations at all epochs (table S2) and by any other SN Ia observed so far (*6*). Therefore, the absence of narrow emission lines above the detection limit does not contradict the presence of partially ionized H up to masses of the order of 0.01 $M_{\odot}$.

However, photoionization alone cannot account for the fact that not all features increase in depth with time (Fig. 2). Indeed, on day +61, components C and D return to the same low intensity values that they had on day −2. One possible explanation is that the gas is re-ionized by some other mechanism, like the ejecta-CSM interaction. In this case, the absorbing material generating components C and D must be close enough to the SN so that the ejecta can reach it in about 1 month after the explosion ($\sim 10^{16}$ cm for maximum ejecta velocities of 4×10^{4} km s^{-1}). Similarly, in order not to be reached by the ejecta more than 4 months after the explosion, component A, component B, and the broad high-velocity components must arise at larger distances ($>5 \times 10^{16}$ cm). This scenario is not ruled out by the lack of radio emission from SN 2006X (*15*). Indeed, in light of our current understanding of the ejecta-CSM interaction mechanism (*22*), the presence of similar shells with masses smaller than a few $10^{-4}\ M_{\odot}$ cannot be excluded by radio nondetections of SNe Ia in general (*7*). Our findings are consistent with upper limits on the radio flux set by our VLA observations, obtained about 10 months after the explosion (SOM text S1), which are comparable to the best upper limits set on the radio luminosity of other normal SNe Ia (*7*).

If we adopt the velocity of the CN lines as indicative of the host galaxy rotation component along the line of sight at the SN location, then our observations provide solid evidence of CSM expanding at velocities that span a range of about 100 km s^{-1} (Fig. 2).

The most important implication of these observations is that this CSM was ejected from the progenitor system in the recent past. For instance, with a shell radius of 10^{16} cm and a wind velocity of ~50 km s^{-1}, the material would have been ejected some 50 years before the explosion. This almost certainly rules out a double-degenerate scenario for SN 2006X, where the supernova would have been triggered by the merger of two carbon-oxygen white dwarfs. In this case, no substantial mass loss would be expected in the phase immediately preceding the supernova. Thus, a single-degenerate model is the favored model for SN 2006X, where the progenitor accreted from a nondegenerate companion star.

Mean velocities for the CSM of ~50 km s^{-1} are comparable to those reported for the winds of early red giant (RG) stars (*22*); velocities matching our observations are also expected for late subgiants. The observed material is moving more slowly than would be expected for winds from main sequence donor stars or from compact helium stars. These wind velocities seem more consistent with the shorter-period end of the symbiotic formation channel than with the other major formation channel proposed for a SN Ia with a nondegenerate donor star (*23*). The observed structure of the CSM could be due to variability in the wind from the companion RG; considerable variability of RG mass loss is generally expected (*24*).

An alternative interpretation of these distinct features is that they arise in the remnant shells of successive novae, which can create dense shells in the slow-moving material released by the companion star (*25*, *26*). This scenario seems to require an aspherical shell geometry in order to match the observed low velocities (SOM text S6). Not only might this be expected a priori (*27*), but observations of the 2006 outburst of RS Ophiuchi also show that there is an equatorial density enhancement that strongly restrains the expansion of the nova shell (*28*–*30*).

One crucial issue to resolve regarding what we have seen in SN 2006X is whether it represents the rule or whether it is an exceptional case. Other cases of SNe Ia showing negative velocity components are known, such as SN 1991T and SN 1998es (fig. S5 and SOM text S5). Unfortunately, multi-epoch high-resolution spectroscopy is not available for these objects (to our knowledge, the SN 2006X data set is distinctive in this respect), and therefore time variability cannot be demonstrated. Nevertheless, the data clearly show components approaching the observer at velocities that reach at least 50 km s^{-1} with respect to the deep absorption that we infer to be produced within the disks of the respective host galaxies. This, and the fact that SN 2006X has shown no optical, UV, and radio peculiarities whatsoever, supports the conclusion that what we have witnessed for this object is common to normal SNe Ia, and possibly to all SNe Ia, even though variations resulting from different inclinations of the line of sight with respect to the orbital plane may exist.

References and Notes

1. A. G. Riess *et al.*, *Astron. J.* **116**, 1009 (1998).
2. S. Perlmutter *et al.*, *Astrophys. J.* **517**, 565 (1999).
3. D. Branch, M. Livio, L. R. Yungelson, F. Boffi, E. Baron, *Publ. Astron. Soc. Pac.* **107**, 1019 (1995).
4. W. Hillebrandt, J. C. Niemeyer, *Annu. Rev. Astron. Astrophys.* **38**, 191 (2000).
5. J. Whelan, I. Iben, *Astrophys. J.* **186**, 1007 (1973).
6. S. Mattila *et al.*, *Astron. Astrophys.* **443**, 649 (2005).
7. N. Panagia *et al.*, *Astrophys. J.* **646**, 396 (2006).
8. S. Immler *et al.*, *Astrophys. J.* **648**, L119 (2006).
9. M. Hamuy *et al.*, *Nature* **424**, 651 (2003).
10. G. Aldering *et al.*, *Astrophys. J.* **650**, 510 (2006).
11. The subluminous SN Ia 2005ke has shown an unprecedented x-ray emission, which has been interpreted as the signature of a possible weak interaction between the SN ejecta and material lost by a companion star (*8*). Nevertheless, this finding and the strong UV excess might be related to the nature of this SN.
12. S. Benetti *et al.*, *Astrophys. J.* **653**, L129 (2006).
13. S. Suzuki, M. Migliardi, *IAU Circ. 8667* (2006).
14. R. Quimby, P. Brown, C. Gerardy, *Cent. Bur. Electron. Telegrams* **421** (2006).
15. C. J. Stockdale *et al.*, *Cent. Bur. Electron. Telegrams* **396** (2006).
16. See supporting material on *Science* Online.
17. R. J. Rand, *Astron. J.* **109**, 2444 (1995).
18. H. Hao *et al.*, *Astrophys. J.* **659**, L99 (2007).
19. N. Panagia, paper presented at the *Supernova 1987A: 20 Years after: Supernovae and Gamma-Ray Bursters Conference*, Aspen, CO, 19 to 23 February 2007 (American Institute of Physics), in press; preprint available at http://arxiv.org/abs/0704.1666.
20. W. A. Pauldrach *et al.*, *Astron. Astrophys.* **312**, 525 (1996).
21. R. A. Chevalier, C. Fransson, in *Supernovae and Gamma-Ray Bursters*, K. W. Weiler, Ed. (Lecture Notes in Physics 598, Springer, New York, 2003), pp. 171–194.
22. P. G. Judge, R. E. Stencel, *Astrophys. J.* **371**, 357 (1991).
23. I. Hachisu, M. Kato, *Astrophys. J.* **558**, 323 (2001).
24. L. A. Willson, *Annu. Rev. Astron. Astrophys.* **38**, 573 (2000).
25. I. Hachisu, M. Kato, *Astrophys. J.* **558**, 323 (2001).
26. W. M. Wood-Vasey, J. L. Sokoloski, *Astrophys. J.* **645**, L53 (2006).
27. I. Hachisu, M. Kato, K. Nomoto, *Astrophys. J.* **522**, 487 (1999).
28. T. J. O'Brien *et al.*, *Nature* **442**, 279 (2006).
29. M. F. Bode *et al.*, *Astrophys. J.* **652**, 629 (2006).
30. M. F. Bode *et al.*, *Astrophys. J.*, in press; preprint available at http://arxiv.org/abs/0706.2745.

31. We thank K. Krisciunas for providing information about the photometric evolution of SN 2006X. We acknowledge K. Steenbrugge, F. Primas, W. M. Wood-Vasey, R. Corradi, G. J. Ferland, P. van Hoof, F. Bresolin, and C. Stockdale for useful discussions. We particularly thank M. F. Bode for sharing some results on RS Ophiuchi before publication. This work is based on observations made with ESO telescopes at Paranal Observatory, obtained under run IDs 276.D-5048, 277.D-5003, and 277.D-5013. Some of the data presented herein were obtained at the W. M. Keck Observatory, which is operated as a scientific partnership among the California Institute of Technology, the University of California, and NASA. This work made use of the Very Large Array telescope of the National Radio Astronomy Observatory (NRAO), which is operated by Associated Universities, Incorporated, under a cooperative agreement with NSF. P.C. is a Jansky Fellow of the NRAO.

Supporting Online Material

www.sciencemag.org/cgi/content/full/1143005/DC1
Materials and Methods
SOM Text
Figs. S1 to S5
Tables S1 and S2
References and Notes

26 March 2007; accepted 29 June 2007
Published online 12 July 2007;
10.1126/science.1143005
Include this information when citing this paper.

Radiationless Electromagnetic Interference: Evanescent-Field Lenses and Perfect Focusing

R. Merlin

Diffraction restricts the ability of most electromagnetic devices to image or selectively target objects smaller than the wavelength. We describe planar subwavelength structures capable of focusing well beyond the diffraction limit, operating at arbitrary frequencies. The structure design, related to that of Fresnel plates, forces the input field to converge to a spot on the focal plane. However, unlike the diffraction-limited zone plates, for which focusing results from the interference of traveling waves, the subwavelength plates control the near field and, as such, their superlensing properties originate from a static form of interference. Practical implementations of these plates hold promise for near-field data storage, noncontact sensing, imaging, and nanolithography applications.

The closely related problems of electromagnetic imaging and focusing beyond Abbe's diffraction limit, set by $\sim\lambda/n$, where λ is the vacuum wavelength and n is the refractive index (*1*), have received considerable attention in the past decade, motivated in part by optical studies using subwavelength apertures to probe the near field (*2*) and related work at microwave frequencies (*3*). Various schemes have been developed to improve the resolution, involving, for example, sharp tips (*4*, *5*), coherent control (*6*) and far-field time-reversal mirrors (*7*), and values as small as $\sim\lambda/100$ have been reported for the THz range (*8*). Subwavelength focusing necessarily involves the evanescent components of the field, that is, the near field. Because of this, standard interference techniques or geometrical optics methods do not apply. More recently, negative refraction has emerged as a topic of interest to near-field studies (*9*, *10*), following proposals of perfect lensing (*11*–*14*) and the subsequent experimental verification of negative refraction at microwave frequencies (*15*, *16*) and imaging beyond Abbe's limit with negative-permittivity slabs (*17*, *18*). In this work, an approach to subwavelength focusing is described that uses patterned, planar structures to induce convergence of the near field. The focusing effect described is reminiscent of, but the physics is substantially different from, that of both negative refraction slabs and Fresnel zone plates (*19*).

Let F be one of the cartesian components of the electric (**E**) or the magnetic (**H**) field , and assume that all the field sources are monochromatic, with time dependence given by $e^{-i\omega t}$ (ω is the angular frequency), and that they lie to the left of a particular plane, defined as $z = 0$. Then, for $z \geq 0$, F satisfies the Helmholtz equation $\nabla^2 F + k^2 F = 0$ and can thus be expressed in the angular-spectrum-representation form (*20*, *21*)

$$F(x,y,z_\alpha) = \frac{1}{4\pi^2}\int_{-\infty}^{+\infty}\!\!\iiint F(x',y',z_\beta) \times e^{i[q_x(x-x')+q_y(y-y')+\kappa(z_\alpha-z_\beta)]}dx'dy'dq_xdq_y \quad (1)$$

providing an exact relationship between the solution to the wave equation in two arbitrary planes, parallel to each other, $z = z_\alpha > 0$ and $z = z_\beta > 0$. Here, $k = 2\pi/\lambda$ and

$$\kappa = \begin{cases} i\left|(q_x^2+q_y^2-k^2)^{1/2}\right| & q_x^2+q_y^2 \geq k^2 \\ \left|(k^2-q_x^2-q_y^2)^{1/2}\right| & q_x^2+q_y^2 < k^2 \end{cases} \quad (2)$$

With the sources located in the half-space $z < 0$, the choice of signs in Eq. 2 is dictated by the requirements that the homogeneous and inhomogeneous (or evanescent) solutions to the wave equation must travel and decay in the positive z direction, respectively.

According to Eq. 1, the field in the region $z \geq 0$ is determined by the boundary values $F(x,y,0)$. Hence, the question of focusing (for both the subwavelength and the conventional, diffraction-limited cases) becomes that of identifying the sources needed to generate the field profile at $z = 0$ that converges to a spot of a predetermined size at the focal plane, $z = f$. Although the angular-spectrum representation shows that $F(x,y,0)$ is, in turn, uniquely determined by the focal-plane values, $F(x,y,f)$, the answer to the focusing problem is not unique, and the search for the optimal solution is not trivial, because "focal spot" is, at best, an electromagnetically vague concept. The difficulty here is that the wrong choice of $F(x,y,f)$ may result in a field that is unsuitable for applications, that diverges, or that does not exist (everywhere in a region or at certain points), or in a boundary field that is difficult to implement in practice. In our approach, $F(x,y,0)$ is defined by the transmission properties of subwavelength-patterned planar structures that behave, in some sense, like the evanescent-wave counterparts to Fresnel's zone plates (*19*). Similar to the latter structures, the waves exit our plates in a pattern set by the plate design, which forces them to converge to a spot on the focal plane, as prescribed by Eq. 1. Unlike the Fresnel plates, which rely on interference involving radiative components of the field, and are thus subjected to Abbe's constraint, our plates affect primarily the evanescent waves leading to interference effects that are electrostatic or magnetostatic in nature and, as a result, the spot size can be arbitrarily small. As with other near-field effects, our plates' ability to focus at large distances is severely limited by the exponential decay of the near field which, in practical applications, constrains the focal length to dimensions much smaller than λ.

The proposed plates can be tailored to give subwavelength focal patterns of various types and symmetries. We concentrate on two key geometries displaying cylindrical and azimuthal symmetry. In the cylindrical or two-dimensional case, $\partial F / \partial x = 0$, the perfect focus is a line, and Eq. 1 becomes

$$F(y,z_\alpha) = \frac{1}{2\pi}\int_{-\infty}^{+\infty}\!\!\iint F(y',z_\beta) \times e^{i[q(y-y')+\kappa(z_\alpha-z_\beta)]}dy'dq \quad (3)$$

where $\kappa(q)$ is given by Eq. 2 with $q_x^2 + q_y^2 \rightarrow q^2$. For electromagnetic fields propagating in the $+z$ direction that have azimuthal symmetry, such as the axicon (*22*) and Bessel beams (*23*), the tangential ϕ component of the electric field, as well as the z and radial ρ component of **H** vanish, whereas the nonzero components $\Psi = H_\phi$ or E_ρ obey

$$\Psi(\rho,z_\alpha) = \int_{-\infty}^{+\infty}\!\!\iint \Psi(\rho',z_\beta)J_1(q\rho')J_1(q\rho) \times e^{i\kappa(z_\alpha-z_\beta)}\rho'd\rho'qdq \quad (4)$$

Replacing the Bessel function J_1 by J_0, one obtains the corresponding expression for E_z. Note that $e^{iq_0y}\exp[i\kappa(q_0)z]$ and $J_1(q_0\rho)\exp[i\kappa(q_0)z]$ are, respectively, solutions of Eqs. 3 and 4 for arbitrary q_0 that become evanescent modes for $|q_0| > k$. For $|q_0| < k$, the corresponding fields are the well-known diffraction-free plane waves and Bessel beams. These states and, more generally, source-free electromagnetic fields with components of the form $f_{q_0}(\boldsymbol{\rho})\exp[i\kappa(q_0)z]$, where $\boldsymbol{\rho}$ is a vector normal to the z axis, play a crucial role in near-field lensing.

Our approach to subwavelength focusing relies on a property of the near field that, to the best of our knowledge, has not been considered before. Assume that $f_{q_0}\exp[i\kappa(q_0)z]$ is part of a full solution to Maxwell's equations and that a

Department of Physics, The University of Michigan, Ann Arbor, MI 48109–1040, USA. Email: merlin@umich.edu

certain field component (cartesian or otherwise) at the source plane, $z = 0$, is of the form $M(\rho) \times f_{q_0}(\rho)$ where M is a modulation function, which is characterized by the length scale $L \gtrsim \ell \equiv 2\pi/|q_0|$ and satisfies the requirements specified below. Then, it can be shown for $|q_0| >> k$ that the field converges to a focal spot of resolution defined by ℓ, after propagating through a distance of order L. This effect is illustrated for both the two-dimensional and azimuthally symmetric case in Fig. 1. The basic concepts of near-field lensing are best understood in the cylindrical geometry. In Eq. 3, take $F(y,0) = M(y)e^{iq_0 y}$ and integrate to calculate $F(y,z)$. For $|q_0| >> k$, the relevant states are evanescent waves. We can therefore approximate $\kappa(q) \approx i|q|$ so that $F(y,z) \approx \iint e^{iqy} e^{-|q|z} M(y') e^{i(q_0 - q)y'} dy' dq/2\pi$ (in this approximation, F is harmonic, i.e., $\nabla^2 F \approx 0$, for arbitrary M). Lensing occurs for a wide variety of modulation functions. Mathematically, a sufficient condition for focusing is that M should have one or more poles in the complex plane with nonzero imaginary components. To prove this, we assume that $M(y)$ is a real and even function, with poles at $\pm iL$. Performing a simple integration we obtain, for $q_0 > 0$, $F(y,z) \propto Le^{-q_0 L} g(y,z)$ where

$$g(y,z) = \left[\frac{e^{q_0(iy+L-z)} - 1}{iy + L - z} + \frac{(iy + L + z)e^{q_0(iy+L-z)} + (-iy + L + z)}{y^2 + (z+L)^2} \right] \quad (5)$$

As anticipated, the expression inside the brackets leads to focusing at $z = L$ such that, for $L >> \ell$, $|F(y,L)| \propto Le^{-q_0 L}|\sin(q_0 y/2)/y|$ (note that the singularity at $z = L$ and $y = 0$ is removable and that the second term gives a small correction of order ℓ/L to the resolution). Because there are no phases associated with evanescent waves, it should come as a surprise that the lensing process shows telltale signs of conventional interference, particularly in the way the waves contributing to Eq. 3 add up constructively and destructively at the focal plane. Because it involves nonradiative modes, we will refer to this unconventional form of focusing as radiationless interference.

Figure 1A shows plots of $|F(y,z)|^2$, obtained from Eq. 3, for $f_{q_0} = e^{iq_0 y}$ and $M = (1 + y^2/L^2)^{-1}$. This form of M is the simplest one for an even function with poles at $y = \pm iL$. The calculations are consistent with Eq. 5 and support our contention that, for $L \gtrsim \ell$, the focal length and the resolution are determined, independently, by the modulation length, L, and the length scale of the unperturbed field component, ℓ. As shown in Fig. 1B, the modulated azimuthally symmetric field (ringlike focus) exhibits a similar effect.

Although our study so far has been limited to simple poles located in the imaginary axis, it can be shown that (i) focusing can also be attained with higher-order poles, (ii) modulation functions with multiple poles give multiple foci, and (iii) the real and imaginary part of a given pole determine, respectively, the off-axis position of the focal spot and the corresponding focal length. Within this context, it is of interest to apply our analysis to a negative-refraction slab that exhibits perfect focusing at $n = -1$ (*11*). For $|1 + n| << 1$ and a source consisting of a line of dipoles, the expression for the field is known analytically (*13*, *14*). In particular, if the slab thickness is d and the source is at a distance $d/2$ from the nearest slab surface and, therefore, its image is at $d/2$ from the other surface (*11*), the evanescent field at the exit side of the slab can be written as $M(y)e^{iq_0 y}$ where

$$M(y) \propto \frac{\cosh(\pi y/2d) - i\sinh(\pi y/2d)}{\cosh(\pi y/2d) + i\sinh(\pi y/2d)} \quad (6)$$

and $q_0 = -\ln|1 + n|/d$ (*14*). As expected, M exhibits a pole at $y = id/2$, reflecting the image location and, moreover, the expression for q_0 is in perfect agreement with the known slab resolution (*13*, *14*, *24*). Because M has an infinite number of additional poles at $y = i(d/2 + 2pd)$, where $p > 0$ is an integer, a near-perfect slab will exhibit not just one, but an infinite number of images for which the intensity decays exponentially with p. These additional images are due to multiple reflections arising from the slight impedance mismatch at the slab-vacuum interfaces.

For the two-dimensional geometry, the above results can be trivially extended from the simple sinusoidal to the general case of a periodic field $P_\ell(y)$, of period ℓ. It is apparent that, for values at the source plane given by $F(y,0) = M(y)P_\ell(y)$, the field will converge at $z = L$ to a focal spot of size $\sim\ell$. This suggests the path for a practical implementation of cylindrical near-field lensing. As a periodic field can be simply realized by letting a plane wave go through an array of periodically placed slits or ribbons, it is clear that a

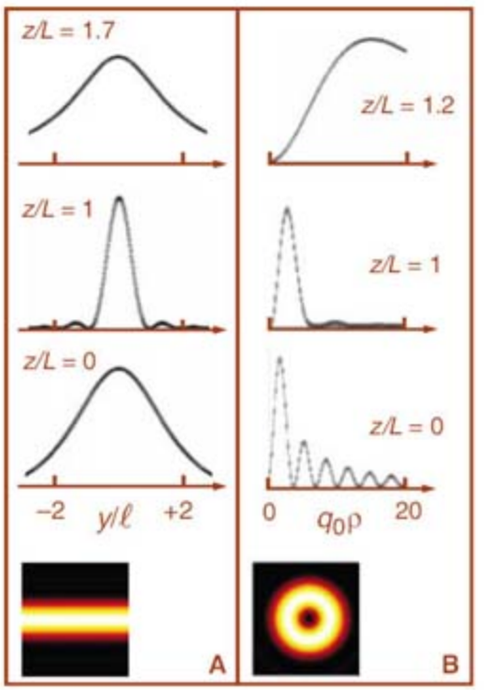

Fig. 1. Subwavelength focusing. (**A**) Two-dimensional case: $|F(y,z)|^2$ versus y/ℓ from Eq. 3 where $F(y,0) \propto e^{iq_0 y}/(1 + y^2/L^2)$ and $L/\ell = 2.5$. (**B**) Azimuthally symmetric geometry: $|\Psi(\rho,z)|^2$ versus $q_0\rho$ from Eq. 4 where $\Psi(\rho,0) \propto J_1(q_0\rho)/(1 + \rho^2/L^2)$ and $L/\ell = 8$. The contour plots show the focal line (A) and ring (B) at $z = L$.

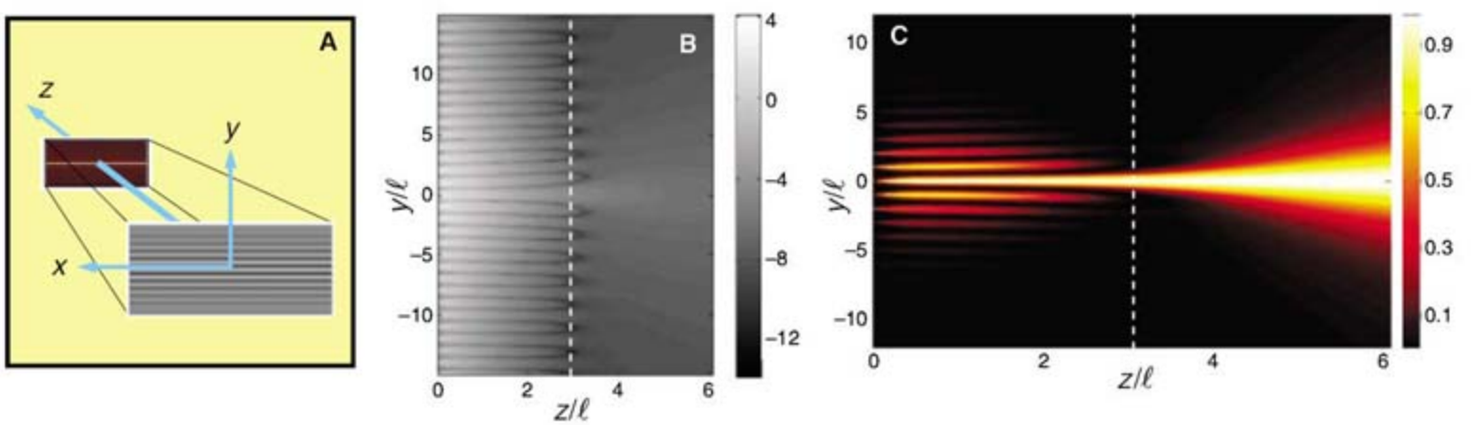

Fig. 2. Radiationless interference. (**A**) Schematic showing a subwavelength plate, represented as a modulated array of linear current sources at $z = 0$ and the plane showing the focal line. $L/\ell = 3$; see Eq. 7. (**B**) Contour plot of $\ln|H_y|$. (**C**) Contour plot of $|H_y(z,y)/H_y(z,0)|^2$. The dashed white line at $z = L$ denotes the focal plane.

field of the form $M(y)P_\ell(y)$ can be obtained by introducing a slowly varying modulation in, say, the width or the properties of the material of which an element is made. Similarly, in the case of azimuthal symmetry, a Bessel beam can be used together with a set of concentric rings of properly modulated width placed at radii satisfying $J_1(q_0\rho) = 0$. The technology for manufacturing plates of this kind for microwave applications has been available for quite some time, whereas nanofabrication methods involving, for example, electron and focused ion beam lithography, can be used for the infrared and optical range. An important consideration in the design of a near-field plate is to avoid as much as possible the presence of terms giving a background that could overwhelm the sharp features of the field. An example of background-free focusing is shown in Fig. 2. These results are for the diffraction of a plane wave by a set of ribbons of very narrow width $<< \ell$ and parameters such that the total current density is $\mathbf{j} = (j_x,0,0)$ where

$$j_x \propto \delta(z) \sum_{s=-\infty}^{\infty} \frac{(-1)^s \delta(y - s\ell)}{(1 + s^2\ell^2/L^2)} \qquad (7)$$

(the incident electric field is parallel to the cylindrical axis). Such an array of currents, with the sign varying from one element to the next, can be realized at infrared and optical frequencies by alternating material with positive and negative permittivity and, in the microwave regime, by using a set of interchanging capacitive and inductive elements. Figure 2B shows a contour plot of the y component of the diffracted magnetic field (logarithmic scale). These results are similar to those reported for negative-index slabs (*14*, *25*), thereby revealing the close relationship between the two phenomena (*26*). Finally, to help ascertain the origin of radiationless interference, we show in Fig. 2C a linear plot of the field intensity, normalized to its largest value at a given z. Reflecting a property of the zeros of H_y, the figure clearly shows behavior reminiscent of beam coupling in that the diffraction of the beam produced by a particular current source is prevented by the presence of its neighbors. It is only after the intensity of its neighbors has decreased a sufficient amount that the central beam is allowed to spread, and the point at which this happens determines the focal length.

References and Notes

1. E. Abbe, *Arch. Mikrosk. Anat.* **9**, 413 (1873).
2. E. Betzig, J. K. Trautman, *Science* **257**, 189 (1992).
3. A. Tselev *et al.*, *Rev. Sci. Instrum.* **74**, 3167 (2003).
4. F. Zenhausern, Y. Martin, H. K. Wickramasinghe, *Science* **269**, 1083 (1995).
5. R. Hillenbrand, T. Taubner, F. Keilmann, *Nature* **418**, 159 (2002).
6. M. I. Stockman, S. V. Faleev, D. J. Bergman, *Phys. Rev. Lett.* **88**, 067402 (2002).
7. G. Lerosey, J. de Rosny, A. Tourin, M. Fink, *Science* **315**, 1120 (2007).
8. P. C. M. Planken, N. C. J. van der Valk, *Opt. Lett.* **29**, 2306 (2004).
9. D. R. Smith, J. B. Pendry, M. C. K. Wiltshire, *Science* **305**, 788 (2004).
10. D. R. Smith, *Science* **308**, 502 (2005).
11. J. B. Pendry, *Phys. Rev. Lett.* **85**, 3966 (2000).
12. N. A. P. Nicorovici, R. C. McPhedran, G. W. Milton, *Phys. Rev. B* **49**, 8479 (1994).
13. G. W. Milton, N. A. P. Nicorovici, R. C. McPhedran, V. A. Podolskiy, *Proc. R. Soc. London Ser. A* **461**, 3999 (2005).
14. R. Merlin, *Appl. Phys. Lett.* **84**, 1290 (2004).
15. R. Shelby, D. R. Smith, S. Schultz, *Science* **292**, 77 (2001).
16. A. Grbic, G. V. Eleftheriades, *Phys. Rev. Lett.* **92**, 117403 (2004).
17. N. Fang, H. Lee, C. Sun, X. Zhang, *Science* **308**, 534 (2005).
18. T. Taubner, D. Korobkin, Y. Urzhumov, G. Shvets, R. Hillenbrandt, *Science* **313**, 1595 (2006).
19. E. Hecht, *Optics* (Addison Wesley, San Francisco, 2002).
20. J. A. Stratton, *Electromagnetic Theory* (McGraw-Hill, New York, 1941).
21. P. C. Clemmow, *The Plane Wave Spectrum Representation of Electromagnetic Fields* (Pergamon, Oxford, 1966).
22. J. H. McLeod, *J. Opt. Soc. Am.* **44**, 592 (1954).
23. J. Durnin, J. J. Miceli Jr., J. H. Eberly, *Phys. Rev. Lett.* **58**, 1499 (1987).
24. D. R. Smith *et al.*, *Appl. Phys. Lett.* **82**, 1506 (2003).
25. G. Shvets, *Phys. Rev. B* **67**, 035109 (2003).
26. We emphasize that, although our plates and negative-index slabs create comparable field distributions, the physical origins are very different in that the plates transform, propagating into evanescent modes, whereas the slabs amplify the near field.

27. The author acknowledges discussions with A. Grbic. This work was supported by the Air Force Office of Scientific Research under contract FA 9550-06-01-0279 through the Multidisciplinary University Research Initiative Program.

16 April 2007; accepted 27 June 2007
Published online 12 July 2007;
10.1126/science.1143884
Include this information when citing this paper.

Coherent Optical Spectroscopy of a Strongly Driven Quantum Dot

Xiaodong Xu,[1] Bo Sun,[1] Paul R. Berman,[1] Duncan G. Steel,[1*] Allan S. Bracker,[2] Dan Gammon,[2] L. J. Sham[3]

Quantum dots are typically formed from large groupings of atoms and thus may be expected to have appreciable many-body behavior under intense optical excitation. Nonetheless, they are known to exhibit discrete energy levels due to quantum confinement effects. We show that, like single-atom or single-molecule two- and three-level quantum systems, single semiconductor quantum dots can also exhibit interference phenomena when driven simultaneously by two optical fields. Probe absorption spectra are obtained that exhibit Autler-Townes splitting when the optical fields drive coupled transitions and complex Mollow-related structure, including gain without population inversion, when they drive the same transition. Our results open the way for the demonstration of numerous quantum level–based applications, such as quantum dot lasers, optical modulators, and quantum logic devices.

The quantum optoelectronic properties of semiconductor quantum dots (QDs) have featured prominently in numerous proposals, including quantum computing, single-photon sources, and quantum repeaters (*1*–*3*). QDs are particularly attractive for these applications because they behave in many ways as simple stationary atomic or molecular systems (*4*) with discrete states where the electron-hole pair can be treated as a well-defined composite-particle state (*5*).

Whereas strong optical excitation of a semiconductor creates a many-body problem because of the extended nature of the wave function (*6*), confinement of the wave function in QDs leads to strong energy-level shifts between one exciton and two or more exciton states, enabling the system to be considered as a relatively simple few-level problem. The strong-field excitation regime of the transition from the ground state to an excited state such as the exciton, a Coulomb bound electron-hole pair, is then defined by $\Omega_R >> 2\gamma$ where the Rabi frequency $\Omega_R = \frac{\mu E}{\hbar}$, $\frac{\gamma}{\pi}$ is a transition linewidth (full width at half-maximum, in Hz), μ is the transition dipole moment, and E is the amplitude of the optical electric field. For time scales less than γ^{-1}, strong excitation leads to Rabi oscillations (*7*–*10*) in time. The effect of vacuum Rabi splitting (*11*) has also been observed in a single QD embedded in a nanocavity (*12*–*14*).

Under strong continuous wave (CW) narrowband resonant optical excitation of a simple atomic system, the fluorescence emission spectrum, which is a narrow emission line at low power (the emission width is the laser bandwidth), consists of three peaks referred to as the Mollow triplet (*15*). A simple picture of the origin of this emission pattern is understood from a dressed-atom picture (*16*). Figure 1B shows the dressed-state picture with fully quantized atom-field states, when the driving-field frequency ω is equal to the electronic frequency ω_0. In this limit,

[1]The H. M. Randall Laboratory of Physics, The University of Michigan, Ann Arbor, MI 48109, USA. [2]The Naval Research Laboratory, Washington, DC 20375, USA. [3]Department of Physics, University of California–San Diego, La Jolla, CA 92093, USA.

*To whom correspondence should be addressed. E-mail: dst@umich.edu

the "bare" states $|3, N-1\rangle$ and $|2, N\rangle$ are degenerate, where N labels the photon number of the driving field. The atom-field interaction lifts this degeneracy and produces "dressed" states $|\alpha(N-1)\rangle$ and $|\beta(N-1)\rangle$ having energy separation $\hbar\Omega_R$ as shown. The dressed states are linear combinations of the bare states. The dashed lines in the figure indicate a triplet of possible emission frequencies, occurring at ω and $\omega \pm \Omega_R$.

In absorption, the spectrum can be more complex. For the three-level V system (Fig. 1A), where the strong field couples levels 2 and 3, theory predicts that the probe absorption from level 2 to level 1 is strongly modified from the usual simple Lorentzian seen in the absence of strong-field excitation. The probe absorption splits into two resonances, known as the Autler-Townes (AT) splitting (*17*). When the probe absorption on the strongly driven transition (between levels 2 and 3) is measured, the spectrum is much richer. New physics beyond that seen in the Mollow fluorescence triplet is observed (*18*–*22*) and arises from the coherent coupling between the two optical fields. When the Rabi frequency of the strong pump field is sufficiently large, the absorption spectrum shows gain without population inversion.

We present experimental results of the AT splitting and complex Mollow absorption spectrum (MAS) using a single semiconductor QD. We coherently control the probe absorption with a strong optical field, thus demonstrating that the single QD coupled with the strong pump can function as a modulator of the probe absorption (*23*). In addition, the spectrum as a function of the probe frequency shows Rabi splitting and gain without population inversion. The results are in good agreement with the standard theory based on the optical Bloch equations. Our work demonstrates that on long time scales, the discrete energy-level spectrum of the dot is maintained even at the high field strengths needed for quantum logic operations (e.g., qubit rotations) and single-photon devices, and that the system behaves in a manner similar to that of a trapped atom. The results suggest that it should be possible to demonstrate numerous quantum level–based applications, such as dressed-state lasers (*24*), QD optical modulators (*23*), and quantum logic devices (*4*).

The system of interest is a single, neutral InAs self-assembled QD embedded in a Schottky diode structure at 5K (*25*). The typical single-beam, linear absorption spectrum of a single QD (Fig. 1C), taken with a CW laser with a 300-KHz linewidth, shows that the neutral exciton has two linearly polarized quantum transitions with orthogonal polarizations. The fine-structure splitting of the exciton states, due to the QD in-plane anisotropy (*26*), is about 15 μeV. In the corresponding energy-level diagram of the states (Fig. 1A), states $|1\rangle$ and $|3\rangle$ represent the exciton states, state $|2\rangle$ is the crystal ground state, and the two linearly polarized transitions are labeled V and H.

To analytically describe our experiments, we follow the approach used in (*17*, *19*), describing the system with the optical Bloch equations $i\hbar\frac{d\rho}{dt} = [H, \rho] + \text{Decay}$ (*27*, *28*), where ρ and H are the density matrix and Hamiltonian of the light-coupled QD system, respectively. The Hamiltonian is given by $H = H_0 - \vec{\mu} \cdot \vec{E}$ where $\vec{E} = \vec{E}_0 + \vec{E}_1$. $\vec{E}_0$ is the strong pump field and $\vec{E}_1$ is the weak probe field. For calculations of the absorption spectrum, we can use the semiclassical approach where the fields are taken to be classical. H_0 is the diagonalized Hamiltonian for the QD structure (Fig. 1A). The results of calculations in the limits appropriate to this work are provided in the Supporting Online Material (*25*). The theory is fit to experimental data with

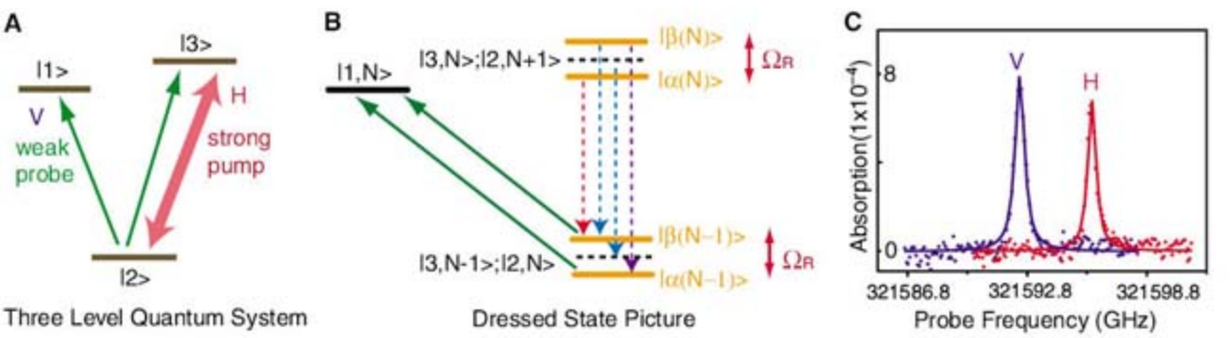

Fig. 1. (**A**) The energy-level diagram of a single neutral QD. The absorption of the weak probe beam by scanning either transition V or H is modified by the strong pump beam, which is near resonant with transition H. (**B**) The dressed-state picture of the system shown in (A). The transitions between states $|\alpha,N\rangle$ ($|\beta,N\rangle$) and $|1,N+1\rangle$, outside the energy range of the diagram, are not shown. If a weak beam probes transition 2-1 as shown by the green arrows, the absorption spectrum consists of a doublet. Ignoring the state $|1\rangle$, the emission spectrum of transition 3-2 consists of three peaks (Mollow triplet): a peak centered at the electronic transition ω, and two Rabi side bands located at $\omega \pm \Omega_R$ (shown by the dashed lines). (**C**) Single-beam, linear absorption profile of a single exciton state. The horizontally (or vertically) polarized light only excites the corresponding linearly polarized exciton transition.

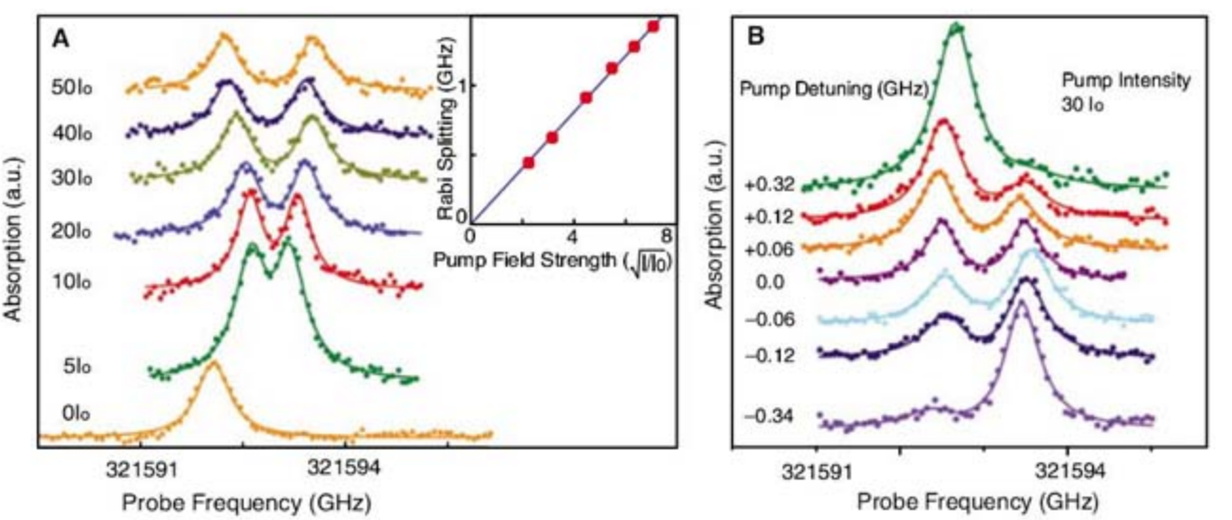

Fig. 2. Autler-Townes splitting by means of a single QD. A strong pump drives transition H, and a weak probe scans across transition V. (**A**) Probe absorption spectra as a function of the pump intensity when the pump is on resonance. I_0 equals 1.2 W/cm^2. The solid lines are theoretical fits to the data. The inset shows the AT splitting (Rabi splitting) as a function of the square root of the pump intensity. A linear fit (solid line) matches the data very well. (**B**) The probe absorption spectra as a function of the pump frequency detuning with fixed pump intensity. The lines are the theoretical fits to the data.

only the linewidth and amplitude as free parameters. The dipole moment is extracted from the linear dependence of the splitting on the field strength.

To experimentally demonstrate the AT effect (*17*), we use two frequency-locked but independently tunable CW lasers with a mutual coherence bandwidth of a few MHz (*25*). We set a horizontally polarized pump beam resonant with the H transition. A weak, vertically polarized probe beam then scans across transition V. The probe absorption spectra for different pump laser intensities are plotted in Fig. 2A with increasing pump intensity. The data are shifted vertically for clarity. In agreement with theory (solid lines) (*25*), the probe absorption splits into a doublet where each peak has equal strength. There is a small energy shift of the response relative to the low-intensity excitation that is probably due to a small screening of the applied field by photoexcited charge in the diode. The shift saturates at a power between the lowest-intensity curve and the next higher-power spectrum. The pump laser is adjusted to follow the shift of the resonance.

The frequency separation between the absorption peaks shows a strong dependence on the pump intensity. We plot the measured splitting as a function of the square root of the pump intensity in the inset of Fig. 2A. The splitting clearly depends linearly on the pump field strength and goes to zero in the absence of the pump, as expected for the dependence of the AT splitting on the Rabi frequency.

Figure 2B shows the probe absorption as a function of the pump detuning with a fixed pump intensity of $30I_0$ (the corresponding photon number per unit volume is ~$1.4 \times 10^{10}/\mathrm{cm}^3$), where $I_0 = 1.2\ \mathrm{W/cm}^2$, corresponding to a Rabi frequency of $\sim \frac{\Omega_R}{2\pi} = 1.1$ GHz. Again, the data are shifted for clarity, and the solid lines are the fit of the data to the theory (*25*) and show good agreement.

In the MAS, where the pump and probe beams coherently couple to the same transition and the pump field is tuned to resonance, we observe a relatively weak maximum centered at zero probe detuning and two Rabi side bands with dispersive line shapes. The pump power dependence of the probe absorption spectra is shown in Fig. 3A. The single-beam absorption data are plotted at the bottom. The spectral shift of the data with the high-power optical field is due to the excitation of the charge states in the buffer layer. The complex line shape of the MAS depends strongly on the pump intensity. The splitting between the two side bands is plotted as a function of the square root of the pump intensity in Fig. 3B, again showing that the splitting linearly depends on the pump field strength and is zero in the absence of the pump field.

The data confirm that the probe beam experiences optical gain in the pump-probe configuration for strong excitation. The MAS data in Fig. 3A show that part of the probe absorption curve is below zero, which is the "gain" effect. Using the data corresponding to $15I_0$ as an example, the absorption/gain ratio is about 0.066%/0.0024% = 27.5. This gain is from the pump and probe beams coherently exchanging energy through the QD and corresponds to gain without inversion because there is no population inversion either in the dressed- or bare-atom pictures.

The AT splitting can provide a method to measure the dipole moment, as the Rabi frequency is a product of the transition dipole moment with the optical field. From the extracted Rabi splitting with the corresponding optical field strength, we can infer a transition dipole moment of about 30 D for this particular QD. The Einstein A coefficient (spontaneous emission rate) of a QD in a medium is given as $\gamma_{sp} = \frac{9n^5}{(2n^2 + n_{QD}^2)^2} \times \frac{\omega_0^3 \mu^2}{3\pi\varepsilon_0 \hbar c^3} = \frac{9n^5}{(2n^2 + n_{QD}^2)^2} \gamma_{spo}$, where n (n_{QD}) is the refractive index of the medium (QD) and γ_{spo} is the spontaneous emission rate of a two-level quantum system in the vacuum (*29*). By taking $n = n_{QD} = 3.44$ and inserting the experimental parameters and the extracted dipole moment into the equation, we obtain $\frac{\gamma_{sp}}{2\pi} = 190$ MHz, which corresponds to a life time of about 840 ps. Assuming there is no other decay and no pure dephasing, this would lead to a natural linewidth expected in the low-power absorption spectrum also equal to $\frac{\gamma_1}{2\pi} = 190$ MHz, where γ_j is the decay rate of level j in Fig. 1A. Compared to the extracted linewidth from the single-beam, low-power absorption data, which is about 500 MHz, γ_{sp} is smaller by a factor of about 2.5. This discrepancy indicates that there is possibly a spectral wandering process that broadens the transition linewidth (*30*). This interpretation agrees with our previous study on a single charged QD, which also suggested the absence of pure dephasing.

We can also extract the exciton decay and dephasing rates from the AT splitting and MAS data. The solid lines in Fig. 2A are the theoretical fit of the AT splitting data assuming that $\gamma_3 = \gamma_1$ and $\Gamma_{13} = 0$, where $\gamma_{ij} = (\gamma_i + \gamma_j)/2 + \Gamma_{ij}$. γ_{ij} is the total dephasing rate, and Γ_{ij} is the contribution to the dephasing rate of the ij transition from sources other than spontaneous emission. From the fits, we find $\frac{\gamma_{21}}{2\pi}$ and $\frac{\gamma_{31}}{2\pi}$ of (176 ± 16) MHz and (357 ± 16) MHz, respectively. The theory fits the data very well and indicates that under these experimental conditions, the single QD behaves like a single atomic system. We also fit the MAS data to theory (*25*) (solid lines in Fig. 3A). The fitting yields $\frac{\gamma_{21}}{2\pi}$ and $\frac{\gamma_1}{2\pi}$ of (230 ± 12) MHz and (315 ± 45) MHz, respectively. The value of $\frac{\gamma_{21}}{2\pi}$ is within 10% of that extracted from the low-pump field profile. The physical parameters from the MAS and AT splitting data show that the decay rate is almost twice the dephasing rate, indicating no appreciable pure dephasing. We speculate that the reason for the discrepancy between the Einstein A coefficient determined from the dipole moment (above) and the fitting parameters is again due to spectral wandering, which leads to a fit of the theory that over-

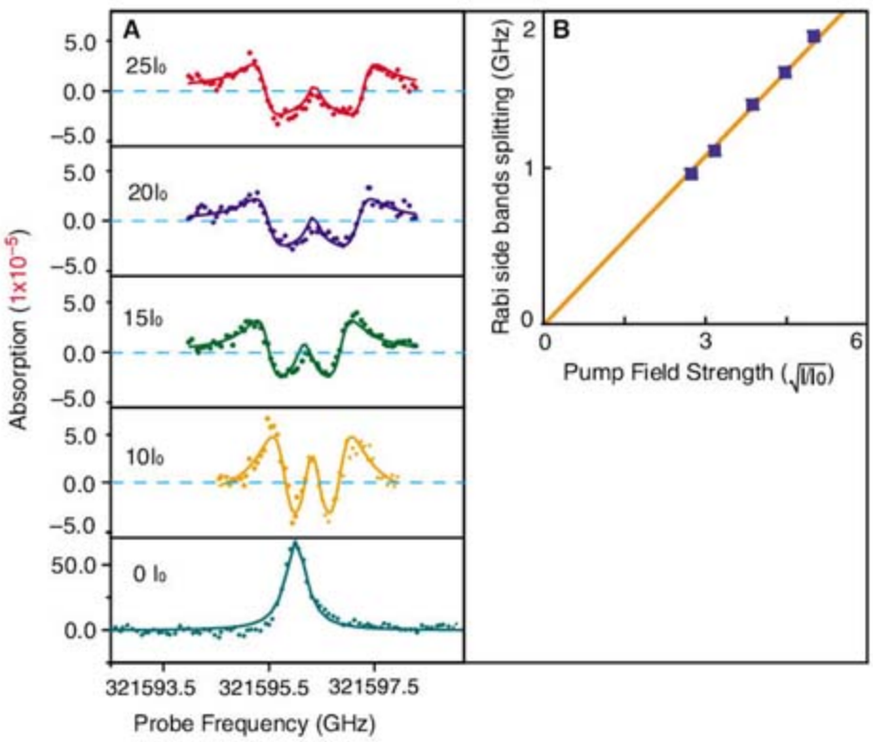

Fig. 3. Mollow absorption spectrum when the strong pump and weak probe beams couple to the same transition. (**A**) Measured probe absorption versus pump field intensity when the pump is on resonance. The lines are the fits to the probe absorption function obtained by solving optical Bloch equations. The MAS data show that the part of the absorption signal is "negative." Using the data corresponding to $15I_0$ as an example, the absorption/gain ratio is about 0.066%/0.0024% = 27.5. (**B**) The splitting between the Rabi side bands versus pump field strength. The solid line is the linear fit to the data.

estimates the population relaxation rate. However, this remains under investigation.

The AT splitting and gain without inversion in the Mollow absorption spectrum imply that the absorption and gain inside a single QD are tunable. In the AT configuration, the absorption of the probe beam can be switched on and off by applying a strong optical field. In contrast, in the MAS experiment, the absorption of the frequency fixed probe beam can be tuned to be positive or negative (gain) by adjusting the pump field strength. Our results are the first step toward the realization of electromagnetically induced transparency and lasing without inversion in the spin-based lambda system and suggest that QDs offer the potential to be used as elements in optoelectronics and quantum logic devices (*4*, *27*).

Note added in proof: Since the submission of this paper, two papers have appeared on http://arxiv.org that report studies of the resonant excitation of quantum dots in the strong excitation regime. The first (*31*) reports a measurement of the fluorescence correlation function that Mollow first calculated, and the second (*32*) reports Rabi oscillations.

References and Notes

1. D. Loss, D. P. DiVincenzo, *Phys. Rev. A.* **57**, 120 (1998).
2. Z. Yuan *et al.*, *Science* **295**, 102 (2002).
3. H.-J. Briegel, W. Duer, J. I. Cirac, P. Zoller, *Phys. Rev. Lett.* **81**, 5932 (1998).
4. D. Gammon, D. G. Steel, *Phys. Today* **55**, 36 (2002).
5. L. J. Sham, T. M. Rice, *Phys. Rev.* **144**, 708 (1966).
6. V. M. Axt, A. Stahl, *Z. Phys. B* **93**, 195 (1994).
7. T. H. Stievater *et al.*, *Phys. Rev. Lett.* **87**, 133603 (2001).
8. H. Kamada, H. Gotoh, J. Temmyo, T. Takagahara, H. Ando, *Phys. Rev. Lett.* **87**, 246401 (2001).
9. H. Htoon *et al.*, *Phys. Rev. Lett.* **88**, 087401 (2002).
10. A. Zrenner *et al.*, *Nature* **418**, 612 (2002).
11. J. J. Sanchez-Mondragon, N. B. Narozhny, J. H. Eberly, *Phys. Rev. Lett.* **51**, 550 (1983).
12. J. P. Reithmaier *et al.*, *Nature* **432**, 197 (2004).
13. T. Yoshie *et al.*, *Nature* **432**, 200 (2004).
14. K. Hennessy *et al.*, *Nature* **445**, 896 (2007).
15. B. R. Mollow, *Phys. Rev.* **188**, 1969 (1969).
16. J. Dupont-Roc, G. Grynberg, C. Cohen-Tannoudji, *Atom-Photon Interactions: Basic Processes and Applications* (Wiley, New York, 1998).
17. S. H. Autler, C. H. Townes, *Phys. Rev.* **100**, 703 (1955).
18. E. V. Baklanov, V. P. Chebotaev, *Sov. Phys. JETP* **34**, 490 (1972).
19. B. R. Mollow, *Phys. Rev. A.* **5**, 2217 (1972).
20. S. Haroche, F. Hartmann, *Phys. Rev. A.* **6**, 1280 (1972).
21. F. Y. Wu, S. Ezekiel, M. Ducloy, B. R. Mollow, *Phys. Rev. Lett.* **38**, 1077 (1977).
22. M. T. Gruneisen, K. R. MacDonald, R. W. Boyd, *J. Opt. Soc. Am. B* **5**, 123 (1988).
23. S. G. Carter *et al.*, *Science* **310**, 651 (2005).
24. N. Lu, P. R. Berman, *Phys. Rev. A.* **44**, 5965 (1991).
25. Materials and methods are available as supporting material on *Science* Online.
26. D. Gammon, E. S. Snow, B. V. Shanabrook, D. S. Katzer, D. Park, *Phys. Rev. Lett.* **76**, 3005 (1996).
27. M. O. Scully, M. S. Zubairy, *Quantum Optics* (Cambridge Univ. Press, Cambridge, 1997).
28. P. Meystre, M. Sargent, *Elements of Quantum Optics* (Springer-Verlag, Heidelberg, Germany, ed. 3, 1998) chap. 9.
29. A. Thranhardt, C. Ell, G. Khitrova, H. M. Gibbs, *Phys. Rev. B* **65**, 035327 (2002).
30. A. Hogele *et al.*, *Phys. Rev. Lett.* **93**, 217401 (2004).
31. A. Muller *et al.*, http://arxiv.org/abs/0707.0656.
32. R. Melet *et al.*, http://arxiv.org/abs/0707.3061.

33. This work is supported by the U.S. Army Research Office, Air Force Office of Scientific Research, Office of Naval Research, NSA/LPS, and FOCUS-NSF.

Supporting Online Material

www.sciencemag.org/cgi/content/full/317/5840/929/DC1
Materials and Methods
SOM Text
Fig. S1
References

26 March 2007; accepted 4 June 2007
10.1126/science.1142979

Deep Ultraviolet Light–Emitting Hexagonal Boron Nitride Synthesized at Atmospheric Pressure

Yoichi Kubota,* Kenji Watanabe, Osamu Tsuda, Takashi Taniguchi

Materials emitting light in the deep ultraviolet region around 200 nanometers are essential in a wide-range of applications, such as information storage technology, environmental protection, and medical treatment. Hexagonal boron nitride (hBN), which was recently found to be a promising deep ultraviolet light emitter, has traditionally been synthesized under high pressure and at high temperature. We successfully synthesized high-purity hBN crystals at atmospheric pressure by using a nickel-molybdenum solvent. The obtained hBN crystals emitted intense 215-nanometer luminescence at room temperature. This study demonstrates an easier way to grow high-quality hBN crystals, through their liquid-phase deposition on a substrate at atmospheric pressure.

Hexagonal boron nitride (hBN) and cubic boron nitride (cBN) are known as the representative crystal structures of BN. hBN is chemically and thermally stable and has been widely used as an electrical insulator and heat-resistant material for several decades; cBN, which is a high-density phase, is almost as hard as diamond (*1*).

Promising semiconductor characteristics due to a direct band gap of 5.97 eV were recently discovered in high-purity hBN crystals obtained by a high-pressure flux method, paving the way for a material that efficiently emits deep ultraviolet (DUV) light (*2*, *3*). Similar to aluminum nitride (AlN) (*4*) and gallium nitride (GaN) (*5*), hBN may have attractive potential as a wide–band gap material. The layered structure of hBN makes the material mechanically weak, but it has greater chemical and thermal stability than GaN and AlN. The interesting optical properties of hBN, such as its huge exciton-binding energy (*2*), are due to its anisotropic structure, whereas a single crystal's basal plane in hBN is not easily broken because of its strong in-plane bonds. Thus far, the excitation of hBN by an accelerated electron beam or by far-UV light above the band-gap energy shows various efficient luminescence bands near the band edge.

National Institute for Materials Science (NIMS), Tsukuba, Ibaraki 305-0044, Japan.

*To whom correspondence should be addressed. E-mail: kubota.yoichi@nims.go.jp

However, the electronic properties of hBN near the band gap, which is fundamental information for developing DUV light–emission applications, are not yet fully understood, as seen by the fact that the origins of the luminescence bands are still controversial (*2*, *6*, *7*). Two opposed models, a Wannier exciton model and a Frenkel exciton model, have been proposed. The former model is based on results of the intrinsic absorption spectra near the band edge from pure single crystals (*2*), and the latter model is based on theoretical calculations and a luminescence study that used powder samples (*7*) showing very intense impurity bands around 4.0 eV (*8*). According to work examining the correlation between impurities and defects and luminescence properties (*8*, *9*), the intrinsic optical properties of samples are hindered by the extrinsic ones if experimenters do not have careful control of the samples' crystallinity and polymorphic purity. In (*7*), the strong 5.46-eV luminescence band, which is attributed to stacking faults (*9*), dominated in the region of the band gap, and the most intense photoluminescence band at 215 nm, observed in a pure single crystal, was not observed from the powder sample. Pure samples with high crystallinity must be indispensable for developing this new material for DUV light–emitting applications. Because high-quality hBN crystals have so far been produced only by high-pressure processes, it is important to discover an alternative synthesis scheme for conventional crystal growth at atmospheric pressure.

DUV-luminous single-crystalline hBN has been created through the reduction of O and C impurities with the use of a reactive solvent of the Ba-BN system under high pressure (*2*, *3*, *8*).

Although the Ba-BN system is a useful solvent to obtain high-purity hBN crystals under high pressure, the system cannot be used at atmospheric pressure, probably because of the decomposition of the solvent itself at high temperature. A closed high-pressure system is required for using Ba-BN as a solvent, because the Ba-BN system is unstable at high temperature and is also extremely reactive with O and in the presence of humidity at atmospheric conditions (*8*).

hBN is thermodynamically stable at high temperatures and at atmospheric pressure. Therefore, it should be possible to obtain high-quality hBN crystals at atmospheric pressure by using an appropriate solvent. Ishii and Sato reported the preparation of hBN single crystals by using a Si flux under 1 atm of N_2 (*10*). Although they claimed that the crystals showed sharp absorption near 5.8 eV, DUV-emitting properties were not observed. Because the band-edge optical properties are strongly affected by O and C impurities (*8*), the emission characteristics of their hBN crystals were probably affected by the C impurity mentioned in their report (*10*). Yano *et al.* reported the synthesis of hBN crystals using a Na solvent under 100 atm of N_2 (*11*). They observed a cathodoluminescence spectrum of the hBN with a peak near 3.8 eV and a weak emission near 5.6 eV.

A variety of solvents have been studied for cBN synthesis at high-pressure and high-temperature conditions: alkali and alkaline earth metals (*12*, *13*), their BN compounds (*3*, *8*, *14*), and some transition metals (*15*, *16*). Because a solvent useful for cBN growth may be useful for hBN growth, we focused on transition-metal solvents, which do not decompose at atmospheric pressure. We recently established a reaction diagram of Ni and BN under high pressures and found that hBN dissolves in molten Ni and precipitates as tiny cBN crystals, and also recrystallizes as hBN at high-pressure and high-temperature conditions (*17*). In the chemical vapor deposition process, Ni seems to have a catalytic action that initiates the formation of the hBN (*18*). A UV-luminous hBN layer was deposited on a Ni substrate, though the layer was not homogeneous (*19*). Yang *et al.* reported that their hBN crystals were formed from a molten surface layer of Ni substrate, although the obtained crystals were only a few micrometers in size (*20*). They did not claim any information about the optical characteristics of the products.

Here we describe the synthesis of high-quality hBN crystals under atmospheric pressure using a Ni base solvent. Although the grown crystals formed aggregates with dimensions of several hundred micrometers, intense DUV emission was observed across the entire region of the grown crystals.

Initially, we used a Ni disk as the solvent and deoxidized hBN powder as a starting material for the atmospheric-pressure synthesis of hBN (*21*). The materials were put into a crucible and heated at 1350° to 1500°C for a soak period of 12 hours in the furnace. After soaking, the furnace was cooled down at a rate of 4°C/hour to 1200°C.

Colorless and transparent crystals with a thin platelike habit were found to grow on the surface of the solidified Ni solvent. The obtained crystal surface was segmented by striae into triangular or hexagonal domains. The largest crystal was about 300 μm across, with thickness of a few micrometers. The Raman spectrum of the crystal showed a single peak at 1365 cm^{-1}, which corresponds to the in-plane vibrational mode of hBN (*22*), with full width at half maximum (FWHM) of 9.3 cm^{-1}. The yield of the reaction was, however, very low, and the recrystallized hBN was observed only on some small parts of the surface of the solvent.

The binary Ni-B and Ni-N phase diagrams show that approximately 30 weight % (wt%) B is in a liquid phase at 1550°C (*23*), whereas the solubility of N in liquid Ni is only 0.0012 wt% at 1550°C at 1 atm of N_2 (*24*). Thus the yield of recrystallized hBN is controlled by the N solubility in the liquid phase of the Ni solvent. Kowanda and Speidel reported that the N solubility of a liquid Ni-Mo alloy increases with an increasing concentration of Mo; the addition of Mo of 40 wt% to the Ni solvent enhances the solubility of N by 40 times as compared to that in the pure Ni (*24*). We thus added Mo to the Ni solvent so as to increase N content in solution.

Many faceted platelike hBN crystals were obtained on the surface of the solidified Ni-Mo solvent (Fig. 1A). The thickness of the crystals grown was typically 10 μm, as characterized by optical microscopy. The largest hBN crystal obtained in this study was on the order of 300 μm × 200 μm. We found that the crystals were aggregated and fully covered the surface of the Ni-Mo solvent, which was 20 mm in diameter (Fig. 1B, inset). Although the grown crystals fragmented into several pieces during the acid treatment, the recovered crystal was transparent, colorless, and about 9 mm × 4 mm in size (Fig. 1B). These results show that the Mo in the Ni-Mo alloy increases the yield of recrystallized hBN, probably by increasing the N solubility of the solvent.

The Raman spectrum of the crystal shows a single peak at 1365 cm^{-1} with a FWHM of 9.0 cm^{-1} (Fig. 2A). The FWHM of our high-quality hBN single crystals obtained by high-pressure and high-temperature synthesis was 9.1 cm^{-1}, suggesting that quality of the crystal from the Ni-Mo binary system was almost comparable to that of the crystal produced by high-pressure and high-temperature synthesis.

Figure 2B shows an x-ray diffraction (XRD) profile of the aggregate crystals that were ground into fine powder. All the peaks can be assigned as those of hBN (Joint Committee on Powder

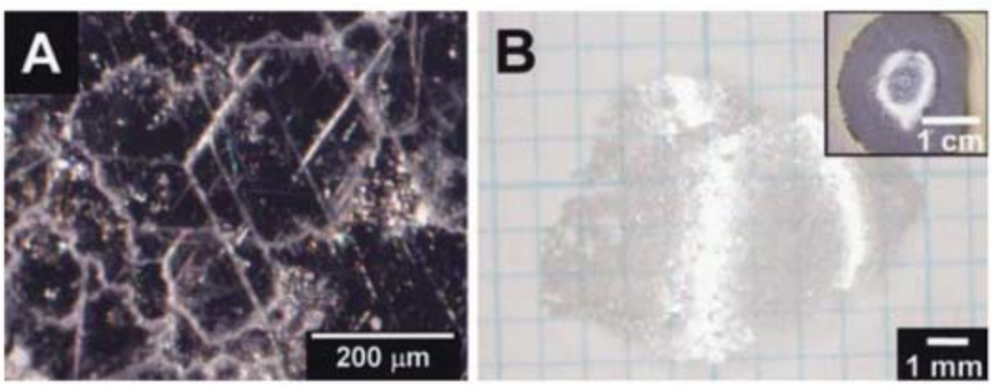

Fig. 1. Optical micrographs of recrystallized hBN obtained with a Ni-Mo solvent. (**A**) Typical hBN crystal on the solidified solvent (as grown). (**B**) A fragment of aggregate hBN crystals after acid treatment (the inset is an optical micrograph of a recovered sample). The shiny white regions are reflected light.

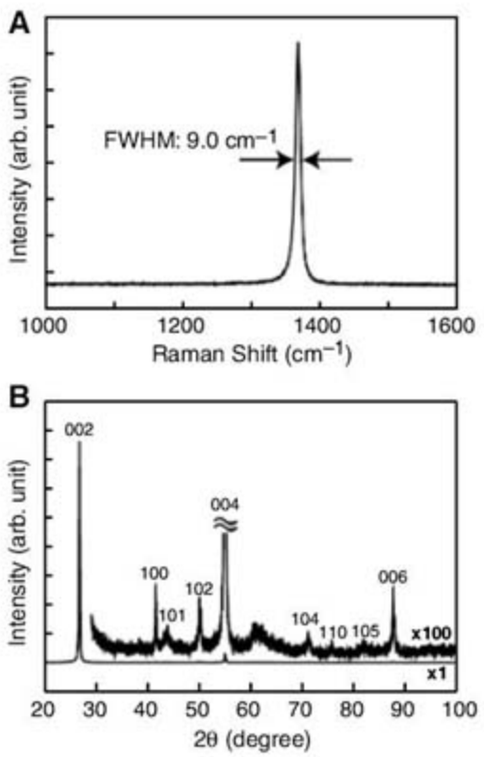

Fig. 2. Characteristics of recrystallized hBN grown in a Ni-Mo solvent at atmospheric pressure. (**A**) Raman spectrum obtained from recrystallized hBN. (**B**) X-ray diffraction profile of recrystallized hBN after being ground to fine powder. arb., arbitrary.

Diffraction Standards card no. 34-421), except the broad peak near 60°, which is attributed to the Si sample holder.

Figure 3 shows typical cathodoluminescence spectra of the hBN crystals grown with the Ni and Ni-Mo solvents. The spectra were measured at room temperature. Each spectrum exhibits an intense free-exciton luminescence peak at 215 nm that is characteristic of a high-quality hBN crystal (*2*). The shoulder structure around 227 nm, which we attribute to a bound exciton caused by a stacking disorder, is relatively low, suggesting that these crystals have low stacking disorder (*9*). We also observed weak broad bands around 300 nm, especially in the Ni solvent system, which were probably due to residual impurities such as O and C (*2*, *8*). It is known that Mo forms carbide whereas Ni does not (*25*, *26*), suggesting that Mo could play the role of the C getter in the Ni solvent. The reduction of C impurities in the crystals was achieved, as suggested by the less-broadband feature near 300 nm. The dominant DUV band near the band edge at 215 nm reveals the low impurity content of our crystals.

Our results show that the atmospheric-pressure Ni-Mo solvent system is as effective for the synthesis of high-quality hBN as are high-pressure and high-temperature solvent systems. We made direct quality comparisons of the emission characteristics of the samples grown in this study and those grown at high pressures. The band-edge emission intensities of the both crystals were of similar order (Fig. 3C).

hBN recrystallization using a metal solvent can lead to large-area deposition of high-quality hBN crystals on a substrate with the use of a liquid-phase epitaxy process under atmospheric-pressure conditions. In order to examine the growth of a hBN crystal on a substrate from the solution, we added a sapphire substrate to the starting materials and applied the same growth process as above, using the Ni-Mo solvent. We observed that hBN crystals with smooth surfaces grew on the substrate (Fig. 4A). The cathodoluminescence spectrum of the hBN crystals showed the similar dominant luminescence band at 215 nm (Fig. 3). Figure 4B shows the intense 215-nm luminescence image at room temperature corresponding to Fig. 4A. The intensity of the 215-nm band is uniform over almost all of the surface. The cathodoluminescence image of striae is substantially enhanced by the scattered 215-nm luminescence in Fig. 4B.

When Mo was added to the Ni solvent, the yield of recrystallized hBN was substantially increased because of the enhancement of N solubility in the Ni-Mo system. The grown hBN crystals were of very high quality, exhibiting their band-edge optical nature of intense 215-nm luminescence. Consequently, we can establish an alternative synthesis route for large amounts of high-quality hBN crystals, as well as their liquid-phase deposition process on a substrate at atmospheric pressure.

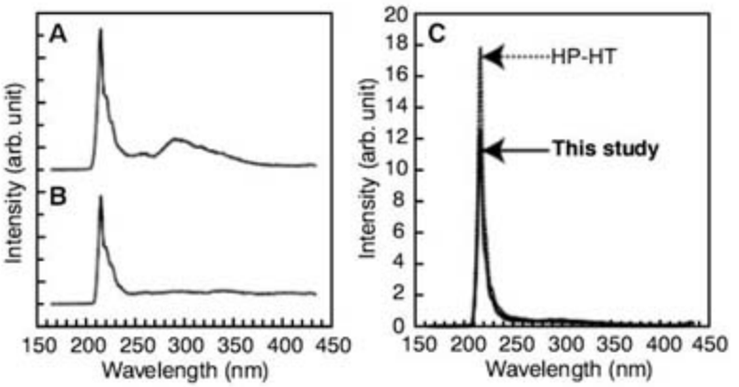

Fig. 3. Cathodoluminescence spectra of recrystallized hBN at room temperature. (**A**) hBN obtained with a Ni solvent. (**B**) hBN obtained with a Ni-Mo solvent. (**C**) Direct quality comparison of the emission characteristics. Solid line, hBN obtained with a Ni-Mo solvent at atmospheric pressure (in this study); dotted line, hBN obtained with a Ba-BN solvent at high pressure and high temperature (HP-HT).

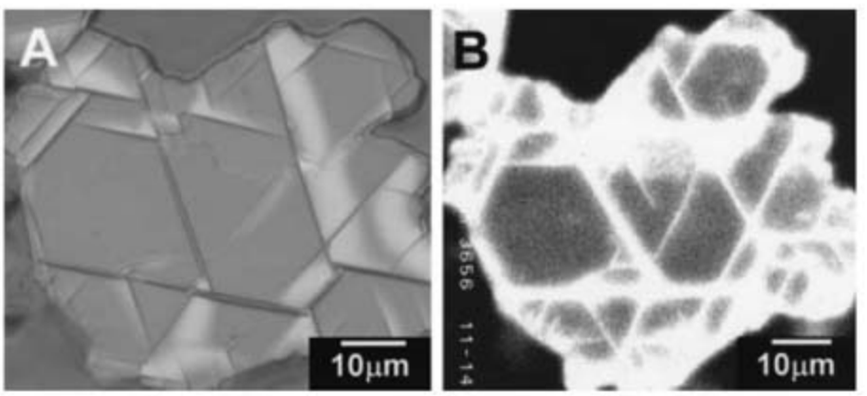

Fig. 4. Images of hBN crystal grown on the *a*-plane sapphire substrate (obtained with a Ni-Mo solvent prepared at 1400°C). (**A**) Differential interference microscopic image. (**B**) Cathodoluminescence image for 215-nm band. We did not find any intensity change of the measured spectra between the grain boundary and the plane surface area when measuring the point-to-point mode of the cathodoluminescence system, where the electron beam remained stationary and the measured luminescence was confined to the exposed spot area.

References and Notes

1. O. Mishima, K. Era, in *Electric Refractory Materials*, Y. Kumashiro, Ed. (Dekker, New York, 2000), chap. 21.
2. K. Watanabe, T. Taniguchi, H. Kanda, *Nat. Mater.* **3**, 404 (2004).
3. T. Taniguchi, K. Watanabe, S. Koizumi, *Phys. Status Solidi A* **201**, 2573 (2004).
4. Y. Taniyasu, M. Kasu, T. Makimoto, *Nature* **441**, 325 (2006).
5. I. Akasaki, H. Amano, *Jpn. J. Appl. Phys.* **36**, 5393 (1997).
6. B. Arnaud, S. Lebegue, P. Rabiller, M. Alouani, *Phys. Rev. Lett.* **96**, 026402 (2006).
7. M. G. Silly *et al.*, *Phys. Rev. B* **75**, 085205 (2007).
8. T. Taniguchi, K. Watanabe, *J. Cryst. Growth* **303**, 525 (2007).
9. K. Watanabe, T. Taniguchi, T. Kuroda, H. Kanda, *Appl. Phys. Lett.* **89**, 141902 (2006).
10. T. Ishii, T. Sato, *J. Cryst. Growth* **61**, 689 (1983).
11. M. Yano *et al.*, *Jpn. J. Appl. Phys.* **39**, L300 (2000).
12. R. H. Wentorf Jr., *J. Chem. Phys.* **34**, 809 (1961).
13. T. Endo, O. Fukunaga, M. Iwata, *J. Mater. Sci.* **14**, 1375 (1979).
14. R. C. DeVries, J. F. Fleisher, *J. Cryst. Growth* **13–14**, 88 (1972).
15. H. Saito, M. Ushio, S. Nagano, *Yogyo Kyokai Shi* **78**, 1 (1970) [in Japanese with an English abstract].
16. T. Taniguchi, *New Diamond Front. Carbon Technol.* **14**, 289 (2004).
17. Y. Kubota, K. Watanabe, T. Taniguchi, *Jpn. J. Appl. Phys.* **46**, 311 (2007).
18. T. Takahashi, H. Itoh, A. Takeuchi, *J. Cryst. Growth* **47**, 245 (1979).
19. O. Tsuda, K. Watanabe, T. Taniguchi, *Jpn. J. Appl. Phys.* **46**, L287 (2007).
20. P. C. Yang, J. T. Prater, W. Liu, J. T. Glass, R. F. Davis, *J. Electron. Mater.* **34**, 1558 (2005).
21. Materials and methods are available as supporting material on *Science* Online.
22. R. Geick, H. Perry, *Phys. Rev.* **146**, 543 (1966).
23. P. K. Liao, K. E. Spear, in *Binary Alloy Phase Diagrams*, T. B. Massalski, Ed. (ASM International, Materials Park, OH, ed. 2, 1990), vol. 1, pp. 508–510.
24. C. Kowanda, M. O. Speidel, *Scripta Mater.* **48**, 1073 (2003).
25. T. B. Massalski, in *Binary Alloy Phase Diagrams*, T. B. Massalski, Ed. (ASM International, Materials Park, OH, ed. 2, 1990), vol. 1, pp. 861–862.
26. M. F. Singleton, P. Nash, in *Binary Alloy Phase Diagrams*, T. B. Massalski, Ed. (ASM International, Materials Park, OH, ed. 2, 1990), vol. 1, pp. 866–867.

27. The authors thank T. Wada of NIMS for his support in the XRD study. This study was supported by a Grant-in-Aid for Scientific Research of the Japan Society for the Promotion of Science (nos. 19205026 and 18360321).

Supporting Online Material

www.sciencemag.org/cgi/content/full/317/5840/932/DC1
Materials and Methods
Fig. S1
References

24 April 2007; accepted 22 June 2007
10.1126/science.1144216

Temporal Variability of the Atlantic Meridional Overturning Circulation at 26.5°N

Stuart A. Cunningham,[1]* Torsten Kanzow,[1] Darren Rayner,[1] Molly O. Baringer,[2] William E. Johns,[3] Jochem Marotzke,[4]* Hannah R. Longworth,[1] Elizabeth M. Grant,[1] Joël J.-M. Hirschi,[1] Lisa M. Beal,[3] Christopher S. Meinen,[2] Harry L. Bryden[1]

The vigor of Atlantic meridional overturning circulation (MOC) is thought to be vulnerable to global warming, but its short-term temporal variability is unknown so changes inferred from sparse observations on the decadal time scale of recent climate change are uncertain. We combine continuous measurements of the MOC (beginning in 2004) using the purposefully designed transatlantic Rapid Climate Change array of moored instruments deployed along 26.5°N, with time series of Gulf Stream transport and surface-layer Ekman transport to quantify its intra-annual variability. The year-long average overturning is 18.7 ± 5.6 sverdrups (Sv) (range: 4.0 to 34.9 Sv, where 1 Sv = a flow of ocean water of 10^6 cubic meters per second). Interannual changes in the overturning can be monitored with a resolution of 1.5 Sv.

Defining the size of the variability in MOC is a fundamental prerequisite to understanding how it may be changing on climate-relevant time scales. Recently, it was suggested that the circulation has slowed by 30% or 8 Sv over the past decade, based on consistent analysis of repeated hydrographic sections along 26.5°N (*1*). Coupled climate models suggest that there will be a decline in the Atlantic overturning circulation as a result of increased CO_2 in the atmosphere but that the change will be gradual over this century (*2*). Is the suggested 8-Sv change in overturning just the result of intra-annual variability in the circulation sampled by each hydrographic section? What size of a change in the overturning can be reliably detected above the intra-annual variability? To answer such questions, we define the size and structure of the intra-annual variability in the MOC at 26.5°N from 1 year of measurements by using the Rapid Climate Change (RAPID) mooring array (*3*).

The 26.5°N Atlantic section is separated into two regions: a western boundary region, where the Gulf Stream flows through the narrow (80 km), shallow (800 m) Florida Straits between Florida and the Bahamas, and a trans-atlantic mid-ocean region, extending from the Bahamas at about 77°W to Africa at about 15°W (fig. S1). Variability in Gulf Stream flow is derived from cable voltage measurements across the Florida Straits (*4*), and variability in wind-driven surface-layer Ekman transport across 26.5°N is derived from QuikScat satellite–based observations (*5*). To monitor the mid-ocean flow, we deployed an array of moored instruments along the 26.5°N section (fig. S2). The basic principle of the array is to estimate the zonally integrated geostrophic profile of northward velocity on a daily basis from time-series measurements of temperature and salinity throughout the water column at the eastern and western boundaries. Inshore of the most westerly measurements of temperature and salinity, the transports of the Antilles current and deep western boundary current are monitored by direct velocity measurements [supporting online material (SOM) text].

We deployed the mid-ocean array from February to March 2004 and recovered it from March to May 2005 (*6*, *7*). The overlapping period when the entire array was working for its first year was 28 March 2004 to 31 March 2005. We have since redeployed the array in spring 2005 and again in spring 2006. In this report, we present results from the first year. The design of the RAPID array for monitoring basin-scale circulation was tested in numerical ocean-circulation models (*8*, *9*), and a companion paper (*10*) demonstrates from the first year's time series that five independently measured transports (Gulf Stream, Ekman, boundary wedge, baroclinic, and barotropic geostrophic transports) are in overall mass balance for time scales longer than 10 days, providing evidence that the monitoring system works (SOM text).

To examine the intra-annual mid-ocean baroclinic variability in layers (Fig. 1), we estimated daily transports above 800-m depth (thermocline recirculation), between 800- and 1100-m depth (intermediate water flow), between 1100- and 3000-m depth (upper North Atlantic deep water or UNADW), and below 3000-m depth (lower North Atlantic deep water or LNADW). We prefer to use 800 m as a boundary for the thermocline recirculation because this is the maximum depth of the Florida Straits; thus, all of the northward transport in the Gulf Stream and Ekman layer occurs above 800-m depth.

The time series of layer transports (Fig. 2) exhibit variability of about 3 Sv around their time-averaged transports (Table 1): The SD in thermocline recirculation and LNADW is ±2.7 and ±3.5 Sv, respectively, indicating the size of the variability in baroclinic structure. Such variability is smaller than the 6 Sv previously reported from a modeling study (*11*). Still, the range in transports is large: The southward thermocline recirculation is as small as –6.6 Sv and as large as –23.3 Sv, and the range in LNADW transport is from 1.0 to –18.2 Sv.

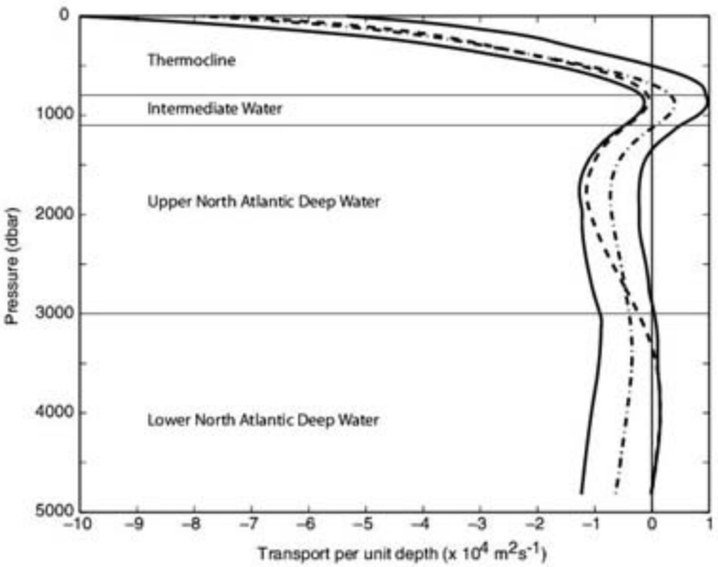

Fig. 1. Vertical profile of the northward mid-ocean transport per unit depth ($m^2\ s^{-1}$). Dynamic height difference (east minus west in $m^2\ s^{-2}$) divided by Coriolis frequency (s^{-1}) equals transport per unit depth and is proportional to the zonally integrated meridional geostrophic velocity; negative difference corresponds to southward velocity across 26.5°N. Reference levels are chosen so that the vertically integrated mid-ocean geostrophic transport equals the northward Gulf Stream transport through the Florida Straits plus the average northward wind-driven Ekman transport across 26.5°N plus the boundary wedge transport. The profile of year-long average (dashed-dotted curve), the profile on 2 November 2004 during the extreme (dashed curve), and the maximum and minimum over the year at each depth (solid curves) are shown.

[1]National Oceanography Centre, Empress Dock, Southampton SO14 3ZH, UK. [2]National Oceanic and Atmospheric Administration (NOAA)–Atlantic Oceanographic and Meteorological Laboratory (AOML)/Physical Oceanography Division, 4301 Rickenbacker Causeway, Miami, FL 33149, USA. [3]Rosenstiel School of Marine and Atmospheric Sciences (RSMAS), University of Miami, 4600 Rickenbacker Causeway, Miami, FL 33149, USA. [4]Max Planck Institute for Meteorology, Bundesstrasse 53, D-20146 Hamburg, Germany.

*To whom correspondence should be addressed. E-mail: scu@noc.soton.ac.uk (S.A.C.); marotzke@dkrz.de (J.M.)

From March 2004 to March 2005, the Florida Straits transport is at its maximum in August (Fig. 3), typical of its long-term seasonal cycle (*12*). The year-long average transport is 31.7 Sv, slightly less than the long-term mean of 32.2 Sv (*12*), and the daily transport variations have a SD of ±3.3 Sv (Table 2). During 2004–2005, the northward wind-driven surface-layer Ekman transport has an annual average value of 3.0 Sv, smaller than the long-term mean Ekman transport of about 3.8 Sv, due in part to anomalous southward transport during February and March 2005. Long-term records of Ekman transport at 26.5°N exhibit small seasonal variability (*13*), but from 2004 to 2005, the maximum northward Ekman transport occurs in December and January. Daily variations in Ekman transport via QuikScat data have a SD of ±4.4 Sv. The mid-ocean thermocline recirculation above 800-m depth is at a minimum in late September and a maximum in December.

The maximum overturning, as is commonly used by modelers in their overturning analyses, is defined here as the sum of northward Gulf Stream, Ekman, intermediate water, and southward thermocline recirculation transports, which gives the maximum amount of northward transport of upper waters (SOM text); maximum overturning has an annual mean transport of 18.7 Sv with a SD of ±5.6 Sv. The overturning reaches a maximum value of 34.9 Sv in September, when the Gulf Stream transport is near its summertime maximum and when the southward upper mid-ocean transport is near its minimum value. The overturning achieves a minimum value of 4.0 Sv in February when the Gulf Stream transport is low, the Ekman transport is southward, and the southward upper mid-ocean transport is relatively strong.

Gulf Stream, Ekman, and upper mid-ocean transport (Fig. 3) are nearly independent time series, and there is no significant correlation among them. There is some compensation inherent in the mid-ocean recirculation because the reference-level velocity depends on the size of the Gulf Stream transport plus Ekman transport on each day, but most of the transport compensation occurs in the deep-water transports that have larger areas. The SD in upper mid-ocean transport (±3.1 Sv) is actually smaller than the variations in Gulf Stream (±3.3 Sv) transport or Ekman (±4.4 Sv) transport. Therefore, the variance in the overturning is nearly equal to the sum of the variances, so each component contributes about equally to its temporal variability.

The most notable event in the year-long time series occurs in early November 2004, when the deep southward flow of LNADW essentially ceased and there was a brief period of net northward transport of deep waters below 3000-m depth. In the time series of temperatures at the western boundary station (fig. S4), the signature of this event is a 700-m downward displacement of isotherms below 2000 m. The vertical profile of dynamic height difference (Fig. 1) shows the sharp decrease in southward velocity in the deep water, as compared to the average profile. In terms of water masses, the cold LNADW effectively disappears at the boundary. Even though the southward flow of LNADW stopped, there is not a large anomaly in overturning. This event is strongly baroclinic (Figs. 1 and 2): The thermocline recirculation is close to its average value whereas the southward flow of UNADW is larger than average, which compensates for the lack of LNADW transport. Thus, the overturning (Fig. 3) is close to its mean value during this event.

There has been no comparable event observed in historical transatlantic sections (*14*–*18*). There was a steep descent of deep isotherms offshore from the western boundary in the 1957 hydrographic section, but the isotherms recovered

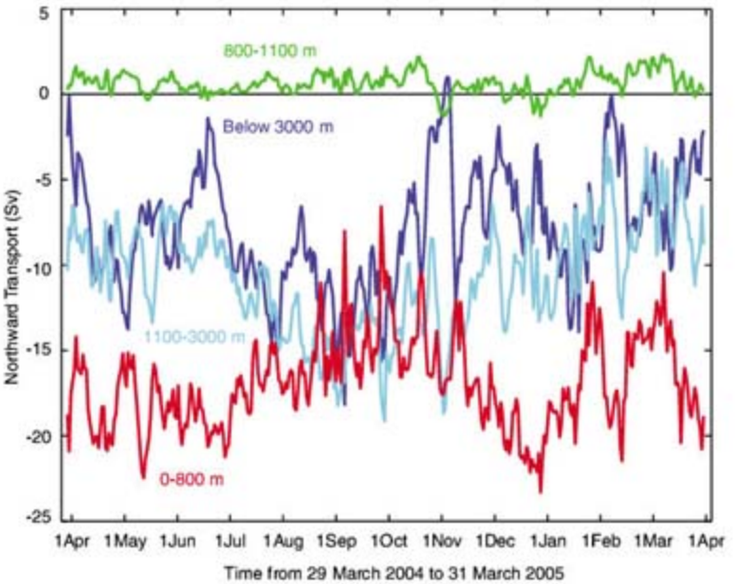

Fig. 2. Year-long time series of layer transports for thermocline recirculation (red), intermediate water (green), UNADW (light blue), and LNADW (dark blue). Negative transports correspond to southward flow.

Table 1. Mid-ocean layer transports (data reported in Sv).

Water depth	Mean	SD	Minimum	Maximum
0 to 800 m (thermocline recirculation)	−16.9	2.7	−23.3	−6.6
800 to 1100 m (intermediate water)	0.7	0.6	−1.3	2.3
1100 to 3000 m (UNADW)	−10.7	3.1	−19.2	−2.7
Below 3000 m (LNADW)	−7.8	3.5	−18.2	1.0

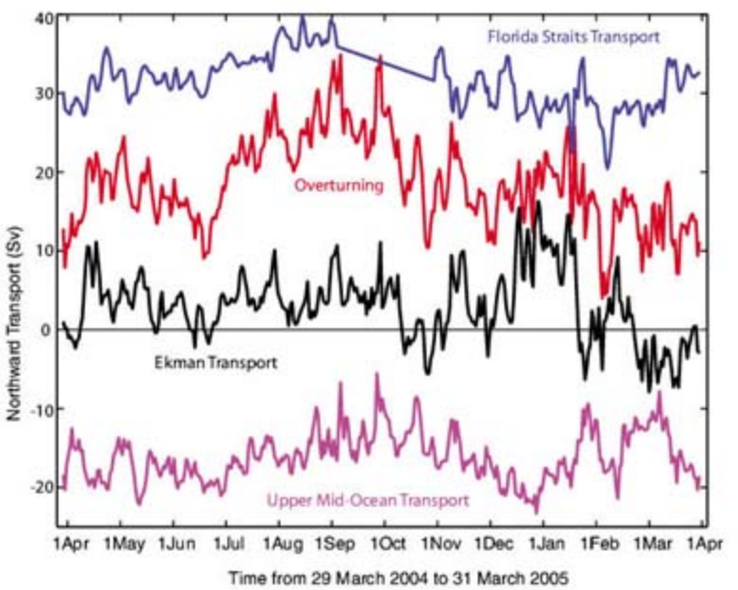

Fig. 3. Daily time series of Florida Straits transport (blue), Ekman transport (black), upper mid-ocean transport (magenta), and overturning transport (red) for the period 29 March 2004 to 31 March 2005. Florida Straits transport is based on electromagnetic cable measurements; a gap in the time series of ~2 months from 4 September to 28 October 2004 is due to Hurricane Frances, which destroyed the facility recording the voltage (linear interpolation is chosen here to fill the gap). Ekman transport is based on QuikScat-determined winds. The upper mid-ocean transport, based on the RAPID time series, is the vertical integral of the transport per unit depth down to the deepest northward velocity (~1100 m) on each day. Overturning transport is then the sum of the Florida Straits, Ekman, and upper mid-ocean transports and represents the maximum northward transport of upper-layer waters on each day (SOM text).

at the boundary, suggesting that there was a deep eddy of recirculating LNADW in this offshore region. With the western station of the RAPID array being so close to the western boundary, there is no room for a deep western boundary current to be inshore of mooring WB2 (SOM text), so we do not consider this November 2004 event to be an eddy. Within 500 km of the Bahamas, the deep western boundary current transport is absent at this time.

In a recent paper, the strength of the MOC calculated from hydrographic sections in 1957, 1981, 1992, 1998, and 2004 was found to have reduced from 22.9 to 14.8 Sv, where the overturning was defined to be the net northward transport above 1000-m depth (*1*). For the 2004–2005 time series, the overturning shallower than 1000 m has a mean value of 19.0 Sv and a SD of ±5.6 Sv. For the year-long time series, the range in daily overturning includes all hydrographic section estimates, suggesting that single hydrographic sections may represent only intra-annual variability rather than a long-term trend. The 2004 hydrographic section started at the western boundary on 7 April 2004, when the thermocline recirculation was large, when LNADW transport was small (Fig. 2), and when the overturning was small (Fig. 3). Thus, relative to the 2004–2005 time series, the 2004 hydrographic section was taken during a period of low overturning relative to the year-long average overturning.

The temporal variability in the overturning resulting from fluctuations in the Florida Straits or Ekman transports can be put into the context of long time series of such transports. The Florida Straits transport time series goes back reliably to 1982, with some cable time series continuing to the 1950s and some dropsonde sections extending to as early as 1964 (*12*, *19*, *20*). Similarly, the National Centers for Environmental Prediction reanalysis project (*21*) archives wind stress values back to the 1950s. Thus, any variability in annually averaged overturning, due to changes in Florida Straits or Ekman transports of more than 1 or 2 Sv, should be immediately recognizable. However, we lack a comparable long time series of mid-ocean transport against which we might examine changes in mid-ocean circulation that would affect the strength of the overturning. There are isolated hydrographic stations on the eastern and western boundaries that provide some additional information on long-term variability in mid-ocean transport (*22*), but these "snapshot" estimates of mid-ocean circulation all lie within the range of variability in the first year's RAPID measurements. Without additional historical estimates to increase the degrees of freedom, it is unlikely that we will be able to conclusively demonstrate a change in the overturning circulation over the past 50 years.

In terms of the future detection of changes in overturning, the prospects are better. The 2004–2005 time series define a year-long average upper mid-ocean transport of –16.1 Sv with a SD of ±3.1 Sv. Based on the integral time scales of variability (SOM text), the SE of the yearly average mid-ocean transport is about 0.8 Sv. Indeed, we can monitor the yearly average mid-ocean layer transports as well as the Florida Straits or Ekman transports. If future years' time series exhibit similar intra-annual variability, we should be able to identify real interannual variability that is larger than 1.6 Sv in mid-ocean transport averaged over a year. Combining the mid-ocean Ekman and Florida Straits transports into a time series of the overturning, we can estimate the yearly average overturning with a SE of about 1.5 Sv. Thus, we can monitor the interannual variability in the overturning at 26.5°N with a resolution of 1.5 Sv. For example, if the circulation passes through a bifurcation (*23*) or if the overturning reduces by 25% [as coupled climate models suggest that it might under increasing atmospheric CO_2 concentrations (*24*)], we should also be capable of identifying the change relative to the 2004–2005 average. There may be interannual variability in the circulation and overturning that would obscure a trend, as found in coupled climate models (*25*); but, with longer time series of mid-ocean transports from the RAPID array (combined with continuing cable measurements of Florida Straits transport and satellite-based wind estimates of Ekman transport), the interannual variability in Atlantic overturning should be defined with a resolution of 1.5 Sv.

Thus, although the intra-annual variability in the overturning demonstrates that we are unlikely to conclusively identify past changes in the overturning using only sparse basin margin densities at a single latitude, the observed temporal variability defines the limit of our ability to identify future changes. Fundamentally, we need longer time series of the overturning to define its interannual variability. Ten additional years of uninterrupted measurements would ensure that any seasonal cycles are well defined and would also refine the nature of interannual variations, whether they are oscillations, trends, or sudden shifts.

Table 2. Component transports of the Atlantic overturning circulation (data reported in Sv) at 26.5°N for the period 29 March 2004 to 31 March 2005. Overturning transport is defined as in Fig. 3. The upper mid-ocean transport is defined as the minimum in southward transport of upper waters on each day. The average depth of the maximum transport is 1041 m (with a SD of ±92 m).

Component	Mean	SD	Minimum	Maximum
Florida Straits transport	31.7	3.3	20.4	39.8
Ekman transport	3.0	4.4	–7.9	16.3
Upper mid-ocean transport	–16.1	3.1	–23.3	–5.5
Overturning	18.7	5.6	4.0	34.9

References and Notes

1. H. L. Bryden, H. R. Longworth, S. A. Cunningham, *Nature* **438**, 655 (2005).
2. U. Cubasch *et al.*, in *Climate Change 2001: The Scientific Basis*, J. T. Houghton *et al.*, Eds. (Cambridge Univ. Press, Cambridge, 2001), pp. 525–582.
3. RAPID is a directed program of the Natural Environment Research Council (NERC). The project to monitor the Atlantic MOC at 26.5°N reported here is a joint UK/US collaboration among the National Oceanography Centre (Southampton), the University of Miami, RSMAS, and NOAA AOML. This joint effort is known as RAPID-MOC/MOCHA (www.noc.soton.ac.uk/rapidmoc/), where MOCHA stands for Meridional Circulation and Heat Flux Array.
4. Florida current transport, AOML, www.aoml.noaa.gov/phod/floridacurrent.
5. SeaWinds on QuikSCAT mission, http://winds.jpl.nasa.gov/missions/quikscat/index.cfm.
6. D. Rayner *et al.*, "RRS *Discovery* Cruises D277/D278, RAPID Mooring cruise report, February–March 2004," Southampton Oceanography Centre Cruise Report 53, Southampton, UK (2005).
7. S. A. Cunningham *et al.*, "RAPID Mooring cruise report, April–May 2005, RRS *Charles Darwin* Cruise CD170 and RV *Knorr* Cruise KN182-2, April–May 2005," National Oceanography Centre Southampton Cruise Report 2, Southampton, UK (2005).
8. J. Hirschi *et al.*, *Geophys. Res. Lett.* **30**, 1413 (2003).
9. J. Baehr, J. Hirschi, J.-O. Beismann, J. Marotzke, *J. Mar. Res.* **62**, 283 (2004).
10. T. Kanzow *et al.*, *Science* **317**, 938 (2007).
11. A. Ganachaud, *J. Atmos. Ocean. Technol.* **20**, 1641 (2003).
12. M. O. Baringer, J. C. Larsen, *Geophys. Res. Lett.* **28**, 3179 (2001).
13. L. M. Duncan, paper presented at the First RAPID Annual Science Meeting, 6 to 8 September 2004, University of Nottingham; www.noc.soton.ac.uk/rapid/sci/AnnualMeeting2004.php.
14. F. C. Fuglister, *Atlantic Ocean Atlas of Temperature and Salinity Profiles and Data from the International Geophysical Year of 1957–1958* (Woods Hole Oceanographic Institution, Woods Hole, MA, 1960).
15. D. Roemmich, C. Wunsch, *Deep-Sea Res.* **32**, 619 (1985).
16. H. L. Bryden *et al.*, *J. Clim.* **9**, 3162 (1996).
17. K. E. McTaggart, G. C. Johnson, C. I. Fleurant, M. O. Baringer, "CTD/O_2 measurements collected on a Climate and Global Change cruise along 24°N in the Atlantic Ocean (World Ocean Circulation Experiment Section A6) during January–February 1998" (NOAA Data Report ERL PMEL-68, U.S. Department of Commerce, NOAA, Environmental Research Laboratories, Seattle, WA, 1999).
18. S. A. Cunningham *et al.*, "A transatlantic hydrography section at 24.5°N: RRS *Discovery* Cruise D279, 04 April–10 May 2004," Southampton Oceanography Centre Cruise Report 54, Southampton, UK (2005).
19. J. C. Larsen, *Philos. Trans. R. Soc. London Ser. A* **A338**, 169 (1992).
20. W. Sturges, B. G. Hong, *J. Phys. Oceanogr.* **31**, 1304 (2001).
21. www.cdc.noaa.gov/cdc/data.ncep.reanalysis.derived.otherflux.html.
22. H. R. Longworth, thesis, University of Southampton (2007).
23. S. Rahmstorf, *Nature* **378**, 145 (1995).
24. J. M. Gregory *et al.*, *Geophys. Res. Lett.* **32**, L12703 (2005).
25. J. Baehr, K. Keller, J. Marotzke, *Clim. Change* 10.1007/s10584-006-9153-z (2007).

26. The authors would like to thank the captains and crews of the research vessels *Charles Darwin*, *Discovery*, *Ronald Brown*, and *Knorr*, and the UK National Marine Facilities-

Sea Systems mooring team. The mooring operations are funded by NERC and NSF. The Florida Current cable data are made freely available by the AOML (www.aoml.noaa.gov/phod/floridacurrent/) and are funded by the NOAA Office of Climate Observations. Wind stress data were obtained from the Centre for Satellite Exploitation and Research, at the Institut français de recherche pour l'exploitation de la mer, Plouzané, France.

Supporting Online Material
www.sciencemag.org/cgi/content/full/317/5840/935/DC1
SOM Text
Figs. S1 to S4
References

14 February 2007; accepted 12 July 2007
10.1126/science.1141304

Observed Flow Compensation Associated with the MOC at 26.5°N in the Atlantic

Torsten Kanzow,[1]* Stuart A. Cunningham,[1] Darren Rayner,[1] Joël J.-M. Hirschi,[1] William E. Johns,[2] Molly O. Baringer,[3] Harry L. Bryden,[1] Lisa M. Beal,[2] Christopher S. Meinen,[3] Jochem Marotzke[4]*

The Atlantic meridional overturning circulation (MOC), which provides one-quarter of the global meridional heat transport, is composed of a number of separate flow components. How changes in the strength of each of those components may affect that of the others has been unclear because of a lack of adequate data. We continuously observed the MOC at 26.5°N for 1 year using end-point measurements of density, bottom pressure, and ocean currents; cable measurements across the Straits of Florida; and wind stress. The different transport components largely compensate for each other, thus confirming the validity of our monitoring approach. The MOC varied over the period of observation by $\pm 5.7 \times 10^6$ cubic meters per second, with density-inferred and wind-driven transports contributing equally to it. We find evidence for depth-independent compensation for the wind-driven surface flow.

The Atlantic meridional overturning circulation (MOC) consists of a near-surface, warm northward flow, compensated for by a southward return flow at depth. Heat loss to the atmosphere makes the increasingly dense northward-flowing surface waters sink at high latitudes to feed the deep return flow (*1*). The vertical temperature contrast associated with this flow results in a northward heat transport of 1.3×10^{15} W at 24°N (*2*), which noticeably moderates the Northeast Atlantic climate (*3*, *4*).

Most of the observation-based estimates of Atlantic MOC strength are based on infrequently acquired zonal hydrographic sections. Because the frequency distribution of the MOC variability is unknown, long-term changes inferred from these snapshot sections (*5*) may not be representative. Basic MOC characteristics, such as magnitude and time scales of natural variability (*6*), response to local wind-stress forcing, or the relative importance of wind-stress and buoyancy forcing on subseasonal-to-decadal time scales (*7*, *8*), have not yet been observed. Our ability to detect future MOC changes depends on the accurate quantification of the MOC's spectral distribution and on understanding the physical processes involved.

We analyzed MOC variability on subseasonal time scales using a 1-year-long mooring-based volume-transport time series from March 2004 to March 2005, acquired in the framework of the rapid climate change/meridional overturning circulation and heat flux array (RAPID/MOCHA) experiment (*9*, *10*). To compute the MOC, the zonally integrated meridional flow across 26.5°N as a function of depth (z) was observed. The backbones of this effort are moorings that measure full water-column profiles of density and ocean-bottom pressure at the western and eastern endpoints of the basin interior (Fig. 1) and on both sides of the Mid-Atlantic Ridge (MAR) (fig. S2). The eastern-to-western boundary-density difference allows for the computation of the temporal evolution of the basin-wide integrated geostrophic-transport profile relative to 4820 dbar

[1]National Oceanography Centre, Empress Dock, Southampton, SO14 3ZH, UK. [2]Rosenstiel School of Marine and Atmospheric Science, 4600 Rickenbacker Causeway, Miami, FL 33149, USA. [3]National Oceanic and Atmospheric Administration Atlantic Oceanographic and Meteorological Laboratory, 4301 Rickenbacker Causeway, Miami, FL 33149, USA. [4]Max-Planck-Institut für Meteorologie, Bundesstraße 53, 20146 Hamburg, Germany.

*To whom correspondence should be addressed. E-mail: tok@noc.soton.ac.uk (T.K.); jochem.marotzke@zmaw.de (J.M.)

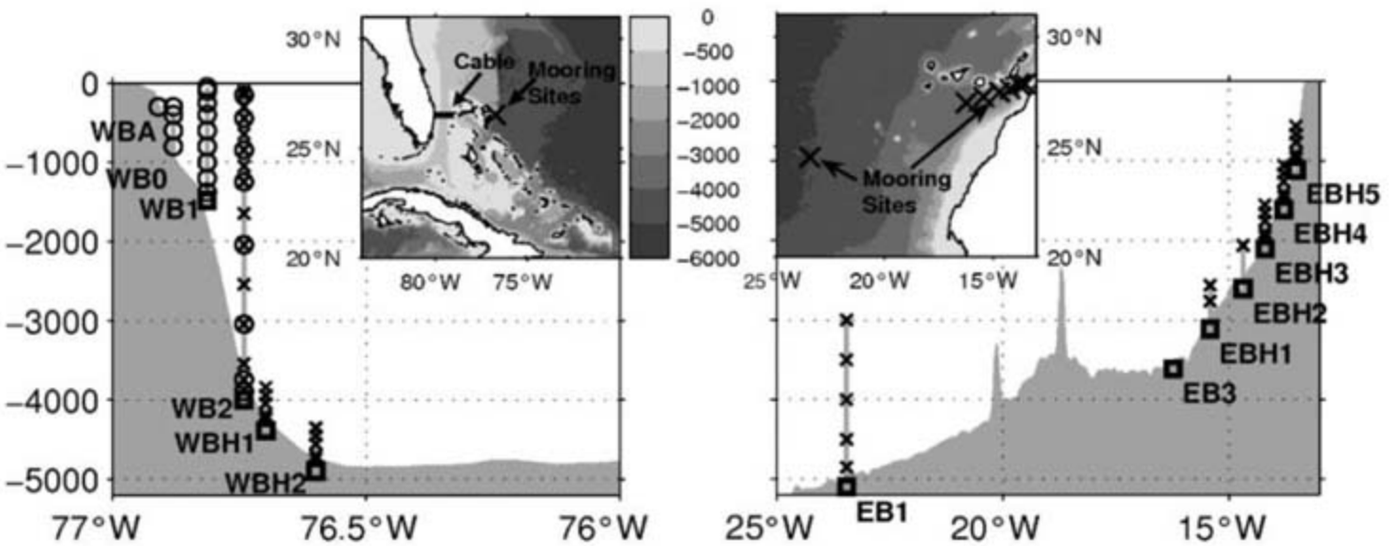

Fig. 1. Distribution of density (crosses) and bottom-pressure sensors (squares) of the RAPID/MOCHA moorings at the western and eastern boundaries of the subtropical North Atlantic near 26.5°N that are used for computing the zonally integrated meridional geostrophic flow. Direct current–meter measurements at the western boundary (circles) complement the observations in the upper part of the western-boundary continental slope. The location of the western- and eastern-boundary mooring sites and that of the Straits of Florida telephone cable can be seen in the insets. WBA, western boundary acoustic doppler current profiler; WBH, western boundary homer; EB, eastern boundary.

(*11*, *12*) [supporting online material (SOM)], referred to as internal transport (T_{INT}). We ignored the presence of the MAR in the calculations of the geostrophic flow; however, its effect is assessed crudely in the SOM. Zonal differences of bottom-pressure fluctuations between adjacent stations provide the temporally varying, zonally integrated reference-level contribution of the geostrophic flow (*11*, *12*) (SOM), referred to as external transport (T_{EXT}). The meridional-transport profile over the continental slope west of mooring western boundary 1 (WB1) (Fig. 1, left)—hereafter referred to as western-boundary wedge transports (T_{WBW})—was estimated from direct current–meter measurements (SOM). Gulf Stream transports through the Straits of Florida (T_{GS}) are monitored by National Oceanic and Atmospheric Administration (NOAA) submarine cable measurements (*13*) (SOM). The coast-to-coast integrated wind-driven Ekman transports (T_{EK}), confined to a thin layer at the sea surface, are derived from spaceborne scatterometry (*14*) (SOM).

The sum of T_{EXT} (geostrophic reference-level contribution), T_{INT} (relative geostrophic contribution), and T_{WBW} yields the geostrophic mid-ocean transport fluctuations (T_{MO}) integrated across the transatlantic section, relative to a time-invariant offset (*11*, *15*). Thus, when MOC variability is addressed, a time-variable flow adjustment is not required, in contrast to traditional hydrographic-section data analyses where mass conservation is imposed to derive absolute transports (*5*, *16*). This gives us two alternative approaches to compute MOC fluctuations from the transport per-unit-of-depth profiles: $T_{INT}(z) + T_{EXT}(z) + T_{WBW}(z) + T_{EK}(z) + T_{GS}(z)$ and the traditional $T_{INT}(z) + T_{WBW}(z) + T_{EK}(z) + T_{GS}(z)$ + mass-conservation constraint. Our observing system allows us to study: (i) the order of magnitude and time scales of MOC variability and (ii) how compensation of volume fluxes is distributed vertically and accomplished among the different transport components. As we show below, (ii) is a prerequisite for (i).

The fluctuations (time-mean–subtracted) of the vertically integrated profiles in Fig. 2A amounted to ±8.3, 12.6, 1.1, 4.4, and 3.3 Sv (*17*, *18*) for $\overline{T_{INT}}$, $\overline{T_{EXT}}$, $\overline{T_{WBW}}$, $\overline{T_{EK}}$, and $\overline{T_{GS}}$, respectively. (Overbars denote transport integrated vertically over the entire depth range.) Assuming that mass is conserved across a transatlantic section, one would expect the different transport contributions shown in Fig. 2A to compensate for each other. As a first indication, $\overline{T_{INT}}$ and $\overline{T_{EXT}}$ display negatively correlated fluctuations on monthly time scales. On the other hand, on daily to weekly time scales, none of the contributions can possibly compensate for the large variability seen in $\overline{T_{EXT}}$ (±8.0 Sv when applying a 10-day high-pass filter). Thus, in the high-frequency limit, zero net flow across the section is not a good approximation.

Because flow compensation for the different components occurs during periods longer than 10 days (fig. S1), we restricted the analysis to low frequencies by applying a 15-day low-pass filter to the transport components. After filtering, fluctuations amounted to ±7.4, 9.1, 1.0, 3.9, and 3.1 Sv for $\overline{T_{INT}}$, $\overline{T_{EXT}}$, $\overline{T_{WBW}}$, $\overline{T_{EK}}$, and $\overline{T_{GS}}$, respectively. We observed a maximum negative correlation of –0.83 between $\overline{T_{INT}}$ and $\overline{T_{EXT}}$ at zero time lag. It appears plausible that random boundary-density fluctuations affecting $\overline{T_{INT}}$, primarily caused by Rossby waves impinging onto the western boundary (*6*) or by boundary waves propagating southward, act to create a mass imbalance, whereas $\overline{T_{EXT}}$, being composed of depth-invariant motions (SOM), responds quickly to maintain mass balance. $\overline{T_{MO}}$ and the sum of $\overline{T_{EK}}$ and $\overline{T_{GS}}$ (referred to as western- and surface-boundary transport $\overline{T_{BOUND}}$) display a negative correlation of –0.74 (ignoring the period from September to October 2004 when $\overline{T_{GS}}$ was not measured) (Fig. 2B). The fact that $\overline{T_{MO}}$ and $\overline{T_{BOUND}}$ (being completely independent measurements) strongly compensate for each other demonstrates that our MOC observing strategy, using moorings at the section end points only to monitor $T_{MO}(z)$, is successful.

$\overline{T_{GS}}$ and $\overline{T_{EK}}$ are essentially uncorrelated (–0.04). However, compensation for both in equal shares is provided by $\overline{T_{MO}}$, with each showing a similar amount of negative correlation to $\overline{T_{MO}}$ (–0.47 for $\overline{T_{GS}}$ and –0.55 for $\overline{T_{EK}}$). $\overline{T_{EK}}$ displays a weak but significant negative correlation (*19*) to $\overline{T_{EXT}}$ (–0.32) and an insignificant correlation to $\overline{T_{INT}}$ (0.05). Thus, compensation for $\overline{T_{EK}}$ variability is primarily provided by $\overline{T_{EXT}}$. Because the 2-month gap in $\overline{T_{BOUND}}$ would have limited our analysis to 10 months, we filled the gap (Fig. 2B) by means of a linear regression between $\overline{T_{MO}}$ and $\overline{T_{BOUND}}$ (SOM).

There is a mass imbalance in the unconstrained total transport, defined as $\overline{T_{MO}} + \overline{T_{BOUND}}$ (Fig. 2B), although it amounts to only ±3.4 Sv, compared to ±4.9 Sv for T_{BOUND} (leaving out the period from September to October). Uncertainties of the five measurement components yielding ±2.7 Sv (SOM) account for a substantial part of the imbalance. The remaining ±2.1 Sv ($\sqrt{3.4^2 - 2.7^2}$ Sv) of the imbalance may arise from deficiencies, such as the flow below 4820 dbar not being included in $T_{MO}(z)$ and the role of the MAR in possibly upsetting the balance between the coast-to-coast integrated meridional flow and the coast-to-coast pressure gradient not being assessed. Observed transport fluctuations through the Bering Strait (*20*) suggest that an imbalance of ±0.66 Sv across 26.5°N on intraannual time scales may exist.

We inferred MOC-transport variability from the vertical distribution of meridional-transport

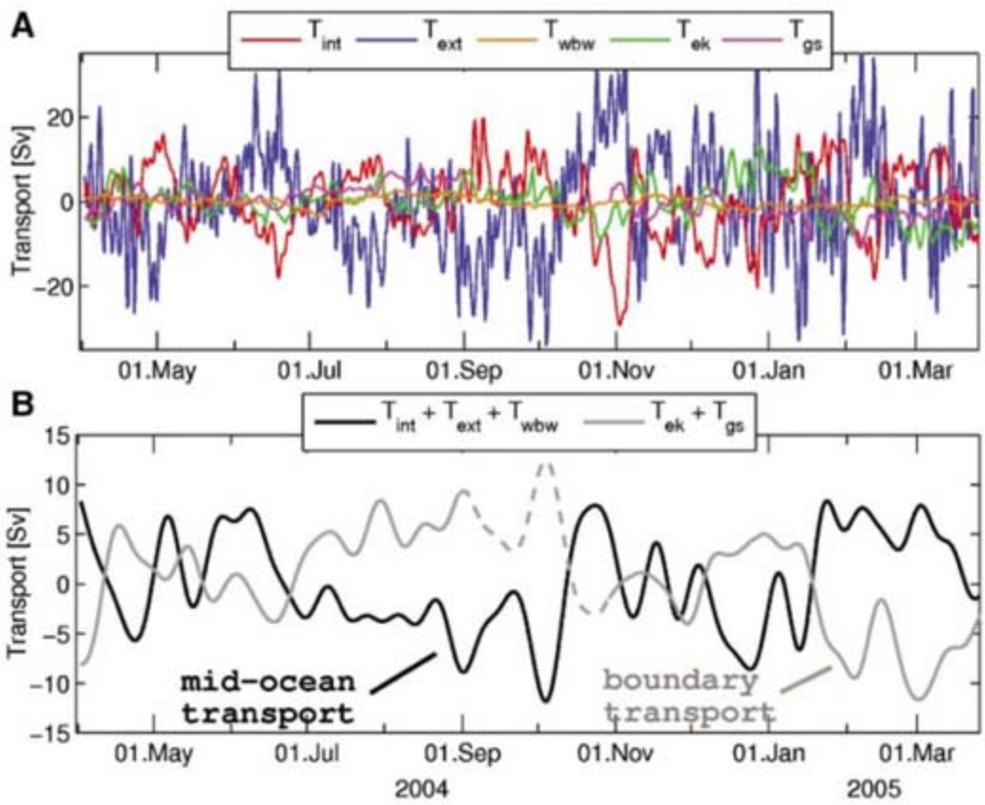

Fig. 2. (**A**) Fluctuations of $\overline{T_{INT}}$, red; $\overline{T_{EXT}}$, blue; $\overline{T_{WBW}}$, orange; $\overline{T_{EK}}$, green; and $\overline{T_{GS}}$, magenta (table S2). There is a 2-month gap in $\overline{T_{GS}}$ between 31 August and 29 September 2004. All time series were 2-day low-pass filtered and subsampled on a half-daily grid. The initial sampling rates were 15 min for the underlying density and current measurements and 10 min for the bottom pressure. (**B**) Fifteen-day low-pass–filtered fluctuations of vertically integrated mid-ocean ($\overline{T_{MO}} = \overline{T_{INT}} + \overline{T_{EXT}} + \overline{T_{WBW}}$) and boundary transports ($\overline{T_{BOUND}} = \overline{T_{EK}} + \overline{T_{GS}}$) as black and gray lines, respectively. The dashed part of the gray line denotes the period when $\overline{T_{GS}}$ could not be measured. A linear regression between $\overline{T_{MO}}$ and $\overline{T_{BOUND}}$ was used to fill this gap (SOM).

fluctuations. Over the 12-month period, the cumulative unconstrained total transport fluctuations (integrated upward from 4820 dbar toward the sea surface) show fluctuations of ±3.9 Sv at 3600 dbar, have their peak value of ±5.7 Sv at 1040 dbar and reduce to ±3.0 Sv at the sea surface (Fig. 3). Given that we observed the maximum value near 1000 dbar, the transports integrated between 1000 and 4820 dbar will be referred to as MOC transports, following the traditional view that the MOC represents a two-layer flow. The small change in the cumulative transports at mid-depths (between 3600 and 1000 dbar) suggests that the MOC variability is dominated by near-bottom and upper-ocean contributions.

We computed the MOC variability using the traditional approach to infer MOC transports from hydrographic-section data (*5*, *16*). Instead of using $T_{EXT}(z)$, we imposed an across-section zero-net-flow constraint at each time step by adding a depth-independent compensation. This allowed us (i) to estimate the relative importance of the density-inferred and locally wind-stress–driven contributions and (ii) to test the reliability of the traditional method by comparing it to the above unconstrained MOC estimate. To isolate the geostrophic contribution to the MOC, we assumed $T_{EK}(z)$ to be time-invariant. Thus, we constrained the vertical integral of $T_{INT}(z) + T_{WBW}(z) + T_{GS}(z)$ to be zero at each time step (Fig. 3, light blue line) and referred to it as constrained total geostrophic transport, assuming $T_{WBW}(z)$ and $T_{GS}(z)$ to be largely in geostrophic balance. This MOC-transport contribution neglecting $T_{EK}(z)$ varies by ±4.1 Sv, peaking at 1160 dbar.

The constrained total transport [zero-net-flow constraint imposed on $T_{INT}(z) + T_{WBW}(z) + T_{EK}(z) + T_{GS}(z)$] displays an Ekman-induced strong increase in near-surface variability (Fig. 3, orange line) with a maximum value of ±4.8 Sv at 920 dbar. This amplitude and the gradual increase below the Ekman layer are similar to the unconstrained total transport. However, with only ±2.3 Sv at 3600 dbar, the cumulative constrained total transport shows a nearly uniform (rather than depth-intensified) increase between the bottom and the depth of maximum variability, as compared with the unconstrained transport. The fact that the peak-level amplitude of the constrained total flow is slightly less than that of the unconstrained total flow can partly be explained by having considered only the baroclinic flow between WB1 and WB2 in the constrained solution to simulate the traditional approach of inferring MOC transports (SOM).

For each of the cases, MOC-transport time series are computed (Fig. 4). The unconstrained MOC fluctuations (Fig. 4, black line) cover a range of 28.3 Sv. For the constrained total geostrophic (Fig. 4, light blue line) and total (Fig. 4, orange line) MOC contributions, the ranges are 21.8 and 24.7 Sv, respectively. The correlations between the unconstrained total MOC transport and the constrained total geostrophic and total MOC transport yield 0.60 and 0.82, respectively. Not only do the overall magnitudes of the unconstrained and constrained total transport variability agree (Fig. 4, black and orange lines), but their temporal evolutions are similar, too. Thus, deriving MOC variability from constrained flows [computed from continuous observations of $T_{INT}(z)$, $T_{WBW}(z)$, $T_{EK}(z)$, and $T_{GS}(z)$] appears to be a reliable technique for periods longer than 15 days. Also, as noted earlier, $\overline{T_{EXT}}$ shows a weak negative correlation to $\overline{T_{EK}}$. When including $T_{EK}(z)$ into the constrained solution [which excludes $T_{EXT}(z)$], the correlation between the resulting MOC transport and that from the unconstrained solution [which uses $T_{EXT}(z)$] increases. We therefore conclude that the depth-independent compensation for $T_{EK}(z)$ is partly contained in $\overline{T_{EXT}}$ (*7*).

In conclusion, the section-wide integrated $T_{MO}(z)$ and $T_{BOUND}(z)$ largely compensate for each other. This is strong evidence that the end-point mooring approach to continuously monitor the MOC is valid. A net flow imbalance of ±3.4 Sv remains, which is mainly attributable to measurement errors of ±2.7 Sv. However, a time-variable transport imbalance of ±0.66 Sv may actually exist, associated with Bering Strait throughflow (*20*). The measurement uncertainty in MOC fluctuations should amount to only ±2.0 Sv and consequently be smaller than the top-to-bottom integrated ±3.4-Sv imbalance, because only the flow deeper than 1000 dbar needs to be considered (SOM).

During periods shorter than 10 days, fluctuations of ±8.0 Sv in $\overline{T_{EXT}}$ remain uncompensated for. Recent evidence from $\overline{T_{EXT}}$ observed in an experiment at 16°N indicates that the high-frequency fluctuations exhibit spatial correlation scales of more than 1000 km (*21*). For the high-frequency flow to be unbalanced would require the average water-column height of the North Atlantic to fluctuate coherently by ±2 to 3 cm during periods <10 days for which indications have been found (*22*, *23*).

At 26.5°N, much of the observed compensation of the (zonally integrated) flows is expected to take place close to the western boundary (*24*); however, this may not hold at other latitudes (*11*, *25*).

Both the unconstrained and constrained total transports display maximum cumulative variability (from the bottom up to 1000 dbar) of ±5.7 and ±4.8 Sv, respectively, with the former showing near-bottom intensified variability resulting from zonally non-uniform contributions in $T_{EXT}(z)$ over variable topography (which the

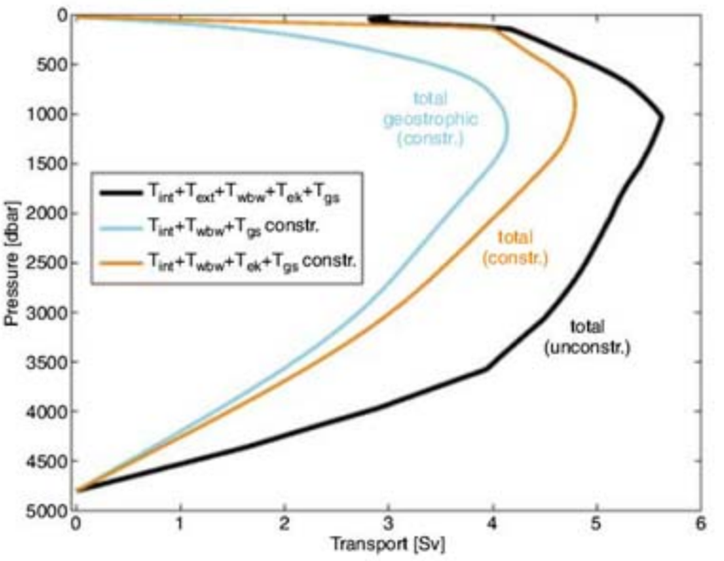

Fig. 3. Standard deviation of cumulative-transport fluctuations integrated upward from 4820 dbar. The black line shows the cumulative total unconstrained transports [$T_{INT}(z) + T_{EXT}(z) + T_{WBW}(z) + T_{EK}(z) + T_{GS}(z)$]. For the remaining two curves, a constraint of zero net flow across the 26.5°N section was imposed at each time step. The cumulative constrained total geostrophic [$T_{INT}(z) + T_{WBW}(z) + T_{GS}(z)$] and constrained total [$T_{INT}(z) + T_{WBW}(z) + T_{EK}(z) + T_{GS}(z)$] transport fluctuations are displayed as light blue and orange lines, respectively (table S3). All time series were 15-day low-pass filtered.

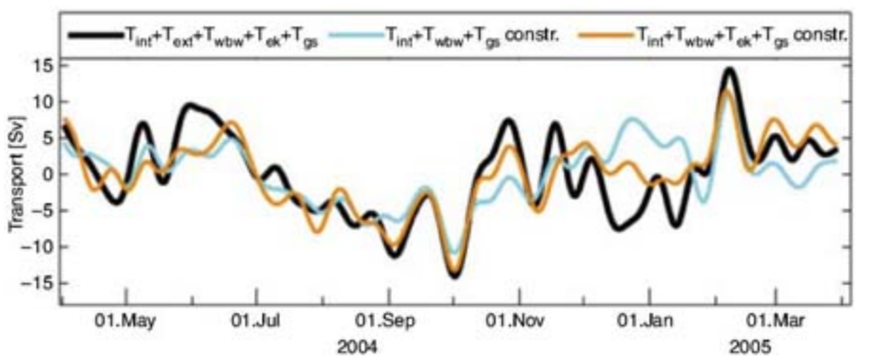

Fig. 4. MOC-transport fluctuations: cumulative-transport variability at 1000 dbar (integrated upward from 4820 dbar) for the three different cases displayed in Fig. 3.

constrained MOC transport does not account for). The presence of the MAR has not been accounted for in our calculations. Including moored-density and bottom-pressure measurements on both flanks of the MAR allows for the computation of $T_{MO}(z)$ below the MAR crest independently for the western and eastern basin (fig. S2). However, the effect of this on the temporal evolution of unconstrained MOC time series is rather small (fig. S3), with the difference between calculations taking into account and neglecting the measurements on the MAR flanks varying by ±1.1 Sv (SOM).

Fluctuations in $\overline{T_{EK}}$ of ±3.9 Sv do not dominate MOC variability on subseasonal time scales at 26.5°N. Rather, we observe an equal share of variability between Ekman and density contributions, with the constrained total geostrophic MOC solution (excluding $\overline{T_{EK}}$) displaying ±4.1 Sv. We have presented evidence that the depth-independent compensation for $\overline{T_{EK}}$ is partly contained in $\overline{T_{EXT}}$. We have demonstrated the validity of our MOC-observing approach and described previously unobserved basic characteristics of the MOC variability near 26.5°N in the Atlantic after 1 year of continuous observations.

References and Notes

1. R. Dickson, J. Brown, *J. Geophys. Res.* **99**, 12319 (1994).
2. A. Ganachaud, C. Wunsch, *J. Clim.* **16**, 696 (2003).
3. M. Vellinga, R. A. Wood, *Clim. Change* **54**, 251 (2002).
4. S. Rahmstorf, *Nature* **421**, 699 (2003).
5. H. L. Bryden, H. R. Longworth, S. A. Cunningham, *Nature* **438**, 655 (2005).
6. J. J.-M. Hirschi, P. D. Killworth, J. R. Blundell, *J. Phys. Oceanogr.* **37**, 1246 (2007).
7. S. R. Jayne, J. Marotzke, *Rev. Geophys.* **39**, 385 (2001).
8. B. W. Dong, R. T. Sutton, *Geophys. Res. Lett.* **28**, 2445 (2001).
9. J. Marotzke, S. A. Cunningham, H. L. Bryden, *Monitoring the Atlantic Meridional Overturning Circulation at 26.5°N* (Southampton Oceanography Centre, Southampton, UK, 2002).
10. S. A. Cunningham, *RRS Discovery Cruise 277/278* (Report No. 53, National Oceanography Centre, Southampton, UK, 2004).
11. T. Kanzow, U. Send, W. Zenk, A. D. Chave, M. Rhein, *Deep-Sea Res. I* **53**, 528 (2006).
12. W. E. Johns, T. Kanzow, R. Zantopp, *Deep-Sea Res. I* **52**, 1542 (2005).
13. J. C. Larsen, T. B. Sanford, *Science* **227**, 302 (1985).
14. J. Graf *et al.*, *Acta Astronaut.* **43**, 397 (1998).
15. T. Whitworth III, *J. Phys. Oceanogr.* **13**, 2045 (1983).
16. S. A. Cunningham *et al.*, *Science* **317**, 935 (2007).
17. Estimates of variability and uncertainty refer to 1 SD.
18. 1 Sv = 10^6 m^3 s^{-1}.
19. Statistical significance is stated at a 5% error probability.
20. A. T. Roach *et al.*, *J. Geophys. Res.* **100**, 18443 (1995).
21. T. Kanzow *et al.*, *J. Geophys. Res.* **110**, C09001 (2005).
22. M. Hirose, I. Fukumori, R. M. Ponte, *Geophys. Res. Lett.* **28**, 2441 (2001).
23. W. Brown, W. Munk, F. Snodgrass, H. Mofjeld, B. Zetler, *J. Phys. Oceanogr.* **5**, 75 (1975).
24. C. S. Meinen, M. O. Baringer, S. L. Garzoli, *Geophys. Res. Lett.* **33**, L17610 (2006).
25. C. S. Meinen, *Deep-Sea Res. I* **48**, 1553 (2001).

26. We thank the captains and crews of the research vessels *Charles Darwin*, *Discovery*, *Ronald Brown*, and *Knorr* and the National Marine Facilities Sea Systems mooring team. The mooring operations have been funded by the Natural Environment Research Council, RAPID, and NSF. The Florida Current cable data are made freely available by the Atlantic Oceanographic and Meteorological Laboratory (www.aoml.noaa.gov/phod/floridacurrent/) and are funded by the NOAA Office of Climate Observations. The wind-stress data were obtained from Centre ERS d'Arquivage et de Traitment the Institut Français de Recherche pour l'Exploration de la Mer in Plouzané, France.

Supporting Online Material

www.sciencemag.org/cgi/content/full/317/5840/938/DC1
Materials and Methods
SOM Text
Figs. S1 to S3
Tables S1 to S3
References

14 February 2007; accepted 12 July 2007
10.1126/science.1141293

Reduced Egg Investment Can Conceal Helper Effects in Cooperatively Breeding Birds

A. F. Russell,[1,2]*† N. E. Langmore,[3] A. Cockburn,[3,4] L. B. Astheimer,[5] R. M. Kilner[6]*

Cooperative breeding systems are characterized by nonbreeding helpers that assist breeders in offspring care. However, the benefits to offspring of being fed by parents and helpers in cooperatively breeding birds can be difficult to detect. We offer experimental evidence that helper effects can be obscured by an undocumented maternal tactic. In superb fairy-wrens (*Malurus cyaneus*), mothers breeding in the presence of helpers lay smaller eggs of lower nutritional content that produce lighter chicks, as compared with those laying eggs in the absence of helpers. Helpers compensate fully for such reductions in investment and allow mothers to benefit through increased survival to the next breeding season. We suggest that failure to consider maternal egg-investment strategies can lead to underestimation of the force of selection acting on helping in avian cooperative breeders.

In cooperative breeding systems, offspring receive food from helpers in addition to their parents. Although parents can reduce the rate at which they feed their offspring in the presence of helpers, this reduction is usually incomplete, and so offspring receive more food when helpers are present than when they are absent (*1*). Given that offspring receive more food when also provisioned by helpers, it is currently unclear why many long-term studies have failed to detect helper effects on offspring growth and survival (*2*) or have detected only weak effects (*3*). This failure to document the benefits to offspring has prompted hypotheses proposing that helping behavior is an unselected consequence of physiological priming to provide care to begging offspring (*4*), is contingent on future reciprocity (*5*), or is a form of "rent payment" (*6*). These alternatives are problematic because helping has been shown to be costly (*7*) and strategically directed to maximize benefits (*3*, *8*), cooperative breeding based on direct reciprocity is inherently unstable (*9*), and rent payment occurs under conditions that will be seldom met (*10*).

In cooperative breeding systems, securing and maintaining a breeding position is particularly challenging but offers substantial fitness benefits (*11*). Consequently, breeders might be expected to be under strong selection to reduce their investment in each reproductive attempt in order to increase the number of attempts that they can have in a lifetime. For example, one of the most commonly reported helper effects in avian cooperative breeding systems is load lightening, where breeding females reduce offspring provisioning with increasing helper numbers (*1*). Load lightening could also occur at the egg stage (*12*). However, despite growing evidence from noncooperative species that female birds can adaptively manipulate investment within eggs (*13*), this possibility has not been explored in cooperatively breeding species. Furthermore, hypotheses regarding such adaptive maternal egg investment typically predict that mothers should increase their level of within-egg investment when breeding in favorable conditions (*14*, *15*). Yet it is also theoretically plausible that mothers breeding in privileged circumstances (in this case, with the benefit of helpers) might also benefit from reductions in egg investment, if the future fitness payoffs from doing so exceed the current fitness payoffs from increasing egg investment. If mothers reduce their investment in eggs when breeding in the presence of helpers, then any benefit that helpers might have on offspring condition and survival will be masked.

[1]Department of Animal and Plant Sciences, University of Sheffield, Sheffield S10 2TN, UK. [2]Centre for the Integrative Study of Animal Behaviour, Macquarie University, Sydney NSW 2109, Australia. [3]School of Botany and Zoology, Australian National University, Canberra ACT 0200, Australia. [4]Percy Fitzpatrick Institute of African Ornithology, Department of Science and Technology/National Research Foundation Centre of Excellence, University of Cape Town, Rondebosch 7701, South Africa. [5]School of Health Sciences, University of Wollongong, Wollongong New South Wales 2522, Australia. [6]Department of Zoology, University of Cambridge, Cambridge CB2 3EJ, UK.

*These authors contributed equally to this work.
†To whom correspondence should be addressed. E-mail: a.f.russell@sheffield.ac.uk

We tested (i) whether helper presence is associated with reductions in maternal investment at the egg stage, (ii) whether these reductions confound estimates of helper contributions to nestling mass, and (iii) whether maternal reductions are adaptive. We investigated these questions in the cooperatively breeding superb fairy-wren *Malurus cyaneus*, a passerine bird endemic to southeastern Australia, whose social mating system comprises both breeding pairs and cooperatively breeding groups (*16*). Previous work on this species has shown that nestlings receive more food in the presence of helpers (*17*), but despite this pattern, helpers have no effect on the mass or survival of chicks (*18*). The same was true in our study population (*16*). Chicks that were provisioned by a breeding pair with helpers received 19% more food than did those that were tended by an unassisted breeding pair (Fig. 1A). Nevertheless, chicks reared by groups were of similar mass to those reared by pairs alone (Fig. 1B). There were no obvious differences in prey loads or species fed to chicks in pairs and groups (*19*).

Consequently, we investigated whether mothers reduced their investment in eggs when breeding in groups. Clutch size and mean egg volumes were uncorrelated [linear mixed-effect model (LME) controlling for repeated measures within territories: $\chi_1^2 = 0.01$, $P = 0.91$, $N = 68$ clutches], and clutches were similar in size in both groups and pairs [LME, $\chi_1^2 = 0.29$, $P = 0.59$, $N = 68$ clutches]. In contrast, mothers breeding in groups laid eggs that were 5.3% smaller than eggs from those breeding in pairs (*16*) (Fig. 2A). Eggs laid by females in groups were also of lower nutritional content than those laid by females in pairs (*16*). Helpers were associated with a 14% reduction in the wet mass of yolks (Fig. 2B) and a 9% reduction in the dry mass of yolks (Fig. 2C), indicating that the reduction in egg volume was not simply due to reductions in albumen or water content. Furthermore, the dried yolks of eggs laid by females in groups had 12% less lipid and 13% less protein than did those laid by females breeding in pairs (Fig. 2D), suggesting that mothers invest less energy in their eggs when breeding in the presence of helpers.

Further analysis of our observational data suggests that this reduced maternal investment at the egg stage conceals helper effects on chick growth (*16*). First, small eggs gave rise to small chicks (measured 6 to 8 days after hatching) (Fig. 3A). Second, after controlling for the differences in egg volumes between groups and pairs (Fig. 2A), we found that helpers had a significant positive effect on chick mass (Fig. 3B). The magnitude of this latter helper effect equates to an 18% increase in chick mass, suggestively close to the 19% increase in food that chicks received when provisioned by helpers (Fig. 1A).

To test fully the possibility that reduced maternal investment obscures helper effects, we conducted a cross-fostering experiment involving permanent reciprocal translocation of complete clutches between females before hatching (*16*). There were two experimental treatments: (i) one in which clutches were moved from nests of pairs to nests attended by groups and vice versa (experimental treatment) and (ii) one in which clutches were swapped between nests attended by the same number of adults (control treatment). First, if mothers reduce their egg investment in the presence of helpers, we would predict that chicks from eggs laid in groups and reared in pairs (grp-pr, Fig. 3C) would be significantly lighter than either control chicks or those laid in pairs and reared in groups (pr-grp, Fig. 3C). In support of this prediction, chicks arising from eggs that were laid in groups and reared in pairs were significantly lighter than those from the other two treatments (Fig. 3C). Second, our cross-fostering experiment also confirmed that maternal reductions in egg investment wholly conceal helper effects. We found that the mean mass of nestlings in the foster territory declined as the number of males in the natal territory increased (prenatal-effect size = −0.54 ± 0.18) (Fig. 3D). However, this negative effect was completely offset by the positive influence of the provisioning rate of foster males (postnatal-effect size = 0.36 ± 0.15) (Fig. 3E), which was itself significantly influenced by the number of foster males contributing (Fig. 3F). Taken together, these results confirm that provisioning frequency is a reliable indicator of chick caloric intake and that the benefits to chicks of receiving food from helpers are concealed by reductions in egg investment by females with helpers.

Given that, in other cooperative breeding systems, offspring of low mass are shown to have reduced chances of recruitment (*20*) and low future reproductive success (*21*), why do females breeding in the presence of helpers lay eggs that yield suboptimal offspring? We know that the durations of incubation and chick rearing are inflexible in superb fairy-wrens and so are uninfluenced by helper presence (*16*, *18*). One possibility is that mothers are constrained from optimal allocation of resources into eggs because of competition with helpers for food in their territory. Alternatively, females breeding in groups might exploit helper contributions to nestling mass by reducing their own investment in reproduction to save resources for future breeding attempts. The latter explanation is more strongly supported by our evidence.

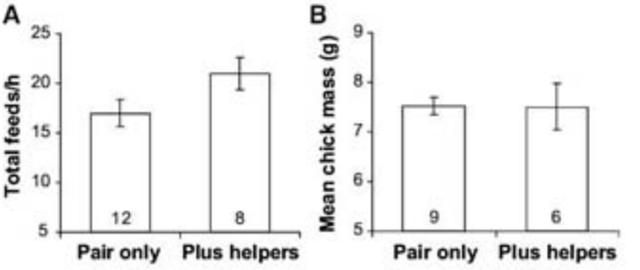

Fig. 1. Relation between helper presence and (**A**) chick provisioning rates or (**B**) chick mass. (A) Helpers had a positive effect on the rate at which chicks were provisioned [general linear model (GLM), $F_{1,18} = 5.82$, $P = 0.027$, $r^2 = 10\%$]. (B) Helpers had no effect on chick mass (GLM, $F_{1,14} = 0.00$, $P = 0.97$). Brood size was fitted as a covariate in (A), as was tarsus length in (B). The predicted means ± SEM (error bars) are shown. The values in each bar are the numbers of independent breeding units.

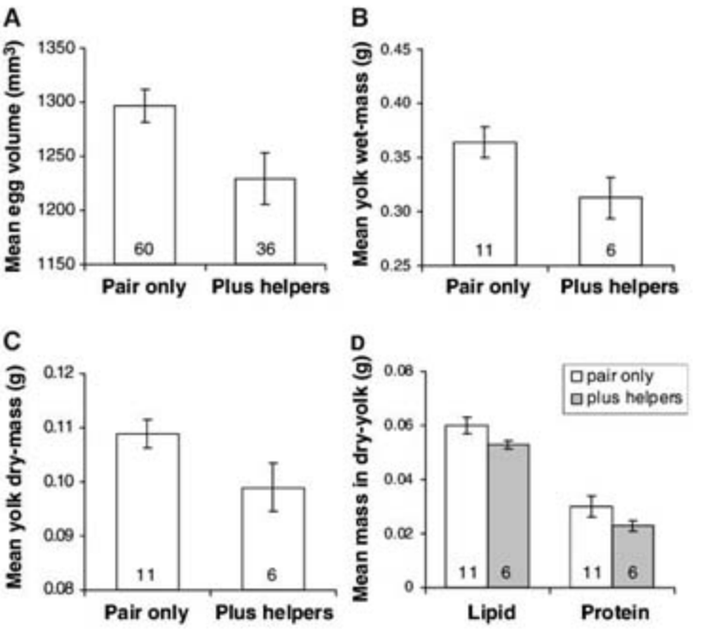

Fig. 2. Relation between helper presence and (**A**) egg volume or (**B** to **D**) egg composition. In the presence of helpers, mothers laid eggs that (A) were smaller [LME, $\chi_1^2 = 5.62$, $P = 0.018$], (B) had a reduced wet mass of yolk (GLM, $F_{1,14} = 5.24$, $P = 0.039$, $r^2 = 14\%$), (C) had a reduced dry mass of yolk (GLM, $F_{1,15} = 5.26$, $P = 0.037$, $r^2 = 21\%$), or (D) had reduced masses of lipid (GLM, $F_{1,14} = 5.92$, $P = 0.029$, $r^2 = 21\%$) and protein (GLM, $F_{1,14} = 5.79$, $P = 0.031$, $r^2 = 19\%$). The territory identity (ID) was fitted as a random factor (1 to 4 clutches per territory), the year was fitted as a covariate in (A), and the lay date was fitted as a covariate in (A) to (D). The predicted means ± SEM (error bars) are shown. The values in each bar are the numbers of independent breeding units.

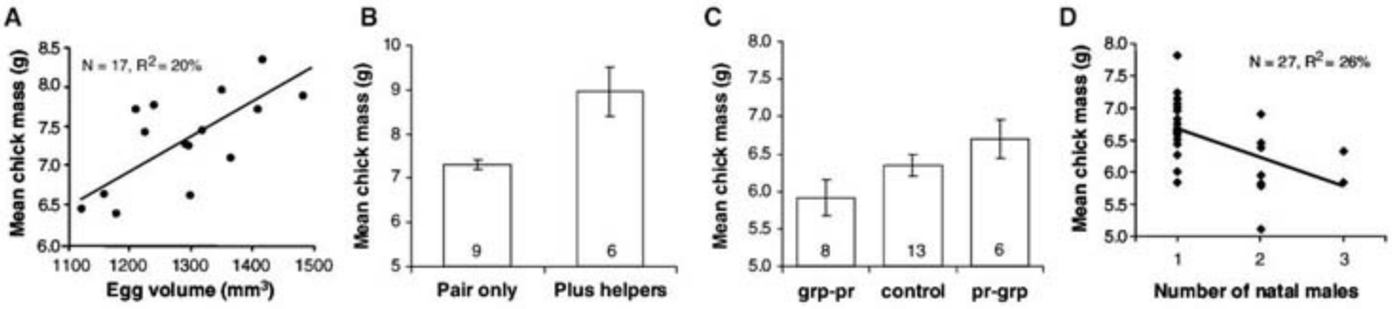

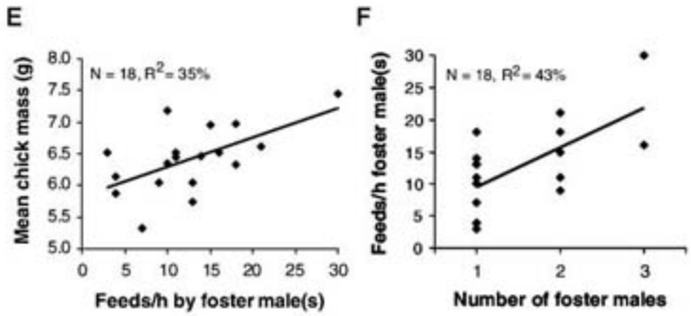

Fig. 3. Correlational and experimental evidence for maternal and helper effects on nestling mass (**A** to **E**) and male-number effects on overall male provisioning rates (**F**). (A) Chick mass increased with egg volume (GLM, $F_{1,14} = 15.86$, $P = 0.003$, $r^2 = 20\%$). $N = 17$ broods. (B) After controlling for differences in egg volume, chick mass was influenced positively by helper presence (GLM, $F_{1,14} = 7.66$, $P = 0.020$, $r^2 = 9\%$). (C) Chick mass varied between treatments (GLM, $F_{2,24} = 3.95$, $P = 0.033$, $r^2 = 19\%$). grp-pr, eggs laid in groups and reared in pairs; pr-grp, eggs laid in pairs and reared in groups. (D) The mass of foster chicks declined with the number of males in their natal territory (GLM, $F_{1,24} = 9.15$, $P = 0.006$, $r^2 = 15\%$). $N = 27$ nests. (E) Chick mass increased with the provisioning rate of males in their foster territory (GLM, $F_{1,14} = 5.59$, $P = 0.033$, $r^2 = 10\%$). $N = 18$ nests. (F) The rate at which chicks received food from foster males increased with the number of foster males (regression, $F_{1,16} = 12.28$, $P = 0.003$, $r^2 = 40\%$). $N = 18$ nests. The tarsus length [(A) and (C to E)], lay-date (A), mean egg volume (B), and number of males in the natal territory (E) were fitted as covariates. The predicted means ± SEM (error bars) are shown. The scatter plots show the predicted values, and the values in each bar in (B) and (C) are the numbers of independent breeding units.

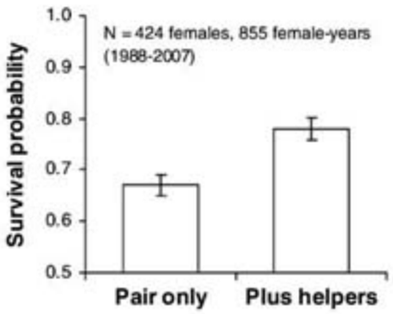

Fig. 4. Relation between helper presence and female survival probability. Females had an increased probability of survival to the following breeding season when they bred in the presence of helpers [GLMM, $\chi_1^2 = 12.13$, $P < 0.001$]. Age and spring rainfall were fitted as covariates, and maternal identity was fitted as a random factor. The predicted means ± SEM (error bars) are shown.

First, females presented with experimentally enlarged broods increased their provisioning frequency to a similar extent irrespective of whether they were in groups or pairs (*16*), indicating that extra group members do not constrain females from increasing investment. Second, analysis of data from the 19-year study of an unmanipulated neighboring population (*16*) revealed that when females bred in the presence of helpers, they had a 22% hazard or mortality until the following year, but when they bred in the absence of helpers, this risk increased to 33%. Helpers are therefore associated with a 30% reduction in mortality risk for mothers (Fig. 4). Relations between helper numbers and adult survival could be spurious, because territories that promote survival are likely to accumulate philopatric helpers (*1*, *2*). However, we found no evidence that breeding males survive better in the presence of helpers [generalized linear mixed model (GLMM), $\chi_1^2 = 0.02$, $P = 0.89$], suggesting that the effect of helpers on females is causal and operates, in part, through a path primarily accessible to females—in this case, strategic reductions in egg investment.

We have shown that in superb fairy-wrens, mothers reduce egg investment when breeding in the presence of helpers and that the subsequent undernourishment of the young at hatching wholly conceals the positive effect of helper contributions to nestling mass. The critical factor that will select for maternal reductions in egg investment in a cooperative bird is a predictable workforce to assist in provisioning young, for this will allow females to make informed decisions at the egg-laying stage concerning how much food their chicks will receive after hatching (*22*). This is true of most cooperative birds: The number of helpers present from the onset of egg laying accurately reflects the number of helpers available to feed the offspring after hatching (*23*). We therefore predict that load lightening of maternal investment at the egg stage will be a general phenomenon in cooperative birds, as is the case with maternal load lightening at the chick-provisioning stage (*1*, *2*). We conclude that all studies conducted on species in which helper numbers are predictable from the onset of breeding have the potential to underestimate the contributions made by helpers to nestling condition and/or maternal survival. Such studies will overlook the significant benefits that helpers stand to gain from breeding cooperatively through kin selection if helpers are related to breeders (*24*) or group augmentation if they are not (*25*).

References and Notes

1. B. J. Hatchwell, *Am. Nat.* **154**, 205 (1999).
2. A. Cockburn, *Annu. Rev. Ecol. Syst.* **29**, 141 (1998).
3. A. S. Griffin, S. A. West, *Science* **302**, 634 (2003).
4. I. G. Jamieson, *Am. Nat.* **133**, 394 (1989).
5. J. D. Ligon, S. H. Ligon, *Nature* **276**, 496 (1978).
6. A. J. Gaston, *Am. Nat.* **112**, 1091 (1978).
7. A. F. Russell, L. L. Sharpe, P. N. M. Brotherton, T. H. Clutton-Brock, *Proc. Natl. Acad. Sci. U.S.A.* **100**, 3333 (2003).
8. A. F. Russell, B. J. Hatchwell, *Proc. R. Soc. London B. Biol. Sci.* **268**, 2169 (2001).
9. T. Clutton-Brock, *Science* **296**, 69 (2002).
10. H. Kokko, R. A. Johnstone, J. Wright, *Behav. Ecol.* **13**, 291 (2002).
11. T. H. Clutton-Brock *et al.*, *Nature* **444**, 1065 (2006).
12. Load lightening describes lower overall levels of investment in the presence of helpers. Mothers may increase clutch size in the presence of helpers (*26*) and to do so may reduce the size of each egg, but this is not load lightening because increases in clutch size will usually be associated with increases (not decreases) in maternal investment.
13. T. D. Williams, *Biol. Rev.* **69**, 35 (1994).
14. N. Burley, *Am. Nat.* **132**, 611 (1988).
15. E. J. A. Cunningham, A. F. Russell, *Nature* **404**, 74 (2000).
16. Materials and methods are available on *Science* Online.
17. P. O. Dunn, A. Cockburn, *Evolution* **50**, 2542 (1996).
18. P. O. Dunn, A. Cockburn, R. A. Mulder, *Proc. R. Soc. London B. Biol. Sci.* **259**, 339 (1995).
19. N. A. MacGregor, A. Cockburn, *Anim. Behav.* **63**, 923 (2002).
20. B. J. Hatchwell *et al.*, *Behav. Ecol.* **15**, 1 (2004).
21. A. F. Russell, A. J. Young, G. Spong, N. R. Jordan, T. H. Clutton-Brock, *Proc. R. Soc. London B. Biol. Sci.* **274**, 513 (2007).
22. Experimental removal of helpers in superb fairy-wrens close to the onset of egg laying causes females to abandon their attempt (*17*), consistent with the prediction that females use helper presence as a cue for egg investment.
23. P. B. Stacey, W. D. Koenig, Eds., *Cooperative Breeding in Birds: Long-Term Studies of Ecology and Behavior* (Cambridge Univ. Press, Cambridge, 1990).
24. W. D. Hamilton, *J. Theor. Biol.* **7**, 1 (1964).
25. H. Kokko, R. A. Johnstone, T. H. Clutton-Brock, *Proc. R. Soc. London B. Biol. Sci.* **268**, 187 (2001).
26. J. Wright, *J. Avian Biol.* **29**, 105 (1998).

27. We thank Environment Australian Capital Territory and the director of the Australian National Botanic Gardens for permission to work at Campbell Park and the Botanic Gardens, respectively; A. Guy for help with egg assays; J. Gardner, G. Maurer, M. Double, H. Osmond, and D. Green for help with field work; and E. Cunningham, R. Heinsohn, and J. Wright for their valuable comments. This work was funded by grants from the Royal Society University Research Fellowship scheme (A.F.R. and R.M.K.), the Australian Research Council (N.E.L., A.C., L.B.A., and R.M.K.), and The Leverhulme Trust (N.E.L. and R.M.K.). Ethics approval was given by Australian National University Animal Experimentation Ethics Committee under protocol F.BTZ.61.03.

Supporting Online Material
www.sciencemag.org/cgi/content/full/317/5840/941/DC1
Materials and Methods
References

4 June 2007; accepted 6 July 2007
10.1126/science.1146037

A Whole-Genome Association Study of Major Determinants for Host Control of HIV-1

Jacques Fellay,[1] Kevin V. Shianna,[2*] Dongliang Ge,[1*] Sara Colombo,[3*] Bruno Ledergerber,[4*] Mike Weale,[1*] Kunlin Zhang,[3] Curtis Gumbs,[1] Antonella Castagna,[5] Andrea Cossarizza,[6] Alessandro Cozzi-Lepri,[7] Andrea De Luca,[8] Philippa Easterbrook,[9] Patrick Francioli,[10] Simon Mallal,[11] Javier Martinez-Picado,[12] José M. Miro,[13] Niels Obel,[14] Jason P. Smith,[2] Josiane Wyniger,[3] Patrick Descombes,[15] Stylianos E. Antonarakis,[16] Norman L. Letvin,[17] Andrew J. McMichael,[18] Barton F. Haynes,[19] Amalio Telenti,[3]† David B. Goldstein[1]†‡

Understanding why some people establish and maintain effective control of HIV-1 and others do not is a priority in the effort to develop new treatments for HIV/AIDS. Using a whole-genome association strategy, we identified polymorphisms that explain nearly 15% of the variation among individuals in viral load during the asymptomatic set-point period of infection. One of these is found within an endogenous retroviral element and is associated with major histocompatibility allele *human leukocyte antigen* (*HLA*)–*B*5701*, whereas a second is located near the *HLA-C* gene. An additional analysis of the time to HIV disease progression implicated two genes, one of which encodes an RNA polymerase I subunit. These findings emphasize the importance of studying human genetic variation as a guide to combating infectious agents.

Humans show remarkable variation in vulnerability to infection by HIV-1 and especially in the clinical outcome after infection. One striking and largely unexplained difference is the level of circulating virus in the plasma during the nonsymptomatic phase preceding the progression to AIDS. This is known as the viral set point and can vary among individuals by as much as 4 to 5 logs (*1*–*6*). We aimed to identify human genetic differences that influence this variation.

To define a homogeneous phenotype for genetic analyses, a consortium of nine cohorts was formed [termed Euro-CHAVI (Center for HIV/AIDS Vaccine Immunology) (*7*)], and a total of 30,000 patients were screened to identify those most appropriate for analysis. All longitudinal viral-load (VL) data were assessed through a computerized algorithm to eliminate VL not reflecting the steady state and were individually inspected by an experienced infectious-disease clinician (Fellay) to exclude suspicious VL data and patients that do not show a clear set point, leaving 486 patients with a consistent and accurately measured phenotype (*7*). For patients with at least four CD4 cell-count results, we defined a progression phenotype as the time to treatment initiation or to the predicted or observed drop of the CD4 cell count below 350 (*7*, *8*).

All samples were genotyped with the use of Illumina's HumanHap550 BeadChip with 555,352 single-nucleotide polymorphisms (SNPs). A series of quality-control steps resulted in the elimination of 20,251 polymorphisms (*7*). We applied methods to identify deletions and targeted copy-number variations and to assess whether they influenced the phenotype (*7*). Our core association analyses focused on single-marker genotype-trend tests of the quality control–passed SNPs, using linear regression (*7*). To control for the possibility of spurious associations resulting from population stratification, we used a modified EIGENSTRAT method (*7*, *9*). We assessed significance with a Bonferroni correction (P cutoff = 9.3×10^{-8}). Analyses incorporating *human leukocyte antigen* (*HLA*) typing were carried out on a subgroup of 187 patients with available four-digit *HLA* class I allelic determination.

These analyses identified two independently acting groups of polymorphisms, associated with *HLA* loci *B* and *C*, that are estimated to explain 9.6 and 6.5% of the total variation in HIV-1 set point, respectively, and can thus be considered as major genetic determinants of viral set point. A third set located >1 Mb away in the major histocompatibility complex upstream of a gene that encodes an RNA polymerase I subunit explains 5.8% of the total variation in disease progression. Together, the three polymorphisms explain 14.1% of the variation in HIV-1 set point.

One polymorphism located in the *HLA* complex *P5* (*HCP5*) gene explains 9.6% of the total variation in set point, despite a minor-allele frequency of 0.05 (Single Nucleotide Polymorphism database number rs2395029, $P = 9.36 \times 10^{-12}$). A single copy of the controlling allele was found to result in a reduction in VL of >1 log (Fig. 1); at $P = 9.36 \times 10^{-12}$, this genome-wide association is significant.

The *HCP5* gene is located 100 kb centromeric from *HLA-B* on chromosome 6 (Fig. 2), and the associated variant is known to be in high linkage disequilibrium (LD) with the *HLA* allele *B*5701* (*10*) ($r^2 = 1$ in our data set). This allele itself has the strongest-described protective impact on HIV-1 disease progression (*11*) and has been associated with low VL (*12*).

Given the strong functional data supporting a role for *HLA-B*5701* in restricting HIV-1, our first hypothesis is that the association observed

[1]Center for Population Genomics and Pharmacogenetics, Duke Institute for Genome Sciences and Policy, Duke University, Durham, NC 27710, USA. [2]Duke Institute for Genome Sciences and Policy, Duke University, Durham, NC 27710, USA. [3]Institute of Microbiology, University Hospital Center; and University of Lausanne, 1011 Lausanne, Switzerland. [4]Division of Infectious Diseases, University Hospital, 8091 Zürich, Switzerland. [5]Clinic of Infectious Diseases, Istituto di Ricovero e Cura a Carattere Scientifico, San Raffaele Hospital, 20127 Milan, Italy. [6]Department of Biomedical Sciences, Section of General Pathology, University of Modena and Reggio Emilia, School of Medicine, 41100 Modena, Italy. [7]Department of Primary Care and Population Sciences, Royal Free and University College Medical School, University College London, London NW3 2PF, UK. [8]Institute of Clinical Infectious Diseases, Catholic University of the Sacred Heart, 00168 Rome, Italy. [9]Academic Department of HIV and Genitourinary Medicine, Kings College London, at Guy's, King's, and St. Thomas' Hospitals, London SE5 9RJ, UK. [10]Service of Infectious Diseases, Department of Medicine and Service of Hospital Preventive Medicine, University Hospital Center, 1011 Lausanne, Switzerland. [11]Centre for Clinical Immunology and Biomedical Statistics, Royal Perth Hospital; and Murdoch University, Perth, WA 6000, Australia. [12]irsiCaixa Foundation and Hospital Germans Trias i Pujol, 08916 Badalona, Spain; and Institució Catalana de Recerca i Estudis Avançats, Barcelona, Spain. [13]Hospital Clinic–Institut d'Investigacions Biomèdiques August Pi i Sunyer, University of Barcelona, 08036 Barcelona, Spain. [14]Department of Infectious Diseases, Copenhagen University Hospital, Rigshospitalet, 2100 Copenhagen, Denmark. [15]Genomics Platform, National Centre of Competence in Research "Frontiers in Genetics," University of Geneva, 1211 Geneva, Switzerland. [16]Department of Genetic Medicine and Development, University of Geneva Medical School, 1211 Geneva, Switzerland. [17]Division of Viral Pathogenesis, Beth Israel Deaconess Medical Center, Harvard Medical School, Boston, MA 02215, USA. [18]Medical Research Council Human Immunology Unit, Weatherall Institute of Molecular Medicine, John Radcliffe Hospital, Oxford OX3 9DS, UK. [19]Duke Human Vaccine Institute, Duke University, Durham, NC 27710, USA.

*These authors contributed equally to this work.
†To whom correspondence should be addressed. E-mail: amalio.telenti@chuv.ch (A.T.); d.goldstein@duke.edu (D.B.G.)
‡On behalf of the Center for HIV/AIDS Vaccine Immunology (CHAVI) and the Euro-CHAVI consortia.

here is due to the effect of *HLA-B*5701*, reflected in its tagging a SNP within *HCP5* (*10*). We emphasize, however, that genetics allows no resolution of whether this effect is exclusively due to *B*5701* or if *HCP5* variation also contributes to the control. In fact, as a human endogenous retroviral element (HERV) with sequence homology to retroviral *pol* genes (*13*) and confirmed expression in lymphocytes (*14*), *HCP5* is itself a good candidate to interact with HIV-1, possibly through an antisense mechanism (*14*). Moreover, *HCP5* is predicted to encode two proteins, and the associated polymorphism results in an amino acid substitution in one of these proteins.

A model in which *HCP5* and *HLA-B*5701* have a combined haplotypic effect on the HIV-1 set point is consistent with the observation that suppression of viremia can be maintained in *B*5701* patients with undetectable VL, even after HIV-1 undergoes mutations that allow escape from cytotoxic T lymphocyte (CTL)–mediated restriction (*15*). However, this observation has also been explained by a decrease in viral fitness associated with the escape variants (*16*). In addition, *B*5701* patients present less frequently with symptoms during acute HIV-1 infection (*12*), suggesting control before the time of a maximal CTL response (*17*).

The second most significant polymorphism we identified, rs9264942, is located in the 5′ region of the *HLA-C* gene, 35 kb away from transcription initiation (Fig. 2) and 156 kb telomeric of the *HCP5* gene. This SNP explains 6.5% of the variation in set point (Fig. 1) and shows a genome-wide significant association ($P = 3.77 \times 10^{-9}$). Despite minor LD between the *HCP5* and *HLA-C* SNPs ($r^2 = 0.05$, $D' = 0.84$), nested regression models clearly demonstrate an independent effect of each of these variants. In a model including the *HCP5* variant, the addition of the *HLA-C* variant results in a highly significant increase in explanatory power, as does the addition of the *HCP5* variant to a model already including the *HLA-C* variant [supporting online material (SOM) text].

This SNP also associates strongly with differences in *HLA-C* expression levels, both in the Sanger Institute Genevar expression database (*18*) (table S1) and in a replication group of 48 healthy volunteers established for this study (SOM text). The protective allele leads to a lower VL and is associated with higher expression of the *HLA-C* gene. This strong and independent association with *HLA-C* expression levels suggests that genetic control of expression levels of a classical *HLA* gene influences viral control. Other *HLA-C* 5′ variants also associate with *HLA-C* expression but do not contribute independently to viral control (SOM text).

Although these data make a strong case for a causal role for *HLA-C* expression levels, extensive LD throughout the MHC region makes it necessary to directly test for alternative causal variants. Specifically, we used nested regression models to assess whether the observed association could be determined by described functional *HLA* class I alleles. In fact, the *HLA-C* expression SNP shows association with certain alleles or group of alleles (Tables 1 and 2). In each case, however, although the *HLA-C* expression variant can explain the effect of these alleles on the HIV-1 set point, the reverse is not true. When a linear regression model includes known *HLA* alleles, the addition of rs9264942 results in a significant increase in the explained variation. On the other hand, none of the *HLA* alleles considered, with the exception of *HCP5/B*5701*, adds significantly to a model that already incorporates the *HLA-C* variant (Tables 1 and 2).

No other single marker reached genome significance, and none of the identified copy-number variations (*7*) showed any association with the HIV-1 set point. An analysis comparing the observed set of *P* values to that expected under the null hypotheses shows no overall inflation of *P* values (indicating little contribution from population stratification) but does show an excess of low *P* values, beginning with the 355th most associated SNP (fig. S1). This indicates that additional real effects are likely to be present among the most associated polymorphisms in this study (complete list available in table S2). Potentially interesting candidates with a lesser association with the set point (listed in tables S3 to S5) were chosen on the basis of their ranking in the study or their link with HIV-1 biology.

We next identified polymorphisms that associate with progression rather than VL: The strongest association included a set of seven polymorphisms located in and near the *ring finger protein 39* (*RNF39*) and *zinc ribbon domain–containing 1* (*ZNRD1*) genes, respectively (rs9261174, rs3869068, rs2074480,

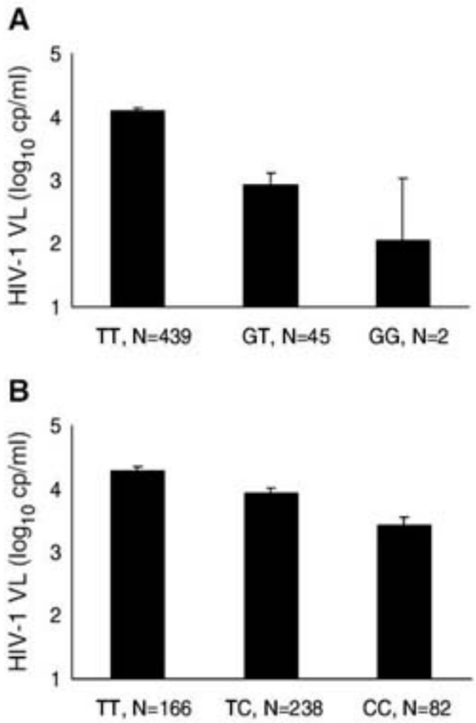

Fig. 1. HIV-1 VL at the set point is highly correlated with (**A**) the *HCP5* rs2395029 genotype, where T is the major allele and G is the minor allele, and with (**B**) the *HLA-C* 5′ region rs9264942 genotype, where T is the major allele and C is the minor allele. Mean and SEM (error bars) are represented for the respective genotypes.

Table 1. The impact of *HLA-C* 5′ expression polymorphism rs9264942 on the set point is independent of its association with *HLA* alleles and groups of alleles previously implicated in HIV-1 control. The addition of rs9264942 to the linear regression model significantly improves the fit for all *HLA* alleles or groups of alleles that have been suspected to have an influence on HIV disease. N.A., not applicable.

Allele	LD between rs9264942 and HLA alleles (r^2)	Models with *HLA* alleles (*P* value)	Addition of rs9264942 to models with *HLA* alleles (*P* value)	Addition of *HLA* alleles to a model with rs9264942 (*P* value)
*HLA-B*27*	0.07	0.19	1.3×10^{-5}	0.91
*HLA-B*5701*	0.05	2.6×10^{-5}	8.5×10^{-5}	4.1×10^{-4}
*HLA-B*35Px*	0.04	0.18	8.1×10^{-6}	0.73
*HLA-B*08*	0.09	0.042	3.6×10^{-5}	0.41
*HLA-B*51*	<0.01	0.44	5.3×10^{-6}	0.36
All 5 above	N.A.	N.A.	3.1×10^{-4}	4.4×10^{-4}
B22 serogroup	0.01	0.28	8.1×10^{-6}	0.59
B7 supertype	0.17	0.007	1.7×10^{-4}	0.35
Bw4 serotype	0.23	0.010	1.7×10^{-4}	0.65
Bw6 serotype	0.16	0.033	6.3×10^{-5}	0.76
*HLA-A*23*	<0.01	0.41	6.9×10^{-5}	0.38
A2 supertype	<0.01	0.72	6.4×10^{-5}	0.53
*HLA-Cw*4*	0.10	0.041	1.3×10^{-4}	0.56
*HLA-Cw*7*	0.25	0.065	1.0×10^{-4}	0.83

rs7758512, rs9261129, rs2301753, and rs2074479). This group of polymorphisms explains 5.8% of the variation in progression, with a relative hazard of 0.64 (fig. S2), and approaches genome-wide significance ($P = 3.89 \times 10^{-7}$). It also associates with VL at the set point ($P = 7.11 \times 10^{-3}$). These variants are >1 Mb telomeric from the previous candidates (fig. S3), and their effect on both progression and set point is independent of *HCP5*- and *HLA-C*–related polymorphisms and *HLA* alleles or groups of alleles previously implicated in HIV-1 control (SOM text and table S6).

Using the Genevar database and our group of 48 healthy volunteers, we observed that *ZNRD1* expression is significantly associated with the identified SNPs (SOM text and table S1). Two of them (rs3869068 and rs9261174) are located in a putative regulatory 5′ region, 25 and 32 kb away from the gene, respectively. Because *ZNRD1* encodes an RNA polymerase I subunit, if this gene is responsible for the restriction of HIV-1, the mechanism could involve interference with the processing of HIV-1 transcripts by the HIV-1 regulatory protein Rev. Rev is known to be localized in the nucleolus (where RNA polymerase I transcribes ribosomal RNA), and the blockade of RNA polymerase I has been shown to influence the distribution of REV, causing a shift from the nucleolus to the cytoplasm (*19*, *20*). Efficiency in provirus transcription is highly variable among individuals; in one study, differences in transcription efficiency accounted for 64 to 83% of the total variance in virus production that was attributable to post-entry cellular factors (*21*).

The second gene, *RNF39*, is poorly characterized but cannot be ruled out as a candidate because two of the associated polymorphisms are located in its coding region and result in amino acid changes (rs2301753 and rs2074479). No other genome-wide significant association was observed in the analysis of the progression phenotype (SOM text).

We established an independent replication cohort of 140 Caucasian patients, drawn from the same participating cohorts. For this follow-up study, we relaxed the interval from a documented negative test to a positive test (for infection) from 2 years to 4 years to identify additional qualifying study participants. We genotyped representative polymorphisms

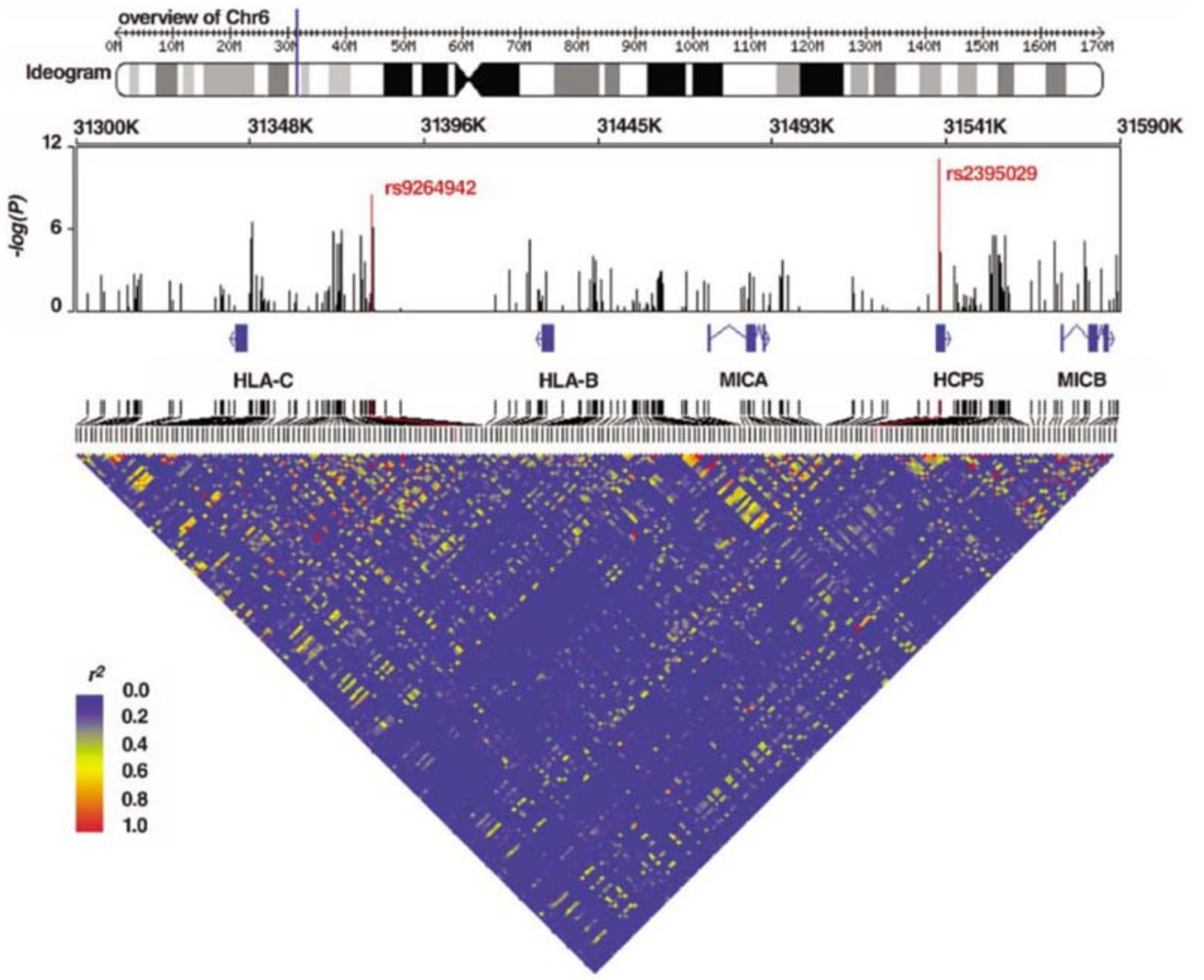

Fig. 2. Partial map of the *HLA* class I region (chromosome 6 p21.3). The *P* values [–log(*P*)] of all genotyped SNPs annotated with the gene structure are indicated. The two independent SNPs that show genome-wide significant association with HIV-1 VL at the set point are marked in red. The graph was drawn with WGAViewer software (www.genome.duke.edu/centers/pg2/index_html/downloads/AnnotationSoftware).

for the associations reported above (*HCP5*, rs2395029; *HLA-C*, rs9264942; and *ZNRD1*, rs9261174). Each association was replicated with effects all in the same direction: *HCP5*, $P = 1.4 \times 10^{-2}$; *HLA-C*, $P = 2.8 \times 10^{-3}$; and *ZNRD1*, $P = 4.8 \times 10^{-2}$.

We have securely identified at least two mechanisms not previously known to restrict HIV-1: *HLA-C*, which has been suspected but never confirmed to contribute to HIV-1 control, and an RNA polymerase subunit that substantially changes the time course of HIV progression (fig. S1). We also suggest the possibility that a HERV-derived gene may contribute to the viral control attributed to the *HLA-B*5701* allele. Our findings confirm and emphasize the central role of the MHC region in HIV-1 restriction, estimate its contribution against all genome influences, and open up new perspectives in the understanding of its mode of action: It is necessary to expand *HLA* analysis to include high-density genotyping. It is also noteworthy that this genome-wide study of host determinants has three clear discoveries, implying that determinants of host response may often include gene variants with major effects. This suggests a degree of urgency in carrying out similar studies for other infectious diseases.

Our results suggest two possible directions for therapeutic intervention. First, if *HCP5* and *ZNRD1* contribute to the control associated with *HLA-B*5701*, they could lead to therapeutic applications. On the other hand, the implication of *HLA-C* in HIV-1 control could present important opportunities, given that the HIV-1 accessory protein Nef selectively down-regulates the expression of *HLA-A* and *-B* but not that of *HLA-C* on the surface of infected cells (*22*). Originally, this strategy was considered advantageous for the virus because *HLA-A* and *-B* present foreign (notably viral) epitopes to CD8 T cells, resulting in cell destruction, whereas *HLA-C* binds self-peptides and interacts with natural killer (NK) cells to avoid NK attack. However, *HLA-C* also has the ability to present viral peptides to cytotoxic $CD8^+$ T cells and consequently to restrict HIV-1 (*23*, *24*). Our observations suggest that *HLA-C*–mediated restriction may be an important element of viral control in specific genetic backgrounds, and that the apparent immunity of *HLA-C* to Nef down-regulation could present an opportunity for vaccine strategies targeting *HLA-C*–mediated responses.

Table 2. In contrast to Table 1, only *HLA-B*5701* has an independent impact after taking into account the effect of rs9264942. The independence of *HLA-C* is also clearly seen in the mean values of the HIV-1 set point for each rs9264942 genotype: The minor allele C is associated with a decrease in VL, independent of all considered alleles and groups of alleles. Numbers refer to a subgroup of 187 patients with available four-digit *HLA* class I allelic results.

rs9264942 genotype	Number of patients	Mean	SD
	All patients		
TT	67	4.37	0.85
TC	87	3.84	1.19
CC	33	3.24	1.28
	Patients without HLA-B*27		
TT	66	4.39	0.83
TC	78	3.86	1.21
CC	25	3.13	1.23
	Patients without HLA-B*5701		
TT	67	4.37	0.85
TC	76	3.97	1.08
CC	27	3.43	1.25
	Patients without HLA-B*35Px		
TT	56	4.32	0.88
TC	84	3.86	1.17
CC	32	3.23	1.30
	Patients without HLA-B*08		
TT	50	4.26	0.87
TC	81	3.83	1.22
CC	33	3.24	1.28
	Patients without HLA-B*51		
TT	56	4.38	0.85
TC	73	3.77	1.17
CC	28	3.21	1.38

References and Notes

1. A. Telenti, D. B. Goldstein, *Nat. Rev. Microbiol.* **4**, 865 (2006).
2. S. J. O'Brien, G. W. Nelson, *Nat. Genet.* **36**, 565 (2004).
3. A. Telenti, G. Bleiber, *Future Virol.* **1**, 55 (2006).
4. M. Carrington, S. J. O'Brien, *Annu. Rev. Med.* **54**, 535 (2003).
5. G. W. Nelson, S. J. O'Brien, *J. Acquired Immune Defic. Syndr.* **42**, 347 (2006).
6. G. Bleiber *et al.*, *J. Virol.* **79**, 12674 (2005).
7. Materials and methods are available as supporting material on *Science* Online.
8. D. C. Douek, L. J. Picker, R. A. Koup, *Annu. Rev. Immunol.* **21**, 265 (2003).
9. A. L. Price *et al.*, *Nat. Genet.* **38**, 904 (2006).
10. P. I. de Bakker *et al.*, *Nat. Genet.* **38**, 1166 (2006).
11. S. A. Migueles *et al.*, *Proc. Natl. Acad. Sci. U.S.A.* **97**, 2709 (2000).
12. M. Altfeld *et al.*, *AIDS* **17**, 2581 (2003).
13. J. K. Kulski, R. L. Dawkins, *Immunogenetics* **49**, 404 (1999).
14. C. Vernet *et al.*, *Immunogenetics* **38**, 47 (1993).
15. J. R. Bailey *et al.*, *J. Exp. Med.* **203**, 1357 (2006).
16. J. Martinez-Picado *et al.*, *J. Virol.* **80**, 3617 (2006).
17. A. J. McMichael, S. L. Rowland-Jones, *Nature* **410**, 980 (2001).
18. B. E. Stranger *et al.*, *PLoS Genet.* **1**, e78 (2005).
19. A. Michienzi *et al.*, *Proc. Natl. Acad. Sci. U.S.A.* **97**, 8955 (2000).
20. M. Dundr *et al.*, *J. Cell Sci.* **108**, 2811 (1995).
21. A. Ciuffi *et al.*, *J. Virol.* **78**, 10747 (2004).
22. G. B. Cohen *et al.*, *Immunity* **10**, 661 (1999).
23. P. J. Goulder *et al.*, *AIDS* **11**, 1884 (1997).
24. S. Adnan *et al.*, *Blood* **108**, 3414 (2006).

25. We thank R. Sahli (University of Lausanne, Switzerland). Funding was provided by the NIH-funded Center for HIV/AIDS Vaccine Immunology. J.F. is supported by the Swiss Foundation for Grants in Biology and Medicine, and A.T. is supported by Infectigen and the Swiss National Science Foundation.

Supporting Online Material

www.sciencemag.org/cgi/content/full/1143767/DC1
Materials and Methods
SOM Text
Figs. S1 to S3
Tables S1 to S6
References

13 April 2007; accepted 2 July 2007
Published online 19 July 2007;
10.1126/science.1143767
Include this information when citing this paper.

Spatial Regulation of an E3 Ubiquitin Ligase Directs Selective Synapse Elimination

Mei Ding,[1] Dan Chao,[1,2] George Wang,[1] Kang Shen[1,2]*

Stereotyped synaptic connectivity can arise both by precise recognition between appropriate partners during synaptogenesis and by selective synapse elimination. The molecular mechanisms that underlie selective synapse removal are largely unknown. We found that stereotyped developmental elimination of synapses in the *Caenorhabditis elegans* hermaphrodite-specific motor neuron (HSNL) was mediated by an E3 ubiquitin ligase, a Skp1–cullin–F-box (SCF) complex composed of SKR-1 and the F-box protein SEL-10. SYG-1, a synaptic adhesion molecule, bound to SKR-1 and inhibited assembly of the SCF complex, thereby protecting nearby synapses. Thus, subcellular regulation of ubiquitin-mediated protein degradation contributes to precise synaptic connectivity through selective synapse elimination.

Synapse elimination is a developmental hallmark of neural circuit refinement (*1*). In the vertebrate neuromuscular junction, the neurotransmitter acetylcholine (ACh) drives elimination of postsynaptic ACh receptor clusters (*2*, *3*). However, little is known about the molecular machinery that eliminates presynaptic specializations, or the mechanisms that selectively eliminate certain synapses while sustaining others.

We investigated synapse elimination in the egg-laying motor neuron of *C. elegans*, the HSNL. In adult animals, the HSNL connects to its targets, the vulval muscles and VC motor neurons, via a cluster of synapses localized exclusively to the vulval region, the primary synapse region (PSR). These synapses were visualized with the vesicle marker synaptobrevin fused to yellow fluorescent protein (SNB-1::YFP) (*4*) (Fig. 1). To determine whether synapses specifically localize to the PSR as a result of synapse elimination, we followed the development of synapses in individual live animals. At early stages of development, we observed that additional SNB-1::YFP puncta formed immediately anterior to the vulva, the secondary synapse region (SSR) (Fig. 1, B and E). Stereotyped elimination of these puncta gave rise to the synaptic pattern present in adult animals (Fig. 1, A to I). The average number of SSR puncta per animal and the percentage of animals with SSR puncta gradually decreased as the animals matured (Fig. 1J). In addition to SNB-1, these SSR puncta contained synaptic vesicle protein RAB-3/rab3 (*5*), active zone protein SYD-2/liprin (*6*) (Fig. 1, K to P), and presynaptic protein UNC-10/RIM (fig. S1). Thus, SSR puncta probably represent bona fide presynaptic structures.

The immunoglobulin superfamily (IgSF) protein SYG-1 (homologous to NEPH1 and IrreC in mouse and *Drosophila*, respectively) is an essential determinant of synaptic specificity in the HSNL (*4*). In *syg-1(ky652)* null mutants, the SNB-1 puncta at the SSR failed to be eliminated and instead persisted into adulthood (Fig. 2A), whereas synapses at the PSR were greatly diminished (*4*). A weak allele of *syg-1*, *wy2*, displayed SSR puncta in 100% of mid-L4 animals; however, only 47.3% of *wy2* adults showed SSR puncta (Fig. 2A). Thus, the level of functional SYG-1 may influence synapse elimination. To test this idea, we generated animals with varying dosages of SYG-1. Heterozygous *syg-1(ky652)* animals exhibited a level of SSR puncta intermediate to those of homozygous and wild-type animals. Furthermore, overexpression of full-length SYG-1 resulted in a lower frequency of SSR puncta relative to the wild type (Fig. 2B). Thus, the level of SYG-1 in the HSNL directly correlates with the extent of SSR puncta elimination.

SYG-1 localizes near the vulva region through its interaction with SYG-2, another IgSF protein expressed in the guidepost epithelial cells (*7*). To understand the relationship between SYG-1 localization and SSR puncta fate, we examined SYG-1 subcellular localization during synapse elimination. In all developmental stages examined, SYG-1 localized exclusively to the PSR where SNB-1 puncta persisted (Fig. 2, C, F, and I). SNB-1 puncta at the SSR (Fig. 2, D and G) did not overlap with SYG-1 fused to cyan fluorescent protein (SYG-1::CFP) (Fig. 2, C to K).

To understand how SYG-1 promotes elimination of SSR synapses, we performed a yeast two-hybrid screen and found that the SYG-1 intracellular domain bound to SKR-1 (fig. S2). This result was confirmed by coimmunoprecipitation (Fig. 3A). SKR-1 is the ortholog of vertebrate Skp1, a core component of the Skp1–cullin–F-box (SCF) complex (*8*). SCF complexes are E3 ubiquitin ligases that transfer ubiquitin to target proteins destined for degradation by the proteasome (*9*). Regulated ubiquitin-proteasome system (UPS) activity controls diverse aspects of neuronal development and function, including neurite outgrowth, synapse growth, and pre- and postsynaptic receptor trafficking (*10*–*14*). To determine *skr-1*'s role in synapse elimination, we performed a loss-of-function analysis using an RNA interference (RNAi) approach. At both the mid-L4 and adult stages, more *skr-1* RNAi–treated animals than control animals displayed SSR puncta (Fig. 3, B and C). RNAi knockdown of CUL-1/Cul1, another obligatory component of the SCF complex (*8*), produced synapse elimination defects similar to those of *skr-1* RNAi–treated animals (fig. S2). Therefore, an SCF complex is essential for proper synapse elimination.

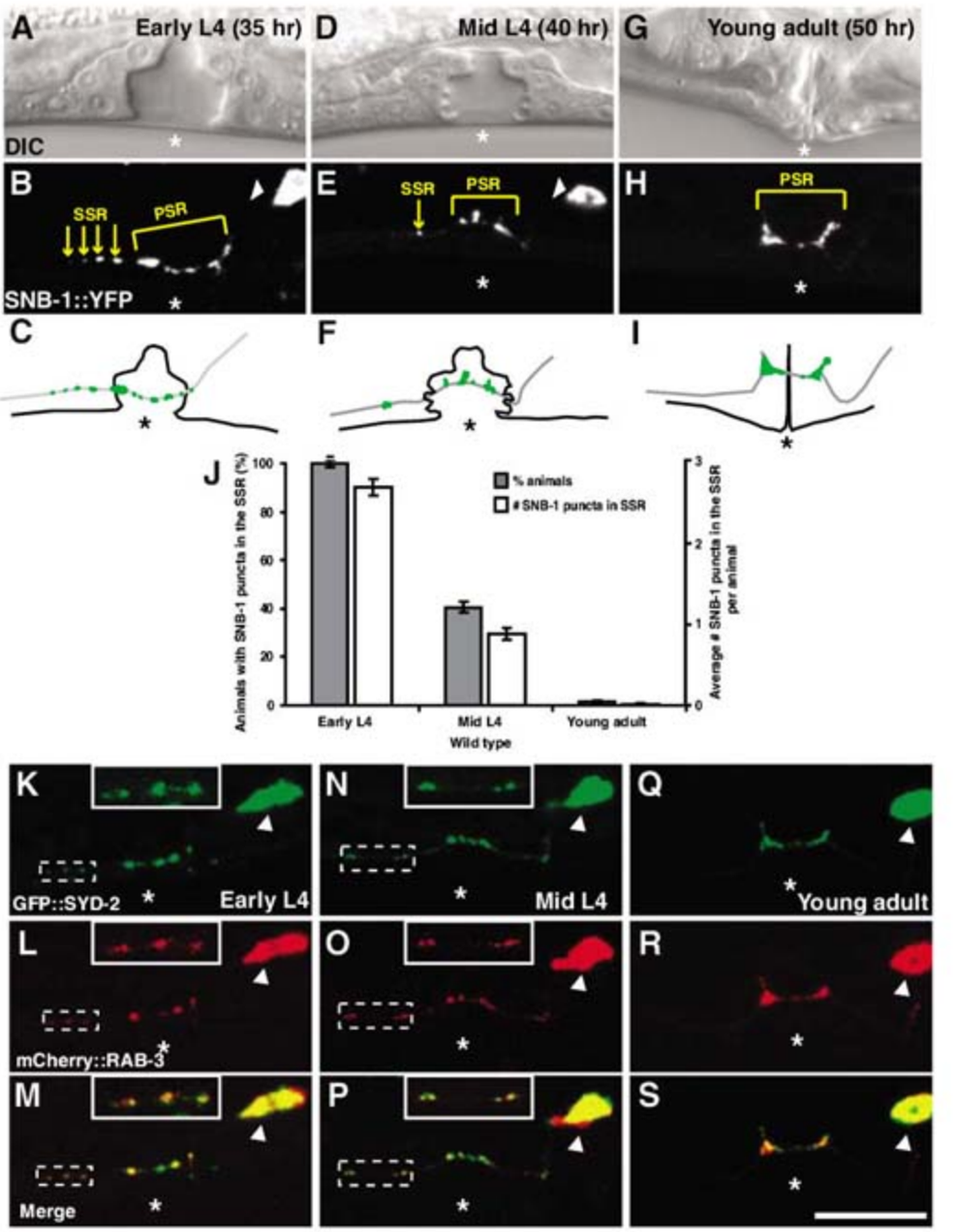

Fig. 1. Synapse elimination at the SSR in the HSNL. The vulval epithelial cells are used as a staging criterion for early L4 (**A** to **C**), mid-L4 (**D** to **F**), and young adult (**G** to **I**) animals. SNB-1::YFP reveals SSR puncta in early and mid-L4 animals [(B) and (E)], which are absent in adult worms (H). Asterisks mark the vulva; arrows and brackets indicate SNB-1::YFP puncta at the SSR and PSR, respectively; arrowheads mark the HSNL cell body. (**J**) Quantification of SNB-1::YFP puncta in the SSR; error bars, SEM. (**K** to **S**) RAB-3 colocalizes with SYD-2 at synapses in both the PSR and SSR [enlarged view in (K) to (P)]. All images are lateral views, anterior to the left and ventral down. Scale bar, 20 μm.

[1]Department of Biological Sciences, Stanford University, Stanford, CA 94305, USA. [2]Neuroscience Program, Stanford University, Stanford, CA 94305, USA.

*To whom correspondence should be addressed. E-mail: kangshen@stanford.edu

F-box proteins provide target specificity for SCF complexes (*8*). We next tested candidates to identify the specific F-box protein that regulates synaptic elimination in the HSNL. FSN-1 and LIN-23, two F-box proteins that have been implicated in presynaptic differentiation and postsynaptic receptor trafficking (*15*, *16*), did not affect the HSNL synaptic pattern (fig. S2). We then investigated another F-box protein, SEL-10, which is known to bind to SKR-1 and functions in the Notch signaling pathway as well as in sex determination in *C. elegans* (*17*, *18*). Interestingly, *sel-10* mutants displayed a phenotype similar to that of *skr-1* knockdown worms: increased SSR puncta as detected with both SNB-1 and the active zone marker SYD-2 (Fig. 3 and fig. S2). Thus, SEL-10 may serve as a specific F-box protein in synapse elimination in the HSNL.

Next, we sought to identify the site of action for *sel-10* in synapse elimination. A transgene containing the *sel-10* promoter driving green fluorescent protein (GFP) labeled a subset of neurons including the HSNL, which suggests that *sel-10* is expressed in the HSNL (fig. S3). Then we expressed the *sel-10* cDNA under the control of various cell-specific promoters and asked which promoters could rescue the mutant phenotype. An *unc-86* promoter driving the *sel-10* cDNA, which confers expression in HSNs, fully rescued the *sel-10* mutant phenotype (Fig. 3, D and E). In contrast, when we used promoters that drove expression in cells adjacent to the HSNL, the *sel-10* defect remained (Fig. 3D). Finally, we examined the subcellular localization of SEL-10. SEL-10::GFP was diffusely localized along the entire axon throughout development (fig. S3). Thus, SEL-10 functions cell-autonomously to regulate synaptic elimination and is present at both the PSR and SSR.

Because SCF E3 ubiquitin ligases participate in UPS-mediated protein degradation (*8*), we asked whether proteasome activity is required for synapse elimination. We found that SSR synapse elimination was drastically compromised in animals treated with lactacystin, a proteasome inhibitor (*19*), which suggests that UPS-mediated protein degradation is required for synapse elimination (fig. S4).

Because the SCF^{SEL-10} complex is present at both the PSR and SSR, why does synapse elimination occur specifically at the SSR but not at the

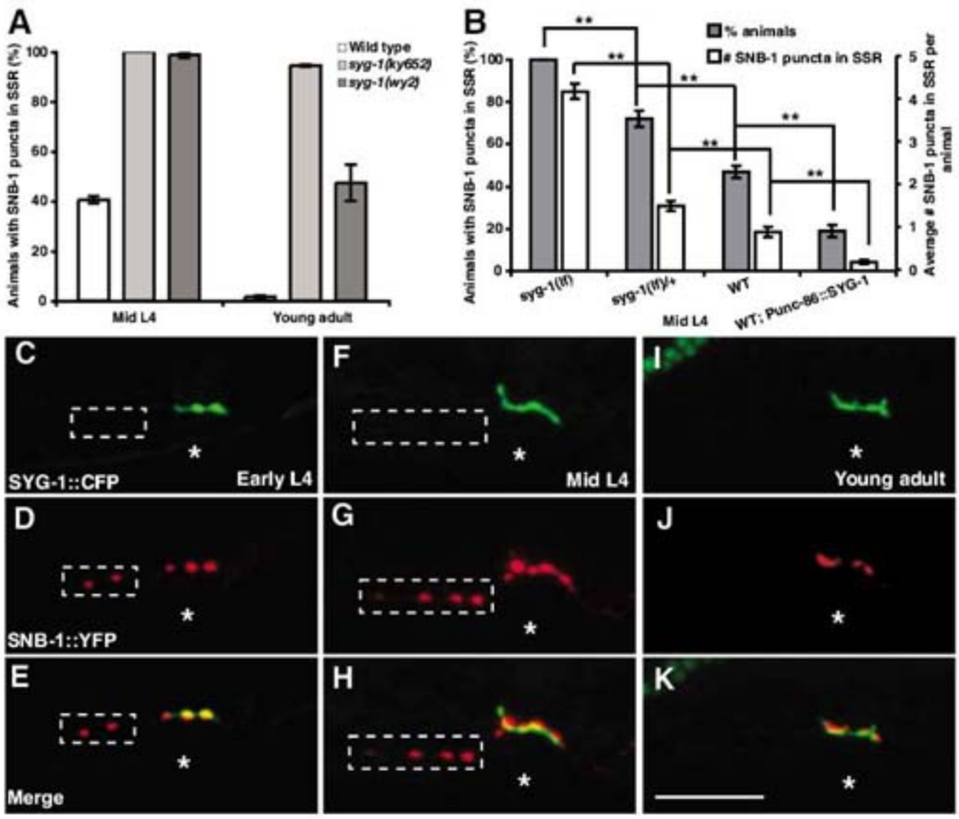

Fig. 2. SYG-1 is required for SSR synapse elimination. (**A**) Quantification of SSR puncta in a null *syg-1(ky652)* allele and a weak *syg-1(wy2)* allele. (**B**) SYG-1 dosage effect on the SSR SNB-1::YFP puncta. $^{**}P < 0.01$; $n \geq 100$. (**C** to **K**) SSR SNB-1::YFP puncta are located anterior to the developing vulva (dashed boxes) and do not overlap with SYG-1::CFP. Asterisks indicate the vulva.

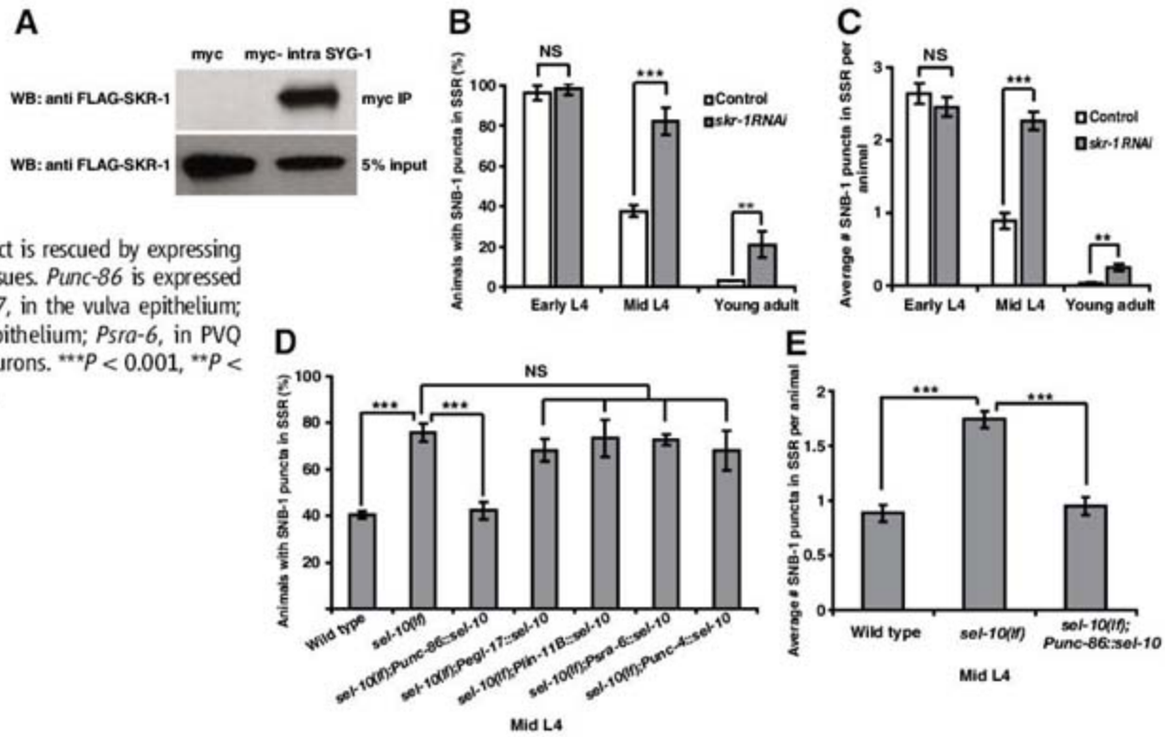

Fig. 3. The SCF^{SEL-10} complex is required for synapse elimination in the HSNL. (**A**) SKR-1 immunoprecipitates the intracellular domain of SYG-1 in 293T cells. (**B** and **C**) The SSR puncta are not eliminated completely in *skr-1* RNAi–treated animals. (**D** and **E**) The *sel-10* synapse elimination defect is rescued by expressing *sel-10* in HSNs but not in other tissues. *Punc-86* is expressed in HSNs and other neurons; *Pegl-17*, in the vulva epithelium; *Plin-11B*, in VCs and the vulva epithelium; *Psra-6*, in PVQ and ASH neurons; *Punc-4*, in VC neurons. $^{***}P < 0.001$, $^{**}P < 0.01$; NS, not significant; $n \geq 100$.

PSR? We considered two models. First, the SCF-UPS pathway could exert its effect by regulating the expression of *syg-1*. SYG-1 would then promote synapse elimination through an unidentified pathway. Alternatively, SYG-1 could regulate SCF complex formation or activity. To distinguish between these models, we examined SYG-1::GFP expression in lactacystin-treated animals and *sel-10* mutants. In these worms, the SYG-1::GFP pattern was indistinguishable from that of wild-type animals (Fig. 4, A and B). Furthermore, the SEL-10 WD-repeat domain, which recruits substrates (*20*), did not bind the intracellular domain of SYG-1 (fig. S4). Therefore, it is unlikely that the SCF complex controls the level or localization of SYG-1.

To investigate whether SYG-1 regulates the formation of the SCF^{SEL-10} complex, we assayed the interaction of SEL-10 with SKR-1 by co-immunoprecipitation. The binding between SKR-1 and SEL-10 was significantly weaker in the presence of the SYG-1 intracellular domain (Fig. 4, C and D), which suggests that the SYG-1–SKR-1 interaction inhibited the assembly of SCF complexes. Because SYG-1 protein was strictly localized to the PSR (Fig. 2, C, F, and I), whereas SCF^{SEL-10} was present at both the PSR and SSR (fig. S3) and synapse elimination only occurred at the SSR, we hypothesized that SCF^{SEL-10} degraded synaptic components and its activity was attenuated at the PSR because of the presence of SYG-1 (fig. S5). Furthermore, in *syg-1* mutants, PSR synapses are significantly reduced and SSR synapses are increased (*4*). One explanation for this observation is that the SCF complex may be limiting within the HSNL; a high level of SCF activity at the PSR causes depletion of SCF at the SSR, and vice versa. Therefore, in the wild type, SYG-1 localizes at the PSR and interferes with the assembly of the SCF complex by binding to SKR-1. As a result, SCF activity is low at the PSR and high at the SSR, leading to synapse stabilization at the PSR and synapse elimination at the SSR (fig. S5). In the absence of SYG-1, SCF activity increases at the PSR, leading to synapse elimination, whereas at SSR the SCF activity is low and synapses persist.

To validate this hypothesis, we tested three additional predictions suggested by the model. First, if the SCF is rate-limiting for synapse degradation, then increasing the SCF complex levels should enhance synapse elimination at both the SSR and PSR sites. Indeed, overexpressing SKR-1 protein resulted in reduced PSR (Fig. 4E) and decreased occurrence of SSR synapses (Fig. 4F). Conversely, overexpressing a dominant negative form of SEL-10 that contained only the F-box domain inhibited synapse elimination and led to more SSR puncta (Fig. 4F).

Second, if SYG-1 protects synapses from degradation through its inhibition of SCF, a form of SYG-1 that is diffusely localized should inhibit SCF assembly and perturb synapse elimination at both the SSR and PSR. Consistent with our model, the expression of a freely diffusing SYG-1 intracellular domain construct increased the PSR puncta intensity in *syg-1* mutants (Fig. 4E and fig. S6) and the SSR synapses in wild-type animals (Fig. 4F).

Third, if the SCF complex also functions in synapse elimination at the PSR, we predict that inhibiting SCF activity should suppress the diminished PSR phenotype of *syg-1* mutants. Indeed, in *syg-1* mutant animals, compromising SCF by *skr-1* RNAi or a *sel-10* mutation significantly enhanced PSR synaptic intensity (Fig. 4E). These three lines of evidence support a model in which SYG-1 protects the synapse at the PSR by antagonizing the function of SCF, and SYG-1 promotes synapse elimination by making more SCF available distantly at the SSR. It is also possible that SYG-1 acts through unknown mechanisms to regulate SCF activity at the SSR, which would not require SCF activity to be limiting.

Synaptic circuit assembly is a highly dynamic process of concurrent formation and elimination of synapses during development (*21*). The UPS is widely used in many cellular processes, including axon pruning, dendrite pruning, and synapse development (*15*, *22*–*26*). Our findings reveal that the UPS also mediates local elimination of synapses without obvious neurite loss, a process that requires precise control of UPS activity. One way to explain the spatial regulation of UPS activity is through local inhibition of the SCF complex by synaptic specificity molecules such as SYG-1. This ensures that synapses are stabilized at appropriate sites but removed from inappropriate sites. A recent study showed that the proteasome could function locally within distal dendrites of vertebrate neurons (*27*). Our results provide a molecular link between spatial regulation of ubiquitin-mediated protein degradation and selective synapse elimination; similar local protection mechanisms may also underlie vertebrate neural circuit formation.

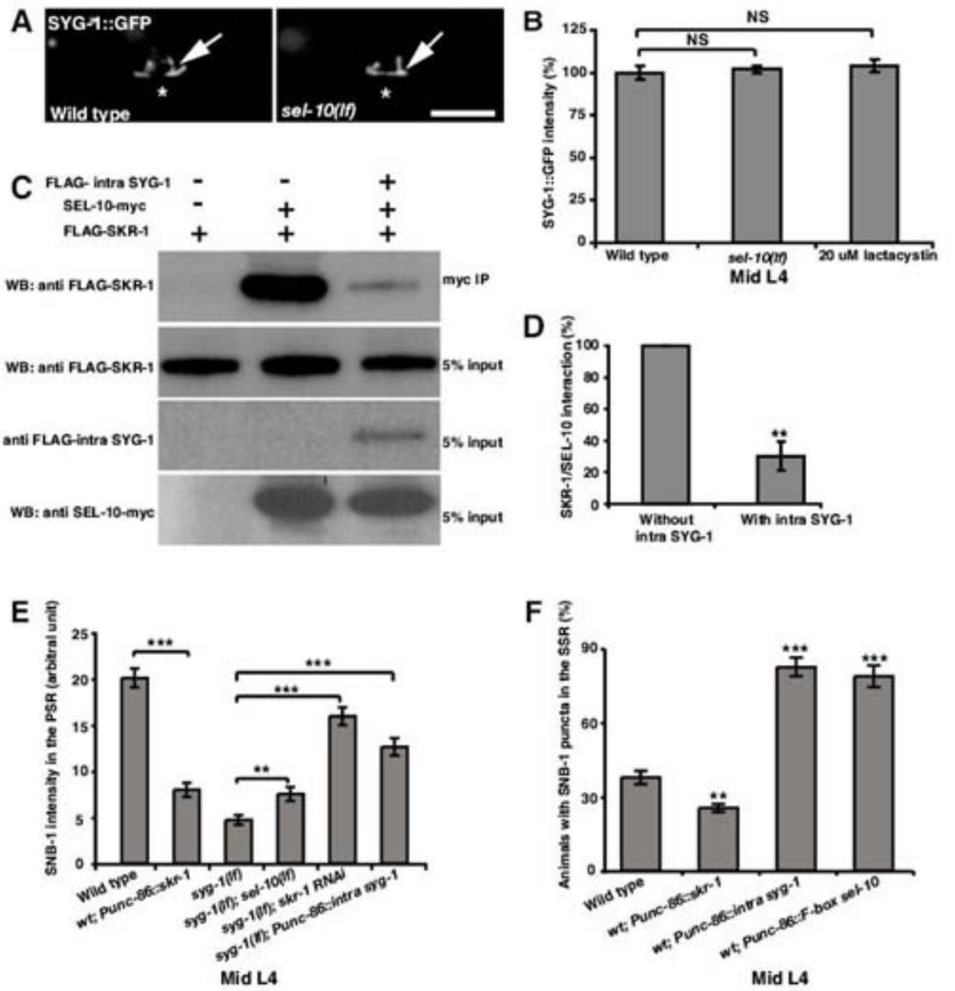

Fig. 4. SYG-1 inhibits SCF^{SEL-10} assembly. (**A**) SYG-1::GFP expression is not altered in *sel-10* mutants. Arrows indicate SYG-1::GFP; asterisks mark the vulva. Scale bar, 20 μm. (**B**) Quantification of SYG-1::GFP intensity. NS, not significant; $n = 20$. (**C**) Coimmunoprecipitation of SKR-1 and SEL-10 is reduced in the presence of SYG-1 intracellular domain. (**D**) Quantification of the SKR-1–SEL-10 interaction. (**E**) Effects of SCF activity and SYG-1 on PSR synaptic intensity. Depletion of SCF or overexpression of SYG-1 intracellular domain enhances PSR synapses; $n = 20$. (**F**) Overexpression of *skr-1* reduces the SSR synapses, whereas overexpression of SYG-1 intracellular domain or the F-box domain of SEL-10 causes an increase in SSR synapses; $n \geq 100$. $^{**}P < 0.01$, $^{***}P < 0.001$.

References and Notes

1. J. W. Lichtman, H. Colman, *Neuron* **25**, 269 (2000).
2. W. Lin *et al.*, *Neuron* **46**, 569 (2005).
3. T. Misgeld, T. T. Kummer, J. W. Lichtman, J. R. Sanes, *Proc. Natl. Acad. Sci. U.S.A.* **102**, 11088 (2005).
4. K. Shen, C. I. Bargmann, *Cell* **112**, 619 (2003).

5. G. Fischer von Mollard *et al.*, *Proc. Natl. Acad. Sci. U.S.A.* **87**, 1988 (1990).
6. M. Zhen, Y. Jin, *Nature* **401**, 371 (1999).
7. K. Shen, R. D. Fetter, C. I. Bargmann, *Cell* **116**, 869 (2004).
8. T. Cardozo, M. Pagano, *Nat. Rev. Mol. Cell Biol.* **5**, 739 (2004).
9. K. I. Nakayama, K. Nakayama, *Nat. Rev. Cancer* **6**, 369 (2006).
10. A. DiAntonio *et al.*, *Nature* **412**, 449 (2001).
11. M. D. Ehlers, *Nat. Neurosci.* **6**, 231 (2003).
12. R. J. Watts, E. D. Hoopfer, L. Luo, *Neuron* **38**, 871 (2003).
13. M. Zhen, X. Huang, B. Bamber, Y. Jin, *Neuron* **26**, 331 (2000).
14. A. M. Schaefer, G. D. Hadwiger, M. L. Nonet, *Neuron* **26**, 345 (2000).
15. L. Dreier, M. Burbea, J. M. Kaplan, *Neuron* **46**, 51 (2005).
16. E. H. Liao, W. Hung, B. Abrams, M. Zhen, *Nature* **430**, 345 (2004).
17. S. Jager, H. T. Schwartz, H. R. Horvitz, B. Conradt, *Proc. Natl. Acad. Sci. U.S.A.* **101**, 12549 (2004).
18. E. J. Hubbard, G. Wu, J. Kitajewski, I. Greenwald, *Genes Dev.* **11**, 3182 (1997).
19. D. H. Lee, A. L. Goldberg, *Trends Cell Biol.* **8**, 397 (1998).
20. R. J. Deshaies, *Annu. Rev. Cell Dev. Biol.* **15**, 435 (1999).
21. C. L. Waites, A. M. Craig, C. C. Garner, *Annu. Rev. Neurosci.* **28**, 251 (2005).
22. S. D. Speese, N. Trotta, C. K. Rodesch, B. Aravamudan, K. Broadie, *Curr. Biol.* **13**, 899 (2003).
23. A. N. Hegde, A. DiAntonio, *Nat. Rev. Neurosci.* **3**, 854 (2002).
24. M. Colledge *et al.*, *Neuron* **40**, 595 (2003).
25. P. Juo, J. M. Kaplan, *Curr. Biol.* **14**, 2057 (2004).
26. A. DiAntonio, L. Hicke, *Annu. Rev. Neurosci.* **27**, 223 (2004).
27. B. Bingol, E. M. Schuman, *Nature* **441**, 1144 (2006).

28. We thank CGC, Japanese NBPR, Y. Kohara, M. Nonet, and J. Audhya for reagents. Supported by NIH grant 1R01NS048392 (K.S.), the McKnight endowment fund (K.S.), the W. M. Keck Foundation (K.S.), and the Searle Scholarship (K.S.).

Supporting Online Material

www.sciencemag.org/cgi/content/full/1145727/DC1
Materials and Methods
Figs. S1 to S6
References

29 May 2007; accepted 22 June 2007
Published online 12 July 2007;
10.1126/science.1145727
Include this information when citing this paper.

Rapid Erasure of Long-Term Memory Associations in the Cortex by an Inhibitor of PKMζ

Reut Shema,[1] Todd Charlton Sacktor,[2] Yadin Dudai[1]*

Little is known about the neuronal mechanisms that subserve long-term memory persistence in the brain. The components of the remodeled synaptic machinery, and how they sustain the new synaptic or cellwide configuration over time, are yet to be elucidated. In the rat cortex, long-term associative memories vanished rapidly after local application of an inhibitor of the protein kinase C isoform, protein kinase M zeta (PKMζ). The effect was observed for at least several weeks after encoding and may be irreversible. In the neocortex, which is assumed to be the repository of multiple types of long-term memory, persistence of memory is thus dependent on ongoing activity of a protein kinase long after that memory is considered to have consolidated into a long-term stable form.

Persistent phosphorylation by the atypical protein kinase C isoform PKMζ is required for maintenance of long-term potentiation (LTP) in hippocampus and for sustaining hippocampus-dependent spatial memory (*1*). It is neocortex, however, which is assumed ultimately to store multiple types of long-term memory in the mammalian brain (*2*, *3*). We set out to determine whether persistent phosphorylation by PKMζ is critical for storage of long-term memory in cortex. We investigated taste memory in the insular cortex (IC), which contains the gustatory cortex (*4*).

We trained rats on conditioned taste aversion (CTA) (*5*) using saccharin as the conditioned stimulus (CS), and 3 days later, microinfused the selective PKMζ pseudosubstrate inhibitor ZIP (*1*, *6*) bilaterally into the IC. Controls received vehicle only. We tested one ZIP group 1 week later and another 1 month later. ZIP in the IC blocked CTA memory in both groups [one-way analysis of variance (ANOVA), $F(2,16) = 7.61$, $P < 0.005$] (Fig. 1A). Post hoc comparisons unveiled no difference between the ZIP groups; however, each was different from the control ($P < 0.05$). The difference persisted in extinction [repeated-measures ANOVA, group effect, $F(2,16) = 6.17$, $P < 0.01$, test effect, $F(2,32) = 8.91$, $P < 0.001$]. The ZIP groups did not differ from each other, but each was different from control ($P < 0.05$).

Although consolidation of memory in the IC is considered to be over within hours, judged by loss of vulnerability to amnesic agents (*7*), we wondered whether the vulnerability to ZIP reflects a longer consolidation process (*8*). We administered ZIP at various times 3 to 25 days after training, followed by CTA testing. The PKMζ inhibitor blocked memory at all time points tested

[1]Department of Neurobiology, The Weizmann Institute of Science, Rehovot 76100, Israel. [2]Departments of Physiology, Pharmacology, and Neurology, The Robert F. Furchgott Center for Neural and Behavioral Science, SUNY Downstate Medical Center, 450 Clarkson Avenue, Brooklyn, NY 11203, USA.

*To whom correspondence should be addressed. E-mail: yadin.dudai@weizmann.ac.il

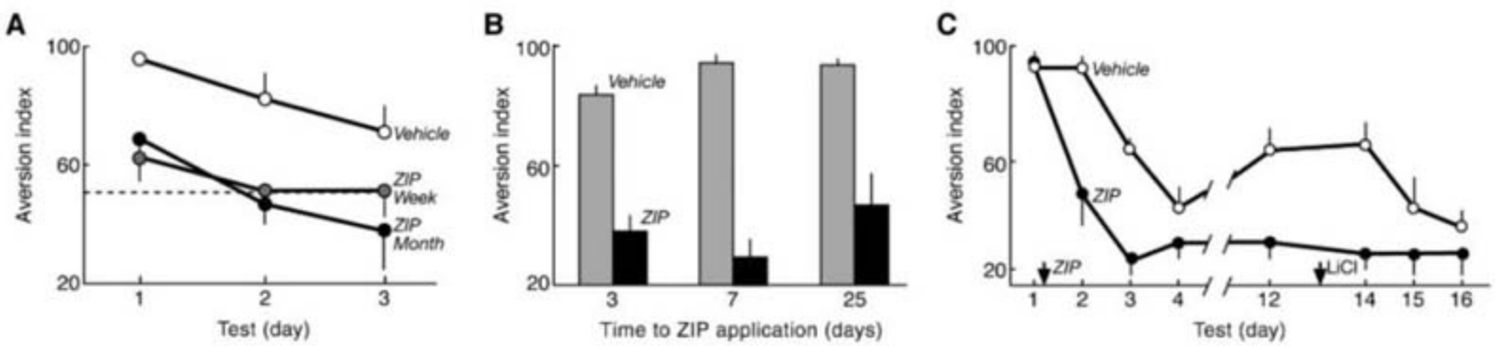

Fig. 1. Erasure of long-term CTA memory by a single application of the PKMζ inhibitor ZIP into the IC. (**A**) ZIP was administered 3 days after training, and memory was tested 1 week or 1 month later. Controls were tested at 1 month. Data are shown for three successive tests, 1 day apart. The dashed line indicates equal preference for the CS and water, i.e., AI = 50 (*5*). A preference for the CS may develop over time in naïve or CTA-extinguished rats, but AI usually does not decline below 20 to 30 even in naïve rats. For statistics, see text. (**B**) ZIP was microinfused into the IC at the indicated times after training, which was a single conditioning session (3 and 7 days groups) or two successive conditioning sessions, a day apart (25 days group). Memory was tested 2 hours (3 and 7 days groups) or 1 day (25 days group) later. (**C**) Rats were trained on CTA and tested once 3 days later, followed 1 to 4 min later by microinfusion of ZIP into the IC. Although spontaneous recovery was seen in the no-test interval between days 4 and 12 in the control group, the ZIP-treated rats showed neither spontaneous recovery nor any indication for UCS-reinstatement (LiCl, day 13).

[(Fig. 1B); $P < 0.001$ for the difference between ZIP groups at 3 days and 7 days and the controls, $P < 0.005$ for the difference between the 25 days group and control]. There is no evidence, therefore, for closure of a consolidation window even after several weeks. The effect of ZIP on long-term memory is rapid [within 2 hours at most; (Fig. 1B), at 3 and 7 days] and is not eliminated by intensifying training [(Fig. 1B), at 25 days after two successive CTA trainings to the same taste].

To exclude the possibility that the effect of the inhibitor is unique to the CS used, we replaced saccharin with glycine. ZIP was administered 3 days after training. Scrambled inactive ZIP was used as control (*1*). A test 1 day later showed an aversion index (AI) = 74.7 ± 6.5 in the ZIP group, and 98.2 ± 1.05 in the control ($n = 8$ each, $P < 0.005$). The effect is thus not unique to the CS used and requires inhibition of PKMζ activity.

In the experiments above, ZIP was administered before the first test. Because reactivation-induced reconsolidation may reinforce the memory trace (*9*–*11*), we wondered whether retrieval under conditions that promote reconsolidation (*8*) might render the trace immune to PKMζ inhibition. We subjected rats to two CTA training sessions, a day apart, followed by a test a week later [before ZIP, AI = 94.5 ± 2.76, $n = 10$; before vehicle, AI = 95.5 ± 2.24, $n = 8$; $F(1,16) < 1$]. We then delivered ZIP a day after the test, and retested a day later. The effect of ZIP was not eliminated [after ZIP, 58.68 ± 7.9; after vehicle, 92.1 ± 3.8; $F(1,16) = 12.27$, $P < 0.005$].

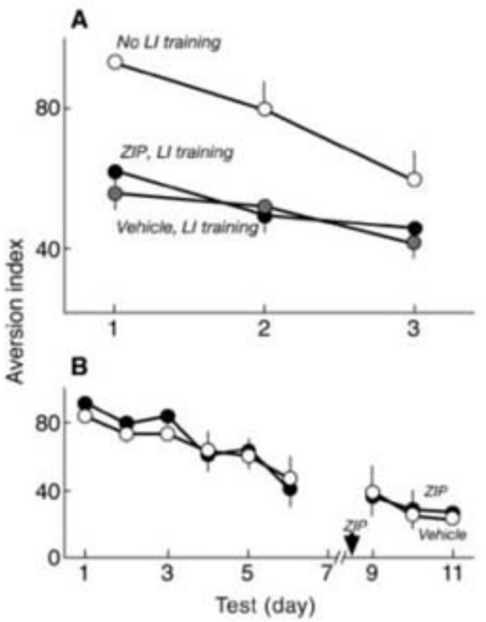

Fig. 2. (**A**) In LI, familiarity with the tastant attenuates the potency of that tastant to serve as CS in subsequent CTA training (compare vehicle, LI training to no LI training). Microinfusion of ZIP into the IC after the exposure to the tastant in the LI protocol (ZIP, LI training) has no effect on familiarity. (**B**) Neophobia declines over repeated nonreinforced exposures to the tastant (days 1 to 6). Application of ZIP into the IC has no effect on familiarity in this protocol either.

To examine the possibility that the inhibitor blocks memory performance only transiently, we continued testing ZIP-treated rats over time, to unveil spontaneous recovery, and in addition, after about 2 weeks, reapplied the unconditioned stimulus (UCS) to elicit potential reinstatement. None of these manipulations yielded evidence for recovered memory in the ZIP group (Fig. 1C). Repeated-measures ANOVA on days 4 and 12 (the no-test interval, in which spontaneous recovery might occur) shows significant group effect, $F(1,12) = 5.79$, $P < 0.05$, and a trend toward group × test interaction, $F(1,12) = 4.29$, $P = 0.06$. Post hoc comparisons reveal nonsignificant difference between groups on test day 4 ($P = 0.28$), but significant difference on day 12 ($P < 0.01$). All in all this indicates spontaneous recovery in the control but not in the ZIP group. The lack of expected extinction in the control between days 12 and 14 (paired t test, $P = 0.84$) suggests a reinstatement effect. No evidence for an effect from UCS reapplication was observed in the ZIP group.

Can ZIP disrupt more than one association at a time? Rats were trained on CTA to saccharin (CS1), and 2 days later to glycine (CS2). These tastants are perceived differently (*12*). One week later, ZIP was microinfused into the IC, and a day later, a test schedule was initiated in which the rats ($n = 8$) were tested on CS1 and CS2, consecutively, 1 day apart over 6 days. Both CS1-UCS and CS2-UCS associations were disrupted: AI on the first test for CS1 association was 94.0 ± 3.16 in the control ($n = 7$), 70.3 ± 7.09 in the ZIP group [$F(1,13) = 8.41$, $P < 0.05$]. AI on the first test for CS2 association was 97.6 ± 0.97 in the control, 78.9 ± 5.8 in the ZIP group [$F(1,13) = 8.61$, $P < 0.05$]. No significant difference was detected among groups in extinction rate, indicating lack of recovery from the ZIP effect on repetitive testing [repeated-measures ANOVA, group × test interactions, $F(2,26) < 1$, not significant].

We tested the effect of the PKMζ inhibitor on the ability to encode, as opposed to retain, CTA memory in the IC. First, we microinfused ZIP into the IC 2 hours before exposure to a glycine

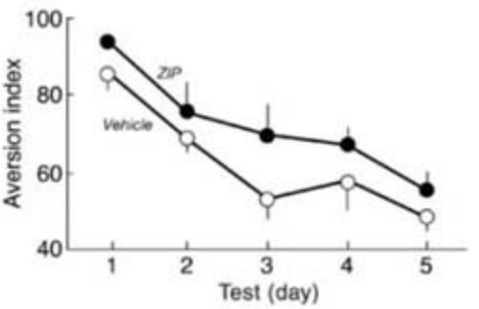

Fig. 3. PKMζ inhibitor in the hippocampus does not impair CTA memory. ZIP was microinfused bilaterally into the hippocampus 3 days after CTA training, and memory was tested starting a day later. These data also demonstrate that the effect of ZIP on CTA memory in the IC is region-specific.

CS in CTA training and tested 3 days later. We found no effect of ZIP on acquisition of CTA [ZIP group, 85.4 ± 5.0, $n = 8$; vehicle, 87.4 ± 5.9, $n = 7$; one-way ANOVA, $F(1,13) < 1$, $P = 0.81$]. Similar results were obtained using saccharin as the CS [ZIP group, 79.6 ± 3.9, $n = 6$; vehicle, 80.0 ± 3.8, $n = 10$; one-way ANOVA, $F(1,14) < 1$, $P = 0.95$]. Second, rats that were trained on CTA to saccharin and then treated with ZIP, were subjected a week later to a new CTA training to glycine. There was no difference between the ZIP and the control rats in their ability to reacquire CTA [ZIP group 93.2 ± 2.3, $n = 9$; vehicle 95.0 ± 2.9, $n = 5$, tested 3 days after retraining; one-way ANOVA, $F(1,12) < 1$, $P = 0.62$].

The IC subserves detection and consolidation of taste familiarity (*13*–*17*). We used two paradigms to determine whether the PKMζ inhibitor disrupts taste familiarity once formed. The first is latent inhibition (LI) (*17*). Preexposure to the CS in a LI protocol attenuates later CTA training to the same CS; hence, CTA performance serves as a familiarity detector (*17*). Introduction of ZIP into the IC after the preexposure to the taste in the LI protocol had no effect on LI [(Fig. 2A); one-way ANOVA for the first test, $F(2,37) = 7.77$, $P < 0.005$]. Post hoc comparisons showed no significant difference between the ZIP-LI and the vehicle-LI groups; however, both groups were significantly different from the no-LI group ($P < 0.01$). Repeated-measures ANOVA showed significant group effect, $F(2,37) = 6.83$, $P < 0.005$, and significant test effect, $F(2,74) = 15.94$, $P < 0.001$. Again, post hoc comparisons showed no significant difference between the two LI groups, and each of these groups was significantly different from the no-LI group ($P < 0.01$).

We also examined attenuation of neophobia (*18*). Here, rats are presented with an unfamiliar tastant that invokes fear-of-the-new and then repeatedly presented with the same tastant. Over time, the neophobia decreases, serving as a measure of familiarity. PKMζ inhibition had no effect in this paradigm [(Fig. 2B), repeated-measures ANOVA, significant attenuation of neophobia in the repeating tests, $F(8,112) = 21.01$, $P < 0.001$]; however, no significant difference was seen between the groups, $F(1,14) < 1$, $P = 0.85$].

PKMζ has been previously shown to maintain LTP and spatial memory in the hippocampus (*1*). The role of the hippocampus in CTA is still unsettled (*19*). Hippocampal lesions do not impair CTA and were even reported to enhance it (*20*). Microinfusion of ZIP into the dorsal hippocampus 3 days after CTA did not impair CTA memory when tested a day after ZIP administration (Fig. 3). If at all, there was a trend toward memory enhancement [repeated-measures ANOVA, $F(1,16) = 2.98$, $P = 0.1$]. Besides demonstrating that PKMζ in the hippocampus is not essential for long-term CTA memory, these data also indicate that the effect of ZIP on memory in the IC is region-specific.

The effect of the PKMζ inhibitor on long-term CTA memory in IC is consistent with

reports that the IC is critical for consolidation, storage, and extinction of CTA (*7*, *13*, *21*, *22*). Although the map of CS-UCS association sites in CTA encoding is still incomplete and probably includes subcortical structures (*23*), once the association is formed, the IC is likely to store elements of the associative hedonic or incentive value of the CS (*24*). In contrast, whereas the IC is documented to detect taste novelty that facilitates encoding of CTA (*4*, *7*, *13*, *14*, *21*), the present data are in line with the possibility that taste familiarity per se is not stored in the IC.

So far, we have found no evidence that the effect of ZIP on associative taste memory in cortex is reversible; hence, we heuristically propose that the PKMζ inhibitor might practically erase some long-term memory associations. We are aware of the difficulties in concluding that a memory trace is erased from the lack of ability to detect a change in performance that is attributed to that trace. This inherent difficulty haunts the long-standing debate on whether amnesia is a storage or a retrieval deficit, yet does not preclude the assumption that amnesia is a storage deficit (*8*, *9*, *25*).

Recent data on reactivation-dependent vulnerability of memory to amnesic agents (*8*, *9*) reemphasize the frailty of the engram—an attribute long recognized by cognitive psychologists (*26*), but somehow mostly ignored till recently by neuroscientists. Our data reinforce the notion that memory traces are prone to swift interferences long after their encoding. In contrast to these earlier studies, however, no reactivation is needed to render the trace susceptible to ZIP. The possibility that the trace reactivates implicitly is low given that classical amnesic agents, e.g., macromolecular synthesis inhibitors, have no effect on the long-term CTA trace that has not been reactivated (*7*, *13*).

The possibility cannot yet be excluded that vulnerability of memory to PKMζ inhibition in cortex might wane. If so, then the temporal window of "cellular consolidation," i.e., the stabilization process that is postulated to occur in synapses and cell bodies after memory encoding (*8*), lingers far longer than originally thought. This conclusion is even more striking given that elemental CTA seems hippocampus-independent, excluding a "systems consolidation" process in which the hippocampal trace invades neocortex over days to weeks (*8*). An alternative possibility is that PKMζ permanently maintains long-term memory and, thus, is a target for amnesic agents as long as the memory persists. In this case, defining consolidation on the basis of vulnerability to amnesic agents (*8*) requires reconsideration.

How does PKMζ inhibition disrupt memory in neocortex? If work on LTP in the hippocampus is a guide, the effect of PKMζ might be on the microstructure of preexisting synapses, resulting in a doubling of the number of functional postsynaptic AMPA-type glutamate receptors (*27*). Our results indicate, however, that these changes, even weeks after learning, are not indelible modifications of synaptic structure, but remain dependent on ongoing enzymatic activity and, thus, are capable of rapid and dynamic alterations by experimental manipulation or, perhaps, in the course of incorporation of new experience into associative knowledge schemas in cortex (*28*). The idea that persistent enzymatic activity keeps memory going has been raised on the basis of theoretical considerations (*29*–*31*). The finding that this takes place, via PKMζ, not only in LTP and hippocampus (*1*, *6*, *27*), but also in long-term memory in neocortex, has, in addition to theoretical implications, potential clinical significance, e.g., in the field of cognitive enhancement.

References and Notes

1. E. Pastalkova *et al.*, *Science* **313**, 1141 (2006).
2. L. R. Squire, P. J. Bayley, *Curr. Opin. Neurobiol.* **17**, 185 (2007).
3. Y. Dudai, *Memory from A to Z: Keywords, Concepts, and Beyond* (Oxford Univ. Press, Oxford, 2002).
4. A. Bahar, Y. Dudai, E. Ahissar, *J. Neurophysiol.* **92**, 3298 (2004).
5. Materials and methods are described in supporting material on *Science* Online.
6. D. S. F. Ling *et al.*, *Nat. Neurosci.* **5**, 295 (2002).
7. K. Rosenblum, N. Meiri, Y. Dudai, *Behav. Neur. Biol.* **59**, 49 (1993).
8. Y. Dudai, *Annu. Rev. Psychol.* **55**, 51 (2004).
9. K. Nader, *Trends Neurosci.* **26**, 65 (2003).
10. Y. Dudai, M. Eisenberg, *Neuron* **44**, 93 (2004).
11. N. C. Tronson, S. L. Wiseman, P. Olausson, J. R. Taylor, *Nat. Neurosci.* **9**, 167 (2006).
12. X. Dugas du Villard, C. Her, P. MacLeod, *Chem. Senses* **6**, 143 (1981).
13. D. E. Berman, S. Hazvi, K. Rosenblum, R. Seger, Y. Dudai, *J. Neurosci.* **18**, 10037 (1998).
14. F. Bermudez-Rattoni, *Nat. Rev. Neurosci.* **5**, 209 (2004).
15. M. T. Koh, E. E. Wilkins, I. L. Bernstein, *Behav. Neurosci.* **117**, 1416 (2003).
16. C. Roman, N. Nebieridze, A. Sastre, S. Reilly, *Behav. Neurosci.* **120**, 1257 (2006).
17. K. Rosenblum, D. E. Berman, S. Hazvi, R. Lamprecht, Y. Dudai, *J. Neurosci.* **17**, 5129 (1997).
18. O. Buresova, J. Bures, *Behav. Brain Res.* **1**, 299 (1980).
19. K. Yefet *et al.*, *Eur. J. Neurosci.* **24**, 1434 (2006).
20. M. E. Stone, B. S. Grimes, D. B. Katz, *Learn. Mem.* **12**, 579 (2005).
21. D. E. Berman, Y. Dudai, *Science* **291**, 2417 (2001).
22. M. Eisenberg, T. Kobilo, D. E. Berman, Y. Dudai, *Science* **301**, 1102 (2003).
23. T. Yamamoto, T. Shimura, N. Sako, Y. Yasoshima, N. Sakai, *Behav. Brain Res.* **65**, 123 (1994).
24. B. W. Balleine, A. Dickinson, *J. Neurosci.* **20**, 8954 (2000).
25. K. Nader, S. H. Wang, *Learn. Mem.* **13**, 530 (2006).
26. E. C. Bartlett, *Remembering: A Study in Experimental and Social Psychology* (Cambridge Univ. Press, Cambridge, 1932).
27. D. S. F. Ling, L. S. Benardo, T. C. Sacktor, *Hippocampus* **16**, 443 (2006).
28. D. Tse *et al.*, *Science* **316**, 76 (2007).
29. F. Crick, *Nature* **312**, 101 (1984).
30. J. D. Buxbaum, Y. Dudai, *J. Biol. Chem.* **264**, 9344 (1989).
31. P. Miller, A. M. Zhabotinsky, J. E. Lisman, X. J. Wang, *PLoS Biol.* **3**, e107 (2005).

32. The support of the Israeli Science Foundation (ISF), Jerusalem, to Y.D. is gratefully acknowledged. T.C.S. is supported by NIH R01 MH53576 and MH57068.

Supporting Online Material

www.sciencemag.org/cgi/content/full/317/5840/951/DC1
Materials and Methods
Fig. S1
References

26 April 2007; accepted 6 July 2007
10.1126/science.1144334

Detection of Near-Atmospheric Concentrations of CO_2 by an Olfactory Subsystem in the Mouse

Ji Hu,[1,2*] Chun Zhong,[1,2*] Cheng Ding,[1] Qiuyi Chi,[3] Andreas Walz,[4] Peter Mombaerts,[4] Hiroaki Matsunami,[3] Minmin Luo[1]†

Carbon dioxide (CO_2) is an important environmental cue for many organisms but is odorless to humans. It remains unclear whether the mammalian olfactory system can detect CO_2 at concentrations around the average atmospheric level (0.038%). We demonstrated the expression of carbonic anhydrase type II (CAII), an enzyme that catabolizes CO_2, in a subset of mouse olfactory neurons that express guanylyl cyclase D (GC-D$^+$ neurons) and project axons to necklace glomeruli in the olfactory bulb. Exposure to CO_2 activated these GC-D$^+$ neurons, and exposure of a mouse to CO_2 activated bulbar neurons associated with necklace glomeruli. Behavioral tests revealed CO_2 detection thresholds of ~0.066%, and this sensitive CO_2 detection required CAII activity. We conclude that mice detect CO_2 at near-atmospheric concentrations through the olfactory subsystem of GC-D$^+$ neurons.

CO_2 is an olfactory stimulus for many invertebrates (*1*, *2*). CO_2 levels fluctuate locally with biological activities, such as animal respiration, plant photosynthesis, and the decomposition of organic matter. CO_2 signals regulate many insect innate behaviors, such as seeking food and hosts, avoiding stressful environments, and ovipositioning (*3*–*6*). CO_2 has no discernable odor to humans, but at high concentrations (>30%), it produces a pungent trigeminal sensation in the nasopharynx (*7*). Carbonic anhydrase (CA), an enzyme that is implicated in CO_2 sensing by peripheral systems such as carotid chemoreceptors (*2*, *8*), is expressed in a subset of olfactory sensory neurons (OSNs) in several vertebrate species (*8*, *9*). Studies indicate that rats can detect CO_2 at levels above 0.5% (*10*, *11*). It remains unknown whether mammals can detect

CO_2 at concentrations near the atmospheric level (0.038%), and if so, whether this detection is mediated by a specialized olfactory subsystem.

In the mouse olfactory epithelium (OE), conventional OSNs use adenosine 3′-5′ monophosphate (cAMP) in odorant-evoked signal transduction, but a minor population of neurons appears to use guanosine 3′-5′ monophosphate (cGMP) (*12*–*14*). Unlike conventional OSNs, this minor population of cells expresses phosphodiesterase 2A (PDE2A), guanylyl cyclase D (GC-D), and cGMP-sensitive cyclic nucleotide-gated (CNG) channels (*12*–*14*). They project axons to the necklace glomeruli, a set of glomeruli that form a "necklace" in the caudal end of the olfactory bulb (OB) (*13*, *15*). The necklace glomeruli have been implicated in detecting suckling pheromones and pheromonal compounds (*16*, *17*). Here we show that mice can sense CO_2 at near-atmospheric levels through the subset of olfactory neurons that express PDE2A and GC-D.

We first examined the gene expression profile of neurons expressing PDE2A (PDE2A$^+$ neurons) by single-cell serial analysis of gene expression of dissociated cells from the caudal OE of mice (*18*). We found that PDE2A$^+$ neurons expressed high levels of CA type II (CAII), whereas conventional OSNs did not (fig. S1, A to C). Expression of *CAII/Car2* mRNA by a subset of OE cells was verified by in situ hybridization (fig. S1D). Immunostaining showed abundant CAII expression by a small population of cells in the caudal OE. Most of these CAII$^+$ cells clustered with bilateral symmetry in the cul-de-sac regions within the caudal recesses of the nasal cavity (Fig. 1A). CAII localized with PDE2A in the OE (Fig. 1, B to D) and in ~20 glomeruli more than 30 μm in diameter in the caudal OB (Fig. 1, E to H; and fig. S2, $n = 6$ mice). Because PDE2A in turn is coexpressed with GC-D (*13*, *14*), we analyzed a mouse strain with a targeted mutation in the *GC-D* locus that produces bicistronic messages causing cotranslation of GC-D with a fusion protein of tau and green fluorescent protein (GFP) (GCD-ITG mice). CAII immunoreactivity and GFP intrinsic fluorescence completely overlapped in the OE (Fig. 1, I to K) and OB (Fig. 1, L to N, $n = 2$ mice). Henceforth, we refer to the subset of CAII$^+$–PDE2A$^+$–GC-D$^+$ neurons as GC-D$^+$ neurons.

CA catalyzes the reversible reaction of $CO_2 + H_2O \rightleftharpoons HCO_3^- + H^+$ (*19*, *20*). Because CA is implicated in CO_2 sensing, we tested whether GC-D$^+$ neurons respond to CO_2 using calcium imaging in an intact OE preparation from GCD-ITG mice (*18*, *21*). OSNs were incubated with rhod-2 acetoxymethyl ester (AM), a calcium-sensitive red fluorescent dye. GC-D$^+$ neurons were identified by intrinsic green fluorescence of GFP in their dendritic knobs and somata (Fig. 2A), and the uptake of rhod-2 AM dye was confirmed by red fluorescence (Fig. 2B). Tissue was continuously superfused with oxygenated HEPES-based Ringer solution. CO_2 was delivered by superfusing CO_2-bubbled Ringer solution into the imaging chamber, resulting in peak CO_2 concentrations of 0.4 to 6.4 mM as calculated by CO_2 solubility (*22*). After CO_2 application, we observed fluorescence enhancement in both dendritic knobs and underlying somata of GC-D$^+$ neurons (Fig. 2C, $n = 428$ cells). CO_2 responses of GC-D$^+$ neurons were dose-dependent, with substantial activation starting at 1.0 mM CO_2 (Fig. 2D). GC-D$^+$ neurons were not activated by CO_2-free Ringer solution with adjusted pH or bicarbonate levels (Fig. 2E and fig. S3A). When tested with 6.4 mM CO_2, most GC-D$^-$ cells were not activated [$n = 256$ out of 260 (256/260) tested], and a few of them were only weakly activated (fig. S4, $n = 4/260$).

To examine the role of CA in CO_2 sensing by GC-D$^+$ neurons, we applied acetazolamide (AZ, 1 mM), a CA enzymatic inhibitor. AZ completely eliminated the CO_2 responses (Fig. 2F and fig. S3B). Calcium signals in response to CO_2 were absent in Ca^{2+}-free Ringer solution, indicating that calcium signals were due to external calcium influx (Fig. 2G and fig. S3C). Low concentrations of L-*cis*-diltiazem (10 μM), a CNG channel blocker (*23*), reversibly blocked the response of GC-D$^+$ neurons to CO_2 (Fig. 2, H and I). Thus, CO_2 specifically activates GC-D$^+$ neurons, and this activation requires CA enzymatic activity and the opening of CNG channels.

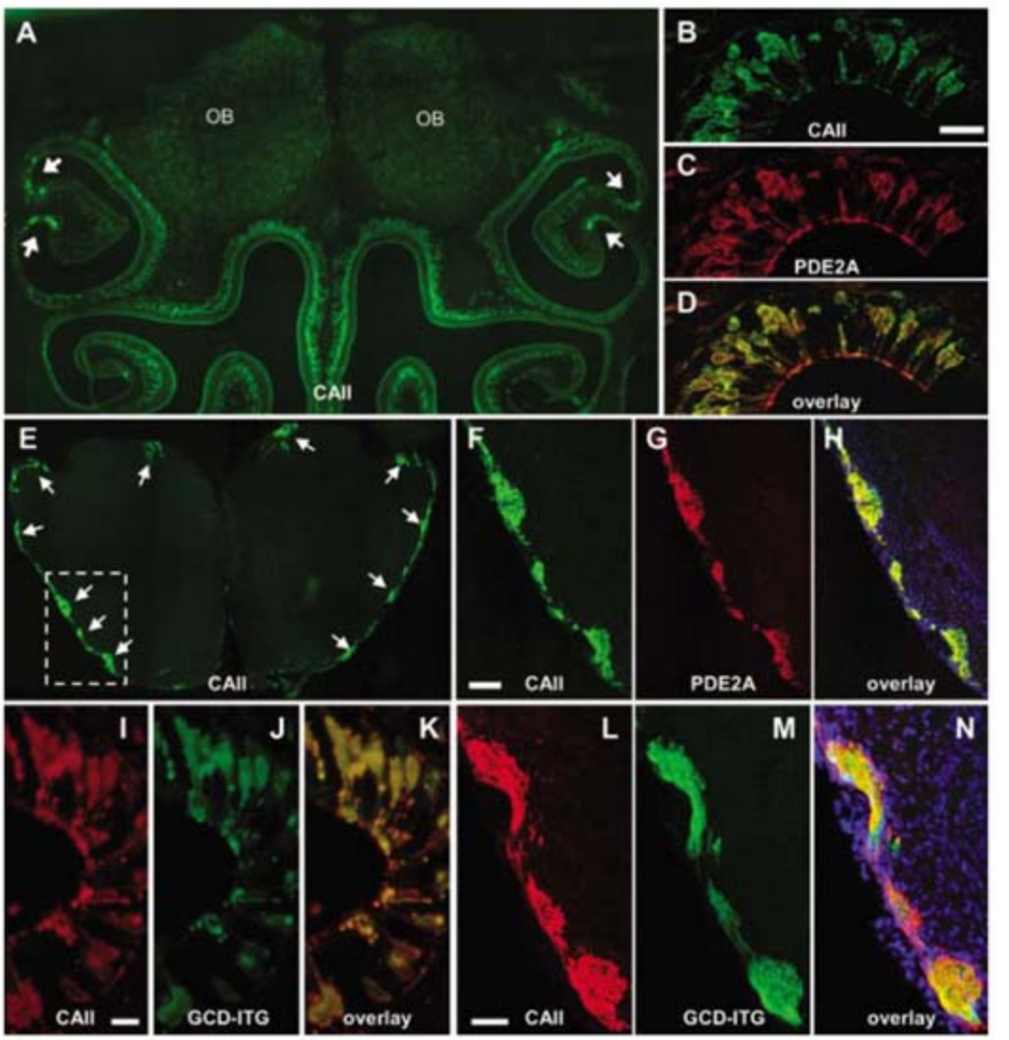

Fig. 1. CAII immunoreactivity in GC-D$^+$ neurons and necklace glomeruli. **(A)** Bilaterally symmetric distribution of CAII$^+$ cells (arrows) in the OE. **(B)** High-power view of CAII immunoreactivity in a CAII$^+$ cluster. **(C)** PDE2A immunoreactivity in the same section as (B). **(D)** Overlay of (B) and (C). **(E)** A coronal section of the caudal OB showing CAII$^+$ glomeruli (arrows) with largely bilateral symmetry. **(F)** High-power view of CAII immunoreactivity within the dashed box in (E). **(G)** PDE2A immunoreactivity. **(H)** Overlay of (F) and (G). Blue, DAPI labeling. **(I to K)** CAII expression overlaps with GFP labeling in the OE of GCD-ITG mice. (I) CAII immunoreactivity. (J) GFP immunoreactivity within the same region as (I). (K) Overlay of (I) and (J). **(L to N)** CAII expression overlaps with GFP labeling in the OB of GCD-ITG mice. (L) CAII$^+$ glomeruli. (M) GFP$^+$ glomeruli within the same region as (L). (N) Overlay of (L) and (M). Scale bars in (B), 20 μm; (F), 100 μm; (I), 10 μm; and (L), 50 μm.

[1]National Institute of Biological Sciences, Beijing, 102206, China. [2]Institute of Biophysics, Chinese Academy of Sciences, Beijing, 100101, China. [3]Department of Molecular Genetics and Microbiology, Duke University Medical Center, Durham, NC 27710, USA. [4]The Rockefeller University, 1230 York Avenue, New York, NY 10021, USA.

*These authors contributed equally to this work.
†To whom correspondence should be addressed. E-mail: luominmin@nibs.ac.cn

To test CO_2 sensitivity in vivo, we recorded from bulbar neurons associated with the necklace glomeruli after exposing anesthetized mice to CO_2 in the airflow delivered to their nostrils (*18*). Out of ~5000 cells tested with 0.5% CO_2 in the gas phase, excitatory responses were found in 260 cells, almost all of which were near the necklace glomeruli. By juxtacellular labeling, we identified five cells with dendritic processes that were delineated clearly and extended into the necklace glomeruli (Fig. 3A). These five cells were activated by external CO_2 at levels above 0.1% (Fig. 3, B and D). Excitatory responses to CO_2 pulses were characterized by initial bursting with short latency [306.3 ± 22.6 ms (mean ± SEM, n = 24 cells)], vigorous firing throughout the stimulus, and brief inhibition after stimulus termination (Fig. 3C). Control pulses (0% CO_2 and 20% O_2) with the same flow rate had no effect, confirming that the responses were evoked by CO_2 but not by increased airflow. The CO_2 responses of bulbar neurons were dose-dependent (Fig. 3, D and E). For the 18 most sensitive cells tested with a range of concentrations, significant activation was observed at 0.1% CO_2. Response amplitudes rose steeply between 0.1 and 0.3% CO_2 and saturated near 0.5% (Fig. 3E). Lower sensitivity to CO_2 was observed in some neurons, with saturation above 2% (n = 30 cells). Activation of GC-D$^+$ glomeruli by CO_2 was further confirmed by immunostaining against c-Fos, a marker of neuronal activation in the olfactory bulb (*17*) (fig. S5).

Finally, we used behavioral assays to examine the sensitivity of CO_2 detection by the mouse (*18*). Water-deprived adult mice were trained to lick a port for water delivery during 0.5% CO_2 pulses and to not lick during control pulses with the same flow rate and oxygen concentrations (fig. S6) (*18*). Training over ~10 days resulted in stable performance at levels of >90% correct responses (Fig. 4A, n =10 mice). During tests, response accuracy remained high for test stimuli with ≥0.1% CO_2 but fell sharply to near-chance level as CO_2 levels decreased further (Fig. 4B). The response ratio at different CO_2 concentrations fitted to a Weilbull psychometric function reporting a CO_2 detection threshold of −1.18 ± 0.07 log units or 0.066% CO_2 (Fig. 4B and fig. S7, n = 8 mice) (*24*), which is just above the average CO_2 concentration in the atmosphere. The behavioral threshold also matched the response sensitivity of bulbar neurons (Fig. 3E). When the OE was ablated by nasal irrigation with zinc sulfate (50 μl at a concentration of 5%), mice were unable to detect 0.5% CO_2 pulses (Fig. 4C). Consistent with OSN regeneration, they slowly regained their ability in 1 to 2 weeks (*25*).

CO_2 repels *Drosophila* (*4*) but attracts mosquitoes to hosts (*3*). In a T-maze assay, we found that mice avoided CO_2 at concentrations as low as 0.2% (n = 31 mice, $P < 0.01$, t test). The avoidance became substantially more marked at higher concentrations (Fig. 4D, 0.4 to 3.2% CO_2). Lesions of the OE by nasal irrigation with zinc sulfate eliminated the avoidance of CO_2 (Fig. 4D). The effects of lesions on mice both trained and untrained for CO_2 detection, in combination with the fast reaction time for CO_2 detection (fig. S8) and the low CO_2 sensitivity of the trigeminal system (fig. S9), demonstrate that the OE has a direct role in CO_2 detection.

Because CAII is expressed exclusively in GC-D$^+$ neurons and its activity is essential for CO_2 responses in these neurons (Figs. 1 and 2), we examined the behavioral phenotype of mice homozygous for a null mutation in the *CAII/Car2* gene that was induced by chemical mutagenesis with *N*-ethyl-*N*-nitrosourea (fig. S10) (*20*, *26*). These mutant mice were unable to detect CO_2 at concentrations below 1% (fig. S11), but their learning curve and detection threshold for detecting amyl acetate (0.10% saturated vapor) were indistinguishable from those of wild-type mice (Fig. 4E, n = 6 for mutant and 7 for wild-type mice) (*18*). After learning the behavioral paradigm with amyl acetate, both wild-type and *CAII*

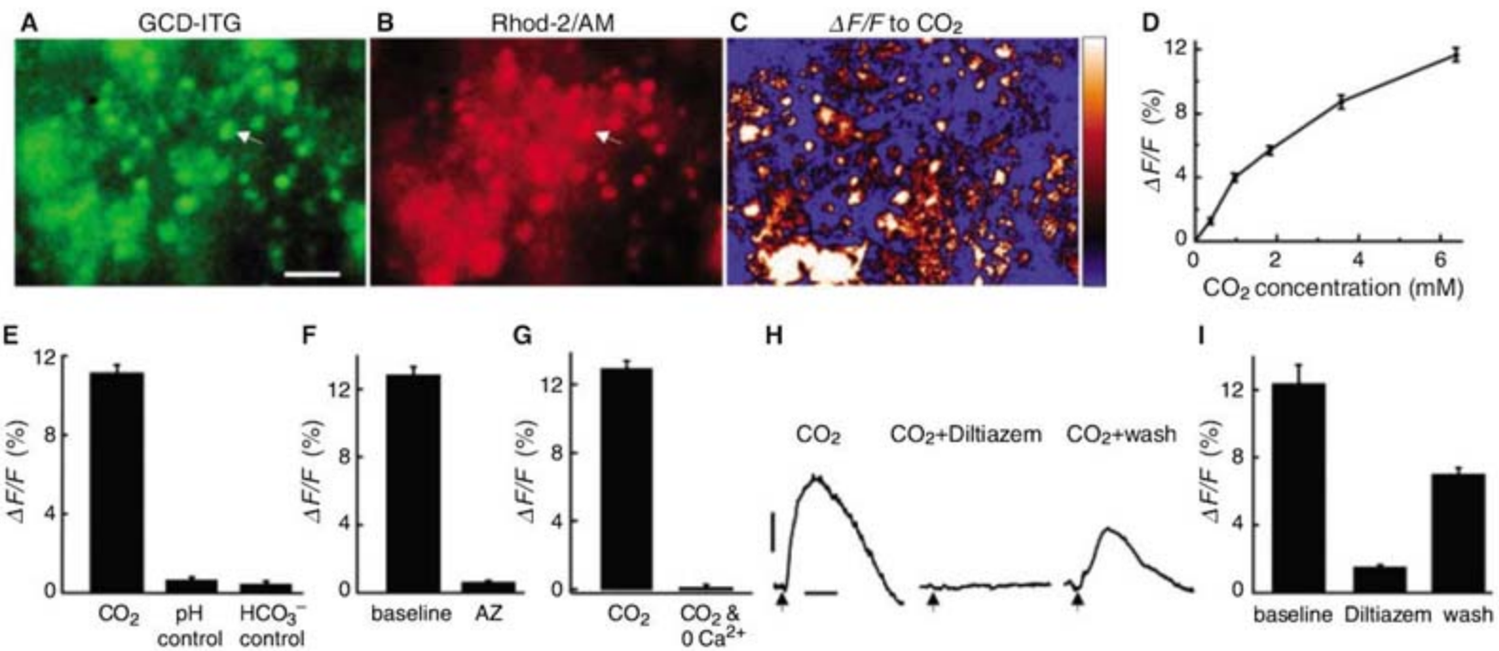

Fig. 2. CO_2 activates GC-D$^+$ neurons, and this activation requires CA activity and the opening of CNG channels. (**A**) GFP labeling of a cluster of GC-D$^+$ neurons within an intact epithelial preparation from a GCD-ITG mouse. The arrow points to a dendritic knob. (**B**) Uptake of the calcium-sensitive dye rhod-2 AM into GC-D$^+$ neurons within the same region as (A). (**C**) Map of normalized fluorescence changes ($\Delta F/F$) within the same region as (A) and (B) showing activation of GC-D$^+$ neurons after CO_2 application. The color scale at the right indicates a $\Delta F/F$ range of 0 to 20%. For all GC-D$^+$ neurons tested, $\Delta F/F$ = 11.1 ± 0.4% (mean ± SEM, n = 428 cells, 8 mice). (**D**) Dose-response curve of the calcium signal to CO_2 (n = 123 cells). (**E**) Group data showing that GC-D$^+$ neurons respond to 6.4 mM CO_2 but not to pH-adjusted and bicarbonate controls ($\Delta F/F$ = 0.7 ± 0.1% for pH-adjusted control, n = 123 neurons, $P < 0.001$, t test, CO_2 versus pH-adjusted control; $\Delta F/F$ = 0.4 ± 0.2% for bicarbonate control, n = 170 neurons, $P < 0.001$, t test, CO_2 versus bicarbonate). Error bars in this and the following figures indicate SEM. (**F**) Group data showing blockade of CO_2 responses by the CA inhibitor AZ ($\Delta F/F$ = 12.8 ± 0.5% in baseline conditions versus 0.5 ± 0.1% in AZ, n = 225 neurons, $P < 0.001$, t test). (**G**) Group data showing the absence of CO_2 responses in Ca^{2+}-free Ringer solution ($\Delta F/F$ = 13.0 ± 0.5% in normal Ringer solution versus 0.0 ± 0.1% for Ca^{2+}-free Ringer, n = 118 neurons, $P < 0.001$, t test). (**H** and **I**) A single example (H) and group data (I) showing the reversible blockade of CO_2 responses by L-*cis*-diltiazem ($\Delta F/F$ = 12.3 ± 1.1% in baseline, 1.8 ± 0.3% during diltiazem application, and 6.9 ± 0.5% during washout; n = 225; $P < 0.001$; t test). Scale bar in (A), 10 μm; in (H), 50 s and a $\Delta F/F$ of 10%.

References and Notes

1. G. Stange, S. Stowe, *Microsc. Res. Tech.* **47**, 416 (1999).
2. S. Lahiri, R. E. Forster 2nd, *Int. J. Biochem. Cell Biol.* **35**, 1413 (2003).
3. M. T. Gillies, *Bull. Entomol. Res.* **70**, 525 (1980).
4. G. S. Suh *et al.*, *Nature* **431**, 854 (2004).
5. C. Thom, P. G. Guerenstein, W. L. Mechaber, J. G. Hildebrand, *J. Chem. Ecol.* **30**, 1285 (2004).
6. W. D. Jones, P. Cayirlioglu, I. G. Kadow, L. B. Vosshall, *Nature* **445**, 86 (2007).
7. D. Shusterman, P. C. Avila, *Chem. Senses* **28**, 595 (2003).
8. E. L. Coates, *Respir. Physiol.* **129**, 219 (2001).
9. M. Kimoto *et al.*, *J. Histochem. Cytochem.* **52**, 1057 (2004).
10. S. L. Youngentob, D. E. Hornung, M. M. Mozell, *Physiol. Behav.* **49**, 21 (1991).
11. K. E. Ferris, R. D. Clark, E. L. Coates, *Chem. Senses* **32**, 263 (2007).
12. H. J. Fulle *et al.*, *Proc. Natl. Acad. Sci. U.S.A.* **92**, 3571 (1995).
13. D. M. Juilfs *et al.*, *Proc. Natl. Acad. Sci. U.S.A.* **94**, 3388 (1997).
14. M. R. Meyer, A. Angele, E. Kremmer, U. B. Kaupp, F. Muller, *Proc. Natl. Acad. Sci. U.S.A.* **97**, 10595 (2000).
15. K. Shinoda, T. Ohtsuki, M. Nagano, T. Okumura, *Brain Res.* **618**, 160 (1993).
16. M. H. Teicher, W. B. Stewart, J. S. Kauer, G. M. Shepherd, *Brain Res.* **194**, 530 (1980).
17. W. Lin, J. Arellano, B. Slotnick, D. Restrepo, *J. Neurosci.* **24**, 3703 (2004).
18. Materials and methods are available as supporting material on *Science* Online.
19. R. G. Khalifah, *J. Biol. Chem.* **246**, 2561 (1971).
20. P. Pan *et al.*, *J. Physiol.* **571**, 319 (2006).
21. M. Ma, G. M. Shepherd, *Proc. Natl. Acad. Sci. U.S.A.* **97**, 12869 (2000).
22. H. Harned, R. J. Davis, *J. Am. Chem. Soc.* **65**, 2030 (1943).
23. T. Y. Chen *et al.*, *Nature* **362**, 764 (1993).
24. A. C. Clevenger, D. Restrepo, *Chem. Senses* **31**, 9 (2006).
25. K. McBride, B. Slotnick, F. L. Margolis, *Chem. Senses* **28**, 659 (2003).
26. S. E. Lewis, R. P. Erickson, L. B. Barnett, P. J. Venta, R. E. Tashian, *Proc. Natl. Acad. Sci. U.S.A.* **85**, 1962 (1988).
27. L. J. Brunet, G. H. Gold, J. Ngai, *Neuron* **17**, 681 (1996).
28. P. N. Pearson, M. R. Palmer, *Nature* **406**, 695 (2000).
29. P. M. Cox, R. A. Betts, C. D. Jones, S. A. Spall, I. J. Totterdell, *Nature* **408**, 184 (2000).

30. We dedicate this paper to the memory of L. C. Katz. We thank H. Zhao for *CNGA2*-knockout mice; J. A. Beavo for antibodies against PDE2A; C. Zhan, Y. Lu, and M. Kubota for technical assistance; M. Ma for technical advice; and A. Person, P. Sterling, and R. Roberts for comments on the manuscript. M.L. is supported by the China Ministry of Science and Technology, a Natural Science Foundation of China Young-Investigator Grant, and a Human Frontier Science Program grant jointly to H.M. and M.L. Support from NIH grants went to H.M., A.W., and P.M. Questions about GCD-ITG mice should be addressed to P.M. (peter@rockefeller.edu).

Supporting Online Material

www.sciencemag.org/cgi/content/full/317/5840/953/DC1
Materials and Methods
Figs. S1 to S13
References

25 April 2007; accepted 12 July 2007
10.1126/science.1144233

Structure of the Membrane Protein FhaC: A Member of the Omp85-TpsB Transporter Superfamily

Bernard Clantin,[1,2,3] Anne-Sophie Delattre,[2,3,4] Prakash Rucktooa,[1,2,3] Nathalie Saint,[5,6] Albano C. Méli,[5,6] Camille Locht,[2,3,4] Françoise Jacob-Dubuisson,[2,3,4]* Vincent Villeret[1,2,3]*

In Gram-negative bacteria and eukaryotic organelles, β-barrel proteins of the outer membrane protein 85–two-partner secretion B (Omp85-TpsB) superfamily are essential components of protein transport machineries. The TpsB transporter FhaC mediates the secretion of *Bordetella pertussis* filamentous hemagglutinin (FHA). We report the 3.15 Å crystal structure of FhaC. The transporter comprises a 16-stranded β barrel that is occluded by an N-terminal α helix and an extracellular loop and a periplasmic module composed of two aligned polypeptide-transport–associated (POTRA) domains. Functional data reveal that FHA binds to the POTRA 1 domain via its N-terminal domain and likely translocates the adhesin-repeated motifs in an extended hairpin conformation, with folding occurring at the cell surface. General features of the mechanism obtained here are likely to apply throughout the superfamily.

Targeting of proteins to their dedicated subcellular compartments is essential for cell function and organelle biogenesis. Translocation of proteins across or insertion into membranes is mediated by protein machineries, some of which have been conserved throughout evolution, such as the transporters of the Omp85-TpsB superfamily. TpsB transporters are components of two-partner secretion (TPS) systems in Gram-negative bacteria. They secrete large, mostly β-helical proteins called TpsA proteins that generally serve as virulence factors (*1*, *2*). TpsB transporters function without accessory factors. The superfamily also includes the Toc75, Sam50-Tob55, and Omp85-YaeT homologs, which are the cores of large hetero-oligomeric complexes involved in protein transport across, and insertion of β-barrel proteins into, the outer membranes of chloroplasts, mitochondria, and Gram-negative bacteria, respectively (*3*–*9*).

Omp85-TpsB transporters have been predicted to comprise a conserved C-terminal transmembrane β barrel and a soluble N-terminal region harboring one to five putative polypeptide-transport-associated (POTRA) domains, which are hypothesized to mediate protein-protein interactions (*10*–*12*). The transporters also harbor conserved C-proximal signature motifs of unknown function in their pore-forming regions (*13*). In spite of their implication in critical physiological processes such as membrane biogenesis and secretion of virulence proteins, the molecular mechanisms of protein translocation or insertion into membranes by those transporters remain poorly understood. To address these issues, we determined the crystal structure of the TpsB prototype FhaC that mediates the translocation to the bacterial surface of filamentous hemagglutinin (FHA), the major adhesin of the whooping cough agent *Bordetella pertussis*.

FhaC was crystallized in space group $C222_1$, and the crystals contained one molecule in the asymmetric unit. The structure was solved by the single-wavelength anomalous diffusion (SAD) method (*14*) and is reported to a resolution of 3.15 Å (table S1 and fig. S1). The protein is a monomer and comprises a 35 Å high β barrel composed of 16 antiparallel β strands (B1 to B16) (Fig. 1A and fig. S2) with a shear number of 20. The β barrel corresponds to the C-terminal moiety of the protein and encompasses residues 209 to 554. The periplasmic and extracellular sides of the barrel are characterized by short turns and longer loops (L1 to L8), respectively, in general agreement with a prior topology model (*15*). The N terminus of the protein is located in the extracellular milieu and folds into a 20-residue-long α helix (H1) that goes right through the transmembrane β barrel (Fig. 1, A and B). The C terminus of helix H1 emerges into the periplasm and is connected to a periplasmic module via a 30–amino acids linker that has no well-defined electron density in the crystal structure. This periplasmic module of 150 residues precedes the β barrel, a feature that had not been predicted earlier (*15*).

The interior of the β barrel is partly hydrophilic, with 17 charged residues pointing inward. Helix H1 is also charged with six Lys and/or Arg and six Asp and/or Glu residues. The charged residues are not uniformly distributed inside the barrel but form three clusters (fig. S3). Cluster 1 runs from the periplasm to the bacterial surface and comprises residues Arg^{280} and Asp^{282} (B5), Lys^{313} (B6), Lys^{333} and Arg^{335} (B7), Asp^{355} (B8), and

[1]UMR8161 CNRS, Institut de Biologie de Lille, Université de Lille 1, Université de Lille 2, 1 rue du Prof. Calmette, F-59021 Lille cedex, France. [2]Institut Pasteur de Lille, Lille, 1 rue du Prof. Calmette, F-59019 Lille cedex, France. [3]IFR142, 59019 Lille, France. [4]INSERM, U629, 59019 Lille, France. [5]INSERM, U554, 34090 Montpellier, France. [6]UMR5048 CNRS, Université de Montpellier 1, Université de Montpellier 2, Montpellier, France.

*To whom correspondence should be addressed. E-mail: francoise.jacob@ibl.fr (F.J.-D.); vincent.villeret@ibl.fr (V.V.)

Arg^{402} (B10) (fig. S3A). They are complemented by residues from H1 (Arg^{13}, Asp^{15}, Asp^{16}, and Arg^{19}). Cluster 2 comprises residues Asp^{218} (B1), Lys^{231} (B2), Arg^{255} (B3), and Glu^{265} (B4) and is located close to the extracellular side. Lastly, cluster 3 comprises residues—Lys^{481} (loop B12-B13), Arg^{516} and Asp^{518} (B14), and Arg^{523} (B15)—close to the periplasmic side of the β barrel (fig. S3B). The large extracellular loop L6 (residues 431 to 469) is folded as a hairpin in the barrel interior, with its tip reaching the periplasm (Fig. 1B). This loop, which is not rigidly bound to the β barrel, covers the inner face of the barrel comprising strands B11 to B16 (fig. S3C). Loop L6 is not well defined in the electron density map and was therefore built as a polyalanine chain. The average temperature factor for Cα in loop L6 is 65 $Å^2$, compared to an overall Cα temperature factor of 38 $Å^2$ in FhaC.

Analyses of the pore dimension (fig. S4A) indicate that the channel in FhaC is too narrow to accommodate the transiting FHA polypeptide because the constricted channel running from the periplasm to the surface between H1 and L6 is only ~3 Å. FhaC forms ion-permeable channels in artificial membranes with conductance values around 1.2 nS in 1 M KCl (*16*). Assuming that the protein forms a perfect cylinder, the pore diameter calculated (*17*) from the measured conductance would be 8.2 Å. However, conductance is not simply related to the size of the channel opening but also to the distribution and environment of the charges inside the channel. Thus, the observed conductance most likely reflects large conformational changes in FhaC in the electrophysiological experiments, possibly with H1 and/or L6 moving out of the pore.

The periplasmic module consists of two globular domains. Both are composed of 75 residues (from 59 to 134 and 135 to 208, respectively) and are organized around a three-stranded β sheet and one α helix (designated hereafter as a POTRA helix). They share the same strand-helix-strand-strand topology. Domain 1 (POTRA 1) corresponds in sequence to the in silico–predicted POTRA domain of the Omp85-TpsB superfamily (*11*). Domain 2 was not previously predicted to also adopt this architecture. Between the first strand and the POTRA helix, the POTRA domains also comprise either an additional turn of α helix and a loop (POTRA 1) or a 10-residue-long additional α helix (POTRA 2) (Fig. 1A and fig. S2). The relative orientation of the POTRA domains was assessed by comparing the angles formed between the axes of helices H2 and H4 with the central axis of the FhaC β barrel. The POTRA 1 and POTRA 2 angles are 148° and 111°, respectively. The two POTRA domains interact with each other via a few hydrogen bonds between loops H2-β2 and H3-H4. POTRA helices H2 and H4, together with strands β5 and β6 (POTRA 2), constitute the surface of the periplasmic module, which is oriented toward the barrel (fig. S5) and close to the translocation pore.

Although well conserved in structure (*18*), the POTRA domains are only 14% identical in sequence. Residues forming the POTRA signature (*11*) either are involved in the hydrophobic core defined by the POTRA helix and the three-stranded β sheet or correspond to glycine residues in loops, such as Gly^{69} and Gly^{109} in loops β1-H2 and H2-β2 for POTRA 1 and Gly^{143} and Gly^{182} in loops β4-H3 and H4-β5 for POTRA 2, respectively (Fig. 2A). Another residue of the POTRA signature, Gly^{134}, is located at the POTRA domains junction. The contribution of these signature residues is essentially structural, and therefore the solvent-accessible surfaces of the POTRA domains are mostly made up of nonconserved, specific residues.

Besides representing the TpsB family, the FhaC structure is also representative of more distantly related transporters of the superfamily, which all share a common architecture consisting of a variable number of POTRA domains in tandem followed by a C-terminal, ≈30-kD β-barrel domain (*10*). In silico analyses of this superfamily have also pinpointed conserved motifs within the β barrel, called motifs 3 and 4 (*13*). In FhaC, motif 3 (amino acids 432 to 474) (Fig. 1) comprises loop L6 and the first half of strand B12. The conserved tetrad VRGY (*19*) (residues 449 to 452) is located at the extremity of the β hairpin in loop L6 and reaches the periplasm. Motif 4 (residues 508 to 536) corresponds to strands B14 and B15, thus comprising residues from the inner and outer faces of the barrel. Residues Met^{508}, Arg^{516}, and Asp^{518} (B14) and Arg^{523}, Ser^{525}, Thr^{527}, and Ser^{529} (B15) are located in the vicinity of loop L6, on the inner face of the β barrel. Motif 4 also comprises residues from the uncharged inner face of the β barrel, along which loop L6 is positioned (fig. S3C).

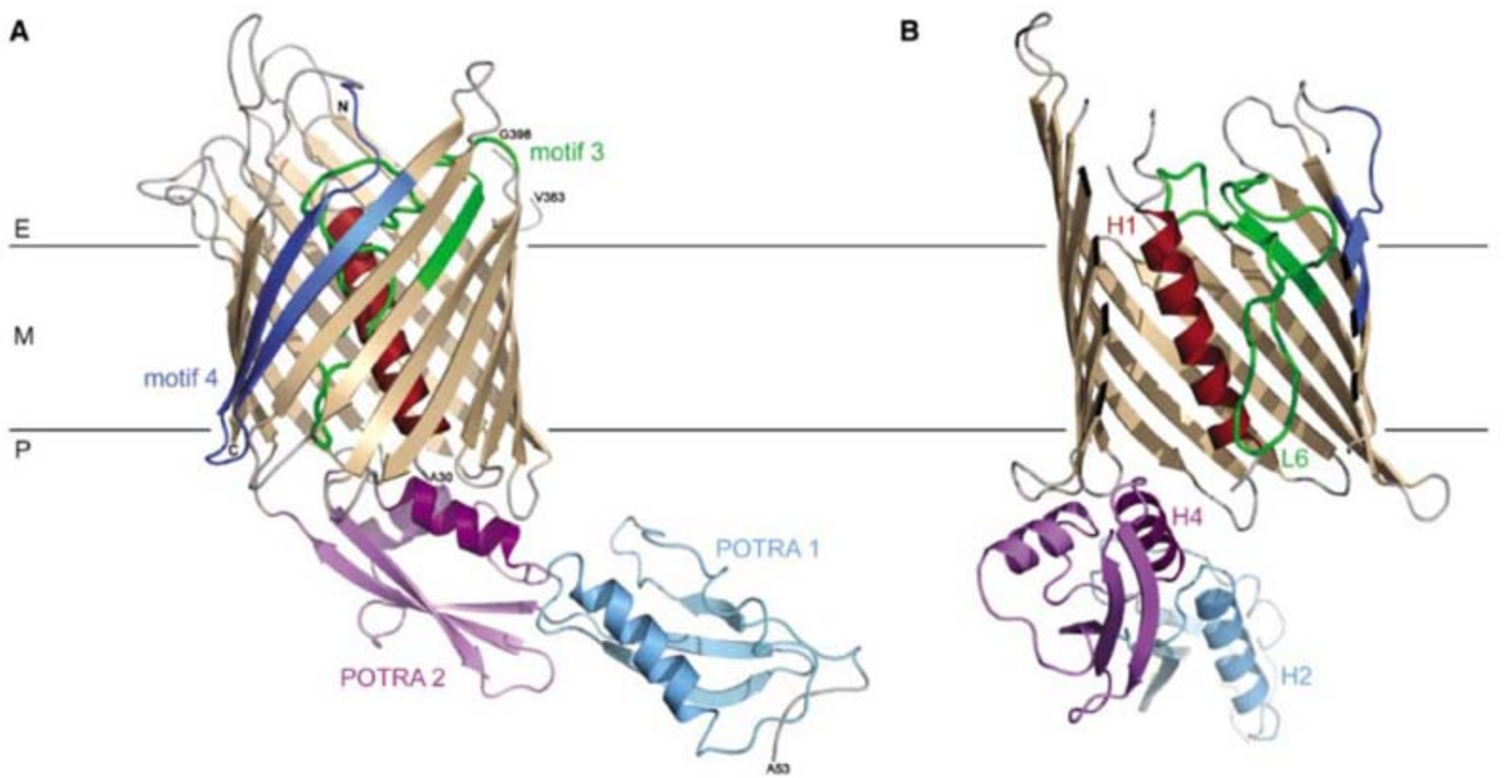

Fig. 1. Crystal structure of FhaC. (**A**) Ribbon representation of FhaC viewed from the membrane plane. Putative position of the membrane (M) boundary is indicated with horizontal lines, with the extracellular side (E) at the top and the periplasm (P) at the bottom. The α helix **H1** is colored red, POTRA **1** light blue, POTRA 2 purple, motif 3 green, and motif 4 blue. (**B**) Cutaway view of FhaC from the membrane plane, rotated about 90° relative to A. The α helix **H1**, POTRA helices **H2** and **H4**, and the loop **L6** are indicated. The images were created with PyMOL (*30*).

In light of the crystal structure, functional aspects of FHA translocation by FhaC have been probed by mutation and deletion studies. FHA secretion has previously been shown to not be affected by removing helix H1 (*15*, *16*), ruling out an essential contribution of H1 in facilitating secretion. FhaC lacking H1 forms channels of similar conductance to that of the wild-type protein in planar lipid bilayer experiments (*16*). Removing H1 would create a ~8 Å large pore (fig. S4B) in FhaC, a size compatible with the conductances observed for both the native and the truncated proteins. These data are in agreement with a model in which H1, found inside the pore in the crystal structure, would be located outside the pore in the electrophysiological experiments. This is similar to previous observations on the crystal structure and electrophysiological data of the translocator domain of the NalP autotransporter (*20*, *21*). Also similar to NalP, the removal of H1 from FhaC enlarges the channel in vivo, as assessed by increased sensitivity to antibiotics (table S2).

In contrast to H1, the deletion of L6 performed in this work abolished secretion, demonstrating its key role in the secretion mechanism (Fig. 3A). This deletion also strongly affected the channel properties of FhaC and decreased the observed conductance to 0.4 to 0.6 nS (Fig. 3). Although removing L6 is predicted to create a 8 Å large channel in FhaC (fig. S4C), the reduction of ion conductance suggests that it affects the conformational stability of the protein and causes important charge rearrangements inside the channel. Crystal structures of OmpF in which the constriction loop L3 has been altered or partially deleted have revealed an increase of the channel size by about 50%, although the ion conductances of these mutants were drastically reduced (*22*–*24*). Evidence for the formation of larger channels by FhaC lacking L6 was obtained from antibiotic sensitivity experiments (table S2), consistent with a role for L6 in plugging the channel. A protease-specific cleavage site inserted after Ser^{462} of FhaC was previously shown to be accessible from the bacterial surface only when FHA is coproduced with FhaC (*15*), indicating conformational changes of L6 during secretion.

The deletion of either POTRA domain, performed here, also abolishes secretion, although FhaC still forms channels in lipid bilayers (Fig. 3, E and F). Therefore, the POTRA domains are strictly required for the secretion process but not for pore formation. The precise orientation of the two POTRA domains is also required, because the insertion of a glycine-serine motif immediately after the conserved Gly^{134} residue of the POTRA sequence signature at the junction of the POTRA domains strongly affects secretion, as shown previously (*15*).

The POTRA domains are involved in FHA recognition, which is likely related to their function in secretion (*25*). Previous work has shown that they recognize a nonnative state of FHA, presumably corresponding to its extended periplasmic conformation in the course of secretion (*25*). In order to identify regions of the POTRA domains involved in these interactions, we interpreted a previously reported insertional analysis in the context of the structure, looking at the effect of insertions in the solvent-exposed regions of the POTRA domains, and we complemented this data with site-directed mutagenesis (Fig. 2B). Insertions of two-residue motifs after positions 72, 73, 79, 88, 93, and 125 (in POTRA 1) and 150, 193, and 206 (in POTRA 2) were shown previously to not affect FHA secretion (*15*), ruling out a major role for these regions in the specific recognition of FHA and in the secretion process. The targeted regions, loop β1-H2 (72-93), loop β2-β3 (125), and helix H3 (150), are located on the faces of the POTRA domains pointing away from the β barrel pore. Thus, the structure rationalizes why they do not affect secretion (Fig. 2B). Insertions in loop β5-β6 (193) and in strand β6 (206) (*15*) are oriented toward the β barrel interior, but because they do not affect secretion they presumably are not major FHA recognition determinants. Therefore, specific interactions of the POTRA domains with FHA likely involve their remaining solvent-exposed surfaces, including helix H2, helix H4, and/or strand β5. Residues located on the exposed faces of these secondary structures that might form hydrogen bonds with FHA, in H2 [K99, Y106, D107, or R108 (*19*)], H4 (D173 or Y177), and strand β5 (T185 or N187), were thus replaced by alanines. Both sin-

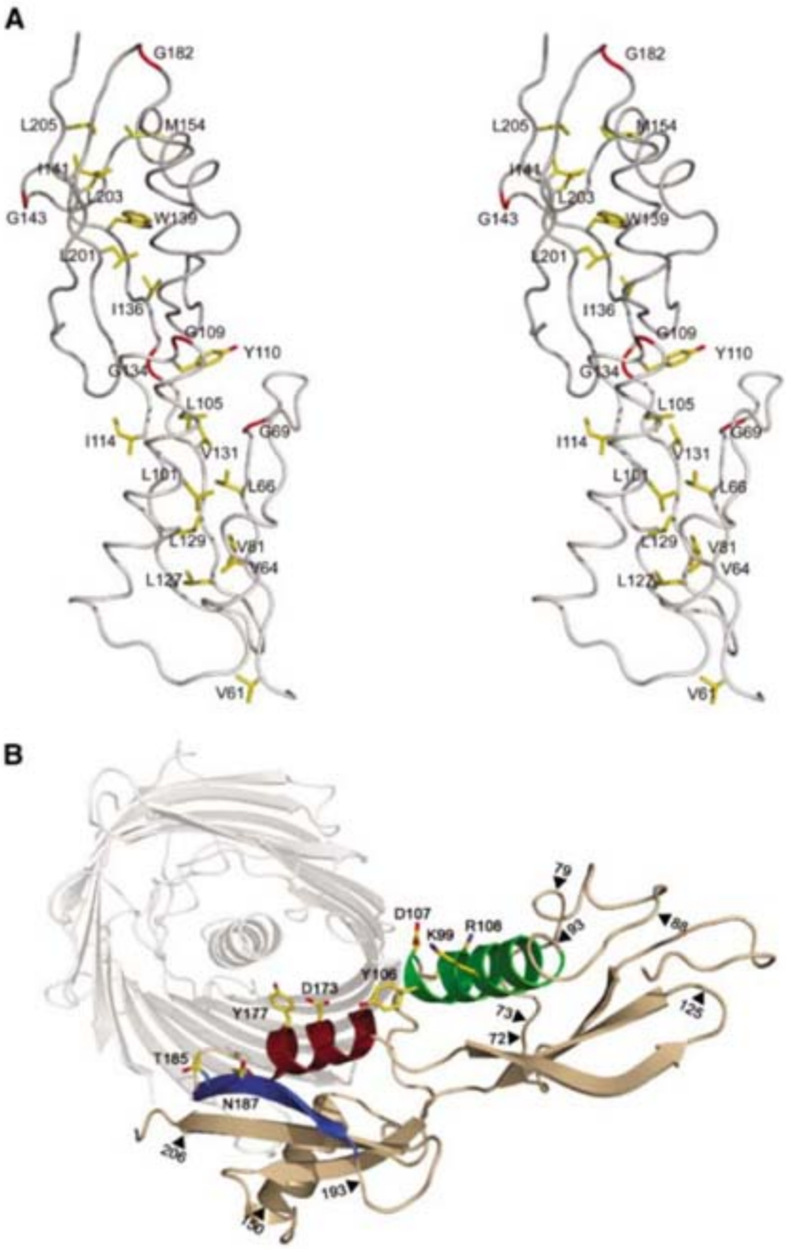

Fig. 2. (**A**) Cα stereoview of the two POTRA domains. POTRA signature residues (*11*) involved in the hydrophobic core are shown in stick representation, whereas the conserved glycines are colored red. V61 and I114 do not belong to the hydrophobic core of POTRA 1. (**B**) Ribbon representation of FhaC viewed from the periplasm. Insertion positions of the two-residue motifs are indicated by black triangles. Side chains of residues analyzed by site-directed mutagenesis are shown with a stick representation. H2, H4, and β5 are colored green, red, and blue, respectively.

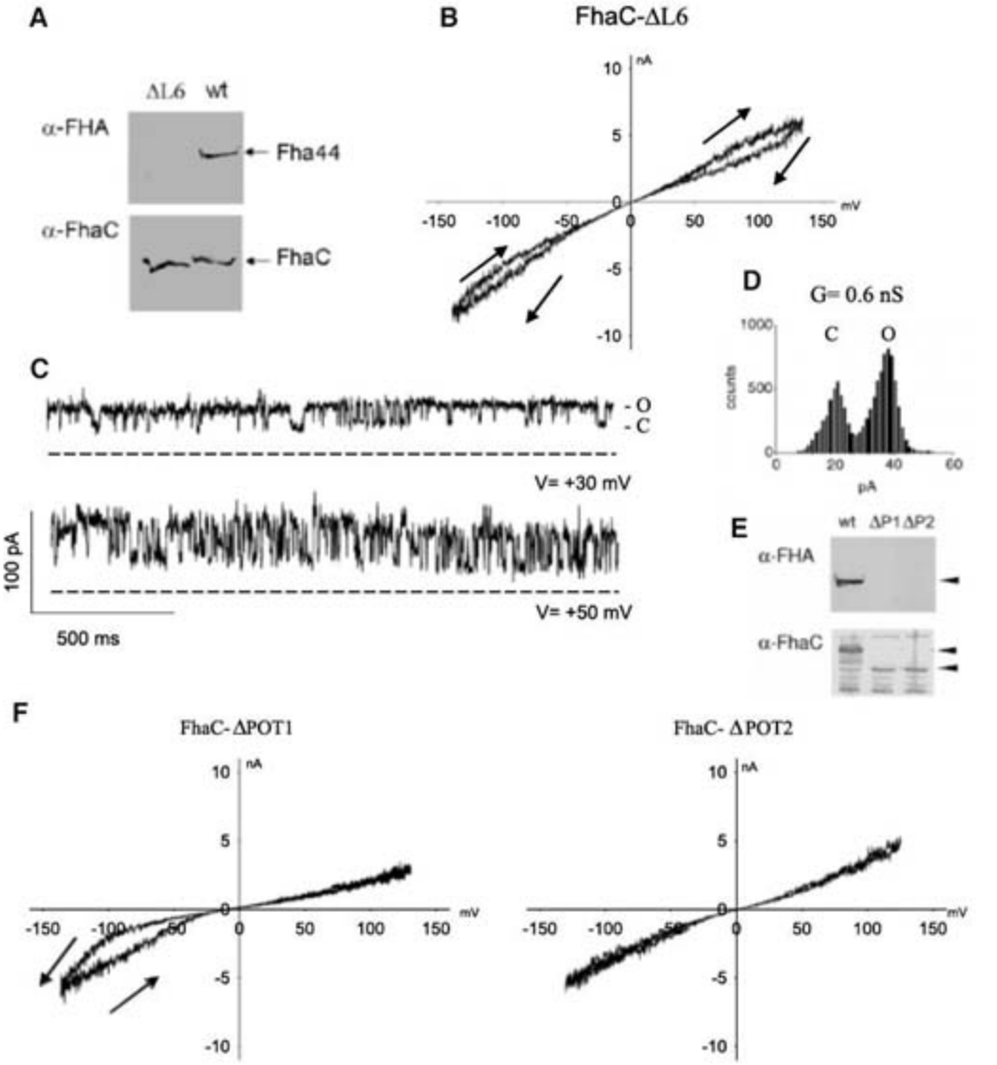

Fig. 3. (**A** to **D**) Behavior of FhaC-ΔL6. (A) Secretion of Fha44, an FHA derivative used as a model FhaC substrate in *Escherichia coli*, by UT5600 (pFJD12, pFc33) (right lanes) and UT5600 (pFJD12, pAS-FcΔL6) (left lanes). Fha44 (top) and FhaC (bottom) were detected with appropriate antibodies by immunoblot analyses of nonconcentrated supernatants and membrane fractions, respectively. wt, wild-type FhaC; ΔL6, FhaC lacking loop L6. (B) Electrophysiological behavior of the FhaC derivative lacking L6. The current-voltage curve is shown, with the arrows indicating the direction of the applied voltage ramp. This *I-V* curve should be compared to that of wild-type FhaC reported in Méli *et al.* (*16*). (C) Single-channel recordings at +30 and +50 mV. The dashed lines represent the zero current level. C and O represent the closed and opened states of one channel, respectively. (D) Amplitude histogram of the single-channel recordings at +30mV, illustrating the distribution of the current values between the closed (C) and opened (O) states of one channel. The main conductance of this channel is equal to 0.6 nS. (**E** and **F**) Behavior of FhaC-ΔPOT1 and FhaC-ΔPOT2. (E) Secretion of Fha44 by UT5600 (pFJD12, pFc33) (left lanes), UT5600 (pFJD12, pAS-FcΔPot1) (middle lanes), and UT5600 (pFJD12, pAS-FcΔPot2) (right lanes). Fha44 (top) and FhaC (bottom) were detected with appropriate antibodies by immunoblot analyses of nonconcentrated supernatants and membrane fractions, respectively. wt, ΔP1, and ΔP2 represent wild-type FhaC and FhaC lacking POTRA 1 or POTRA 2, respectively. The positions of the relevant proteins are indicated by arrowheads. The anti-FhaC immunoblot had to be developed for a long period of time, most likely because the deletion variants were poorly recognized by the antibodies and their levels of production were lower than that of the wild-type protein. (F) Electrophysiological behavior of FhaC-ΔPOT1 and FhaC-ΔPOT2. Current-voltage (*I-V*) curves are shown for the two proteins. These *I-V* curves should be compared to that of wild-type FhaC reported in Méli *et al.* (*16*). The arrows indicate the direction of the applied voltage ramp. Note that the I-V curve of FhaC-ΔPOT1 is similar to that of the wild-type protein, unlike that of FhaC-ΔPOT2, in keeping with the respective positions of the two domains relative to the barrel.

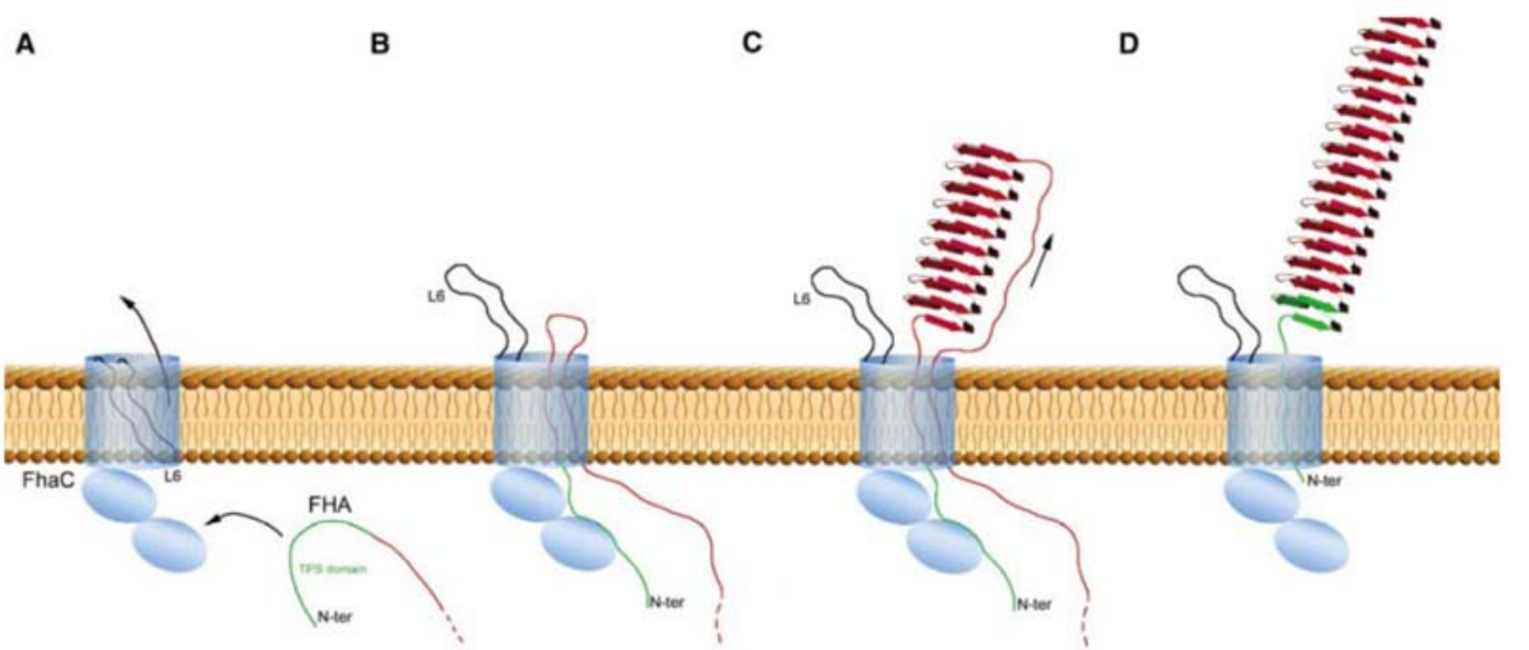

Fig. 4. Proposed model of FHA transport across the outer membrane. (**A**) The TPS domain of FHA in an extended conformation interacts with POTRA 1 of FhaC. (**B**) The channel opens after conformational changes of loop L6, and translocation initiates, with FHA adopting transiently an extended β hairpin structure. (**C**) FHA progressively folds and elongates into its β-helical fold. (**D**) After the C terminus of FHA has reached the surface, the TPS domain dissociates from POTRA 1 and is translocated. The folding of the TPS domain caps the N terminus of the FHA β helix.

gle and double substitutions were created in each of these secondary structures, and the ability of FhaC variants to interact with FHA was assessed (fig. S6) by using an overlay assay developed previously (*25*). Modifications in H2 affected FHA recognition by FhaC in this overlay assay, indicating that helix H2 forms part of the specific recognition surface of FHA.

Collectively, previous data (*15*) and our new mutagenesis data indicate that the L6 loop–motif 3 and the POTRA domains, which are the hallmark features of the superfamily, constitute the active secretion elements of FhaC. FHA is a 50-nm elongated right-handed parallel β helix (*26*–*28*), with the adherence determinants presented on loops or extrahelical motifs along the β helix. The helix interior is essentially filled with stacks of aliphatic residues (Val, Leu, Ile, Ala, and Gly), a characteristic often observed in such β helices. In the light of our structural and functional analysis of FhaC, we propose the following model for transport of FHA across the outer membrane (Fig. 4). The N-terminal TPS domain of FHA, which is characteristic of TpsA proteins and harbors specific secretion signals, initially interacts in an extended conformation with the POTRA 1 domain in the periplasm. Given the orientation of the POTRA domains relative to the channel, the FHA-FhaC interactions bring the region corresponding to the first repeats of the central β-helical domain of FHA in proximity to the tip of loop L6. Conformational changes in FhaC would then expel loop L6 out of the β barrel, opening a 8 Å to 16 Å large (depending on whether H1 is inside or outside the channel during secretion) channel for FHA translocation (fig. S4, C and D). In either case, the channel would not be wide enough to support internal folding of the repeated β-helical motifs of FHA; thus, this event likely takes place at the cell surface. FHA may form a hairpin made up of two extended polypeptide chains in the channel, with its TPS domain anchored in the periplasm. The first repeats of the adhesin could then reach the cell surface, where they could progressively fold into β-helical coils. The formation of the FHA rigid β helix may provide the energy to drive its translocation through FhaC. Transport of FHA in this direction is in agreement with the observation that the C terminus of FHA is exposed to the cell surface before its N terminus (*29*). After the C terminus of FHA has reached the surface, the TPS domain could dissociate from the POTRA domains and be translocated, capping the N terminus of the FHA β helix. Lastly, loop L6 could move back into the barrel.

Because most TpsA proteins are predicted to fold into β helical structures (*26*, *27*), the transport mechanism proposed here may apply more generally to the secretion of TpsA proteins by their dedicated TpsB transporters. All members of the Omp85-TpsB superfamily harbor one to several POTRA domains followed by a β barrel, as well as conserved motifs corresponding to the L6 loop within the barrel, and they mostly handle substrate proteins rich in β structure. Therefore, the major features described here are likely to remain valid throughout the family, although more complex molecular events are expected for some of those transporters, given that they are part of macromolecular assemblies.

References and Notes

1. M.-R. Yen *et al.*, *Biochim. Biophys. Acta* **1562**, 6 (2002).
2. F. Jacob-Dubuisson, R. Fernandez, L. Coutte, *Biochim. Biophys. Acta* **1694**, 235 (2004).
3. S. C. Hinnah, K. Hill, R. Wagner, T. Schlicher, J. Soll, *EMBO J.* **16**, 7351 (1997).
4. B. Bolter, J. Soll, A. Schulz, S. Hinnah, R. Wagner, *Proc. Natl. Acad. Sci. U.S.A.* **95**, 15831 (1998).
5. V. Kozjak *et al.*, *J. Biol. Chem.* **278**, 48520 (2003).
6. S. A. Paschen *et al.*, *Nature* **426**, 862 (2003).
7. R. Voulhoux, M. P. Bos, J. Geursten, M. Mols, J. Tommassen, *Science* **299**, 262 (2003).
8. I. Gentle, K. Gabriel, P. Beech, R. Waller, T. Lithgow, *J. Cell Biol.* **164**, 19 (2004).
9. T. Wu *et al.*, *Cell* **121**, 235 (2005).
10. I. E. Gentle, L. Burri, T. Lithgow, *Mol. Microbiol.* **58**, 1216 (2005).
11. L. Sanchez-Pulido, D. Devos, S. Genevrois, M. Vicente, A. Valencia, *Trends Biochem. Sci.* **28**, 523 (2003).
12. R. Voulhoux, J. Tommassen, *Res. Microbiol.* **155**, 129 (2004).
13. S. Moslavac *et al.*, *FEBS J.* **272**, 1367 (2005).
14. Materials and methods are available as supporting material on *Science* Online.
15. S. Guédin *et al.*, *J. Biol. Chem.* **275**, 30202 (2000).
16. A. C. Méli *et al.*, *J. Biol. Chem.* **281**, 158 (2006).
17. P. Van Gelder, F. Dumas, M. Winterhalter, *Biophys. Chem.* **85**, 153 (2000).
18. The POTRA domains superimpose with an RMS displacement of 1.6 Å, calculated for the Cα. Well-conserved secondary structures include helices H2 and H4, strands β2 and β5, and strands β3 and β6 from POTRA 1 and POTRA 2, respectively.
19. Single-letter abbreviations for the amino acid residues are as follows: A, Ala; C, Cys; D, Asp; E, Glu; F, Phe; G, Gly; H, His; I, Ile; K, Lys; L, Leu; M, Met; N, Asn; P, Pro; Q, Gln; R, Arg; S, Ser; T, Thr; V, Val; W, Trp; and Y, Tyr.
20. C. J. Oomen *et al.*, *EMBO J.* **23**, 1257 (2004).
21. Planar lipid bilayer experiments on the translocator domain of NalP revealed openings and closings of pores of two sizes, with single-channel conductances of 0.15 nS and 1.3 nS that correspond to pore dimensions of 2.4 Å and 8.4 Å, respectively (*20*). Displacement of the α helix from the pore would result in an open channel that may correspond to the observed 1.3-nS conductance steps in planar lipid bilayer experiments. Furthermore, deletion of the α helix in NalP was also shown to increase pore activity (*20*). This helix must be outside the channel to allow for secretion of the passenger domain and could subsequently move in to plug the pore.
22. K. L. Lou *et al.*, *J. Biol. Chem.* **271**, 20669 (1996).
23. N. Saint *et al.*, *J. Biol. Chem.* **271**, 20676 (1996).
24. P. S. Phale *et al.*, *Proc. Natl. Acad. Sci. U.S.A.* **94**, 6741 (1997).
25. H. Hodak *et al.*, *Mol. Microbiol.* **61**, 368 (2006).
26. A. V. Kajava *et al.*, *Mol. Microbiol.* **42**, 279 (2001).
27. B. Clantin *et al.*, *Proc. Natl. Acad. Sci. U.S.A.* **101**, 6194 (2004).
28. FHA comprises an N-terminal TPS domain folded into a β helix, with three extrahelical motifs, a β hairpin, a four-stranded β sheet, and an N-terminal capping (*27*). The reported structure of a 30-kD N-terminal fragment of FHA (Fha30) also reveals several β-helical repeats that form the central right-handed β helix domain of the full-length adhesin.
29. J. Mazar, P. A. Cotter, *Mol. Microbiol.* **62**, 641 (2006).
30. W. L. DeLano, PyMOL Molecular Graphics System (2002); www.pymol.org.

31. We thank H. Hodak for the gift of Fha30 and FhaC-N^{myc} and for advice with the overlay assay experiments, E. Willery and M. L. Parsy for the antibiotic susceptibility experiments, H. Belrhali for support at beamline BM14 at the European Synchrotron Radiation Facility (ESRF, Grenoble), and H. Drobecq for expert assistance with the mass spectrometry experiments. A.C.M. and P.R. are the recipients of predoctoral fellowships from the French Minister de l'Education Nationale and Recherche and Technologie. B.C., F.J.-D., and V.V. are researchers of the CNRS. This work was supported in part by an ACI BCMS2004 grant from the French Ministry of Research. V.V. is supported by an Action Thématique et Incitative sur Programme program from the CNRS and by the Region Nord-Pas de Calais through the Contrat de Plan État-Région and Fonds Européen de Développement Régional programs. Coordinates and structure factors have been deposited in the Protein Data Bank with accession code 2QDZ.

Supporting Online Material

www.sciencemag.org/cgi/content/full/317/5840/957/DC1
Materials and Methods
Figs. S1 to S6
Tables S1 and S2
References

16 April 2007; accepted 11 July 2007
10.1126/science.1143860

Structure and Function of an Essential Component of the Outer Membrane Protein Assembly Machine

Seokhee Kim,[1] Juliana C. Malinverni,[2] Piotr Sliz,[3,4] Thomas J. Silhavy,[2] Stephen C. Harrison,[3,4] Daniel Kahne[1,3]*

Integral β-barrel proteins are found in the outer membranes of mitochondria, chloroplasts, and Gram-negative bacteria. The machine that assembles these proteins contains an integral membrane protein, called YaeT in *Escherichia coli*, which has one or more polypeptide transport–associated (POTRA) domains. The crystal structure of a periplasmic fragment of YaeT reveals the POTRA domain fold and suggests a model for how POTRA domains can bind different peptide sequences, as required for a machine that handles numerous β-barrel protein precursors. Analysis of POTRA domain deletions shows which are essential and provides a view of the spatial organization of this assembly machine.

Although most biological membranes contain exclusively α-helical proteins, the outer membrane of Gram-negative bacteria and the organellar membranes of mitochondria and chloroplasts contain β-barrel proteins (*1*). These integral β-barrel proteins, called outer membrane proteins (OMPs), are folded and inserted into membranes by a process, conserved between prokaryotes and eukaryotes (*2*–*4*), that involves the action of a multiprotein

machine (*5*, *6*). Genetic and biochemical experiments have identified many parts of this machine in several organisms, including *Saccharomyces cerevisiae* and *E. coli* (*3*–*13*). The only conserved component in prokaryotes and eukaryotes is an integral β-barrel membrane protein, represented by YaeT in *E. coli*, Sam50 in mitochondria, and a Toc75 isoform in chloroplasts. A substantial region of all three proteins projects into the intermembrane space and contains one or more predicted polypeptide transport–associated (POTRA) domains (*3*, *4*, *14*).

Proteins destined for the outer membrane of *E. coli* are synthesized in the cytoplasm and transported across the inner membrane through the SecYEG protein secretion machinery (Fig. 1) (*15*). The signal sequence targeting them for secretion is removed at the outer face of the inner membrane. The processed OMP then traverses the periplasmic compartment to β-barrel assembly sites in the outer membrane. Chaperones may assist in periplasmic passage (*16*). It is presumed that the processed OMPs contain structural features that allow them to be recognized by the β-barrel assembly machinery, which in *E. coli* consists of at least five interacting components: four lipoproteins (YfgL, YfiO, NlpB, and SmpA) and the conserved integral membrane protein, YaeT (*5*, *13*).

There are homologs of YaeT in organisms from bacteria to humans (*17*). Recent experiments with *E. coli* YaeT and *S. cerevisiae* Sam50 have shown that these proteins are essential for viability. Furthermore, levels of folded β-barrel proteins decrease and levels of misfolded β-barrel proteins increase when they are depleted (*4*, *5*, *7*, *8*, *18*, *19*). YaeT was reported to bind C-terminal peptides of OMPs (*20*). The POTRA domain in Sam50 was shown to bind unfolded β-barrel precursors, suggesting that this POTRA domain plays an important role in assembling other β-barrel proteins in the mitochondrial membrane (*21*). Biochemical studies of truncated variants of Toc75 have also implicated its POTRA domains as docking sites for proteins destined to be targeted to, or across, biological membranes (*22*). No structure of a POTRA domain has yet been reported.

We expressed and purified the periplasmic domain of *E. coli* YaeT containing all five POTRA domains ($YaeT_{21-420}$) (*23*, *24*). Crystallization of this construct was unsuccessful, but a shorter fragment containing four POTRA domains (residues 21 to 351) yielded well-ordered crystals with diffraction to spacings of 2.2 Å (*23*, *24*).

The overall structure of $YaeT_{21-351}$ has a fishhook-like shape, with successive POTRA domains rotated in a right-handed direction (Fig. 2, A and B). Despite having low sequence similarity, the POTRA domains have similar

[1]Department of Chemistry and Chemical Biology, Harvard University, Cambridge, MA 02138, USA. [2]Department of Molecular Biology, Princeton University, Princeton, NJ 08544, USA. [3]Department of Biological Chemistry and Molecular Pharmacology, Harvard Medical School, Boston, MA 02115, USA. [4]Howard Hughes Medical Institute and Children's Hospital Laboratory of Molecular Medicine, Boston, MA 02115, USA.

*To whom correspondence should be addressed. E-mail: kahne@chemistry.harvard.edu

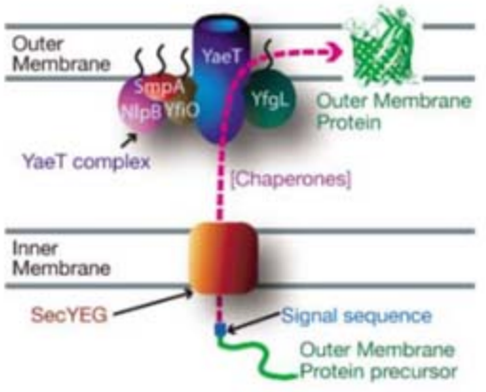

Fig. 1. Diagram of bacterial outer membrane protein (OMP) biogenesis.

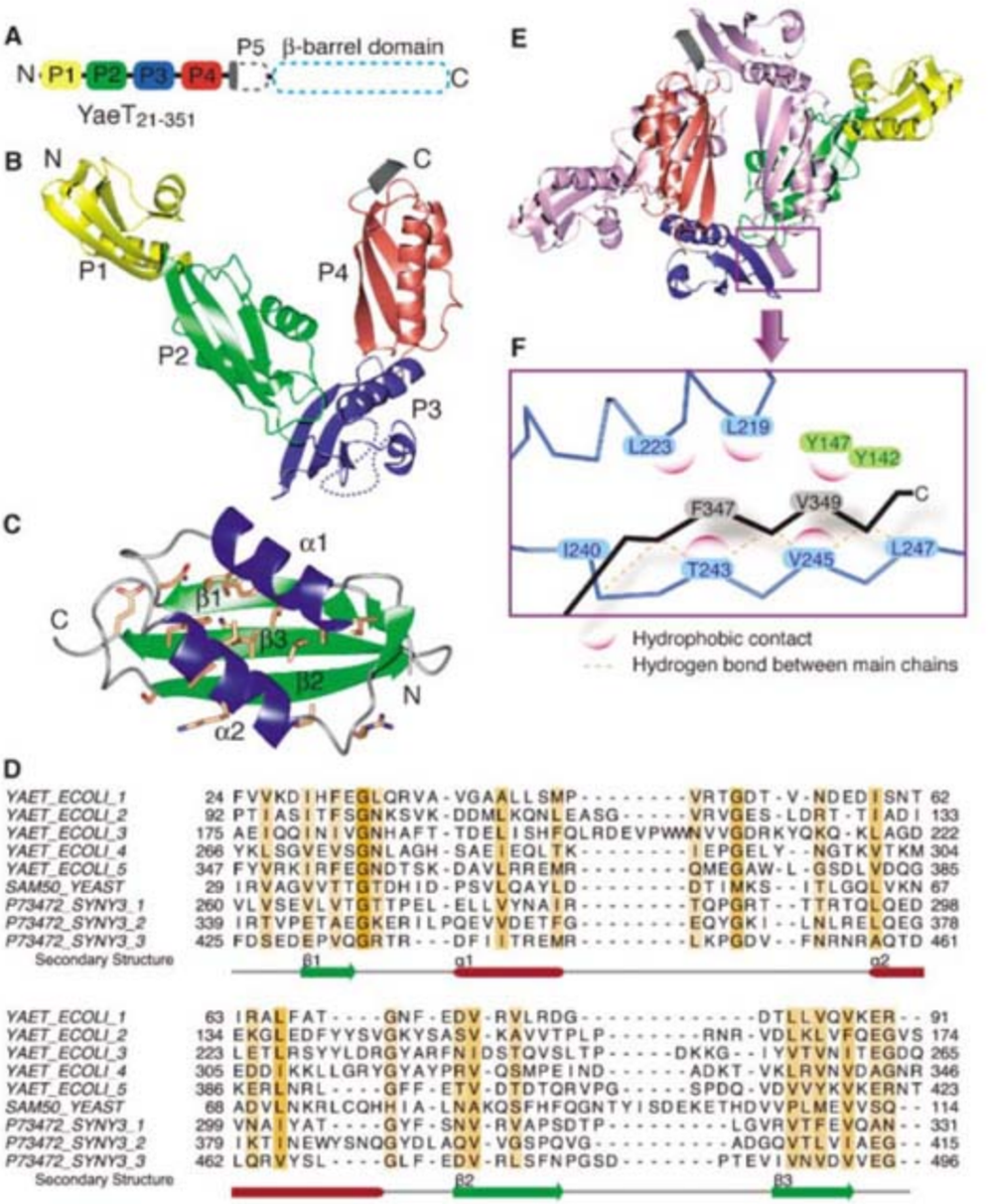

Fig. 2. Structure of YaeT. (**A**) Domain organization. (**B**) X-ray structure of $YaeT_{21-351}$. POTRA domains P1 to P4 are colored yellow, green, blue, and red, respectively. The eight residues from P5 are colored gray. The missing electron density in the P3 domain is represented by a dashed line. (**C**) Ribbon diagram of a POTRA domain (P2) with side chains of the conserved residues shown. (**D**) Sequence alignments of POTRA domains from selected members of the YaeT/Omp85, Sam50, and Toc75 families, found in Gram-negative bacteria, mitochondria, and chloroplasts or cyanobacteria, respectively [adapted from Sánchez-Pulido *et al.* (*14*)]. Conserved residues are highlighted (*28*). The intensity of the orange color reflects the level of conservation in physicochemical properties. (**E**) X-ray structure of the dimer. The POTRA domains in one monomer are colored as in (B); the other monomer is purple. (**F**) Dimer interface showing the C-terminal residue contacts of one monomer (gray) to the P2 (light green) and P3 (light blue) domains of the other monomer. Labels represent hydrophobic residues. L, Leu; Y, Tyr; F, Phe; V, Val; I, Ile; T, Thr.

folds, comprising a three-stranded β sheet overlaid with a pair of antiparallel helices (Fig. 2C). The order of secondary-structure elements is β-α-α-β-β (disproving a previous prediction) (*14*); the first and second β strands form the two edges of the sheet, with the β3 strand sandwiched between them. The conserved residues that define the POTRA domains are primarily in the hydrophobic core or loop regions, suggesting that they are important for the structural integrity of POTRA domain (Fig. 2, C and D).

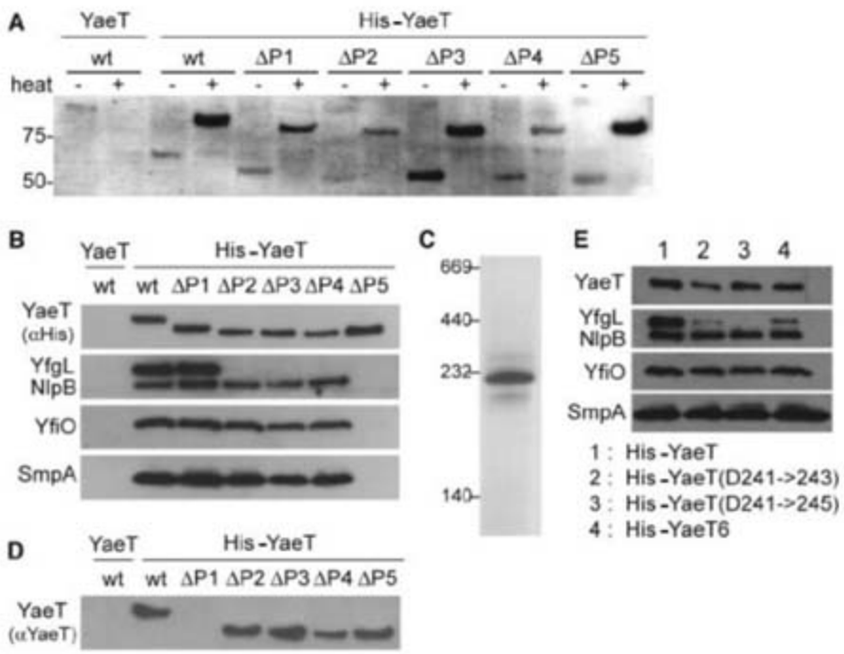

Fig. 3. (**A**) SDS-PAGE analysis of YaeT wild-type (wt) and deletion mutants from whole-cell lysates, without (–) and with (+) prior heat treatment. Proteins were detected by Western blot analysis with the use of an antibody recognizing the His tag. (**B**) His-tagged YaeT wild-type or deletion mutants (ΔP1 to ΔP5) and associated proteins following Ni-affinity chromatography. Eluted samples were blotted against His-tag, YfgL, NlpB, SmpA, and YfiO antibodies. (**C**) The purified YaeT complex run on a Blue-Native PAGE with molecular weights from a standard lane indicated. (**D**) Same as in (B), but YaeT was blotted with an antibody to YaeT. YaeTΔP1 cannot be detected with our YaeT peptide antibody. (**E**) His-tagged wild-type YaeT and P3 mutants after purification by Ni-affinity chromatography and analysis, as in (B).

$YaeT_{21\text{-}351}$ is a dimer in the crystal (Fig. 2E). The two monomers are intertwined, burying 1900 $Å^2$ of solvent-accessible surface of each monomer. The longest contiguous set of contacts between monomer units involves a series of main-chain hydrogen bonds between the β2 edge of the P3 domain of one monomer (Asp^{241} to Leu^{247}) and the first residues (Asn^{345} to Lys^{351}) of the truncated P5 domain of the other monomer (Fig. 2F). These residues form a parallel β strand with respect to the β2 edge of the P3 domain and bury ~1000 $Å^2$, more than half the total buried surface. There are no other extensive contacts between monomers, suggesting that dimerization is mediated by this parallel β-stranded interface. Formation of this interface may have been necessary for growth of well-ordered crystals given that slightly shorter ($YaeT_{21\text{-}348}$) or longer ($YaeT_{21\text{-}355}$) constructs failed to crystallize. Nonetheless, highly ordered contacts are conserved at the interfaces between successive POTRA domains (fig. S1), suggesting that the fishhook conformation is present in the monomer.

We do not think that the dimer is physiologically relevant for several reasons. First, $YaeT_{21\text{-}351}$ elutes as a monomer from a size exclusion column (fig. S2), implying that the stability of the dimer observed in the crystal is weak. Second, the N terminus of P5, which forms one of the β strands of the dimer interface, would not be available to interact with P3 in the full-length protein because the interacting residues

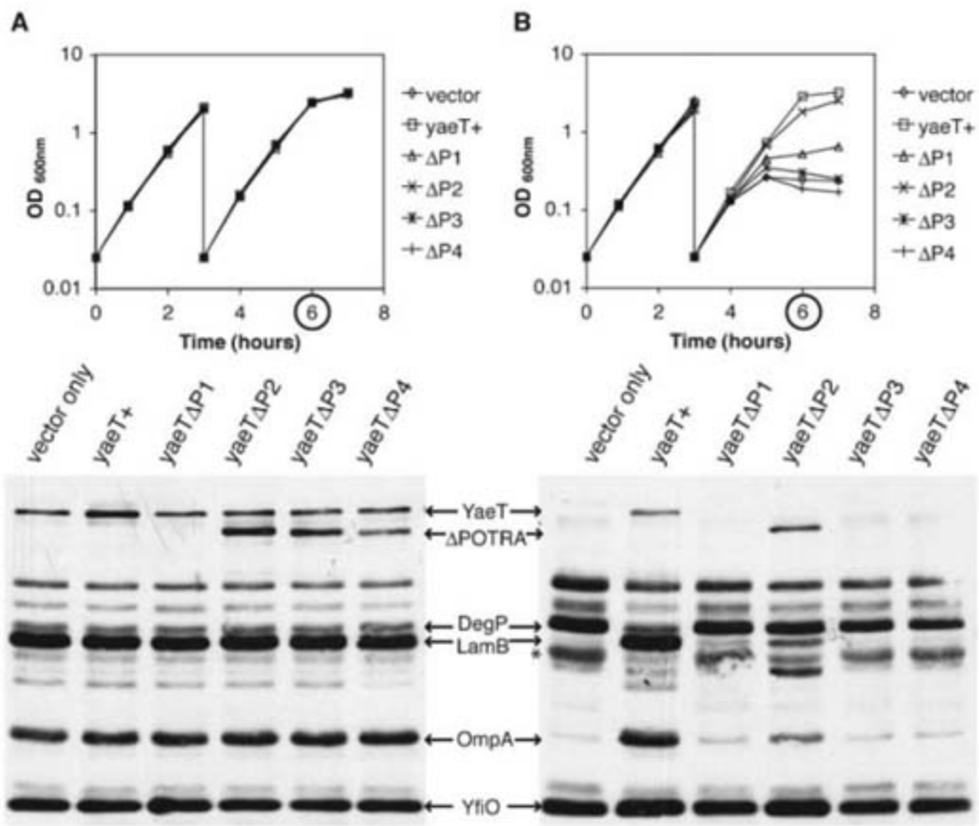

Fig. 4. Essentiality of POTRA domains. Cultures were grown with L-arabinose (**A**) or D-fucose (**B**) to induce or inhibit wild-type *yaeT* expression, which is driven by the ara P_{BAD} promoter (*5*). Plasmid-borne *yaeT* variants were constitutively expressed. Samples taken after 6 hours were subjected to Western analysis. (**A**) Strains expressing plasmid-borne *yaeT* variants grew normally when wild-type *yaeT* was expressed. YaeTΔP1 cannot be recognized with our YaeT peptide antibody (Fig. 3). Strains have low levels of DegP and normal OMP levels (LamB and OmpA). (**B**) When wild-type YaeT is absent, strains producing mutant YaeT variants exhibit growth defects. Strains expressing ΔP1 and ΔP2 grow better and have higher levels of OMPs than ΔP3, ΔP4, and the vector-only control. Although levels of ΔP1 cannot be quantified, ΔP2 is stable, indicating insertion into the membrane even in the absence of wild-type YaeT. Nevertheless, all strains lacking wild-type YaeT exhibit a strong extracytoplasmic stress response (increased DegP) indicative of OMP-assembly defects. Asterisk in (B) corresponds to proteolyzed DegP. OD, optical density.

would be buried in the P5 hydrophobic core. Nevertheless, the dimer interface shows that one way in which other polypeptides can interact with POTRA domains is by β augmentation (*25*).

The lipoproteins in the OMP assembly complex reside in the periplasmic space along with the five POTRA domains of YaeT. One function of the POTRA domains in YaeT could be to provide a scaffold to organize these lipoproteins. Using the crystal structure as a guide, we prepared five N-terminally His-tagged YaeT deletion constructs, each lacking a POTRA domain. All five deletion constructs (YaeTΔP1 to YaeTΔP5) could be expressed in an *E. coli* strain containing a wild-type chromosomal *yaeT* gene; all were targeted to the outer membrane and folded as judged by heat modifiability (Fig. 3A). Each deletion construct was purified by Ni-affinity chromatography, and eluents were assayed to determine which lipoproteins were present. Any of the first four POTRA domains can be deleted without disrupting the interactions with YfiO, NlpB or SmpA; however, the P5 deletion loses all three of these lipoproteins (Fig. 3B). YfgL disappears when any POTRA domains except P1 are deleted (Fig. 3B). These studies show that the periplasmic portion of YaeT scaffolds the other four proteins; and the studies also outline the spatial organization of the OMP assembly complex. Although YaeT purified from inclusion bodies is reported to form higher-order oligomers (*20*), the multiprotein OMP assembly complex behaves as a monomer. It has a mobility on Blue-Native polyacrylamide gel electrophoresis (PAGE) corresponding to a mass less than 230 kD (Fig. 3C). Furthermore, wild-type YaeT does not associate with the His-tagged YaeT POTRA domain deletion mutants (Fig. 3D).

To assess the functional importance of each POTRA domain, we constructed five POTRA domain deletion mutants without His tags for complementation studies in an *E. coli* YaeT-depletion strain. The ΔP1 and ΔP2 mutant proteins retained partial function: Strains expressing these proteins can survive YaeT depletion but grow poorly (Fig. 4). Strains producing the ΔP3 and ΔP4 mutant proteins did not survive YaeT depletion (Fig. 4), showing that P3 and P4 are essential for viability even though neither scaffolds an essential lipoprotein. The ΔP5 construct could not be introduced into the YaeT-depletion strain even under conditions where wild-type YaeT was expressed. Apparently, the ΔP5 mutant protein is toxic to cells in this context. Because we cannot detect an interaction between the mutant protein and wild-type YaeT or any of the lipoproteins, we suggest that ΔP5 mishandles nascent β-barrel substrates, producing harmful misfolded or aggregated OMPs.

P3 has a feature not present in the others—a β bulge (Ile^{240} and Asp^{241}) in strand β2. This strand is at the edge that binds the vestigial residues of P5, and the bulge appears to expose the strand for β augmentation. To determine whether this feature of P3 is involved in an essential function of YaeT or in its association with YfgL, we moved Asp^{241} two and four residues along the β strand to alter the likely location of the bulge and to reduce or disrupt the potential for β augmentation. These bulge translation mutants were expressed at wild-type levels. The two- and four-residue shifts decreased and abolished, respectively, binding to YfgL (Fig. 3E), but both mutants complemented the YaeT deletion strain. These results show that the edge of P3 participates in binding YfgL but that the essential functions of P3 do not involve the modified edge of the domain, nor do they require its interactions with YfgL, as expected from the nonessential nature of this lipoprotein.

The crystal structure may also hold clues to other functionally important regions of P3. The only residues in the polypeptide chain that are not resolved in the crystal structure are located within the loop between the α1 and α2 helices of P3. We have previously isolated a mutant that encodes a YaeT variant, YaeT6, which contains a two–amino acid insertion in the same region of the α1-α2 loop (*12*) of P3. YaeT6, which retains the ability to bind YfgL (Fig. 3E) as well as the other three proteins of the OMP assembly complex, compromises OMP assembly in a wild-type background, but suppresses the outer membrane permeability defects conferred by *imp4213*, a mutant allele of an essential gene that encodes an OMP that is required for lipopolysaccharide assembly (*26*). The α1-α2 loop of P3 may interact with Imp, providing an explanation for why mutations that alter the loop suppress the permeability defects caused by *imp4213*.

Notably, β-strand augmentation (*25*), observed in the dimer interface of the YaeT crystal structure, occurs in other complexes that bind unfolded OMPs—for example, the PDZ domain of DegS, which helps clear misfolded OMPs from the periplasm (*27*). We have shown that P3 may bind YfgL in this way, and it is possible that other POTRA domains, which also contain exposed edges, interact with polypeptides by β-strand augmentation. This mode of capture would allow POTRA domains to participate in assembling the β barrels of OMPs in a manner that is insensitive to the diversity of their primary sequences but dependent on their common hydrophobic periodicity.

References and Notes

1. W. C. Wimley, *Curr. Opin. Struct. Biol.* **13**, 404 (2003).
2. S. Reumann, J. Davila-Aponte, K. Keegstra, *Proc. Natl. Acad. Sci. U.S.A.* **96**, 784 (1999).
3. R. Voulhoux, M. P. Bos, J. Geurtsen, M. Mols, J. Tommassen, *Science* **299**, 262 (2003).
4. S. A. Paschen *et al.*, *Nature* **426**, 862 (2003).
5. T. Wu *et al.*, *Cell* **121**, 235 (2005).
6. N. Wiedemann *et al.*, *Nature* **424**, 565 (2003).
7. V. Kozjak *et al.*, *J. Biol. Chem.* **278**, 48520 (2003).
8. I. Gentle, K. Gabriel, P. Beech, R. Waller, T. Lithgow, *J. Cell Biol.* **164**, 19 (2004).
9. N. Pfanner, N. Wiedemann, C. Meisinger, T. Lithgrow, *Nat. Struct. Mol. Biol.* **11**, 1044 (2004).
10. S. A. Paschen, W. Neupert, D. Rapaport, *Trends Biochem. Sci.* **30**, 575 (2005).
11. N. Ruiz, B. Falcone, D. Kahne, T. J. Silhavy, *Cell* **121**, 307 (2005).
12. N. Ruiz, T. Wu, D. Kahne, T. J. Silhavy, *ACS Chem. Biol.* **1**, 385 (2006).
13. J. G. Sklar *et al.*, *Proc. Natl. Acad. Sci. U.S.A.* **104**, 6400 (2007).
14. L. Sánchez-Pulido, D. Devos, S. Genevrois, M. Vicente, A. Valencia, *Trends Biochem. Sci.* **28**, 523 (2003).
15. A. K. Veenendaal, C. van der Does, A. J. Driessen, *Biochim. Biophys. Acta* **1694**, 81 (2004).
16. J. E. Mogensen, D. E. Otzen, *Mol. Microbiol.* **57**, 326 (2005).
17. S. Moslavac *et al.*, *FEBS J.* **272**, 1367 (2005).
18. W. T. Doerrler, C. R. Raetz, *J. Biol. Chem.* **280**, 27679 (2005).
19. J. Werner, R. Misra, *Mol. Microbiol.* **57**, 1450 (2005).
20. V. Robert *et al.*, *PLoS Biol.* **4**, e377 (2006).
21. S. J. Habib *et al.*, *J. Cell Biol.* **176**, 77 (2007).
22. F. Ertel *et al.*, *J. Biol. Chem.* **280**, 28281 (2005).
23. Residues 1 to 20 represent the signal sequence.
24. Materials and methods are available as supporting material on *Science* Online.
25. S. C. Harrison, *Cell* **86**, 341 (1996).
26. M. P. Bos, B. Tefsen, J. Geurtsen, J. Tommassen, *Proc. Natl. Acad. Sci. U.S.A.* **101**, 9417 (2004).
27. C. Wilken, K. Kitzing, R. Kurzbauer, M. Ehrmann, T. Clausen, *Cell* **117**, 483 (2004).
28. M. Clamp, J. Cuff, S. M. Searle, G. J. Barton, *Bioinfomatics* **20**, 426 (2004).

29. This work is supported by NIH grants GM66174 (D.K.) and GM34821 (T.J.S.). S.C.H. is a Howard Hughes Medical Institute investigator. Data was collected at beamline ID19 at the Advanced Photon Source, Argonne National laboratory, which is supported by the U.S. Department of Energy, under contract no. W-31-109-ENG-38. We thank J. J. Miranda and R. Meijers for technical support. Coordinates and structure factors have been deposited in the Protein Data Bank with the accession codes 2QCZ and 2QDF.

Supporting Online Material

www.sciencemag.org/cgi/content/full/317/5840/961/DC1
Materials and Methods
Figs. S1 to S3
Tables S1 and S2
References

18 April 2007; accepted 3 July 2007
10.1126/science.1143993

Dynamic Live Cell Research

The Leica AM TIRF MC (total internal reflection fluorescence, multi-color) allows the entire fluorescence excitation spectrum to be used for real-time visualization of live cell dynamics. Leica's unique scanner sensor automatically matches the TIRF angle at all wavelengths to the required penetration depth, and positions the laser so that the TIRF penetration depth remains constant even when the wavelength is changed. The Leica AM TIRF MC integrates four solid-state lasers for the excitation of fluorophores at wavelengths from 405 nm to 632 nm. The system features extremely short switching times and an ultra-high synchronized frame rate. For the scientist, this means flexibility for experiments with multiple fluorophores. The system is particularly useful for exploring molecular interactions at cell membranes and molecular interactions of proteins and receptors involved in transport mechanisms. With this instrument, a scientist can examine single molecules near the cell membrane, study co-localization and vesicle transport, and combine TIRF and fast fluorescence resonance energy transfer.

Leica Microsystems For information +49 (0) 6441/29-2550 www.leica-microsystems.com

Spectrophotometer Cells

Spectrophotometer cells with precisely controlled path lengths down to 8 microns are available. These cells are suitable for the measurement of low transmittance samples when dilution is not an option. To achieve the required accuracy, path length is measured by near-infrared interferometry. Using this technique, absolute path lengths in the range of 8 to 200 μm can be measured with an uncertainty budget of ±0.2 μm. This is an order of magnitude better than is achievable using mechanical measurement techniques. The windows are ultraviolet-grade quartz and the cells are available in fully fused, demountable, and flow cell formats. They can be used in any conventional spectrophotometer.

Starna Scientific For information +44 (0) 20 8501 5550 www.starna.com

Allprotect and AllPrep

Allprotect Tissue Reagent immediately stabilizes DNA, RNA, and protein in tissue samples for long-term storage without freezing. The AllPrep DNA/RNA/Protein Mini Kit allows simultaneous purification of these three analytes from the same sample. Immediately submerging fresh tissues in Allprotect Tissue Reagent preserves the in vivo profile of DNA, RNA, and protein is preserved. Tissues are stabilized at room temperature and can be safely stored for up to six months at 2 to 8° C or longer at −20° C or −80° C. Tissues also remain stabilized at 15 to 25° C for up to seven days, allowing shipment without ice. With the AllPrep DNA/RNA/Protein Mini Kit, separate fractions of DNA, RNA, and protein are simultaneously purified from the same tissue sample in a simple spin-column–based procedure without phenol and acetone. There is no need to split the sample into three parts prior to purification. Genomic DNA and total RNA purified using Allprotect and AllPrep deliver optimal performance in all downstream applications.

Qiagen For information 800-426-8157 www.qiagen.com

Whole Transcriptome Kit

The Quantitect Whole Transcriptome Kit delivers high and reproducible complementary DNA (cDNA) yields from limited amounts of RNA by whole transcriptome amplification. The cDNA is intended for use in real-time polymerase chain reaction (PCR) and contains uniformly amplified targets to ensure reliable gene expression analysis. Comprehensive gene expression analysis of rare samples is often not possible due to low RNA amounts. The QuantiTect Whole Transcriptome Kit overcomes this by amplifying all messenger RNA transcripts in a sample. From as little as 1 ng RNA, up to 40 μg cDNA is generated for unlimited real-time PCR analysis and archiving. The kit achieves highly uniform amplification of all mRNA transcripts. The 5′ and 3′ regions of each transcript are equally amplified, and the relative abundance of each transcript is preserved after amplification. This ensures unbiased results in subsequent gene expression analysis.

Qiagen For information 800-426-8157 www.qiagen.com

High Resolution Image Analyzer

The G:BOX Chemi XL automated image analyzer is suitable for producing precise images of protein immunoblots labeled with any Qdot color. This new instrument features a high resolution (5.5 megapixel) 16-bit charge-coupled device, cooled camera with digital zoom inside a dark room fitted with a motor driven sample stage. When Syngene's nine-position filter wheel, lighting unit, and Qdot filter options are added, the system can provide fast, accurate imaging of multiple Qdot antibodies on the same blot without the need for re-probing the sample. The camera features an ability to separate close, different colored band images. It includes easy-to-use image analysis and image capture software. More researchers are using Qdots to label protein immunoblots because they can tag their proteins with different colored fluorescent markers on one blot, which makes it easier to differentiate total and post-translationally expressed proteins, but requires an imager that can visualize different fluorescent wavelengths.

Syngene For information +44 (0) 1223 7727123 www.syngene.com

Genetic Research Database

The iControlDB is the first industry-hosted genotyping control repository for use by researchers conducting case–control whole-genome association studies. Case–control studies compare groups of patients who already have a disease (case) with a group of patients without the disease (control) to identify risk factors that may contribute to a medical condition. The iControlDB provides a cost-efficient and quick way for investigators to obtain control samples, allowing them to focus resources on genotyping disease samples. Combined with the database of Genotype and Phenotype, the new database enables the scientific community to access nearly 10,000 control samples that have been donated by researchers using Illumina's technology for single-nucleotide polymorphism genotyping.

Illumina For information 312-997-2436 www.illumina.com/iControlDB

Newly offered instrumentation, apparatus, and laboratory materials of interest to researchers in all disciplines in academic, industrial, and government organizations are featured in this space. Emphasis is given to purpose, chief characteristics, and availability of products and materials. Endorsement by *Science* or AAAS of any products or materials mentioned is not implied. Additional information may be obtained from the manufacturer or supplier.

Zooming in. Catherine Wu at Dana-Farber Cancer Institute forged her own path in translational research, but new training programs are making that career path easier.

Carving a Career in Translational Research

An influx of public and private funding is invigorating a field that challenges some traditional notions of science

As a first-year hematology-oncology fellow at Dana-Farber/Partners CancerCare 10 years ago, Catherine Wu recognized that if she wanted to bridge research and clinical practice, she needed to understand her options. Every day for 2 months, she questioned senior and junior faculty members on the basic and clinical ends of the research spectrum—no small task for someone working 13-hour days, typically without a break.

She ultimately chose to study leukemia patients' immune responses to bone marrow transplants, an area conducive to translational research in part because the work involves treating patients with human cells, which can be prepared at academic health centers. Now a medical oncologist at the Dana-Farber Cancer Institute in Boston, Wu is professionally fulfilled by work that involves a steady interplay between clinic and lab. "There is something truly incredible about seeing whether your patients benefit from the therapy that you've devised," she says. "It inspires you to do better, to think more broadly, to generate the tools that you need to understand what's going on in your patients."

Bridging the divide that separates laboratory biomedical research from improvements at the clinic has always been difficult. Now, translational research has emerged as a field in its own right, aided in large part by the National Institutes of Health (NIH) Roadmap for Medical Research, a collection of initiatives that prioritize efforts to shepherd biomedical discoveries into clinical application. As translational research has gained momentum, training opportunities in the field have expanded rapidly.

Still, embarking on a career in translational research is hazardous, says Anthony Hayward, clinical research director for NIH's National Center for Research Resources. "It's a tremendous leap of faith for young investigators to commit themselves to translational research. It takes a special sort of person; you have to be willing to take risks."

Follow the money

Part of that risk is in funding: Budgets for biomedical research are tight and may remain so for several years. However, funding for translational research appears to be growing. Perhaps the most visible evidence of growth is NIH's new Clinical and Translational Science Awards (CTSA) program. The first 12 CTSAs were bestowed last October, and more will be announced in September. NIH plans to fund 60 awards altogether, worth about $500 million annually by 2012. CTSAs are required to include training and career-development components, and the initial dozen devote about 13% of their budgets to these areas.

"This is what American medicine has tried to do for many, many years," says Robert Rizza, who directs the recently awarded CTSA program at the Mayo Clinic in Rochester, Minnesota.

Training opportunities abound

M.D.-Ph.D. programs are one obvious approach to training young investigators who want to do translational research. An M.D. degree followed by a research fellowship or a postdoc is another.

But institutions all over the United States are developing shorter, more integrated programs that cater to both physicians and Ph.D. scientists. The Mayo Clinic, for example, offers a master's program and a 1-year certificate program in clinical and translational science, both aimed mostly at M.D.'s. Demand for these programs, both now integrated into Mayo's CTSA, has mushroomed, says Sherine Gabriel, director of education resources at the Mayo Clinic's CTSA. "There is such a hunger to do this," Gabriel says. "My biggest challenge is dealing with the queue outside my door." The master's program in clinical and translational science, she says, enrolls more students than all other master's programs at Mayo together.

Other research-oriented programs, many funded by private foundations, try to capture the interest of M.D.'s earlier. The Howard Hughes Medical Institute (HHMI) in Chevy Chase, Maryland, operates two programs that allow medical students to take a year out of medical school to conduct basic laboratory research. The Doris Duke Charitable Foundation in New York City runs a similar program focused on clinical research. Some schools also independently offer such "1 year out" programs.

Translational research training for Ph.D. scientists has been getting more attention, too. Gary Koretzky, associate director of the University of Pennsylvania's M.D.-Ph.D. program, says institutions have started to recognize that "if you give [basic scientists] the vocabulary of medicine and a sense of how physicians think about problems that they encounter with patients, they'll find it easier to do research that is both scientifically

CREDIT: COURTESY OF CATHERINE WU

rigorous and relevant to disease processes and patient care."

M.D.-Ph.D. neurobiologist Ben Barres, who directs a new master's of medicine program for science Ph.D. students at Stanford University in Palo Alto, California, welcomes the shift. Students do the math, Barres says, and "realize that if they did all the traditional training for both degrees, they'd be almost 40 before they finished. It's just too much."

Stanford's program is one of 13 new "Med Into Grad" programs that HHMI launched last year. Students complete the same 1½-year course sequence that all medical students complete, taking classes alongside med students while also working on Ph.D. requirements. Other Med Into Grad programs offer more targeted pieces of the medical school curriculum to science students—for example, steering neuroscience students toward neuroanatomy courses.

These programs are still in their early years, but it's evident that they will be popular. Barres says Stanford's program has been flooded with applications. "There's been a sea change of interest from the Ph.D. students compared with 5 or 10 years ago," he says. Twenty percent of incoming Ph.D. students from Stanford's biosciences programs applied for the program in its first year, Barres says.

Other options are proliferating. This year the Mayo Clinic, like many other CTSA recipients, enrolled its first students in a new Ph.D. program in clinical and translational science. Students work with a multidisciplinary mentoring team to develop research projects and take on a core curriculum that includes rotations in bench science, patient-based clinical research, and population-based research. Coursework is designed to build skills in designing clinical trials, responsible conduct of research, and grant writing. "We want students to explore questions that cross disciplinary boundaries, then develop research projects that are every bit as deep and rigorous as any traditional research project," says Gabriel.

Funding independent research

The transition from trainee to independent investigator is a particularly vulnerable point in a translational researcher's career. William Crowley, director of clinical research for Massachusetts General Hospital in Boston, observes that, although NIH's many programs to support training in clinical and translational research have been "spectacular," the academy is now filled with well-trained translational researchers, all trying to land independent research grants just as the NIH pay line is plummeting. "We're about to lose a generation of young translational investigators," he says.

To avert that outcome, "we need long, steady investments in translational research, not dramatic ups and downs," says Queta Bond, president of the Burroughs Wellcome Fund (BWF) in Research Triangle Park, North Carolina. Her organization and others have stepped in to help. BWF's Career Awards for Medical Scientists provide $700,000 over 5 years to bridge postdoctoral or fellowship training and the early years of independent research. BWF Clinical Scientist Awards in Translational Research provide $750,000 over 5 years to faculty members in the late-assistant-professor or early-associate-professor stages of their careers. The intention of the translational awards, says Bond, is to buy time for junior faculty members "to keep them in research and keep them training younger investigators." Last year, HHMI gave out its first early-career awards—initially to 13 investigators, a group that soon expanded to 20. Awardees receive $375,000 over 5 years.

CREDIT: COURTESY OF BEN BARRES

Translational training. Ben Barres of Stanford directs a new master's of medicine program for science Ph.D. students.

The pharmaceutical industry is another potential player in providing career support for young investigators, but so far it's untapped. The Clinical Research Forum, a consortium of leading academic health centers headed by Crowley, has asked pharmaceutical companies for a combined $10 million per year for 3 years (the minimum length of time the group expects NIH budget problems to persist), to create "bridging awards" for young investigators who have completed an NIH clinical research training grant, have narrowly missed receiving funding for an independent grant, and are employed at institutions that will match the funding and allow recipients to spend at least 75% of their time on research.

It's a creative strategy, but Crowley won't place odds on the initiative's success. "I just don't know how pharma views its collective social responsibility," he says. Some companies have indicated interest, he says, but "no checks are in the mail."

Translating success into tenure

Scarce funding isn't the only barrier that young translational researchers encounter. Other factors challenge traditional measures of scientific success. For example, grant and tenure success depends on researchers' ability to publish in top journals, but as Wu observes, "translational research deals with patients, and patients aren't a model system. Establishing causality is always a challenge. It's not a slam-dunk that you're going to get into *Science* or *Nature*."

Some translational researchers worry that their individual efforts on multidisciplinary teams will go unrecognized, hindering chances for promotion and grant success. In 2006, NIH began accepting grant applications that identify more than one principal investigator, a measure that may partially address this concern.

Physician-scientists—an important part of the translational-research work force—face mounting pressure to generate income through patient care. That makes it tougher than ever to carve out time for research, says William Galey, HHMI's director of graduate and medical education. Crowley adds that complex and conflicting requirements from multiple regulatory bodies "make translational research look as daunting to a young investigator as a steeplechase racecourse looks to a horse."

These obstacles and others add up to the conclusion, Crowley says, that "there's a lot of easier ways to make a living." Nevertheless, he says, "there has never been a better time or opportunity to do good and alleviate human suffering by research than now. If I have one regret about my career in translational research, it's that I'm not 30 years younger."

Time will tell whether institutions and funding agencies will sustain support for translational research and continue to plumb the storehouse of basic biomedical advances to help sick people. Meanwhile, researchers entering the fray should do so with optimism and caution. And, Wu advises, "go with what you passionately care about, because it's a long row, no matter how you hoe it."

–SIRI CARPENTER

Siri Carpenter is a freelance science writer in Madison, Wisconsin.

Translational Institute Unites Unlikely Partners at Penn

Translational research breaks barriers between the lab and the clinic and, at one institute, brings together some unlikely collaborators

The Hospital of the University of Pennsylvania and the Children's Hospital of Philadelphia (CHOP) sit side by side on the south edge of campus. But a few years ago, when they launched a joint translational research initiative, the separation loomed like an ocean. The two hospitals have completely separate finances, and their research arms compete with each other. So getting them to collaborate, says Penn pharmacology professor Garret FitzGerald, was like "Franco-German rapprochement."

FitzGerald is director of Penn's Institute for Translational Medicine and Therapeutics (ITMAT), launched in 2005 to unite and expand clinical and translational research programs across the Penn campus, including those at the two hospitals. Last year, Penn was one of a dozen institutions awarded a National Institutes of Health (NIH)–sponsored Clinical and Translational Science Award (CTSA), a $68 million, 5-year grant (see p. 966). Penn is investing $30 million of its own money in the effort.

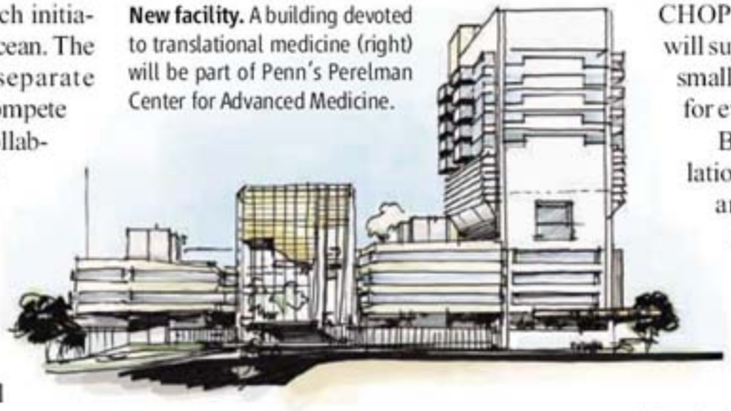

New facility. A building devoted to translational medicine (right) will be part of Penn's Perelman Center for Advanced Medicine.

Despite some "bumpy bits" during negotiations between Penn and CHOP, says FitzGerald, "[we] have worked more and more together, and this has gone extremely well."

Establishing research and training

Building infrastructure to support translational investigators is key. "The previous model before was, you do the whole thing yourself," notes Carl June, director of translational research at the Abramson Cancer Center at Penn. But tougher regulatory requirements and more complex science now make that impossible. To help investigators, Penn employs clinical trial application specialists and has core facilities in everything from bioinformatics to proteomics, as well as a translational imaging center. Meanwhile, CHOP is constructing a new building that will support mouse model work—including small-animal imaging—which is essential for evaluating new cancer therapies.

Because the skills needed for translational science are so diverse, FitzGerald argues for a completely new "interdisciplinary" discipline. Penn offers a master's degree in translational research and a joint MTR-Ph.D. program. In addition, Penn has a grant from the Howard Hughes Medical Institute in Chevy Chase, Maryland, to develop courses to expose Ph.D. students to clinical research to inspire them to find cures for diseases.

In terms of research experience, Penn offers seven fellowships for translational

EUROPEAN PROGRAMS OFFER TRANSLATIONAL TRAINING

Birgit Pless got her first glimpse of translational research in 2003 when, as a student working toward a master's degree, she did an internship at Berlin's Benjamin Franklin University Hospital. She spent the summer searching for new drugs for inflammatory bowel diseases. Once she had been dazzled by the bright promise of helping patients in their daily life, basic research paled.

But it wasn't until April of this year that she found another training opportunity in translational research. That was when she heard about the new, Frankfurt-based International Research Graduate School for Translational Biomedicine (FIRST), where she just enrolled this summer. "Only [FIRST] combined basic research with applied medicine and taught pharmaceutical basics," she says.

Translational research is fast becoming a priority in Europe. The European Commission set the tone by targeting most of its €6 billion health research budget for 2007–2013 at pan-European translational projects. Dedicated training programs such as FIRST are multiplying, but they remain few, vary greatly in approach, and are often works in progress. Three new European programs exemplify the range of approaches to training in translational research.

Injecting medicine into basic science

The new Medical Research Council (MRC) Centre for Translational Research in Neuromuscular Disease, based at University College London (UCL) and Newcastle University, aims to provide a broad understanding of clinical context to influence research questions, says Michael Hanna, a neurologist at UCL's Institute of Neurology. The center, which will open its doors this October under Hanna's direction, received a £3.5 million grant from the MRC to support its first 5 years, including the Ph.D. training of six biology students and two medical doctors.

Basic-science students will get direct contact with clinicians and patients at partner hospitals to pique their interest in research questions relevant to clinical care, Hanna says. Students will spend a year taking introductory courses on neuromuscular disorders and learning neuroscience techniques before starting a 3-year research project.

The two physicians will research a 3-year Ph.D. project in which they will work closer to patients than most basic scientists can, Hanna says. Hanna hopes to soon get more funding for training. "The intention will be to … have a lot more [students] in the future," he says.

A roundtrip, bench-to-bedside

In 2004, the University of Milan–Bicocca in Italy launched an international doctoral program in translational and molecular medicine called DIMET. DIMET connected the department of biotechnology and biosciences with the faculty of medicine so students could move easily between basic and applied biomedical research.

Some DIMET students' projects take a disease-driven approach, whereas others start with a basic finding and aim to develop clinical applications. Combining the two approaches is as fundamental for translational researchers as it is challenging, says DIMET coordinator Andrea Biondi, a clinician and cancer researcher at the university.

Some science students got to work at the interface between the lab and the clinic. After generating T cells against cytomegalovirus, medical

CREDIT: RAFAEL VIÑOLY ARCHITECTS

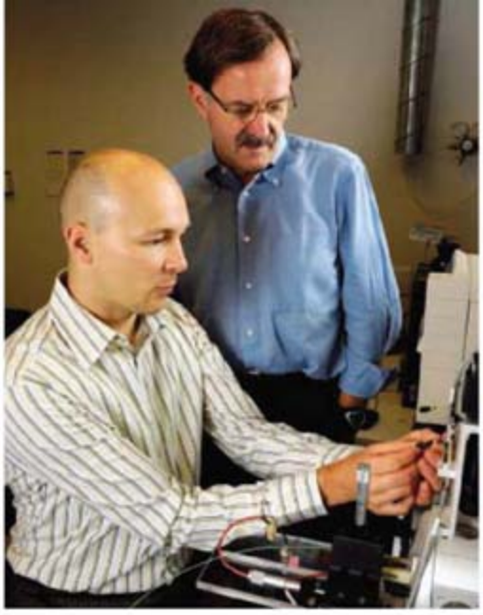

Bench to bedside. Assistant professor Tilo Grosser (*left*) and ITMAT Director Garret FitzGerald are bringing translational research to the forefront at Penn.

research, along with 12 offered through the CTSA, and five more fellowships through NIH T32 research training grants.

To encourage cross-disciplinary research, only researchers from different departments who haven't worked together can qualify for a $150,000 transdisciplinary ITMAT seed grant. Six pairs of senior investigators won grants in the latest funding round.

Penn is trying to push translational research in nontraditional directions. One novel center is Personalized Medicine in Translation (PERMIT). This center will fund the expert staff and facilities needed to examine how genetic variants affect drug response and will give traditional clinical studies a new dimension by identifying which individuals are most likely to benefit or suffer side effects.

FitzGerald's own lab worked out the likely mechanism of Cox-2 inhibitor cardiac toxicity, and PERMIT is designed to detect and individualize such problems before drug launch, not after. FitzGerald is now probing why people differ in their response to all nonsteroidal anti-inflammatory drugs.

Cautions

As a postdoc in FitzGerald's lab, Tilo Grosser played a big role in the Cox-2 work. He is now an assistant professor setting up his own lab at Penn, and he just applied for his first R01 grant. Grosser knows that a career in translational research is risky compared to basic science. "I am aware of the issues, particularly the [smaller] number of publications," he says. "These studies take a lot of time." Grosser points out that a single small clinical trial looking at drug-response variability could take 3 years, including patient screening and data analysis. And clinical research involves sharing credit, which could also devalue his accomplishments.

"I have seen several instances since I've been at [Penn] where promising translational researchers had to go back and just do basic research in order to assure their promotion," says June. "That's not good." Grosser thinks that the breadth of clinical research opportunities at Penn, encompassing genomics, mechanistic work, and animal modeling, makes such career setbacks less likely.

Although tenure committees at Penn are still dominated by R01-type scientists, says FitzGerald, they are gradually taking into account the team contributions and lower publication rates among translational researchers. "That's an ongoing issue," June says.

Thomas Curran, a CHOP neurobiologist, cancer researcher, and ITMAT member, agrees that fears of failed clinical trials and nonexistent publications are real, but they shouldn't be career killers. "First, if you have all of those concerns, you're in the wrong job, because this is a risk-taking enterprise," he says. "Second is, plan for success, never plan for failure. … Come into it with the attitude [that] whatever you do, you're going to do the highest quality [work], and you're going to be successful—recognizing there's an element of doubt."

–KEN GARBER

Ken Garber is a freelance writer in Ann Arbor, Michigan.

Head first. Birgit Pless is among the first students to attend the Frankfurt-based International Research Graduate School for Translational Biomedicine.

biotechnologist Erica Dander, 26, wrote in collaboration with her multidisciplinary team a successful clinical trial protocol to test whether injecting the T cells could kill infected cells in transplant patients. Working at the nearby San Gerardo Hospital, she was "in the right environment to find help" with the protocol, she says.

The program's biggest limitation is its budget, Biondi says; it only receives a few thousand euros a year from the university, and most scholarships are raised by the participating professors. Still, DIMET will enroll 25 students for the next academic year. "We are just at the beginning, but we have seen from the first year a progressive increase in applications," Biondi says.

Promoting drug development

The FIRST program at the University of Frankfurt aims to address a lack of Ph.D. graduates who really understand the drug-development process, says Dieter Steinhilber, the coordinator of FIRST and a pharmacologist at the university's Institute of Pharmaceutical Chemistry.

Starting in October, scientists will learn about medical science and pharmacology while physicians and pharmacists study molecular and cellular biology. During the 3-year research program, students will also take courses on all the steps of drug development, including preclinical and clinical studies, regulatory affairs, and the marketing of medicines.

To form the program, the science and medicine faculties of the University of Frankfurt partnered with the private Georg Speyer Haus research institute and the Paul Ehrlich Institute, the federal health authority agency for biopharmaceuticals. They also count on pharmaceutical companies to provide additional expertise, traineeships, and €300,000 a year.

This money will complement the annual budget of about €1 million FIRST gathered from the university and the integration of two already-funded pilot Ph.D. programs. Starting in 2008, the university plans to recruit 20 basic scientists and 10 medical doctors each year, provided the German government decides in October to give additional support to the program.

"The opportunity for this career development is now," says Graham Lord, director of translational research development at the National Institute for Health Research Biomedical Research Centre at King's College London and Guy's and St. Thomas' hospitals. "I think the job opportunities that follow on that will be very substantial."

–ELISABETH PAIN

Elisabeth Pain is a contributing editor for ScienceCareers.org.

CREDITS (TOP TO BOTTOM): DANIEL BURKE PHOTOGRAPHY; JOHANNA BLESS

POSITIONS OPEN

FACULTY OPENING
Stanford University
Department of Chemical Engineering

The Department of Chemical Engineering at Stanford University is seeking applicants for tenure-track faculty positions at the junior level **(ASSISTANT or UNTENURED ASSOCIATE PROFESSOR).** Applicants are expected to have earned a Ph.D. degree in chemical engineering or related disciplines.

We will consider applicants knowledgeable in the general area of chemical engineering science. While all areas encompassed by chemical engineering are acceptable, there are several broad areas of particular interest, including surface reactivity and catalysis, fuel cells, environmental or atmospheric studies, molecular transport processes and mechanics, soft materials physics and chemistry, computation and simulation, biochemical and biomolecular engineering, nanomaterials processing, and the energy sciences. In general, we give higher priority to the overall originality and promise of the candidate's work than to the sub-area of specialization.

The successful candidate will be expected to teach at the graduate and undergraduate level, to develop advanced graduate courses in a research specialty, as well as to develop a world-class research program with an emphasis on the fundamental physical, chemical, and engineering aspects of chemical engineering science. Applicants should be seeking a stimulating interdisciplinary environment in which to pursue teaching and research. We anticipate that the faculty members will contribute to and develop leadership roles and interactions among faculty not only in Chemical Engineering, but also Electrical, Mechanical, Civil and Environmental, and Material Science and Engineering in the School of Engineering; in Physics, Chemistry, and Biology in the School of Humanities and Sciences; in the departments and programs in the School of Medicine, as well as Bioengineering located in the Schools of Engineering and Medicine, and at the Stanford Synchrotron Radiation Laboratory.

Applicants should send curriculum vitae (including research accomplishments, teaching experience, and publications) a transcript of doctoral graduate study, a detailed research and teaching plan, and supporting letters from at least three references to: **Professor Curtis W. Frank, Chair, Search Committee, Department of Chemical Engineering, Stanford University, Stanford, CA 94305-5025.** Applications are due by December 1, 2007, but we will continue to accept applications until the positions are filled.

Stanford University is an Equal Opportunity, Affirmative Action Employer.

CARNEGIE MELLON UNIVERSITY. The Department of Chemistry invites applications for a **TENURE-TRACK POSITION** at the junior level in the area of biophysics/biophysical chemistry. The successful applicant will benefit from the Department's highly collaborative atmosphere, interdisciplinary approach, and its strengths in core areas of experimental and theoretical biophysics. The Molecular Biosensor and Imaging Center, the NIH National Technology Center for Networks and Pathways, and the Pittsburgh Nuclear Magnetic Resonance Center for Biomedical Research also provide attractive opportunities for collaboration. Candidates are expected to build a vigorous externally funded research program and exhibit a very strong commitment to teaching at both the undergraduate and graduate levels. Applications should contain (1) curriculum vitae, (2) a list of publications, (3) a description of research plans, and (4) three letters of recommendation and be sent to **Professor Linda Peteanu** at **e-mail: biophysics-search@andrew.cmu.edu.** Hard copies of this information can also be mailed to: **Dr. Linda Peteanu, Department of Chemistry, Carnegie Mellon University, 4400 Fifth Avenue, Pittsburgh, PA 15213.** Review of applications will begin on October 1, 2007. *CMU is an Equal Opportunity/Affirmative Action Employer committed to building a diverse faculty; women and minorities are strongly encouraged to apply for this position.*

POSITIONS OPEN

The Bioinformatics Research Center at University of North Carolina, Charlotte invites applications for a **DIRECTOR of BIOINFORMATICS SERVICES.** The individual accepting this position will supervise a staff of bioinformatics research specialists who will work in close collaboration with scientists from academia and industry. Successful applicants must hold a Ph.D. in bioinformatics, biology, computer science, or a related field. Experience with managing medium to large-scale bioinformatics or biotechnology projects is preferred. For more information and application instructions, please see our **website:** http://www.coit.uncc.edu/bioinformatics/site/open_positions.cfm. *The University of North Carolina at Charlotte is an Equal Opportunity/Affirmative Action Employer.*

ASSISTANT/ASSOCIATE PROFESSOR
Prion Biology
Colorado State University

The Department of Microbiology, Immunology, and Pathology at Colorado State University is seeking a scientist at the Assistant or Associate Professor level (tenure track) with research interests in the pathogenesis of transmissible spongiform encephalopathies (prion diseases) or amyloid-related diseases. Candidates with expertise in methods in investigative pathology, prion biology, molecular biology, and/or animal models of prion disease are encouraged to apply. The successful applicant will be expected to develop an extramurally funded research program and participate in Departmental teaching activities. Applicants must have a D.V.M., M.D. and/or Ph.D. (or equivalent degree). Postdoctoral research experience is preferred.

Please electronically submit a letter expressing interest and qualifications for the position, curriculum vitae, and arrange to have three letters of reference sent to:

Prion Biologist Search Committee
c/o Mr. Ryan Abbott
(E-mail:ryan.abbott@colostate.edu)
Department of Microbiology, Immunology, and Pathology
Colorado State University
College of Veterinary Medicine and Biomedical Sciences
1619 Campus Delivery
Fort Collins, CO 80523-1619 U.S.A.

Applications will be accepted until the position is filled. However, evaluation of applications will begin November 15, 2007.

CSU is an Equal Opportunity/Affirmative Action Employer.

ASSISTANT PROFESSOR of PHYSIOLOGY

The Department of Physiology of the School of Medicine of the University of Puerto Rico invites applications from scientists for a tenure-track position at the rank of Assistant Professor. Exceptional candidates may be considered for more senior positions. Candidates must have a Ph.D. and/or M.D. with appropriate postdoctoral fellowship training, a strong record of research accomplishments, and the ability to establish and maintain an independent research program that complements existing strengths within the Department. The ideal candidate should have an externally funded research program in the areas of cardiovascular, renal, or endocrine physiology. He/she will also participate in medical, dental, and graduate training. The closing date for applications is October 31, 2007. Applicants should send curriculum vitae, a description of past research and future plans, and the names of three potential references to: **Dr. N. Escobales, Ph.D., Chair, Physiology Search Committee, Department of Physiology, University of Puerto Rico-School of Medicine, P.O. Box 365067, San Juan, Puerto Rico 00936-5067 (e-mail: nescobales@rcm.upr.edu).** *The University of Puerto Rico is a state-funded institution and is an Equal Opportunity/Affirmative Action Employer.*

HUMAN GENETICIST
Tenure-Track/Tenure Position

The newly formed intramural Laboratory of Translational Genomics (LTG) in the Division of Cancer Epidemiology and Genetics (DCEG), National Cancer Institute (NCI), National Institutes of Health (NIH), Department of Health and Human Services (DHHS), is recruiting two tenure-track/tenured investigators. The mission of the LTG is to investigate the genetic basis of strong association signals identified by candidate gene approaches, linkage analyses in high-risk families, or genome-wide association studies (GWAS), particularly loci identified by the ongoing Cancer Genetic Markers of Susceptibility (CGEMS) program involving GWAS of several major cancers. Investigators in the LTG are expected to develop an independent research portfolio in cancer genomics focused on (1) fine mapping and re-sequencing of loci relevant to cancer susceptibility and/or outcomes, (2) investigation into the causal gene variants that provide biological plausibility for each locus, and (3) bioinformatic analyses of publicly available datasets derived from germline annotation of genetic variation and somatic alterations in cancers. Each investigator is expected to leverage the NCI resources in molecular epidemiology, high-throughput genotyping and whole genome scans, biostatistics and bioinformatics, as well as in basic and clinical sciences. The incumbent will receive research support for developing a state-of-the-art genomics laboratory, and recruiting two post-doctoral fellows/bioinformaticians and a technician.

Applicants must have an M.D. and/or Ph.D. in a relevant field, extensive post-doctoral experience, and a record of publications demonstrating potential for creative independent research in human cancer genetics. Facility with bioinformatics databases and high dimensional data are highly desirable along with strong communication skills. Interested individuals should send a cover letter, curriculum vitae and a brief summary of research accomplishments and goals, along with copies of three to five publications or preprints, and three letters of reference to:

Ms. Judy Schwadron, Division of Cancer Epidemiology and Genetics, National Cancer Institute, 6120 Executive Blvd. EPS/8073, Bethesda, MD 20892.

Recommendations can be included with the package or sent directly by the recommender to Ms. Schwadron. Candidates should submit applications by **October 15, 2007**; at this time, the committee will begin to look at suitable candidates. However, the search will continue until qualified scientists are found. Additional information about staff and ongoing research in the NCI Division of Cancer Epidemiology and Genetics is available at **http://www.dceg.cancer.gov**. Please contact **Dr. Stephen Chanock (phone 301-435-7559 at chanocks@mail.nih.gov) or Dr. Peggy Tucker (phone 301-496-8031 at tuckerp@mail.nih.gov)** for questions about the position(s).

Department of Health and Human Services
National Institutes of Health
National Cancer Institute
Postdoctoral Positions in Immune Defense and Transcriptional Regulation

The Laboratory of Cellular and Molecular Biology in the intramural research program of the National Cancer Institute has several postdoctoral positions available for individuals who have obtained a Ph.D. and/or M.D. degree within the past 2 years. These individuals will join a research group that investigates 1) the regulation of RANTES expression in T lymphocytes and 2) the role of granulysin in immune defense. A strong background in molecular and/or cellular immunology is preferred. Excellent written and oral communication skills are essential.

Relevant publications describing recent work from the group include:

- Dynamic interplay of transcriptional machinery and chromatin regulates "late" expression of the chemokine RANTES in T lymphocytes
  Mol Cell Biol. 27(1):253-66 (2007)
  PMID: 17074812

- Granulysin-mediated tumor rejection in transgenic mice
  J Immunol.178(1):77-84 (2007)
  PMID: 17182542

Applicants should submit their curriculum vitae, a brief description of research interests and experience, and contact information for three references to:

Carol Clayberger, Ph.D., Laboratory of Cellular and Molecular Biology, National Cancer Institute, National Institutes of Health, 37 Convent Drive, Room 4016, MSC 4256, Bethesda, MD 20892, E-mail: Claybergerc@mail.nih.gov.

Applications will be considered as they are received, but it is preferred that they be submitted by **October 1, 2007**.

WWW.NIH.GOV

Tenure-Track Investigator Position in the Laboratory of Immunology

The Laboratory of Immunology (LI), Division of Intramural Research, National Institute of Allergy and Infectious Diseases, National Institutes of Health invites applications for a tenure-track investigator position in immunology. Applicants should have a Ph.D., M.D., or equivalent degree; an outstanding record of postdoctoral accomplishment; and an interest in any area of biomedical research related to immunology.

Specifically, we seek a highly creative individual who will establish an independent, forward-looking, world class research program that takes full advantage of the special opportunity afforded by the stable, long-term funding of the Intramural Research Program at NIH. She/he should be interested in developing and applying novel approaches to the study of problems of major biological and /or medical importance, which could include a major clinical research effort. There are ample opportunities to participate in trans-NIH initiatives involving technology development, translational investigation, and multidisciplinary science.

Generous ongoing support for salary, technical personnel, postdoctoral fellows, equipment, and research supplies will be provided. Available cores or collaborative facilities include flow cytometry, advanced optical imaging, microarray generation and analysis, computational biology, production of transgenic and gene- manipulated mice, chemical genomics and support for projects involving RNAi screening. In addition to an outstanding international postdoctoral community, a superior pool of graduate and undergraduate students is available to the successful applicant.

NIAID's Laboratory of Immunology has a distinguished history of accomplishment in immunology. We strongly encourage outstanding early career investigators who can continue and enhance this record of achievement to apply. Current LI principal investigators are Ronald Germain, Michael Lenardo, Rose Mage, David Margulies, William Paul, Ethan Shevach and Tsan Xiao.

Application Process: To apply, e-mail your CV, bibliography, and an outline of a proposed research program (no more than two pages) to **Ms. Wanda Jackson at jacksonwa@niaid.nih.gov or mail to Ms. Wanda Jackson, 10 Center Drive MSC 1356, Building 10, Rm. 4A-26, Bethesda, Maryland 20892-1356. E-mail is preferred**.

Reference Letters: Three letters of recommendation must be sent directly from the referees to **Ms. Wanda Jackson via e-mail or U.S. mail**. Please refer to **Ad #016** on all communications. Further information about this position may be obtained by contacting **Dr. William Paul (301 496-5046; wpaul@niaid.nih.gov)**. Applications must be received by **October 19, 2007**.

A full package of benefits (including retirement, health, life and long term care insurance, 401-k plan) is available. Women and minorities are especially encouraged to apply. U.S. citizenship is not required.

Division of Cancer Biology
Health Scientist Administrator/ Chemist/Microbiologist/Biologist

With nation-wide responsibility for improving the health and well being of all Americans, the Department of Health and Human Services (DHHS) oversees the biomedical research programs of the National Institutes of Health (NIH) and those of NIH's research Institutes.

The National Cancer Institute (NCI) at the NIH is seeking two interdisciplinary scientists at the GS-13 or GS-14 level, one in the Cancer Cell Biology Branch (CCBB) and one in the Tumor Biology and Metastasis Branch (TBMB) of the Division of Cancer Biology. The scientists will serve as Program Directors and oversee an active research grant portfolio and manage a scientific program in cancer biology. Candidates should have significant research experience in an area of cancer biology and be familiar with applications of new molecular technology. Such research experience may focus on a specific tumor type or include more generic in vitro systems. An M.D. or a doctoral level degree in a biomedical related field and evidence of experience in the administration of a science program are highly desirable. The Program Director will perform the full range of administrative and scientific duties required in a large research grants program, as directed by the Branch Chief. The positions are located in Rockville Maryland.

The CCBB supports basic research projects covering a broad spectrum of topics directed at understanding the biological basis of cancer, including studies on the genes, proteins and networks responsible for the cancer phenotype; investigation of aberrantly modified regulatory processes that promote cancer; and the identification of connecting pathways that ensure tumor cell survival. An emerging interest which will be a focus of this current position is the role of nutrient stress and cellular metabolism in cancer cell survival and tumor growth. The ultimate goal of the Cancer Cell Biology Branch program is the discovery of new information that has practical application to disease detection, prevention, or treatment.

The TBMB supports research covering diversified areas of tumor progression and metastasis, including the interactions of cancer cells with the tumor and/or host microenvironment, role of stem cells in tumor biology, tumor dormancy, angiogenesis and lymphangiogenesis, cell migration, invasion, tumor progression, and metastasis. This includes examination of cell-cell and cell-matrix interactions, the roles of growth factors and cytokines, adhesion molecules, cytoskeleton and the nuclear matrix, and matrix-degrading enzymes, inflammation, glycoproteins, steroid hormones and their receptors, as well as studies on the pathology and biology of solid tumors and tumor bearing animals. Research supported by the Branch also includes novel 3-dimensional or organotypic models and in vivo models to address research focusing on tumor progression and metastasis. A full Civil Service package of benefits (including health and life insurance options, retirement, paid holidays, vacation and sick leave) is available.

The NCI vacancy announcement for the CCBB position will be available on **August 17, 2007** and posted under announcement # **NCI-07-208137-DE**. The vacancy announcement for the TBMB position will be available on **August 17, 2007** and posted under announcement # **NCI-07-208132-DE**. Both positions close on September 21, 2007. The vacancy announcements for these positions contain complete application procedures, list all mandatory information which you must submit with your application and may be obtained from the **https://www.usajobs.opm.gov**. Questions can be directed to **Eugene McDougal on (301) 435-5722**. Please see vacancy announcement for application submission requirements.

Head, Department of Cellular Biology and Anatomy
Louisiana State University Health Sciences Center in Shreveport

The School of Medicine at LSU Health Sciences Center in Shreveport is seeking applicants for Head of the Department of Cellular Biology and Anatomy from world-class researchers in cardiovascular sciences with an interest in developing a nationally competitive program. Investigators having research interests in the area of cardiovascular complications of metabolic syndrome and diabetes are particularly encouraged to apply.

The salary for this tenured position is fully supported by state funds, with additional compensation possible through an institutional research incentive compensation plan. The position also comes with a $2 million Endowed Chair from the Malcolm Feist Cardiovascular endowment. The new Department Head will receive a generous seed package to support his/her research program and state-of-the art laboratory space. A multi-year strategy and supporting financial resources are in place to substantially enhance the national stature of research and training programs in the Department. This includes the state-funded salary lines, research space, and seed package support to recruit 6 faculty members. In addition, $1 million will be provided to expand the research infrastructure of the Department to complement the new emphasis on cardiovascular sciences.

Successful candidates should have a graduate degree (Ph.D. and/or M.D.), current NIH funding, an outstanding record of achievement in cardiovascular research, and experience mentoring graduate students, postdoctoral fellows, and junior faculty. The responsibilities of the position include development and leadership in departmental Ph.D. and postdoctoral training programs, research activities, and multidisciplinary research endeavors as well as a commitment to maintain/strengthen the education obligations of the Department.

The LSU Health Sciences Center-Shreveport, established in 1969, is located in northwest Louisiana and is one of the fastest developing regions within the state. The Shreveport-Bossier City area, with a population of ~325,000, has evolved into a major regional cultural and recreational center, and is in short driving distance to larger metroplexes such as the Dallas-Fort Worth and Houston areas.

Interested applicants and nominations should include a curriculum vitae and a letter of interest. Correspondence should be directed to: **Nicholas Goeders, Ph.D., Professor and Head, Department of Pharmacology, Toxicology and Neuroscience, LSU Health Sciences Center, P.O. Box 33932, Shreveport, LA 71130**. Applications will be accepted by mail or via e-mail (**ngoede@lsuhsc.edu**) until **September 30, 2007**.

LSUHSC is an Affirmative Action Employer.

Adolor Corporation is a biopharmaceutical company located in suburban Philadelphia specializing in the discovery, development and commercialization of novel prescription pain management products. Adolor has more than 120 employees working in areas including discovery research, drug development, clinical research, manufacturing, business development and marketing.

Visit our website **www.adolor.com** or go to **sciencecareers.org** to view job descriptions in detail.

Postdoctoral Fellow
Cell and Molecular Signaling

Postdoctoral Fellow
Cell and Molecular Signaling/
In-Vivo Pharmacology

Research Investigator
Cell and Molecular Signaling

Research Scientist
Cell and Molecular Signaling

Research Scientist II
Pharmacology

ASSOCIATE OR FULL PROFESSOR TO SERVE AS ENDOWED CHAIR

the City College of New York

FLSA Status: Exempt

Compensation: An associate or full professor's salary will be supplemented with the interest earnings from a sizable endowment.

College Web Site: www.ccny.cuny.edu

Notice Number: FY - 13304

Closing Date: Open until filled.

POSITION DESCRIPTION AND DUTIES

The City College of New York, the first free public institution of higher education in the U.S., seeks a distinguished scholar and educator to fill the newly created Zitrin Professorship in Bioethics as an Associate or Full Professor. Candidates for this endowed chair should have a record of scholarship, national appointments, grants, and awards appropriate to the position, with evidence of outstanding university-level teaching. The Zitrin Professor's home department at the City College will depend on the candidate's discipline and interests; applications are welcome from bio-ethicists with academic credentials in bioengineering, biology, law, medicine, philosophy, public health, and other relevant fields. The Zitrin Professor will have interdisciplinary responsibilities and privileges that may include the Honors College, the Department of Bioengineering, and the Sophie Davis School of Biomedical Education.

QUALIFICATION REQUIREMENTS

The successful candidate will be an accomplished and distinguished analyst/practitioner with a M.D., Ph.D., or J.D. Depending on applicant's qualifications and experience, appointment will be made at Associate or full Professor level.

The City College of New York has a strong institutional commitment to the principle of diversity. In that spirit, we are particularly interested in receiving applications from a broad spectrum of individuals, including women and under-represented groups. Upon request, reasonable accommodations provided for individuals with disabilities.

All candidates must provide documentation to prove employment eligibility in compliance with IRCA.

TO APPLY

Send letter of interest, C.V., sample publications, and the names and contact information of three professional references to: **Professor Nickolas Pappas, Dept of Philosophy, NAC 5/144, The City College of New York, 160 Convent Avenue, New York, NY 10031 or e-mail to: philosophy@ccny.cuny.edu.**

The City University of New York is an Equal Employment Opportunity/Affirmative Action/Immigration Reform and Control Act/Americans with Disabilities Act Employer

CITY COLLEGE IS CUNY

Universität Karlsruhe (TH)
Forschungsuniversität · gegründet 1825

KIT Karlsruhe Institute of Technology

The Universität Karlsruhe (TH) and the Forschungszentrum Karlsruhe are joining forces to form the **Karlsruhe Institute of Technology (KIT)** and are planning to integrate their research activities both structurally and strategically. In a Germany-wide competition within the Excellence Initiative, University Karlsruhe was selected as one of three top universities. Within the future concept of the University, several new research groups will be established. The funding of each research group will comprise the position of the group leader, two scientists and an annual budget for consumables.

The **Faculty of Physics and the Institute of Nanotechnology** are seeking at the earliest possible date a

Group Leader (E 15)
of the Shared Research Group "Electronic Properties of Graphene"

Research in this group shall focus on the electronic transport properties of graphene, and complement the existing expertise in the field of physical properties of nanostructures at the University and the Forschungszentrum.

Young scientists with outstanding experience in the field of mesoscopic and nanoscale physics are invited to apply for the position of the group leader. The group will be able to draw on resources in lithography, nanofabrication, characterization and low temperature measurements. Applicants should submit a curriculum vitae including their academic career, a research plan and a list of publications with up to three reprints.

The initial appointment phase is for 4 years with the possibility of a renewal, and will be paid according to E 15 TV-L of the German civil service remuneration system. The research group will be based in the Institute of Nanotechnology in the Forschungszentrum. Active participation in teaching at the University is possible.

For further information please contact Prof. Dr. Hilbert v. Löhneysen (H.vL@pi.uka.de, Tel. 0049-721/608-3450).

To increase the number of women involved in science and technology, female applicants are specifically encouraged. Handicapped applicants will have higher preference in case of equal qualifications.

Applications should be addressed until **15.09.2007** to the **Universität Karlsruhe (TH), Prof. Dr. Hilbert v. Löhneysen, Physikalisches Institut, 76128 Karlsruhe, Germany.**

FACULTY POSITIONS AT YALE UNIVERSITY

Department of Molecular Biophysics and Biochemistry

The Department of Molecular Biophysics and Biochemistry seeks applications for a tenure track position at the Assistant Professor level in the field of biochemistry, molecular biology, or molecular genetics. Our department uses tools ranging from structural biology to genetics to investigate current biological problems at the molecular and atomic levels. In addition to establishing an innovative and interactive research program, new faculty will engage in the teaching and training of undergraduates, graduate students and medical students, as the department is located in both the Faculty of Arts and Sciences and the School of Medicine. More information on the department is available at: **http://www.mbb.yale.edu/**. Applications should include a curriculum vitae, a statement of research interests, no more than three selected reprints or preprints, and the names of three individuals who have been asked to send letters of reference to:

Faculty Search Committee (Biochemistry)
Department of Molecular Biophysics and Biochemistry
Yale University
P.O. Box 208114, 260 Whitney Ave.
New Haven, CT 06520-8114
Telephone: (203) 432-5593

Application Deadline: **October 15, 2007**

Department of Molecular, Cellular, and Developmental Biology

The Department of Molecular, Cellular and Developmental Biology at Yale University invites applications for a tenure-track faculty appointment at the level of Assistant Professor from individuals working in any area of molecular, cellular or developmental biology. The Department encourages applications from candidates using any experimental system (animals, microorganisms or plants) to investigate outstanding questions in contemporary biology at the cellular or molecular level. The successful candidate is expected to develop an active research group, interact with the department's faculty, and participate in interdisciplinary research and training activities. In addition, the successful candidate should demonstrate excellence in teaching at both the undergraduate and graduate levels.

Our web site **http://www.yale.edu/mcdb/** contains additional information on the Department.

The search committee will start screening applications on **October 15, 2007**. Applications close **December 1, 2007**. Please submit a curriculum vitae, a description of research interests and the names of at least three individuals who have been asked to send letters of recommendation to:

Faculty Search Committee
Department of Molecular, Cellular and Developmental Biology
Yale University
P.O. Box 208103
New Haven, CT 06520-8103
Telephone: 203-432-3460

Yale University is an Affirmative Action/Equal Opportunity Employer. Women and members of underrepresented minority groups are especially encouraged to apply.

Cornell University

Institute for Cell and Molecular Biology
Senior and Junior Faculty Positions

As part of a New Life Science Initiative, Cornell University has established and endowed a new Institute for Cell and Molecular Biology (for complete information, see **www.icmb.cornell.edu**). The Institute will consist of 12 faculty as the core component in a $160M new research building, now nearing completion, designed by renowned architect Richard Meier. Dr. Scott Emr recently relocated to Cornell as the founding Director of the new Institute. The goal of the Institute is to build a vibrant center of scientific excellence in basic biology integrated with existing outstanding programs in chemistry and chemical biology, physics, computational biology and engineering. Institute faculty will have full academic appointments in basic science departments to which they will contribute teaching and service.

Three faculty positions are available this year, one of which will be an Endowed Professorship (department open) and the others appointed at the Assistant or Associate Professor levels within the department of Molecular Biology & Genetics (**www.mbg.cornell.edu**). Priority will be given to candidates using model systems employing novel approaches to address fundamental questions in cell biology (including cell cycle control, signal transduction, regulation of the cytoskeleton, organelle biogenesis and function, regulation of membrane architecture, protein quality control, etc.). Individuals with expertise in X-ray crystallography, biochemical reconstitution, mass spectrometry, functional genomics, and live cell imaging are of special interest. However, outstanding candidates in any area of cell and molecular biology will be considered.

Please submit (electronically) a curriculum vitae (highlighting 3-5 publications with title and abstract), research plan (2-3 pages) and teaching interests. Please limit total file to 10MB. In addition, applicants must arrange for three letters of recommendation to be sent to the address below, concurrent with the other application materials. The committee will begin reviewing applications by September 20, 2007, with applications being accepted until the positions are filled. We encourage women and minorities to apply.

Applications must be submitted electronically, as a single pdf, to:
Dr. Scott Emr, c/o Dianna Marsh at dmm20@cornell.edu

You may also upload your application materials to the Institute website at: **www.icmb.cornell.edu**

Located in Ithaca, N.Y., Cornell University is a bold, innovative, inclusive and dynamic teaching and research university.

Cornell University is an Affirmative Action/ Equal Opportunity Employer and Educator.

U.S. Department of Energy
Associate Director
Office of Science for
Biological and Environmental Research
Announcement # SES-SC-HQ-014 (kd)

The U.S. Department of Energy's (DOE's) Office of Science is seeking qualified candidates to lead its Biological and Environmental Research (BER) Program. With an annual budget of more than $500 million, the BER Program is the nation's leading program devoted to applications of biology to bio-energy production and use and to environmental remediation. The BER Program supports major research programs in genomics, proteomics, systems biology, and environmental remediation. The Program is also one of the nation's leading contributors to understanding the effects of greenhouse gas emissions, aerosols, and atmospheric particulates on global climate change.

The Director of Biological and Environmental Research is responsible for all strategic program planning in the BER Program; budget formulation and execution; management of the BER office including a federal workforce of more than 30 technical and administrative staff; program integration with other Office of Science activities and with the DOE technology offices; and interagency integration. The position is within the ranks of the U.S. government's Senior Executive Service (SES); members of the SES serve in key positions just below the top Presidential appointees. For more information on the program please go to **http://www.sc.doe.gov/ober/**.

For further information about this position and the instructions on how to apply and submit an application, please go to the following website: **http://jobsearch.usajobs.opm.gov/getjob.asp?JobID=58520806&AVSDM=2007%2D06%2D06+13%3A44%3A02&Logo=0&q=SES-SC-HQ-014+(kd)&FedEmp=N&sort=rv&vw=d&brd=3876&ss=0&FedPub=Y&SUBMIT1.x=47&SUBMIT1.y=18**. To be considered for this position you must apply online. It is important that you follow the instructions as stated on the announcement **SES-SC-HQ-014 (kd)** located at the website above.

FACULTY POSITIONS FOR PHYSICIAN-SCIENTISTS IN TRANSLATIONAL ONCOLOGY

The Human Oncology and Pathogenesis Program (HOPP) at Memorial Sloan-Kettering Cancer Center (MSKCC) invites applications for tenure track faculty appointments at the level of Assistant, Associate, or Full Member. HOPP is assembling outstanding physician-scientists across clinical disciplines in a single program to foster translational oncology research at the laboratory/clinical interface in an environment that encourages collaborative team science. Current research by HOPP faculty encompasses oncogenomic studies of various cancers, analysis of aberrant signal transduction pathways, preclinical evaluation of molecularly targeted agents and mechanisms of drug resistance. Successful candidates must demonstrate the ability to develop an independent research program as well as an interest in translational oncology. HOPP faculty will be housed in state-of-the-art laboratories in the new Zuckerman Research Center and jointly appointed in the Department of his/her appropriate clinical specialty at MSKCC. Faculty will also be eligible to hold appointments in the newly established Gerstner Sloan-Kettering Graduate School of Biomedical Sciences as well as the Weill Medical School and Graduate School of Medical Sciences at Cornell University.

MSKCC offers a unique and vibrant research environment with programs in Immunology, Pharmacology, Chemistry, Molecular Biology, Computational Biology, Genetics, Cell Biology, Developmental Biology, Cellular Biochemistry, and Structural Biology and close links with the Rockefeller and Cornell communities. The presence of world-renowned clinical programs in cancer research, treatment, and prevention offers unique opportunities for creative collaboration. Applicants must have an M.D. or M.D. Ph.D, postdoctoral experience, and an active clinical interest.

Please send curriculum vitae, a summary of current and proposed research programs, and arrange for three letters of recommendation to be sent to: **Charles L. Sawyers, M.D., Chair, Human Oncology and Pathogenesis Program, c/o Erika Bernardino, Memorial Sloan-Kettering Cancer Center, 1275 York Avenue, Mailbox #20, New York, NY 10021; E-mail: bernare1@mskcc.org. Applications should be received by November 30, 2007.** Memorial Sloan-Kettering Cancer Center is an affirmative action, equal opportunity employer.

Memorial Sloan-Kettering Cancer Center
The Best Cancer Care. Anywhere.
www.mskcc.org

All Souls College Oxford

Senior Research Fellowships

All Souls College intends to elect three Senior Research Fellows with effect from 1st October 2008 (or an agreed later date): in Philosophy, in History, and in Theoretical Life Sciences (all subjects broadly conceived). The Fellowships are open to women and men.

The College regards a Senior Research Fellowship as being of comparable academic standing to an Oxford University Professorship, and applicants are expected to have a correspondingly distinguished record of achievement in research.

Further particulars, including details of emoluments and terms of appointment, application form, and copies of a memorandum for referees may be obtained from the Warden's Secretary, **All Souls College, Oxford OX1 4AL; mary.yoe@all-souls.ox.ac.uk**. See also the College's website: **www.all-souls.ox.ac.uk**. Applications, on the application form, should reach the Warden not later than **Monday, 10th September 2007.**

UNIVERSITY OF ROCHESTER MEDICAL CENTER

The Center for Vaccine Biology and Immunology and the New York Influenza Center of Excellence are seeking:

Post Doctoral Research Fellow(s) - IMMUNOLOGY

Five post-doctoral fellowship positions are available in the David H. Smith Center for Vaccine Biology and Immunology at the University of Rochester. Two of these are in the new, NIAID-funded, New York Influenza Center of Excellence at the University of Rochester Medical Center, with the major aim of investigating the host immune responses to influenza. Other major areas of research include investigating the role of amphiregulin and T cell responses in human asthma and a mouse asthma model; T and B cell responses to influenza infection or vaccination; and dynamic integrin activation during cell migrations in live animals using state-of-the-art optic microscopy systems.

URMC is a highly interactive environment with excellent collaborations between basic and clinical scientists. Outstanding facilities include strong flow cytometry analysis and sorting capabilities, bioinformatics, proteomics, mathematical modeling of immune responses, sophisticated image analysis of fluorescent images including Fluorospot assays, and the support of the Human Immunology Center. State-of-the-art laboratory and animal facilities from biosafety level 2 to enhanced biosafety level 3 are available. The successful candidate will have the opportunity to join a highly interactive, collaborative community of researchers from the Departments of Microbiology and Immunology, Medicine, Computational Biology and Biostatistics, and other research centers and divisions.

For additional information, please see our ads at **ScienceCareers.org** under "URMC-Immunology".

The University of Rochester is an Equal Opportunity Employer.

Chairperson of Biomedical Engineering

FIU
Florida International University

Florida International University is seeking a dynamic and innovative leader to serve as chairperson of the Department of Biomedical Engineering (BME). The department is endowed with $11 million from the Wallace H. Coulter Foundation, the Ware Foundation and the State of Florida. Applicants must have a Ph.D. degree in Biomedical Engineering or a closely related field and must possess credentials that meet the qualifications for appointment at the rank of Full Professor, based on a substantial record of scholarly work, excellent record of extramurally funded research, professional service, and the demonstrated ability to provide significant leadership and vision to a growing academic department. Candidates with the ability to forge interdisciplinary collaborations will be favored. Successful candidates are expected to develop a high-quality funded research program and must be committed to excellence in teaching at both the graduate and the undergraduate levels. ***Candidates with exceptional credentials of scholarly work and research funding may be considered for the Wallace H. Coulter Eminent Scholars Chair of Biomedical Engineering.***

FIU has a student body of over 38,000 and is located in Miami, Florida, a diverse and dynamic metropolitan area with a strong biomedical industry. FIU offers over 190 baccalaureate, masters and doctoral degree programs in 19 colleges and schools. It is ranked as a Research University in the High Research Activity category of the Carnegie Foundation's classification system. FIU is one of only two institutions in the state of Florida that offers BS, MS and PhD degrees in BME. Its undergraduate program is ABET accredited. BME is a dynamic and expanding department with active interdisciplinary research programs in tissue engineering and drug delivery, systems biology, bioinstrumentation and biosignal processing, imaging, neuroengineering, and bionanotechnology and enjoys strong support of the University administration. BME faculty is funded by NIH, DOD, AHA, NSF, FL DOH and industry. The BME has over 30 clinical and industry partners in South Florida, and is taking a leadership role in the development of the new College of Medicine at FIU. There are numerous research centers and institutes available for collaboration both in the College of Engineering and Computing (**www.eng.fiu.edu**) and in the university (**www.fiu.edu**). Additional information about the department can be found at **www.bme.fiu.edu**.

Please send nominations or applications via e-mail to: BME Chair Search and Screen Committee, **bmeinfo@fiu.edu**, or apply online at: **https://www.fiujobs.org/applicants/jsp/shared/frameset/Frameset.jsp?time=1181244925142**. Applications will be evaluated as they are received and review will continue until the position is filled. Application materials should include curriculum vitae, teaching, research and administrative experience, a vision statement, and a list of at least five references. Inquiries, applications, and nominations will be kept in confidence. For more information, contact the email address above or call **305-348-1352** or **305-348-3947**.

Women and minorities are strongly encouraged to apply. FIU is a member of the State University System of Florida and an Equal Access/Equal Opportunity Employer and Institution.

Kumamoto University

Open Recruitment of Young Researchers (1st Stage)

1. Open Recruitment of Researchers (1st stage)
Special project researchers (all given the title of "specially appointed assistant professor")
A maximum of 10 researchers

2. Qualification Requirements
(1) Academic degree, etc.: Young researchers who have obtained a PhD degree within approximately the past 10 years (as of April 1, 2008)
(2) Achievements/ability: Has outstanding research capabilities and/or research achievements in one of the specialty areas outlined in number 3.

3. Arrival
As soon as possible between October 2007 and February 2008

4. Period of Employment
Those hired in stage 1 will be employed through March 2012.
(Contracts will be for one year each and will be renewed once a year through March 31, 2012.)
*Employment contract is based on Article 14 of the Labour Standards Law.
(Note: After having gone through career advancement evaluations and after the end of one's term of employment, it is possible for one to be promoted to the position of "Associate Professor" in the Leading Graduate School System. A total of approximately 8 people from stages 1 and 2 will be chosen for these positions.)

5. Application Deadline
Applications must reach the university by no later than September 7, 2007 (Friday).

6. Inquiries
Any inquiries should be made by e-mail to the Research Cooperation Section (person in charge of research strategy) of Kumamoto University at the e-mail address written below:
k-senryaku@jimu.kumamoto-u.ac.jp

http://sendou.kuma-u.jp/
Please be sure to allow enough time before the application deadline for a response to be made to you.

THE UNIVERSITY OF THE WEST INDIES

CAVE HILL CAMPUS, BARBADOS

Applications are invited from suitably qualified persons for the following posts:

LECTURER/ASSISTANT LECTURER IN ATMOSPHERIC SCIENCE

The successful applicant should have a first degree and PhD in Atmospheric Science (or a related subject).

The successful applicant will teach the introductory ERSC1002 Oceans and Climate course and develop and teach two advanced courses, building on this, in the Earth Sciences programme. Preference will be given to applicants whose area of specialization is of particular relevance to the Caribbean, such as climatology or physical oceanography. The Faculty already has a major in Meteorology, taught by staff of the affiliated Caribbean Institute for Meteorology and Hydrology and collaboration in teaching and research with the Institute staff is expected.

LECTURER/ASSISTANT LECTURER IN GEOLOGY

The successful applicant should have both a first degree and a PhD in Geology (or a closely related subject).

Specialisation in any area of Geology is acceptable but competence to teach geomorphology or environmental risk management could be an advantage. The appointee will teach an introductory Geology course ERSC1001 Dynamic Earth and will develop and teach two advanced courses, building on this, in the Earth Sciences programme.

The appointees for these posts should possess university, or other tertiary level, teaching and research experience, and evidence of publication. They will be expected to develop an active research programme of relevance to the region and will be expected to supervise graduate students registered for MPhil and PhD degrees. There will also be the opportunity to develop advanced level or postgraduate courses in areas of special expertise.

The successful applicants will be expected to assume duties as soon as possible.

Detailed applications (two copies) giving full particulars of qualifications and experience, biodata and the names and addresses of three referees should be sent as soon as possible to the **Campus Registrar, University of the West Indies, P O Box 64, Bridgetown, Barbados. Fax (+1 246) 417-0330; Email: humanresources@cavehill.uwi.edu. In order to expedite the appointment procedure, applicants are advised to request their referees to send references under CONFIDENTIAL cover DIRECTLY to the Campus Registrar without waiting to be contacted by the University. Further particulars including remuneration package for this post are available from our website at www.cavehill.uwi.edu.**

The closing date for applications is 15 September 2007.

CELL BIOLOGY
Vassar College

The Department of Biology at Vassar College invites applications for a tenure-track faculty position at the level of assistant professor beginning Fall 2008. We seek a broadly trained cell biologist whose research and teaching interests may include but are not limited to the following: eukaryotic cell structure, cell signalling, cell trafficking, genetic and epigenetic processes, and protein interaction networks. The successful candidate will be expected to develop an upper-level course in his/her specialty as well as teach at the introductory and intermediate levels, including genetics, cell biology, or another intermediate course. Development of a productive research program with student participation will be expected. Start-up funding, shared equipment, and personal laboratory space will be provided. A Ph.D. is required and postdoctoral experience is preferred.

Consideration of applications will begin on **1 October 2007**. Applicants should submit a curriculum vitae, two representative reprints, a document that describes both research interests & goals and teaching interests & philosophy, and three letters of reference. To apply please visit **https://employment.vassar.edu/**. Referees should send reference letters directly to **cellbiology@vassar.edu**. Website: **http://biology.vassar.edu/**.

Vassar College is an Equal Opportunity/ Affirmative Ection Employer and is strongly and actively committed to diversity within its community.

U.S. Department of Energy
Office of Science
Deputy for Programs
Announcement #*SES-SC-HQ-013 (kd)*

The U.S. Department of Energy's (DOE) Office of Science is seeking highly qualified candidates with outstanding scientific achievements to fill the Deputy for Programs position. The Office of Science is the single largest supporter of basic research in the physical sciences in the United States, with a 2007 budget of $3.8 billion. It oversees the Nation's research programs in high-energy and nuclear physics, basic and fusion energy sciences, and biological, environmental and computational sciences. The Office of Science is the Federal Government's largest single funder of materials and chemical sciences, and it supports unique and vital parts of U.S. research in climate change, geophysics, genomics, life sciences, and science education. The Office of Science also manages 10 world-class laboratories and oversees the construction and operation of some of the Nation's most advanced R&D user facilities, located at national laboratories and universities. These include particle and nuclear physics accelerators, synchrotron light sources, nanoscale science research centers, neutron scattering facilities, bio-energy research centers, supercomputers and high-speed computer networks. More information on the Office of Science can be found at **http://science.doe.gov**.

The Deputy for Programs provides scientific and management oversight of the six program offices by ensuring program activities are strategically conceived and executed; formulating and defending the Office of Science budget request; establishing policies, plans, and procedures related to the management of the program offices; ensuring the research portfolio is integrated across the program offices with other DOE program offices and other Federal agencies; and representing the organization and make commitments for the Department in discussions and meetings with high-level government and private sector officials. The position is within the ranks of the U.S. government's Senior Executive Service (SES); members of the SES serve in key positions just below the top Presidential appointees.

To apply for this position, please see the announcement and application instructions at **http://jobsearch.usajobs.opm.gov/ses.asp** under the vacancy announcement of **#SES-SC-HQ-013 (kd)**. Qualified candidates are asked to submit their online applications by **August 29, 2007**.

From primates to proteomics

For careers in science, turn to *Science*

Don't get lost in the career jungle. At *Science* Careers we know science. We are committed to helping you find the right job, and to delivering the useful advice you need. Our knowledge is firmly founded on the expertise of *Science*, the premier scientific journal, and the long experience of AAAS in advancing science around the world. *Science* Careers is the natural selection.

Features include:

- Thousands of job postings
- Career advice
- Grant information
- Resume/CV Database
- Career Forum

www.ScienceCareers.org

Science Careers
From the journal *Science* AAAS

KECK SCHOOL OF MEDICINE USC

Zilkha Neurogenetic Institute
Keck School of Medicine
University of Southern California

Cellular/Molecular/Systems Neurobiologist

The Zilkha Neurogenetic Institute (ZNI) is recruiting a candidate to fill a tenure-track position at the level of Assistant or Associate Professor. The ZNI, which is supported by major funding from W.M. Keck Foundation and other significant philanthropic sources, is housed in a recently completed facility of 125,000 gsf. The goal of the ZNI is to catalyze a major expansion in basic neuroscience research at the Keck School of Medicine (KSOM). We seek a neurobiologist, Ph.D. and/or M.D., with an outstanding academic record and an innovative research program in cellular, molecular, or systems level processes as they pertain to fundamental aspects of neural development and function. The successful candidate will receive a generous start-up package and will become part of an active and growing research group within the ZNI. The successful candidate will have a primary academic appointment in a basic science department within the KSOM. He or she will have the opportunity to participate in the scientific and teaching activities of the department, as well as in USC's neuroscience graduate program.

Applicants should submit a curriculum vitae, a research plan, and three letters of recommendations to:

Jeannie Chen, Ph.D.
Chair, Search Committee
Zilkha Neurogenetic Institute
Keck School of Medicine of USC
1501 San Pablo Street, ZNI-101
Los Angeles, CA 90033

Women and minority candidates are encouraged to apply.
Equal Opportunity for outstanding men and women.

University of California Los Angeles
Tenure-Track Faculty Position
Microbiology, Immunology and Molecular Genetics

The Department of Microbiology, Immunology and Molecular Genetics at the David Geffen School of Medicine at UCLA is opening a broad search for an outstanding investigator, preferably at the Assistant Professor level. The department has very strong research and teaching programs (**http://www.mimg.ucla.edu**) with extensive ties and opportunities for interdisciplinary collaboration with laboratories in the Schools of Medicine and Engineering, the College of Letters and Sciences, the California NanoSystems Institute, the Jonsson Comprehensive Cancer Center, and the UCLA Institute of Stem Cell Biology and Medicine. This tenure-track position offers a guaranteed salary base, outstanding fringe benefits, and an attractive start-up package with state-of-the-art research facilities in a new building. The successful candidate will also be the first recipient of the endowed Shaper Family Career Development Chair.

Applications will be screened beginning **November 1, 2007**, and accepted until the position is filled. Applicants should submit full curriculum vitae and a brief summary describing their accomplishments and future goals in research and teaching. Applicants should also arrange for three letters of recommendation to be sent under separate cover directly to the Chair of the Search Committee. Electronic submissions will not be considered. All materials should be mailed to:

Chair, Faculty Search Committee
Department of Microbiology, Immunology
and Molecular Genetics
University of California, Los Angeles
1602 Molecular Science Building
Box 951489
Los Angeles, CA 90095-1489

The University of California is an Equal Opportunity/Affirmative Action Employer. All qualified candidates are encouraged to apply.

UCDAVIS
COLLEGE OF AGRICULTURAL & ENVIRONMENTAL SCIENCES

Initiative in Global Environmental Change and Conservation Biology

The College of Agricultural and Environmental Sciences, University of California, Davis, is participating in an initiative in the area of global environmental change and conservation biology that includes the recruitment of six new positions. Three positions were filled last year, and the remaining three positions are being recruited now. These three positions will be tenure-track at the ASSISTANT PROFESSOR level, with the possibility of an appointment in the California Agricultural Experiment Station.

The positions currently under recruitment are:

- **GLOBAL CHANGE INFORMATICS SCIENTIST:** This position will focus on integrating concepts from informatics into research on global change and conservation biology. Research applications could include atmospheric and oceanic climate, hydrologic cycles, biogeochemical cycles, ecosystem health, invasive species, species distributions, ecosystem services, and human interactions with these. To ensure full consideration applications must be submitted by **October 8, 2007**.

- **QUANTITATIVE PLANT CONSERVATION ECOLOGIST:** This position will focus on the plant conservation impacts of large-scale environmental change by combining field and/or laboratory studies with innovative modeling and statistical techniques. Research applications could include the development of landscape and plant population models needed to forecast best practice strategies for maintenance of biodiversity in natural and managed ecosystems. To ensure full consideration applications must be submitted by **October 1, 2007**.

- **CONSERVATION VALUATION ANALYST:** This position will explore how society values biodiversity, species conservation, ecosystem services, natural capital and wildlands by combining methods from various approaches and disciplines including economics, cognitive psychology, survey design, statistics and ecology. The submission date to ensure full consideration of applications has not yet been set for this position.

Recruitments that have been completed in this initiative are:

- **QUANTITATIVE ANIMAL CONSERVATION ECOLOGIST:** This faculty member has skills and interest in investigating how large-scale environmental change will affect the abundance, distribution, and role in ecosystem functioning of animals, particularly fishes or amphibians.

- **ECOSYSTEM BIOGEOCHEMICAL MODELER:** This faculty member has skills and interests in understanding and forecasting ecosystem and biogeochemical dynamics in the context of global and regional environmental change.

- **BIOECONOMIC MODELER:** This faculty member has skills and interests in integrating concepts from economics and ecology into quantitative bioeconomic models.

Please visit **http://recruitments.caes.ucdavis.edu/** for application requirements and for additional information about these positions and the Global Environmental Change and Conservation Biology initiative at UC Davis. Please contact us at **recruitments@caes.ucdavis.edu**, if you experience problems with the website.

UC Davis is an Affirmative Action/Equal Employment Opportunity Employer and is dedicated to recruiting a diverse faculty community. We welcome all qualified applicants to apply, including women, minorities, veterans, and individuals with disabilities.

Take your next career step.

RESEARCH ZOOLOGIST

Department of Vertebrate Zoology

National Museum of Natural History

Smithsonian Institution

The Smithsonian's National Museum of Natural History seeks an outstanding systematic zoologist to conduct an integrative, collections-based research program in vertebrate systematics in the specialty areas of herpetology, ichthyology, mammalogy and/or ornithology. The successful candidate is expected to implement current methods in research, e.g., phylogenetics, morphology, molecular genetics, studies of anatomy, fine structure and/or developmental biology, in pursuing a research focus in systematics and one or more of the following: evolution, biogeography, biodiversity or conservation. Frequent publication in peer-reviewed journals and curation of collections, including collection-building, in specialty area is expected, as well as demonstrated ability of participation in the scientific community in a manner commensurate with emerging leadership in the area of specialty.

This position is a full-time, initially four-year term appointment, and will be filled at the GS-12 level (current salary range of $66,767 - $86,801 per year, commensurate with experience, with an anticipated Federal salary increase in January 2008); US citizenship required. Completed applications may be submitted in any of the following four ways:

- Mailed to **Smithsonian Institution, Office of Human Resources, P.O. Box 23772, Capital Gallery Suite 5060, MRC 517, Washington, D.C. 20026-3772**
- Sent via Fax to **(202) 633-6402**, with announcement number on all pages faxed
- Hand Delivered or sent via FEDEX to **600 Maryland Avenue SW, Capital Gallery Bldg. Suite 100W, Washington, DC 20024**

E-mail applications will not be accepted

Applications must include (1) complete CV including list of all professional publications and all extramural grants received with agencies, funding periods, and amounts; (2) one set of selected publications; (3) list, with contact information, including e-mail address, of at least 5 individuals from whom letters of professional evaluation may be sought; and (4) cover letter specifically addressing the quality ranking factors that appear in the vacancy announcement which is available at **www.si.edu/ohr**. Applications must be received by **September 28, 2007** and must reference announcement number **07-RC 7253**. For further information, call **Office of Human Resources** (OHR) representatives at **(202) 633-6370** or **(202) 633-6409** (TTY). Applicants who have completed education in foreign colleges or universities must demonstrate that such education is at least equivalent to that gained in conventional U.S. education programs; see Vacancy Announcement or contact OHR for further details.

The Smithsonian Institution is an Equal Opportunity Employer.

POSITIONS OPEN

TECHNICAL OPERATIONS MANAGER

The American Institute of Biological Sciences seeks a senior nonacademic individual to serve as Operations Officer in the Scientific Peer Advisory and Review Services (SPARS) Department. The Technical Operations Manager, who reports to the SPARS Director, will provide technical and administrative oversight of the business unit and supervisory responsibility for senior and support staff. The position provides high-level policy, scientific and technical support, and senior leadership to the Institute. Qualifications: The ideal candidate will have an advanced degree (M.B.A., or Ph.D. with business acumen strongly preferred). Minimum of five years of experience and demonstrated success in a large and complex research enterprise, preferably in a business, foundation, or government setting. Thorough understanding of scientific peer review process, and excellent communication skills, written and oral, are essential. Demonstrated managerial skills sufficient to identify and communicate project goals, to motivate and support various levels of personnel, and to effectively oversee organizational change and provide leadership while guiding the changes. Experience with personnel issues and demonstrated skills in contract and grant management and fiscal analysis. Ability to analyze information to resolve conflicts and discrepancies. Skill in writing, editing, and proofreading. Demonstrated organizational skills required. Ability to work independently and as a member of a team. Excellent communication skills required to negotiate contracts, supervise staff, and interface with individuals at all levels. Demonstrated knowledge of federal policies governing the administration of contracts, grants, interagency agreements, cooperative agreements, and subcontracts. Advanced degree in business management, biological sciences, or engineering preferred. Demonstrated knowledge of project management techniques and practices. Skills to work in a fast-paced complex environment at a senior level with little oversight. Strong interpersonal skills and demonstrated ability to articulate the program to a variety of audiences. Applicants should send their cover letter, salary requirements, and curriculum vitae to **e-mail:** hresources@aibs.org.

The Physics Department at Wheaton College (Illinois) invites applications for a tenure-track **ASSISTANT PROFESSOR** position starting fall 2008. Field of expertise is open, with special consideration given to candidates with backgrounds in astronomy or biophysics. Applicants must be committed to excellence in both teaching and scholarship in a liberal arts environment. Faculty who can develop innovative and/or physics education research-based curricula are being sought. The successful candidate would also establish a research program involving undergraduates. Ph.D. is required. The College is located 25 miles west of Chicago and is near two national laboratories. For more information, please visit **website: http://www.wheaton.edu/physics.** Review of applications will begin November 16, 2007, and continue until the position is filled. Applicants should send curriculum vitae and a description of the applicant's teaching philosophy and research interests to: **Dr. Stewart DeSoto, Chair of the Physics Department, Wheaton College, Wheaton, IL 60187.** Application materials will be sent to eligible candidates. *Wheaton College is an evangelical Protestant Christian liberal arts college whose faculty and staff affirm a Statement of Faith and adhere to lifestyle expectations. The College complies with federal and state guidelines of nondiscrimination in employment. Women and minority applicants are encouraged to apply.*

POSITIONS OPEN

ASSISTANT or ASSOCIATE PROFESSOR
Microbial Ecology

We invite applications for a tenure-track position at the Assistant or Associate Professor level in research areas related to microbial ecology or environmental microbiology. We welcome applicants who use modern molecular and/or biogeochemical approaches, and apply them to environmental systems or prokaryote-eukaryote interactions in the natural environment. The successful candidate will have the opportunity to interact with established interdisciplinary groups in microbiology, cell biology, comparative immunology, freshwater and northern ecology, and marine biology. The candidate must have a Ph.D., two or more years of postdoctoral experience with a strong record of research, and have demonstrated potential for excellence in teaching. The University of Alberta offers a competitive salary commensurate with experience and an excellent benefits plan.

The Department of Biological Sciences **(website: http://www.biology.ualberta.ca/),** with 72 faculty members and 275 graduate students, offers an exciting environment for collaborative research. Exceptional infrastructure includes molecular biology, microarray and microscopy/imaging services, biogeochemical analysis laboratory, and field stations including Meanook and the Bamfield Marine Sciences Centre.

Candidates should submit curriculum vitae, a one-page summary of research plans, a statement of teaching interests, and reprints of their three most significant publications preferably electronically to **e-mail: positions@biology.ualberta.ca.**

Applicants must also arrange for three letters of reference to be sent to the Chair. The earliest date of employment could be January 1, 2008. Closing date: October 15, 2007.

Interested applicants may apply to **e-mail: positions@biology.ualberta.ca.**

Dr. L. S. Frost, Chair
Department of Biological Sciences
CW 405 Biological Sciences Building
University of Alberta
Edmonton, Alberta, Canada T6G 2E9

All qualified candidates are encouraged to apply; however, Canadians and permanent residents will be given priority.

The University of Alberta hires on the basis of merit. We are committed to the principle of equity in employment. We welcome diversity and encourage applications from all qualified women and men, including persons with disabilities, members of visible minorities, and Aboriginal persons.

VERTEBRATE ECOLOGIST
ASSISTANT PROFESSOR
Agnes Scott College

The Department of Biology seeks outstanding candidates in vertebrate ecology for a tenure-track Assistant Professor position. A commitment to undergraduate education and an undergraduate-accessible research program are required. Teaching responsibilities include upper-division courses in ecology and vertebrate biology, behavioral ecology, and inquiry and communication in biology. Qualifications: Ph.D. in biology, postdoctoral experience, demonstrated research and teaching excellence, superb communication skills, and the ability to work as a member of a team. Review of applications will begin September 21, 2007. Mail letter of application, curriculum vitae, statement on teaching philosophy, summary of research interests and future plans, and contact information for three references to: **Ecologist Search Committee Chair, Department of Biology, Agnes Scott College, 141 E. College Avenue, Decatur, GA 30030.** Please visit **website: http://www.agnesscott.edu** for more details. Agnes Scott College is a highly selective, independent national liberal arts college for women located in metropolitan Atlanta. For more information about the College, visit our **website: http://www.agnesscott.edu.** *Agnes Scott College has a strong commitment to diversity and urges members of underrepresented groups to apply. Equal Opportunity Employer.*

From life on Mars to life sciences

For careers in science, turn to *Science*

If you want your career to skyrocket, visit *Science* Careers. We know science. We are committed to helping you find the right job, and to delivering the useful advice you need. Our knowledge is firmly founded on the expertise of *Science*, the premier scientific journal, and the long experience of AAAS in advancing science around the world. *Science* Careers is the natural selection.

www.ScienceCareers.org

Features include:

- Thousands of job postings
- Career advice
- Grant information
- Resume/CV Database
- Career Forum

Science Careers

From the journal *Science* AAAS

POSITIONS OPEN

BIOINFORMATICS
Franklin and Marshall College

The Biology Department invites applications for a tenure-track **ASSISTANT PROFESSOR** position in the broad area of bioinformatics, beginning fall 2008. We seek an outstanding teacher and researcher who uses genome-scale approaches to understand fundamental biological questions. Research interests may include, but are not limited to, functional or comparative genomics, cellular systems such as signaling or transport, gene expression, or evolutionary genomics. Candidates should have a Ph.D. and demonstrated strength in teaching and research. Teaching responsibilities (three/two load) include lecture and laboratory sections of a junior-level course in molecular genetics, an advanced elective in bioinformatics or genomics or systems biology, and participation in the general education curriculum. In addition to the biology major, we offer interdisciplinary majors in biochemistry and molecular biology and in biological foundations of behavior (neuroscience and animal behavior). Possible research opportunities are available in collaboration with the Clinic for Special Children **(website: http://www.clinicforspecialchildren.org/).** Franklin and Marshall College has a tradition of excellence in science and student research. A new Life Sciences Building opened in August 2007.

Please send a letter of application, a statement that includes plans for actively engaging undergraduates through teaching and research and explains your goals for development as a teacher and scholar, curriculum vitae, and undergraduate and graduate transcripts to: **Professor Ira Feit, Department of Biology, Franklin and Marshall College, Lancaster, PA 17604-3003.** Applicants should also have three reference letters sent directly to **Professor Feit.** Priority will be given to completed applications received by September 24, 2007. Electronic submissions will not be accepted.

Franklin and Marshall College is a highly selective liberal arts college with a demonstrated commitment to cultural pluralism. Equal Opportunity Employer.

MOLECULAR BIOLOGIST, ASSISTANT PROFESSOR, tenure track, Ph.D. required. Position will begin in September 2008. The candidate is expected to supervise undergraduate research and to teach introductory biology classes, introduction to research, molecular biology, and microbiology. The applicant will have the opportunity to develop courses in his/her specialty and will be expected to develop a research program accessible to undergraduates as well as maintain his/her own research. Department facilities include a tissue culture laboratory, an electron microscope laboratory, an imaging facility, an animal collection, an herbarium, a greenhouse, an aquarium room, and a 289-hectare biological field station. Candidates should submit their curriculum vitae, statements of teaching philosophy and research interests, and three letters of recommendation to: **Dr. Stuart Allison, Biology Department, Knox College, Galesburg, IL 61401.** We will start reviewing applications on October 1, 2007, and continue until the position is filled. For more information about biology at Knox check **website: http://www.knox.edu/biology.xml.**

In keeping with its 171-year commitment to equal rights, Knox College particularly welcomes applications from women and members of other historically underrepresented groups.

ASSISTANT PROFESSOR. Tenure-track faculty position in Department of Chemical Engineering and Materials Science at University of California, Davis, in experimental thermodynamics of materials. Ph.D. in materials science, chemical engineering, chemistry, or related discipline required. Apply at **website: http://www.chms.ucdavis.edu/employment/.** Position open until filled; but to assure full consideration, submit applications no later than October 30, 2007. Start date July 1, 2008. *UC Davis is an Affirmative Action/Equal Opportunity Employer, and is dedicated to recruiting a diverse faculty community.*

POSITIONS OPEN

USDA ARS Agricultural Research Service
www.ars.usda.gov

SUPERVISORY RESEARCH PHYSIOLOGIST/SUPERVISORY RESEARCH NUTRITIONIST
Salary Range of $94,139 to $143,955 per annum

The USDA, Agricultural Research Service (ARS) Western Human Nutrition Research Center at the University of California, Davis, invites applications for the **RESEARCH LEADER** position in the Obesity and Metabolism Research Unit. This Unit conducts cutting-edge research in obesity and metabolism, and vitamin and mineral interventions to improve human health and function. In addition to responsibility for research leadership and management of fiscal and human resources, the candidate will conduct a strong research program on integrative nutrition interventions to prevent obesity that may include whole-organism physiology in humans and animals, and techniques to elucidate underlying mechanisms of action. Desirable qualifications include Ph.D. or equivalent degree in nutrition, physiology, biochemistry, endocrinology, or related science that includes metabolism, working knowledge of research with human subjects, and evidence of multidisciplinary team leadership. *U.S. citizenship required.* For details and application directions see **website: http://www.usajobs.com.** Direct specific questions to **Drs. Lindsay H. Allen or Nancy Keim** at **telephone: 530-752-5268.** Announcement closes October 9, 2007. *USDA/ARS is an Equal Opportunity Employer and Provider.*

ASSISTANT PROFESSOR of Organic Chemistry

Mills College invites applications for a full-time, tenure-track position at the rank of Assistant Professor, beginning August 2008. Primary teaching duties will include organic chemistry and some upper-division courses, which could focus on areas such as organometallic or bio-organic chemistry. The candidate is expected to develop an active research program involving undergraduates. A Ph.D. is required; postdoctoral work and college teaching experience is preferred. Applicants should submit a cover letter detailing teaching experience, philosophy, and research interests, along with curriculum vitae and the names and contact information for three professional references to: **Professor John Brabson, Department of Chemistry and Physics, Mills College, Oakland, CA 94613.** Application deadline is October 1, 2007. Located in the San Francisco Bay Area, Mills is a selective liberal arts college for women, with coeducational graduate programs (see **website: http://www.mills.edu).** *Persons of color and those committed to working in a multicultural environment are encouraged to apply. Affirmative Action/Equal Opportunity Employer.*

Applications are invited for an academic-year, tenure-track **ASSISTANT PROFESSOR** position in riparian ecology with the Fish and Wildlife Department at the University of Idaho. Requires a Ph.D. with a focus on riparian ecology emphasizing impacts of humans on riparian system dynamics from headwater systems to large rivers, biotic-abiotic interactions, and restoration; successful research productivity through external funding and refereed publications; and a commitment to teaching excellence. Postdoctoral or equivalent experience is desired. The successful candidate is expected to develop a comprehensive, externally funded research program involving graduate students, and will teach an undergraduate course in riparian ecology and management; participate in other undergraduate courses as needed; teach a graduate course in riparian ecology, management, and restoration; and a graduate course in specialty area. For a complete description and to apply online, please visit **website: http://www.hr.uidaho.edu.** Application review begins October 12, 2007. *Affirmative Action/Equal Opportunity Employer.*

POSITIONS OPEN

TENURE-TRACK FACULTY POSITION
Marine Genomics

The Department of Biological Sciences, University of Rhode Island invites applications for a tenure-track position in marine genomics at the **ASSISTANT or ASSOCIATE PROFESSOR** level available fall 2008. Research interests in genomic biology relating to physiology, development, ecological genetics, or evolutionary genetics of marine organisms preferred. Additional background in systematics preferred. Ph.D. in biological sciences or related area required. Postdoctoral research and teaching experience preferred. Teaching duties will include introductory and advanced courses in areas of specialty that enhance our undergraduate and graduate degree programs. Candidates must demonstrate through education, publications, research plan, statement of teaching philosophy, letters of recommendation and/or experience, potential for excellence in teaching, and for developing a high quality, nationally recognized and externally funded research program in marine genomics. Visit our Department **websites: http://www.uri.edu/cels/bio/** and **http://www.uri.edu/human_resources** for additional information. Send (no e-mails or faxes, please) a cover letter, current curriculum vitae, statement of teaching philosophy, research plan, copies of up to three published papers, and arrange to have three letters of reference sent by October 1, 2007, to: **Dr. Jacqueline F. Webb, Search Chair (Requisition #SCI011828), University of Rhode Island, P.O. Box G, Kingston, RI 02881.** *URI is an Affirmative Action/Equal Employment Opportunity employer that values diversity and is also an NSF ADVANCE institutional transformation university, working to advance the careers of women faculty, especially in the science and engineering disciplines.*

The Department of Biological Sciences at Wellesley College invites applications for a tenure-track position at the rank of **ASSISTANT PROFESSOR** to begin August 2008. We are seeking a broadly-trained **BIOLOGIST** who is strongly committed to excellence in both teaching and research in a liberal arts college environment. The position is open to any field of biology; however, we are interested in candidates in developmental biology, endocrinology, or behavior. The successful candidate will teach courses at all levels of the curriculum and develop an active research program that involves undergraduates. A Ph.D. and postdoctoral experience are required. Applications should include a cover letter, curriculum vitae, statements of teaching and research interests, and three letters of recommendation.

Materials should be submitted in Word or PDF format to **e-mail: bio07search@wellesley.edu** or mailed to: **Kaye Peterman, Department of Biological Sciences, Wellesley College, Wellesley, MA 02481.** The deadline for receipt of all application materials is October 15, 2007. For more information about becoming a faculty member at Wellesley, please visit **website: http://www.wellesley.edu/DeanCollege/Diversity/Open_pos/prospective.pdf.**

EVOLUTIONARY DEVELOPMENTAL BIOLOGY

The Department of Ecology and Evolutionary Biology at the University of Colorado seeks to hire an **ASSISTANT PROFESSOR** in evolutionary developmental biology. We encourage applications from those addressing questions at the genomic, molecular, cellular, and/or organismic levels, involving any group of eukaryotes. Applicants must submit curriculum vitae and statements of research and teaching interests in the form of a single PDF file via **e-mail: evodevo@colorado.edu.** Applicants should also arrange for three letters of reference to be sent to the same e-mail address. Review of applications will begin on September 24, 2007. *The University of Colorado at Boulder is committed to diversity and equality in education and employment.*

Q AAAS

Who inspires brainwaves while I study water waves?

"I study the mathematical equations that describe the motion of water waves. Different equations represent different waves – waves coming onto a beach, waves in a puddle, or waves in your bathtub. Then when I've surfed the math, I like nothing better than to spend the rest of the day surfing the waves.

This field is very important. The better we can model water waves, the better we can predict the patterns of beach erosion and natural disasters such as the tsunami in South East Asia. And this research can be applied to all sorts of regions around the world.

Being a member of AAAS means I get to learn about areas of interest I might not otherwise encounter. It gives me valuable opportunities to exchange ideas with colleagues in other fields. And this helps me find new approaches to my own work."

Dr. Katherine Socha is an assistant professor of mathematics at St. Mary's College, Maryland. She's also a member of AAAS.

See video clips of this story and others at **www.aaas.org/stories**

Katherine Socha, Ph.D.
Assistant Professor of Mathematics
and AAAS member

AAAS
ADVANCING SCIENCE, SERVING SOCIETY

POSITIONS OPEN

FACULTY POSITION
in Drug Delivery
ASSISTANT/ASSOCIATE PROFESSOR
in Pharmaceutics

The Department of Pharmaceutical Sciences at Wayne State University (WSU) invites applications for a 12-month tenure-track faculty position in pharmaceutics/drug delivery at the Assistant/Associate Professor level. The Department occupies state-of-the-art space in the new 270,000 square-foot College of Pharmacy and Health Sciences building on the WSU Medical Campus located in the cultural center of Detroit. Further information about the Department can be found at **website: http://www.cphs.wayne.edu/psc.html.** Plentiful local and regional collaborative opportunities exist within the Department, WSU Nanoscience and Nanotechnology Initiative **(website: http://research.wayne.edu/nano/),** School of Medicine, and the Karmanos Cancer Institute.

Applicants should have Ph.D. training in pharmaceutics, engineering, chemistry, or related areas. Successful candidates are expected to establish and lead an extramurally funded program in the broadly defined area of drug delivery and be responsible for teaching pharmacokinetics/drug delivery in the Pharm.D. program, as well as graduate courses. The position includes a competitive startup package and benefits.

To ensure full consideration, applicants must use the online application **website: http://jobs.wayne.edu.** Search Postings using Department H1822-Pharmaceutical Sciences, and submit documents online under the Pharmaceutics posting. Please include curriculum vitae, summary of research plans and teaching interests, and names and addresses of three references. Review of applications will begin on September 1, 2007, and continue until the position is filled. Direct inquiries to the **Search Committee Chair, Dr. David Oupicky,** at **e-mail: oupicky@wayne.edu.**

Wayne State University is an Equal Opportunity Employer.

ORGANIC CHEMISTRY
Dartmouth College

Applications are invited for a faculty position at the **ASSISTANT PROFESSOR** level starting July 2008. The Chemistry Department seeks an individual who will establish a nationally recognized research program in organic chemistry at Dartmouth, and who will excel at teaching in our undergraduate and Ph.D. curriculum. We are particularly interested in individuals with a strong background in the organic chemistry of materials or biomaterials. Candidates will be expected to be able to teach introductory and advanced courses in organic chemistry, as well as graduate courses in their area of research. Applicants should submit curriculum vitae, a description of their research plans, and a brief statement about their teaching interests. Applicants should also arrange to have three letters of recommendation sent on their behalf. All inquiries and applications will be treated confidentially. The Committee will begin to consider completed applications on October 15, 2007. Application materials should be sent to: **Chair, Organic Chemist Search Committee, Department of Chemistry, 6128 Burke Laboratory, Dartmouth College, Hanover, NH 03755-3564.** *With an even distribution of male and female students and over a quarter of the undergraduate student population members of minority groups, Dartmouth is committed to diversity and encourages applications from women and minorities. Dartmouth College is an Equal Opportunity and Affirmative Action Employer.*

FACULTY POSITION
Physical/Industrial Pharmacy

The University of Minnesota College of Pharmacy, Department of Pharmaceutics invites nominations and applications for the position of **ASSISTANT/ASSOCIATE PROFESSOR.** Visit **website: http://www.pharmacy.umn.edu/employment** for position description. *The University of Minnesota is an Equal Opportunity Educator and Employer.*

POSITIONS OPEN

BIOCHEMISTRY TENURE-TRACK FACULTY POSITIONS

Department of Chemistry and Molecular Biology, North Dakota State University (NDSU) has two full-time, nine-month tenure-track faculty positions available August 2008. Ph.D. in biochemistry, chemistry, or molecular biology (strong background in chemistry/biochemistry) required. Postdoctoral experience preferred. Applicants with research interests in metabolic regulation, regulation of gene expression, or related areas are encouraged to apply. Teaching duties may include core biochemistry courses at the undergraduate or graduate levels and a graduate course related to specialty area. Each candidate must have the potential to develop an externally funded, competitive research program and a commitment to teaching and service. It is expected that the successful candidate for the regulation of gene expression position, in addition to developing a research program, will also participate in collaborative research with the staff of the newly created NDSU Forensic DNA Facility. Positions are open at the rank of **ASSISTANT PROFESSOR.** Screening will begin October 1, 2007. For further information and full application requirements see **website: http://www.ndsu.edu/ndsu/jobs/non_broadbanded/positions/00021444.shtml.**

Contact person: **Dr. S. Derek Killilea, Department of Chemistry and Molecular Biology, North Dakota State University, Fargo, ND 58105. Telephone: 701-231-7946, fax: 701-231-8324.**

NDSU is an Equal Opportunity Institution.

EVOLUTIONARY/ECOLOGICAL GENOMICS

The Department of Ecology and Evolution and the Institute of Genome and Systems Biology are jointly seeking to fill a faculty position with an individual applying large-scale data approaches to questions in ecology or evolution. The successful candidate will address scientific problems or biological systems with potential to be applied. Rank is open, with a preference for candidates at the level of **ASSISTANT or ASSOCIATE PROFESSOR.** Interested applicants should submit curriculum vitae, selected reprints and preprints, statements of research and teaching interests, and the names and addresses of three references to **website: http://genomics-search.uchicago.edu.** Applications will be accepted until the position is filled, but applications should be received before 15 October 2007, to ensure full consideration. *The University of Chicago is an Affirmative Action/Equal Opportunity Employer.*

CAREER OPPORTUNITY

This unique program offers the candidate with an earned Doctorate in the life sciences the opportunity to obtain the Doctor of Optometry (O.D.) degree in 27 months (beginning in March of each year). Employment opportunities exist in research, education, industry, and private practice. Contact the **Admissions Office, telephone: 800-824-5526** at the **New England College of Optometry, 424 Beacon Street, Boston, MA 02115.** Additional information at **website: http://www.neco.edu, e-mail: admissions@neco.edu.**

POSTDOCTORAL POSITIONS (two to four-year) at University of California, Irvine to study stress responses of human embryonic and neural stem cells. Cells subjected to oxidative stress and irradiation will be analyzed for changes in survival, proliferation, and fate in various rodent models. Desired skills: stem cell growth and characterization, animal/stereotactic surgery, expertise in redox and radiation biology. Send curriculum vitae to: **Dr. Limoli, Department of Radiation Oncology, University of California, Irvine, Medical Sciences I, Irvine CA 92697-2695. E-mail: climoli@uci.edu.** *UCI is an Equal Opportunity/Affirmative Action Employer.*

ANNOUNCEMENTS

POSTDOCTORAL POSITION in cancer genetic epidemiology and genomics. Starting fall/winter 2007, a Postdoctoral position is available to perform whole genome association studies. The focus of this translational laboratory is on inherited susceptibility to cancers of the breast, ovary, colon, and prostate and lymphoma. Access to high-throughput genotyping platforms and a large number of research samples from a genetic isolate (Ashkenazi) is available. Methodology includes candidate gene association studies (see *Science* **297:**2013, 2002; *Cancer Res.* **66:**5104-10, 2006 and **64:**8891-900, 2004) and linage disequilibrium mapping (see *Genetic Epidemiology* **30:**48-61, 2006). Applicants will generally have a strong background in molecular genetics and statistical genetics. Send curriculum vitae and three letters of reference to: **Kenneth Offit, M.D., M.P.H., Clinical Genetics Service, P.O. Box 192, Memorial Sloan-Kettering Cancer Center, 1275 York Avenue, New York, NY 10021. Fax: 212-434-5166. E-mail: offitk@mskcc.org.** *Memorial Sloan-Kettering Cancer Center is an Equal Opportunity Employer with a strong commitment to enhancing the diversity of its faculty and staff. Women and applicants from diverse racial, ethnic, and cultural backgrounds are encouraged to apply.*

An NIH-funded **POSTDOCTORAL POSITION** is available in **Dr. Xu Luo's** Laboratory at the Eppley Institute for Cancer Research, University of Nebraska Medical Center. The project involves the biochemical study of apoptosis in mammalian cells. Candidates with recent Ph.D. degree in molecular biology or biochemistry are welcome to apply. For more information, please see **website: http://www.unmc.edu/Eppley/faculty.htm/**; **N.M. George, J.D. Evans, and X. Luo,** *Genes Dev.* **21:**1937-48, 2007; **X. Luo, I. Budiharjo, H. Zou, C. Slaughter, and X. Wang,** *Cell* **94:**481-490, 1998. Please send curriculum vitae and three reference letters to: **Dr. Xu Luo, Eppley Institute for Cancer Research, 987696 Nebraska Medical Center, Omaha, NE 68198-7696, e-mail: xuluo@unmc.edu.**

MARKETPLACE

AAAS & NPA

Here's your link to career advancement

AAAS is at the forefront of advancing early-career researchers—offering job search, grants and fellowships, skill-building workshops, and strategic advice through ScienceCareers.org and our Center for Careers in Science & Technology.

NPA, the National Postdoctoral Association, is providing a national voice and seeking positive change for postdocs—partnering with AAAS in career fairs, seminars, and other events. In fact, AAAS was instrumental in helping the NPA get started and develop into a growing organization and a vital link to postdoc success.

If you're a postdoc or grad student, go to the AAAS-NPA link to find out how to spell career success.

AAAS.org/NPA

NATIONAL POSTDOCTORAL ASSOCIATION

Science
AAAS

MORE TOPO. TOPO. TOPO.

More free time and better cloning efficiency in just three simple steps. TOPO® cloning technology allows you to perform benchtop cloning reactions in just five minutes—with up to 95% recombinants. So you always have the clones you need for downstream experiments. With more than 10 years of established performance and over 4,000 scientific citations, TOPO® cloning is the method of choice for researchers around the world. Whether you're doing general subcloning, sequencing, *in vitro* transcription, or expression in *E. coli*, mammalian cells, or our Gateway® system, there's a TOPO® cloning solution for you. Revolutionize your research at www.invitrogen.com/topo.

invitrogen™